DEVELOPMENTAND MANUFACTURE OF SUSTAINED RELEASE CAPTOPRIL BEADS

By

Farai Arthur Mhaka

A Thesis Submitted to Rhodes University

in Fulfilment of the Requirements for the Degree of

MASTER OF SCIENCE (PHARMACY)

February 2015

Faculty of Pharmacy

RHODES UNIVERSITY

Grahamstown, South Africa

ABSTRACT

Hypertension has a high mortality rate in developing countries such as South Africa. Although the prevention and control of hypertension is a health priority, efforts to decrease the global burden of hypertension and improve control over the condition are inadequate. The use of angiotensin converting enzyme (ACE) inhibitors such as captopril (CPT) have been effective for the management of hypertension when used as first line therapy alone or in combination. Commercially available immediate release dosage forms containing 12.5, 25 and 50 mg of CPT are administered two or three times a day to treat hypertension. CPT degrades in aqueous media with the sulfhydryl functional moiety responsible for adverse effects such as hypersensitivity, taste disturbances and/or presenting with a dry hacking cough. CPT has a short elimination half-life of between 1.6 and 1.9 hours, which means that the compound is a suitable candidate for inclusion in sustained release (SR) dosage forms. Manufacturing a SR dosage form of coated beads for twice daily dosing may reduce the incidence and intensity of undesirable adverse effects, improve the stability of CPT and improve patient adherence.

A stability indicating reversed-phase high performance liquid chromatographic (RP-HPLC) method was developed and optimised using a central composite design approach. As part of this approach the interactive effects of input factors, *viz.* pH, methanol (MeOH) content and column temperature on retention time, were investigated to achieve a separation with well-resolved and symmetrical peaks for CPT and salicylic acid. The method was validated using ICH guidelines and was found to be simple, linear, precise, accurate, selective and rapid for the *in vitro* quantitation of CPT. The method was successfully applied for the analysis of both commercially available and test formulations.

Preformulation studies were undertaken to establish the physical and chemical properties of CPT, excipients and dosage forms to ensure the production of stabile and bioavailable products. Powder blends were assessed for flow properties using angle of repose (AOR), and bulk and tapped density, which were subsequently used to calculate Carr's Index (CI) and the Hausner ratio (HR). The addition of talc resulted in the most powder blends with AOR, CI and HR that were within a range indicative of satisfactory to good flow properties. The use of talc was necessary to ensure that blending prior to wet granulation and extrusion-spheronisation would produce homogenous powders. Thermogravimetric analysis (TGA), differential scanning calorimetry (DSC) and Fourier

Transform Infrared Spectroscopy (FT-IR) were used for the identification and purity of CPT alone and 1:1 binary mixtures with excipients in an effort to establish if CPT was likely to undergo physical and/or chemical modification during production. The DSC thermograms for all CPT-excipient mixtures revealed the presence of a melting endotherm that was wider, occurring at 110.93 °C (T_{peak} for pure CPT). The characteristic peaks for specific functional groups were present in the FT-IR spectra for powder mixtures, indicating the absence of incompatibilities. Dialysis studies were used to investigate if the ammonium oleate present in Surelease® E-7-19010 interacted with CPT. The results suggests that an interaction between CPT and Surelease® E-7-19010 during processing of CPT beads was unlikely to occur. Preliminary investigations reveal that Methocel® K100M, Methocel® E4M, Avicel® PH102, Eudragit® RS PO, Surelease® E-7-19010 and talc are compatible with CPT and could be used for the manufacture of SR CPT beads.

CPT beads were manufactured using extrusion-spheronisation and coated using a fluidised bed drier fitted with a Wurster insert. The amount of granulating fluid, coating levels, curing time and formulation composition were varied to achieve CPT release with specific criteria to develop a preliminary formulation. The coated beads met all desired quality attributes in respect of micromeritic and flow properties, content uniformity and friability. Response Surface Methodology was used to further optimise the SR CPT formulation. The Plackett-Burman design was used for this process to produce an SR dosage form with desirable quality attributes achieved by altering formulation composition, extrusion-spheronisation variables and coating parameters. ANOVA data revealed significant responses for yield, aspect ratio, sphericity, coating efficiency and cumulative percent CPT released at 2 and 12 hours.

Formulations in which the high molecular weight HPMC were used in increased concentrations resulted in the formation of a sticky wet mass and extrudate, resulting in a decrease in yield. The application of a permeable, but insoluble Surelease® coat onto the surface of the beads formed a barrier that complements the activity of the hydrophilic matrix in preventing rapid dissolution and retarding the release of CPT from the beads. The amount of CPT released over 12 hours revealed that increasing the Methocel® K100M content entrapped CPT and retained it more efficiently in the hydrated matrix, resulting in a slow rate of CPT release.

In vitro release data were fitted to a number of models in an attempt to elucidate mechanistic aspects of transport processes specific to CPT from the coated bead formulations. The results of

fitting data from optimised batches revealed that the goodness of fit based on the adjusted correlation coefficient ranged between 0.953 and 0.976 for the Higuchi model, indicating that diffusion is a predominant factor that controls CPT release from the coated beads. The results of fitting data to the Korsmeyer-Peppas model suggest that the mechanism of CPT release includes transport of the dissolution medium from the vessel reservoir into the core of the bead due to osmotic potential, dissolution of CPT, mass transfer of the dissolved CPT within the core, partitioning between the solution and polymeric film, mass transfer of dissolved CPT through the film to ultimately reach the bulk dissolution fluid.

A SR CPT bead formulation that has potential for further development and optimisation for scaled-up production using RSM approaches and Design of Experiments such as CCD or Box-Behnken has been successfully developed and manufactured using extrusion, spheronisation and coating processes. Assessment of all batches of beads manufactured exhibited satisfactory to good flow properties and demonstrated SR profiles over 12 hours that met USP criteria for SR dosage forms.

ACKNOWLEDGEMENTS

I would like to express my sincere gratitude to the following people:

- My supervisor, Professor R.B. Walker, for his expert guidance, assistance, encouragement, continuous support and patience during the research and the writing of this thesis.

- My co-supervisor, Dr S. Khamanga, for his advice and assistance with my day to day laboratory work as well as their continuous encouragement and interest in my work.

- The Dean and Head of Department, Professor R.B. Walker and the staff of the Faculty of Pharmacy for the use of their facilities in the Faculty at Rhodes University.

- Mr T. Samkange for his technical support and Mr L. Purdon for his continuous help throughout the duration of this project.

- Mr R.J. and Mrs W. Mhaka, Mr M.R. and Mrs C.B.E Mutsvairo, Mrs M. Mutepha for their love, motivation and understanding. Thank you for supporting me financially and for helping me through accomplishing this thesis. You have indeed been the most amazing and supportive people in my life and I hope I have made you proud.

- My colleagues and friends in the Department of Pharmacy for their help and support: Mr Chiluba Mwila, Mr Tawanda Dube, Mr Tendai Chanakira, Mr Denzel Mubare, Ms Ayeesha Fauzee, Ms Cheidza Zindove, Mr Pedzisai Makoni, Ms Samantha Mukozhiwa, Ms Bianca Dagnolo, Ms Laura Magnus, Ms A. Katsidzira and Ms K. Rutsate for their friendship and encouragement during the trials and tribulations of this research.

- My sisters Tafadzwa, and Takudzwa for their love, encouragement and support. Thank you for everything and the being understanding. I love you lots.

- The Almighty for giving me protection, strength and resolve to succeed throughout my life.

STUDY OBJECTIVES

Hypertension accounts for 17 million deaths annually [1] and in developing countries the treatment of hypertension includes the use of angiotensin converting enzyme (ACE) inhibitors such as captopril (CPT) that is as effective as diuretics in reducing the mortality and morbidity of hypertension when used as first line therapy [2]. Challenges exist with immediate release CPT tablets as they require frequent dosing due to the short half-life of CPT [3]. CPT is therefore a suitable candidate for inclusion in sustained release (SR) dosage forms. CPT exhibits dose dependant undesirable adverse effects [4] and is unstable in aqueous solutions that may result in treatment failure. Therefore, developing a SR dosage form of coated beads may reduce the incidence and intensity of undesirable adverse effects, improve the stability of CPT and improve patient adherence.

The objectives of this study were to:

1. To develop and validate a stability indicating reversed-phase high performance liquid chromatographic (RP-HPLC) method for the quantitative analysis of CPT.
2. To perform preliminary studies to assess the suitability of powder blends for extrusion and spheronization.
3. To investigate the CPT excipient interactions using thermal analysis, infra-red spectroscopy and dialysis studies.
4. To investigate the effect of changing amount of granulating fluid, coating levels, curing time and formulation composition on the manufacture and performance of coated beads.
5. To design, develop, screen and optimize a formulation for the production of coated CPT beads using a Plackett-Burman experimental design approach.
6. To study the kinetics and mechanism ofCPT release using statistical and mathematical models.

TABLE OF CONTENTS

LIST OF TABLES

LIST OF FIGURES

CHAPTER ONE
CAPTOPRIL

1.1 INTRODUCTION

Cardiovascular disease (CVD) and the associated risk factors account for approximately 17 million deaths annually [1] and is therefore a major cause of mortality. Hypertension, as a CVD risk factor, is responsible for more deaths than any other and has a high mortality rate in developing countries, including South Africa [2, 5]. Reports that relate to hospitalised hypertensive patients in the developing countries do not necessarily reflect the actual pattern of hypertension in that country [2].This fact suggests that there is a high burden of this disease [6]. Although the prevention and control of hypertension is a health priority, efforts to decrease the global burden of hypertension and improve control of the condition have not been adequate [1, 2, 6]. The control of hypertension is initiated and commences when the blood systolic blood pressure of a patient is > 160 mmHg and the diastolic pressure is > 95-100 mmHg when measured on at least three separate occasions [3].

The treatment of hypertension includes the use of angiotensin-converting enzyme (ACE) inhibitors such as captopril (CPT) that are as effective as diuretics in reducing mortality and morbidity of hypertension when used as first line therapy [8]. CPT is freely soluble in water [3], unstable in light and ionises at the sulfhydryl functional group (-SH) [4]. CPT undergoes first order oxygen-facilitated, free radical oxidation at the sulfhydryl functional group in solution to yield captopril disulfide [3, 4, 9]. Although hydrolysis at the amide linkage is possible, this only occurs when the reaction is forced [4]. Oxidation is reported to be delayed in solutions of acidic pH or by addition of a chelating antioxidant or an increase in the amount of CPT in the dosage form [10]. CPT is a potent active pharmaceutical ingredient (API) for the management of hypertension [3, 4], cardiac failure, diabetic nephropathy and post-infarction with left ventricular function when used alone or in combination therapy. The antihypertensive effect of CPT is enhanced in patients that adhere to a low salt diet [8].

CPT binds to zinc at the active site of the ACE [11, 12] and the CPT binding site contains a sulfhydryl functional group that interacts with intracellular sulfhydryl containing compounds such as glutathione of the ACE, resulting in a change in the protein structure or function of the enzyme [13-15]. The sulfhydryl functional moiety is responsible for the adverse effects experienced by patients, including the presence of a sulphide like odour and a characteristic metallic taste [15]. A pruritic macula-papular skin rash is another adverse effect that occurs in patients that are hypersensitive to the CPT [13, 15].

CPT immediate release oral tablet formulations that are commercially available in South Africa include Adco-Captomax®, Sandoz-Captopril®, Merck Captopril®, Zapto-50®, Capacee®, CaptoHexal® and Capoten®. Therapeutic doses of CPT range between 12.5 mg and 50 mg up to a maximum of 150 mg daily, administered two or three times a day for the management of hypertension [16]. CPT has a short elimination half-life of between 1.6 and 1.9 hours [3] suggesting that there may be a need for additional CPT to be administered to effectively control hypertension. CPT is partly absorbed in the small intestine due to the presence of an amino acid proline structure [17] and the bioavailability of the API is decreased in the presence of food [16], suggesting that CPT is a suitable candidate for inclusion in sustained release (SR) dosage forms. SR dosage forms of CPT should allow for a reduced frequency of dosing to one or two times daily to promote patient adherence to therapy. Moreover, sustained release dosage forms should reduce the incidence and intensity of the undesirable adverse effects caused by excessively high plasma concentrations of CPT that are typically observed following multiple dose administration of conventional immediate release dosage forms [9, 18-20].

1.2 PHYSICO-CHEMICAL PROPERTIES

1.2.1 Description

CPT is 1-[3-mercapto-2-D-methyl-1-oxopropyl]-L-proline [3] and occurs as a white to off-white crystalline powder that has a slight sulphurous odour [9]. CPT exhibits two asymmetric carbon centres, of which one is associated with the proline moiety and the other with the 3-mercapto-2-methylpropionic acid side chain (Figure 1.1). CPT is not less than 98% pure when calculated on an anhydrous basis [3].

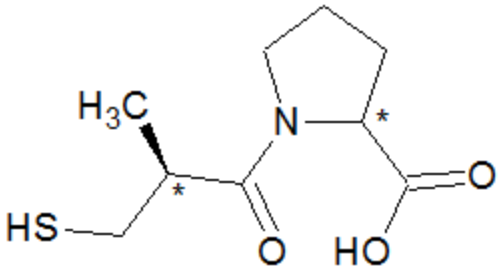

Figure 1.1*Molecular structure of CPT, C9H15NO3S (MW=217.3) * indicates the S,S optically active centres.*

1.2.2 Biological activity

All four isomers of CPT can bind to zinc at the active site of the ACE-enzyme [21] and exhibit biological activity for which potency is dependent on the configuration of the mercaptoalkanoyl side chain that binds to the active site [22]. The S,S isomer is approximately 100 fold more active than the R,S isomer [23-25] and is the only potent optically active inducer of the ACE-enzyme that reduces plasma angiotensin II (AT-II) levels and increases plasma renin activity, resulting in a significant decrease in blood pressure in hypertensive patients. The biological and antihypertensive effects of CPT lasts for up to 6 hours [3] as CPT has a short biological half-life and is eliminated rapidly from the plasma. CPT is readily converted into a disulphide dimer and forms a disulphide conjugate with endogenous sulfhydryl compounds, which does not correlate the relative bioavailability of CPT to a decrease in blood pressure [9, 26, 27]. As a consequence, the monitoring of the free unchanged CPT molecule in plasma [27] is not an adequate indicator of the blood pressure lowering effects and patient adherence to therapy.

The biological activity of CPT can be characterised following radioimmunoassay [28] to determine the plasma-renin activity (PRA) of CPT administered to treat reno-vascular hypertension in comparison to therapy with an international reference standard. The use of radioimmunoassay is a screening approach in which baseline PRA evaluation is established. The patient is then administered an oral dose of radioactive CPT and blood pressure measurements are recorded immediately and at 60 minutes following administration, at which time a second PRA assessment is undertaken. Patients presenting with reno-vascular hypertension demonstrate a larger decrease

in blood pressure and increases in PRA following CPT administration when compared to patients that present with essential hypertension [28]. CPT exhibits several other activities and can be used to treat arthritis, reverse diabetic retinopathy, enhance insulin sensitivity, lower thrombotic risk, decrease atherosclerosis and renal failure, lower the incidence of radiation-induced pulmonary damage and fibro-sarcoma [29].

1.2.3 Solubility

The solubility of CPT in water is 160 mg/mL at 25°C. CPT is freely soluble (< 100 mg/mL) in methanol, ethanol, isopropanol, chloroform and/or methylene chloride [9]. A solubility-temperature profile of CPT was linear up to 40°C and at temperatures higher than 40°C, CPT exhibited extraordinarily high water solubility of more than 250 mg/mL [3].

1.2.4 Dissociation constant (pKa)

The pKa of the carboxylic acid attached to the proline ring of most ACE inhibitors ranges between 2.5 and 3.5 [30]. CPT is an active pharmaceutical ingredient (API) that exhibits weakly acidic properties and ionises at physiological pH, whereas other ACE inhibitors are amphoteric in nature [31]. The dissociation constants for CPT are 3.7 and 9.8 for the carboxyl and sulfhydryl groups, respectively. CPT is zwitterion and has an isoelectric point of 6.8 [31].

1.2.5 Hygroscopicity

CPT is hygroscopic under hot and humid conditions and absorbs large amounts of moisture. It is unstable and storage conditions or manufacturing processes require stringent monitoring of temperature and humidity to ensure that a stable and effective CPT dosage form is produced [3].

1.2.6 Melting range

CPT has a melting range of 106 – 109°C and decomposes at temperatures between 160 and 450 °C in a two or three step process that is dependent on the conditions to which the API is exposed [9, 32].

1.2.7 Optical rotation

The specific optical rotation of the two enantiomers of CPT at 25 °C in absolute ethanol is α_D^{25} = -127.8 °. The R and S isomers have an optical rotation of approximately +5 ° [3].

1.2.8 Polymorphism

Two polymorphic forms of CPT have been identified *viz*. an unstable β and stable α polymorph. The unstable β polymorph melts at 88 °C and the stable α polymorph melts at 106°C [3].

1.2.9 Storage conditions

CPT should be stored at temperatures < 30 °C in well-closed containers. It must be protected from heat, sunlight and moisture. Individuals must avoid breathing CPT powder as it may cause a dry hacking cough and a rash may be observed if CPT comes into contact with skin and membranes, particularly if the individual is allergic to sulphur [9, 17].

1.2.10 Infra-red (IR) absorption spectrum

The IR absorption spectrum of a compound is unique and is useful for elucidation of the chemical structure of an organic compound or as a means to identify that compound [33].The precise interaction of the atoms in a molecule generates a unique spectrum for a specific molecule [33]. The IR spectrum is a specific characteristic of any compound, although certain groups of atoms in organic molecules produce characteristic absorption bands in the same IR region [33] irrespective of the structure of the molecule. The IR absorption spectrum of CPT is depicted in Figure 1.2 and was generated between 4000 and 650 cm^{-1} with Spectrum 2000 FTIR Spectrophotometer (Perkin Elmer Instruments LLC, Shelton, CT, USA) using Nujol® or heavy liquid paraffin (UniLab, Redmont WA, USA).

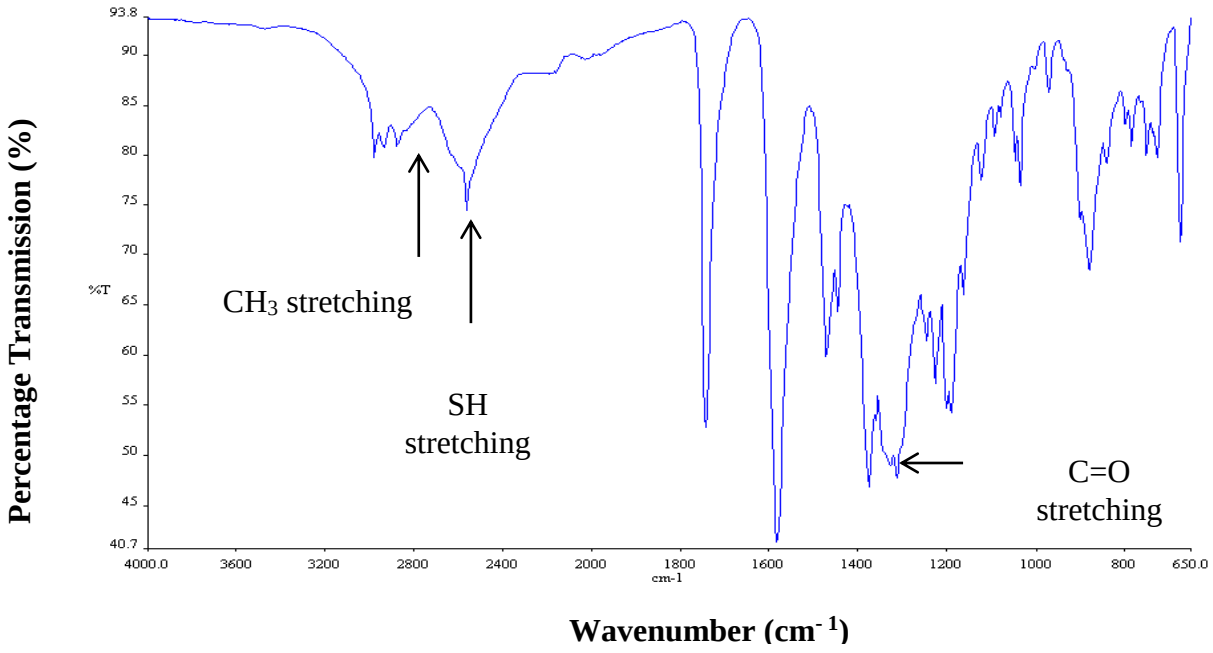

Figure 1.2 *Infrared Absorption Spectrum of CPT.*

The IR spectrum for CPT exhibits characteristic CH_3 stretching bands at 2980 cm^{-1} and CH_2 stretching bands at 2877 cm^{-1} that are representative of alkane functionalities. The broad peak at 2565 cm^{-1} corresponds to SH stretching, which is a characteristic of mercaptan compounds. The peaks observed at 1744 cm^{-1} and 1588 cm^{-1} are due to C=O stretching vibrations of the carboxylic acid and amide functionalities, respectively. The peaks observed at 1227 cm^{-1} and 1246 cm^{-1} corresponded to -C-H and/or -CH_3 bending or symmetric vibrations [33]. The IR absorption spectrum for CPT is similar to what has been reported in literature as illustrated in Table 1.1 [3].

Table 1.1 *IR band assignment for CPT peaks obtained and reference peaks.*

Functional Group	***Wave Number (cm^{-1})**	****Wave Number (cm^{-1})**
-C-H/-CH_3 bending/symmetric vibration	1227, 1246	1300
-C-N amide band	1588	1500
-COOH (-C=O)	1744	1750
-SH stretching vibration	2565	2600
-CH_3 stretching vibration (symmetric)	2980	2980

* IR spectrum bands generated.
** Reference IR spectrum bands [3].

1.2.11 Ultra-violet (UV) absorption spectrum

The UV spectrum of CPT in methanol (MeOH) and water in a ratio of 65:35% v/v over a wavelength range of 190-300 nm was generated at a scan speed of 600nm/min using a double beam UV-VIS Model GBC 916 spectrophotometer (GBC Scientific Equipment Pty Ltd, Melbourne, Australia) and is depicted in Figure 1.3. The wavelength of maximum absorption (λ_{max}) for CPT was 199.3, which is slightly lower than the value of 205 nm generated in 50:50% v/v MeOH water reported in the literature [34]. Changes in the mobile phase composition therefore have the effect to reducing λ_{max} associated with changes in intensity and reflectivity grating when rays pass through a quartz container with sample solution because of angular dispersion in the different medium phases. The λ_{max} was used for the analysis of CPT dosage forms by RP-HPLC as described in Chapter 2, *vide infra*.

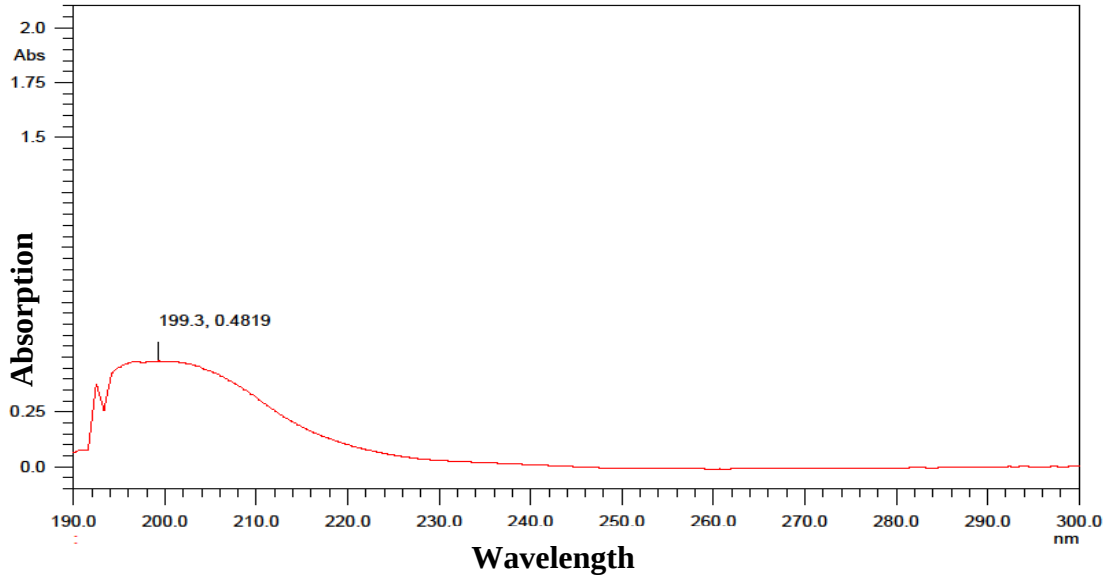

Figure 1.3 *UV absorption spectrum of CPT in MeOH: water in a ratio of 65:35% v/v.*

1.3 STEREOCHEMISTRY

1.3.1 Stereo-specificity

Despite significant differences in the pharmacological, pharmacodynamic and pharmacokinetic responses of individual enantiomers of a compound, many molecules are commercially available as racemic mixtures [35]. Some enantiomers of a compound are more active, toxic or totally inactive [36] when compared to the others. CPT has two asymmetric carbon centres and exists as four stereoisomers, one of which is *R*-captopril, 1-[3-mercapto-2(*S*)-methyl-1-oxopropyl]-*R* (D)-

proline [23], and the others exhibit biological activity of *S*-captopril that is available as S,S stereoisomer [36]. *R*-captopril possesses no ACE inhibiting activity [25]. It is known that the (*S*, *R*) epimer of captopril has a 100-fold lower activity than the *S*-captopril isomer [35].

1.4 SYNTHESIS

1.4.1 Synthetic procedure/pathway

The chemical synthesis of CPT is based on a coupling reaction that is depicted in Figure 1.4.

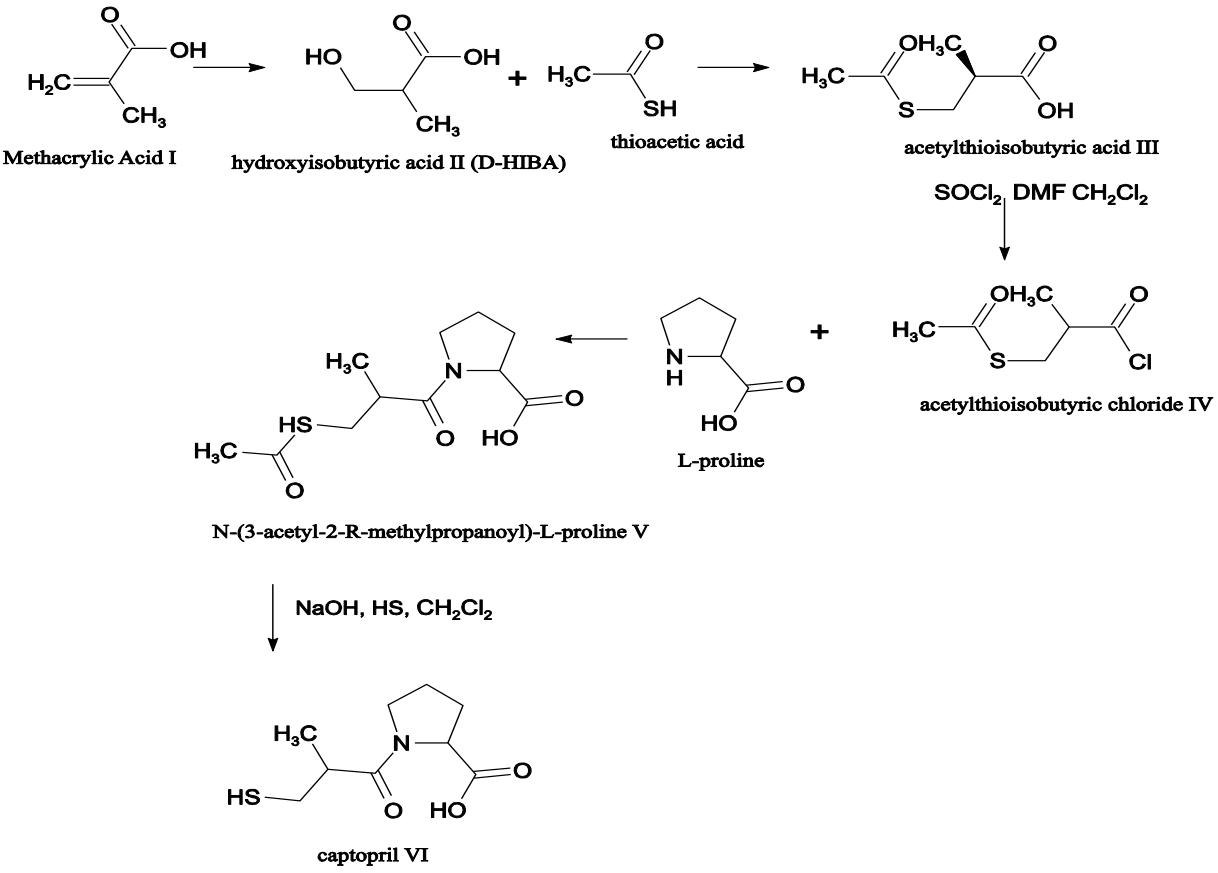

Figure 1.4 *Synthesis of CPT(VI) from methacrylic acid(I) [37]*.

Methacrylic acid (I) undergoes hydroxylation to form D-β- hydroxyisobutyric acid (D-HIBA) (II). D-HIBA is an optically active intermediate in the synthesis of CPT or a raw material for use in the biocatalytic synthesis of CPT [37]. D-HIBA is then acetylated in the presence of thioacetic acid to produce acetylthioisobutyric acid (III) [3]. Acetylthioisobutyric acid is then treated with thionyl chloride ($SOCl_2$), N,N-dimethyl formamide (DMF) and dichloromethane (CH_2Cl_2). A distillation process is performed to produce an intermediate 3-acetyl-2-methylpropanoyl chloride (IV) [22].

The next step of the reaction involves coupling the intermediate produced with L-proline by means of a Schotten-Baumann reaction [38]. Two equivalents of sodium hydroxide and CH_2Cl_2 are used to produce N-(3-chloro-2-R-methyl propanoyl)-L-proline (V). The carboxylic acid function on the L-proline is protected using the process described by Hongo *et al.*,[38-40]. The direct substitution of the chlorine atom with a sulfhydryl functional group on the proline side chain is the penultimate step that produces a racemic mixture of CPT (VI). Retention of the stereochemistry is achieved by use of DMF, dimethyl sulphoxide with hydrogen sulphide (HS) or trithiocarbonate as a nucleophilic reagent [14, 22].

The yield of CPT using the coupling method described is > 28 % [22, 37]. *R*-captopril is a by-product of the reaction and is an impurity in the racemic mixture [37] obtained through chemical synthesis. Purification or resolution of the racemic mixture to obtain the biologically active *S*-captopril is essential [23-25] and therefore enantio-purity tests on the S-captopril product to ensure the production of pure material are essential. Since chemical synthesis of chiral compounds requires resolution of the racemic mixture, the overall yield is closer to 50%. To increase the yield of CPT, Seong *et al.,* [40]proposed an economical model to produce the optically active D-HIBA raw material. The production of D-HIBA from *Candida rugosa* [11] does not require a post-manufacture, resolution process. The main advantage of microbial catalysed synthesis over chemical synthetic procedures is that the reaction is more effective with respect to regional, chemical and stereo specificity. An additional advantage of microbial synthesis is that there is a decrease in the production of unwanted by-products [11], minimum waste and the procedureto produce a higher yields of active CPT is simple.

1.4.2 Structure-activity relationship

CPT is structurally similar to endogenous L-alanyl-L-proline and it consequently characterises L-alanyl-L-proline binding ability to ACE in a similar manner. Studies of the structure and binding of L-alanyl-L-proline to the C-terminal residue of ACE [13] reveal that the L-alanyl-L-proline moiety is responsible for antihypertensive activity, which is also the case for CPT. The presence of a free carboxyl functional group is essential for high levels of activity. The carboxyl functional group is negatively charged and binds to the positively charged amino acid residue of the enzyme

through ionic interactions, as depicted in Figure 1.5. The activity of L-alanyl-L-proline is similar to the ACE inhibition activity demonstrated by CPT.

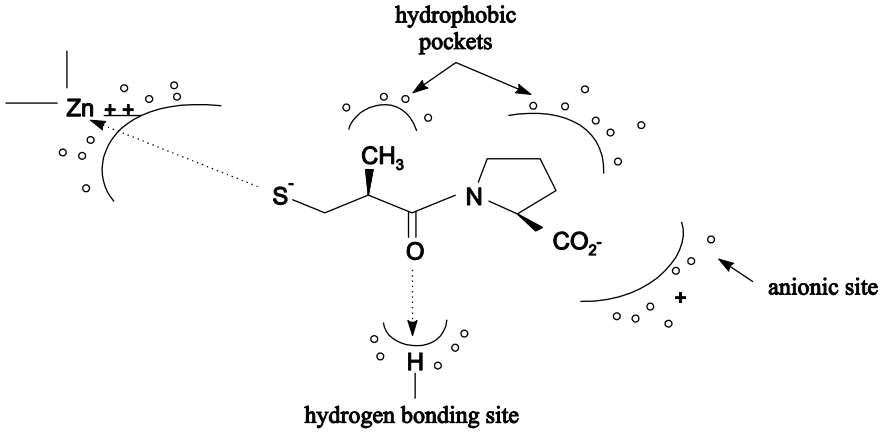

Figure 1.5 *CPT interactions at the catalytic sites of the ACE enzyme.*

Substitution of the proline moiety with a phosphoryl derivative of L-alanyl-L-proline resulted in the production of an ACE inhibitor that is more potent than CPT. Replacement of the sulfhydryl group with a phosphoryl derivative functional group led to the development of enalapril that is approximately three- to fourfold more potent than CPT, but exhibits a slower onset and longer duration of action [13, 14]. The pyrrolidine ring on CPT was substituted with a thiazolidine ring without loss of activity. The proline moiety provides a specific binding site for the ACE pockets through hydrophobic interaction. Subsequent substitution of the sulfhydryl (–SH) functional groups with a hydroxyl (–OH) functional group led to a total loss of activity [13], suggesting that the sulfhydryl functional group of CPT is essential for inhibitory activity of the ACE enzyme [30]. The sulfhydryl functional group is also responsible for the common side effects of CPT. The side effects are reduced when lower doses of CPT are administered or CPT use is discontinued. The side effect profile of CPT prompted the development of sulfhydryl-free derivative ACE inhibitors [22, 30]. The carbonyl oxygen on the alkanoyl chain is essential for ACE inhibition activity and the nitrogen in the proline ring and the carbonyl oxygen of CPT are important for hydrogen bonding. The carbonyl oxygen acts as a proton acceptor, whereas the amino acid residue at or near the active site of ACE acts as a proton donor. The methyl group of the propionic side-chain contributes to the overall binding affinity of CPT to the active site of the enzyme [30]. Many of the class II ACE inhibitors are ester pro-drugs that have a much greater oral bioavailability, yet they are 100 - 1000-fold less potent than the active metabolites of these compounds [13].

1.5 STABILITY

1.5.1 Solid state stability

CPT in the solid state exhibits excellent stability and no significant decomposition was detected for up to six months in bulk samples that were stored at 5 °C, 33 °C and 50 °C [3, 7]. CPT was stable in light when exposed to 900 foot-candles in a light box for up to 30 days [3].

1.5.2 Solution stability

CPT is unstable in solution and undergoes first order free radical oxidation [10] at the sulfhydryl functional group to yield captopril disulfide. The rate of oxidative degradation of CPT in the pH range between 2 and 5.6 at 50 ^{o}C was investigated by Timmins *et al.*,[41], who concluded that oxidation is the predominant route of degradation of CPT. Stability studies of CPT in aqueous solutions of pH 6.6 – 8.0 yielded captopril disulfide as the sole degradation product as a result of oxidation [10]. The rate of degradation of CPT in acetate, citrate and phosphate buffers of different concentrations at a pH 6.0 revealed that all degradation reactions exhibited first-order kinetics [8] and the rate of degradation increased with an increase in buffer concentration. The first-order rate of degradation of CPT in citrate buffer solutions was low due to the chelating effect of citrate ions that reduce metal ion catalysis in oxidative processes [8]. Oxidation was delayed at a low pH and the addition of a chelating antioxidant, nitrogen or use of low oxygen head spaces during production may enhance stability. The oxidation of CPT is known to be pH-dependent and maximum stability is observed in solutions of pH < 4.0 [41].

1.6 CLINICAL PHARMACOLOGY

1.6.1 Mechanism of action

1.6.1.1 Overview of ACEinhibition

Pharmacological therapy by interruption of the renin-angiotensin-aldosterone system (RAAS) in the1970's [42] was considered to be beneficial for patients that presented with hypertension due to high-renin levels. This finding resulted in the development of API, which is known to inhibit ACE [15, 29, 43]. The RAAS is an important regulator of hemodynamic stability and regulates extracellular fluid volume, sodium balance and cardiovascular function through direct and indirect effects on the kidney and other organ systems [44]. Renin is a proteolytic enzyme that has local activity on angiotensinogen in the kidney and general circulation. Angiotensinogen is a protein precursor that is produced by the liver and is cleaved by renin to form the inactive peptide angiotensin I (AT-I) [44-46].

Physiological substrates of ACE include AT-I and bradykinin where AT-I is converted into the active vasopressor AT-II [45] by removal of a single terminal carboxyl dipeptide. The vasodilatory peptide bradykinin is deactivated by the consecutive removal of two terminal carboxyl dipeptides during the metabolism of bradykinin. The effect of AT-II is mediated through the AT-1 receptor, which results in arteriolar vasoconstriction, and water and salt retention as depicted in Figure 1.6. The RAAS is therefore activated in response to fluctuations in blood pressure and the extracellular fluid volume [17].

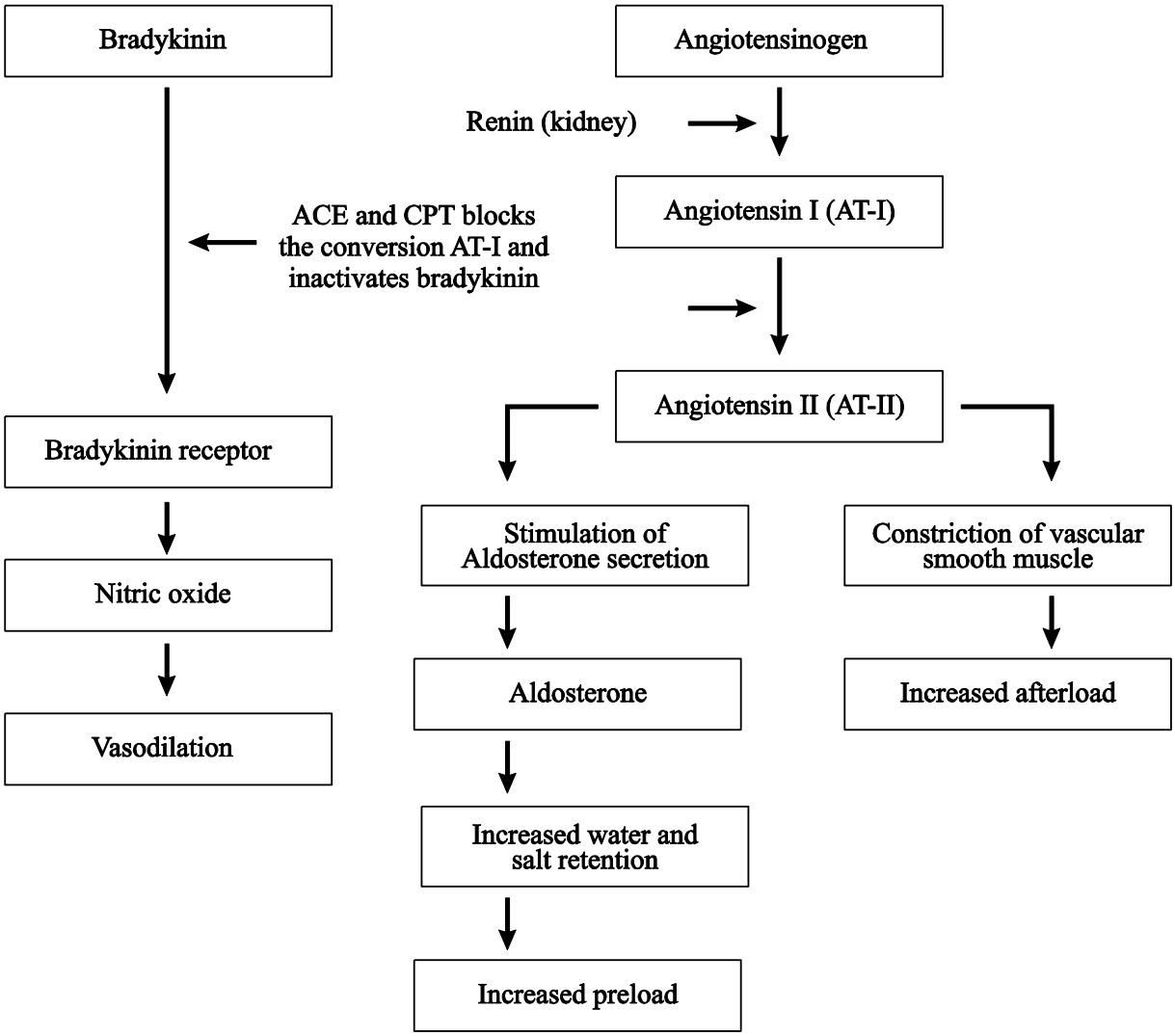

Figure 1.6 *The Renin-Aldosterone-Angiotensin System (RAAS).*

The blockade of an activated RAAS has become a key target in patients that present with hypertension, heart failure, renal and atherosclerotic cardiovascular disease [29, 44, 46, 47] through the use of ACE inhibitors, since ACE is a zinc metalloenzyme attached to the plasma membrane with the epithelial cells that have active sites exposed on the extracellular surface of the cells [46]. ACE inhibitors improve the prognosis in mild, moderate and severe heart failure in addition to preventing the onset of heart failure in patients with left-ventricular dysfunction and myocardial infarction (MI) [43]. Although ACE inhibitors were first used for their antihypertensive effect, it has been proposed [48] that ACE inhibitors potentiate bradykinin beyond blocking hydrolysis through inhibition of desensitisation receptors.

ACE inhibitors may have beneficial effects on the fibrinolytic balance in the body through AT-II inhibition, which is thought to be prothrombotic [45]. Consequently, AT-II inhibition promotes antithrombotic effects through bradykinin accumulation. Further research aimed at investigating the effect and degree of ACE inhibitory tissue activity on the vascular response is required. The beneficial effects of ACE inhibitors include a reduction in the production of AT-II and an increase in bradykinin levels [45, 48] that effectively lowers extracellular fluid volume, sodium balance and cardiovascular function through direct and indirect effects on the kidney and other organ systems.

1.6.1.2 Hypotensive effect

CPT reduces blood pressure in patients with essential hypertension, reno-vascular hypertension [44] and hypertension associated with chronic renal failure [49] by acting as a competitive inhibitor of the ACE in the kidney and vascular walls. CPT inhibition of ACE is believed to be important for the reduction of blood pressure, especially in patients with high PRA. The inhibition of ACE has also proved to be effective in patients with normal and low levels of PRA [43]. The mechanism by which CPT reduces high blood pressure associated with low or normal PRA has not been fully elucidated, but the antihypertensive effect of CPT is enhanced when concomitantly administered with a diuretic in patients on a low salt diet [17].

1.6.1.3 Cardiac failure

CPT is effective in all four classes of heart failure and not only alleviates the symptoms, but also reduces the incidence of infarct decompensation and mortality [50]. CPT significantly decreases left ventricular dilatation and long-term treatment with CPT does not result in improved aerobic exercise capacity following an acute MI [50]. CPT can be combined with diuretics, digitalis preparations and nitrates to treat cardiac failure and is effective as valsartan in patients at high risk for cardiovascular events following MI [51]. Concurrent use of CPT and valsartan results in an increased incidence of adverse events without improving survival rate.

1.6.1.4 Diabetic nephropathy

Diabetic nephropathy is a common cause of end-stage renal disease, especially in patients who present with early stages of insulin-dependent diabetes mellitus (IDDM) [1]. The renal plasma flow (RPF) and glomerular filtration rate (GFR) have higher values [47, 52] than those observed in healthy volunteers. Some IDDM patients who present with early abnormalities in protein excretion or albuminuria have been observed and this phenomenon is thought to be a predictor of clinically overt diabetic nephropathy [47]. The high glomerular hydraulic pressure and/or plasma flow rates [47] are thought to be responsible for proteinuria and the progression of diabetic nephropathy. CPT use in patients with deteriorating renal function, especially IDDM patients, has revealed a reduced progression of diabetic nephropathy by a mechanism that is independent of its antihypertensive effects [47, 52].This is a consequence of altered glomerular hemodynamics in patients with diabetes.

1.6.2 Contra-indications

CPT is contraindicated in patients who are sensitive to sulphur or any excipient used in formulations of the API. CPT must not be used in patients who have experienced angioedema during therapy with other ACE inhibitors and it is also contraindicated in pregnancy [43].

1.6.3 Overdose

Clinical trials have revealed that high doses of CPT of approximately 450 mg per day result in side effects such as dry cough, dose-dependent macula-papular rash, taste alteration, angioedema and neutropenia that is associated with zinc and/or copper depletion [53]. The symptoms of overdose include emesis and hypotension [53]. The correction of hypotension is of major concern in emergency cases. Volume expansion using an intravenous infusion of normal saline for the restoration of blood pressure is the preferred treatment. CPT can be removed from the systemic circulation by hemodialysis [43].However, the effectiveness of hemodialysis for removing CPT in neonates and children has not yet been established. Peritoneal dialysis is not effective [43] for the removal of CPT due to inadequate filtration and insufficient exchange transfusion from the general circulation of neonates. Overdose of CPT has been effectively treated with naloxone due to reversal or blockade of the hypotensive activity of CPT [53].

1.6.4 Drug interactions

Non-steroidal anti-inflammatory drugs (NSAID) attenuate the antihypertensive effects of CPT. Co-administration of CPT with NSAID such as diclofenac sodium, mefenamic acid and/or selective cyclooxygenase-2 inhibitors (COX-2) may cause deterioration of renal function and may precipitate acute renal failure [43]. Monitoring renal function, particularly the serum creatinine levels, in patients treated with CPT and NSAID therapy is recommended and the concomitant administration of CPT and NSAID must be undertaken with caution, particularly in elderly patients or those with pre-existing renal impairment [43].

The addition of a diuretic to the therapeutic regimen of a patient treated with CPT usually enhances the antihypertensive effect of the API. Reports [14] suggest that patients presenting with intravascular volume depletion on initiation of diuretic therapy may result in an excessive reduction in the blood volume within the first hour of commencing therapy. The possibility of hypotensive effects may be minimised by discontinuation of the diuretic or by adequate hydration and increased salt intake prior to commencement of therapy [45]. The patient must be observed closely for several hours following the initial dose of the CPT until the blood pressure has stabilised. The transient hypotensive response is not a contraindication to administration of additional doses that can be administered without difficulty once blood pressure has increased following blood volume expansion therapy [43].

ACE inhibitors are potassium-sparing agents and CPT decreases the production of aldosterone, which may result in elevated potassium levels in serum [17]. Potassium-sparing diuretics such as spironolactone, triamterene or amiloride and the use of potassium supplements [45] should be considered only in patients with documented hypokalemia and should even then be used with caution. Potassium sparing diuretics may lead to a significant increase in serum potassium levels and patients should use a low salt diet when taking potassium sparing diuretics concomitantly with CPT [6].

1.6.5 Adverse reactions

Patients on ACE inhibitor treatment present with a variety of adverse reactions, including hypotension, dry hacking cough and taste disturbance. Uncommon adverse events include first-dose hypotension, macula-papular skin rash, palpitations, angioneurotic oedema, angina and insomnia. Rare adverse effects include neutropenia, which may be accompanied by thrombocytopenia or pancytopenia, pulmonary infiltrate, alopecia and impotence [17].

The incidence of cough varies between 2 and 15 % depending on the ACE inhibitor used [45], dose and duration of therapy. The cough appears to be more common in women than men, is often worse when the patient is lying down and may be due to increased bronchial reactivity [45]. This side effect can be resolved or diminished on continued use or following a reduction of dose, but usually reoccurs following the reintroduction of CPT therapy. The cough most likely occurs due to stimulation of the pulmonary cough reflex by bradykinin and/or prostaglandins that accumulate due to ACE inhibition. Once a patient has developed an intolerable cough, an attempt may be made to switch the patient to an alternate ACE inhibitor or another class of anti-hypertensive compounds such as calcium channel blockers [45, 48].

Severe life-threatening angioedema has been reported in rare cases following CPT use. The overall incidence is approximately 0.1 % - 0.2 % and gender has no impact on the incidence of angioedema or the predisposition to angioedema in patients with heart failure or hypertension [16]. The majority of reported cases of angioedema revealed that the symptoms occurred during the first week of therapy [16].However, the onset of angioedema may be delayed for weeks or even months. Patients may present with multiple episodes of angioedema with long intervals without the related symptoms of angioedema. The aetiology is thought to be non-immunogenic, may be related to bradykinin activity and may occur with or without urticaria, but usually involves non-pitting oedema of the skin, the subcutaneous tissues and mucous membranes [16].

Angioedema of the face, extremities, lips, tongue, glottis and/or larynx have also been reported [27] in patients treated with CPT, and if observed, therapy must be discontinued immediately with appropriate monitoring instituted to ensure complete alleviation of the symptoms. If the swelling is confined to the face and lips, angioedema may be resolved without treatment or following administration of antihistamines. Angioedema associated with laryngeal oedema is potentially life-

threatening and patients should be hospitalised and/or treated with adrenaline and oxygen immediately [17] where involvement of the tongue, glottis or larynx is likely to cause an airway obstruction. Patients that respond to medical treatment should be monitored for the possible re-emergence of symptoms of angioedema and patients with a history of angioedema should not be treated with an alternate ACE inhibitor [16].

1.6.6 High risk groups

1.6.6.1 Pregnancy

The use of agents that act on the renin-angiotensin system during the second and third trimesters of pregnancy may reduce renal function and increase foetal and neonatal morbidity and death [16]. CPT is classed as a Category C compound for the first and a Category D for the second and third trimesters of pregnancy [17]. There are no adequate and well-controlled studies reporting CPT use in pregnant women, and teratogenic effects have not been established following administration of large doses of CPT in hamsters, rats and rabbits [16]. The administration of ACE inhibitors to rabbits at doses of approximately 0.8 to 70 times on a mg/kg basis related to the maximum recommended human dose [16] resulted in a low incidence of craniofacial malformation. No teratogenic effects of ACE inhibitors were evident in studies in which doses were approximately 150 times that of the maximum recommended human dose in pregnant hamsters and 625 times in pregnant rats [16]. Post-marketing experience with ACE inhibitors suggests that exposure *in utero* following administration may be associated with hypotension and decreased renal perfusion in the foetus [16],which may result in foetal death.This indicates that ACE inhibitors should be contraindicated in pregnancy.

Oligohydramnios is a condition in pregnancy characterised by a deficiency of amniotic fluid with presenting clinical features of a smaller fundal height, foetal malpresentation, undue prominence of foetal parts and reduced amounts of amniotic fluid [17]. Oligohydramnios has been reported as a result of decreased foetal renal function and can be associated with foetal lung hypoplasia and skeletal deformation [16]. Potential adverse effects in neonates include skull hypoplasia, anuria, hypotension, renal failure or death [16] following administration of ACE inhibitors in the second and/or third trimesters of pregnancy. CPT use must be discontinued immediately when pregnancy is detected. When ACE inhibitors, including CPT, have been used during the second and third

trimesters of pregnancy, foetal hypotension, renal failure, skull hypoplasia and death [16]have been reported, presumably as a consequence of systemic hypotension in the foetus. There is limited information to whether exposure limited to the first trimester can adversely affect foetal outcomes [43] and consequently women who are pregnant and are using ACE inhibitors must be switched to more appropriate antihypertensive therapy.

1.6.6.2 Lactation

Following oral administration, the concentrations of CPT in human breast milk are 1 % or lower than those observed in the systemic circulation of mothers, and the effect of CPT on breastfed infants has not yet been established. Consequently, caution should be exercised when CPT is administered to breastfeeding mothers [17].

1.6.6.3 Paediatric patients

CPT is not registered for paediatric use in South Africa. However, it has been suggested that doses of 0.1 - 1.0 mg/kg/dose of CPT titrated carefully against a therapeutic response may be administered to paediatric patients as summarised in Table 1.2 [54].

Table 1.2 *CPT doses for paediatric use.*

Category	Recommended dose
Premature neonates **Term neonates ≤ 7 days of age**	0.01 mg/kg/dose every 8 to 12 hours, titrate dose accordingly
Term neonates > 7 days of age	0.05 to 0.1 mg/kg/dose every 8 to 24 hours, titrated upward to maximum dose of 0.5 mg/kg/dose administered every 6 to 24 hours
Infants	0.15 to 0.3 mg/kg/dose titrated upward to maximum dose of 6 mg/kg/day in 1 to 4 divided doses. Usual required dose - 2.5 to 6 mg/kg/day
Children	0.3 to 0.5 mg/kg/dose, titrated upward to a maximum dose of 6 mg/kg/day in 2 to 4 divided doses

There is a paucity of information relating to the safe use of CPT in paediatric populations [55]. The doses based on weight are comparable or lower than those used to treat adults. Infants, especially newborns, may be more sensitive to the adverse haemodynamic effects of CPT exhibited by excessive, prolonged and unpredictable decreases in blood pressure associated with CPT doses of ≥ 0.5 mg/kg/dose [54]. CPT should therefore only be used in paediatric patients if alternative measures of controlling blood pressure have not been effective and if the potential benefits of use justify the risk.

1.6.6.4 Geriatric patients

A dose of CPT of 12.5 mg and 25 mg were administered twice daily to sixteen hypertensive patients between the ages of 65 and 80 years and the outcomes compared to placebo therapy in a double-blind cross-over study [56]. The mean systolic and diastolic baseline blood pressure following treatment was found to be 204.7 ± 24.5 mmHg and 111.8 ± 11.1 mmHg, respectively. Of the 14 patients who completed the study CPT was found to reduce the systolic and diastolic blood pressures significantly when compared to baseline and placebo arm values [56]. The fall in blood pressure was greater following four weeks of therapy when compared to data following two weeks of treatment. No significant changes in blood pressure were noted from baseline values for patients in the placebo arm and no significant and/or serious side-effects were observed during the study. It was concluded that CPT was an effective antihypertensive agent that can be safely used in elderly patients [56].

1.6.6.5 Food

The absorption of CPT is reduced by approximately 25 - 40 % in the presence of food. CPT decreases the excretion of potassium from food and the use of salt substitutes containing potassium increases the risk of hyperkalemia [17]. The antihypertensive effects of CPT may be attenuated by a high salt intake. Bayberry, blue cohash, cayenne, ephedra, ginger, ginseng, kola and liquorice are some of the herbs that may reduce the antihypertensive properties of CPT [30, 46, 47].

1.7 CLINICAL PHARMACOKINETICS

1.7.1 Dosage

The usual dose of CPT is 25 or 50 mg administered twice or three times daily up to a maximum daily dose of 450 mg [43]. Initiating hypertensive therapy using CPT requires consideration of the extent of blood pressure elevation, salt restriction and medical history, among other clinical data. Prior to commencing therapy with CPT patients should discontinue existing antihypertensive therapy for at least one week [16].

The initial adult dose of CPT for the treatment of hypertension is 12.5 mg administered twice or three times daily.It is increased, if necessary, to 25 mg two to three times daily following one or two weeks of therapy [43]. The dose may be increased to 50 mg two or three times a day if there is satisfactory evidence that there has been no significant reduction in blood pressure. A restriction of sodium intake may also be beneficial when CPT is administered alone. If the blood pressure has not been satisfactorily controlled after one to two weeks of therapy, an appropriate dose of a thiazide diuretic should be added to the regimen [17]. If further blood pressure reduction is required, the dose may be increased up to 100 mg twice or three times a day and then, if necessary, up to 150 mg twice or three times a day [43]. Caution must be taken at these doses and monitoring for toxicity of CPT must be undertaken.

1.7.2 Absorption

CPT is a Biopharmaceutical Classification System (BCS) class III compound [3] that exhibits permeability rate-limited absorption across the epithelial cells of the GIT resulting in high variability in the rate and extent of absorption. Following oral administration, CPT is rapidly absorbed and peak plasma concentrations are observed within 60 - 90 minutes and antihypertensive effects manifest within 15 - 60 minutes, lasting for approximately 6-12 hours [42, 53]. The average absorption of CPT is approximately 60 -75 % following administration to healthy individuals in the fasting [43]. The presence of food in the GIT reduces the absorption of CPT and it is recommended that CPT be administered at least one hour before meals [43]. The oral bioavailability of CPT is increased in patients when used chronically [21] and it is possible to reduce the dose of CPT in such patients while maintaining adequate control of blood pressure.

1.7.3 Distribution

CPT binds primarily to albumin and other plasma proteins and distribution appears to be best described by a three compartment model in human subjects [57]. The terminal phase volume of 2 L/kg is due to deep tissue distribution and CPT in the free and oxidised-forms rapidly accumulates in tissues to reach a maximum level within 30 minutes [57]. Tissues studies [58] revealed substantial levels of CPT in the kidneys cells and lower concentrations in the liver, lung, heart, blood cells, spleen and plasma. *S*-methyl captopril was also present in all tissues examined with the highest levels occurring in the liver and kidney cells.

1.7.4 Metabolism

The metabolism of CPT is interrelated and can be reviewed in Figure1.7.

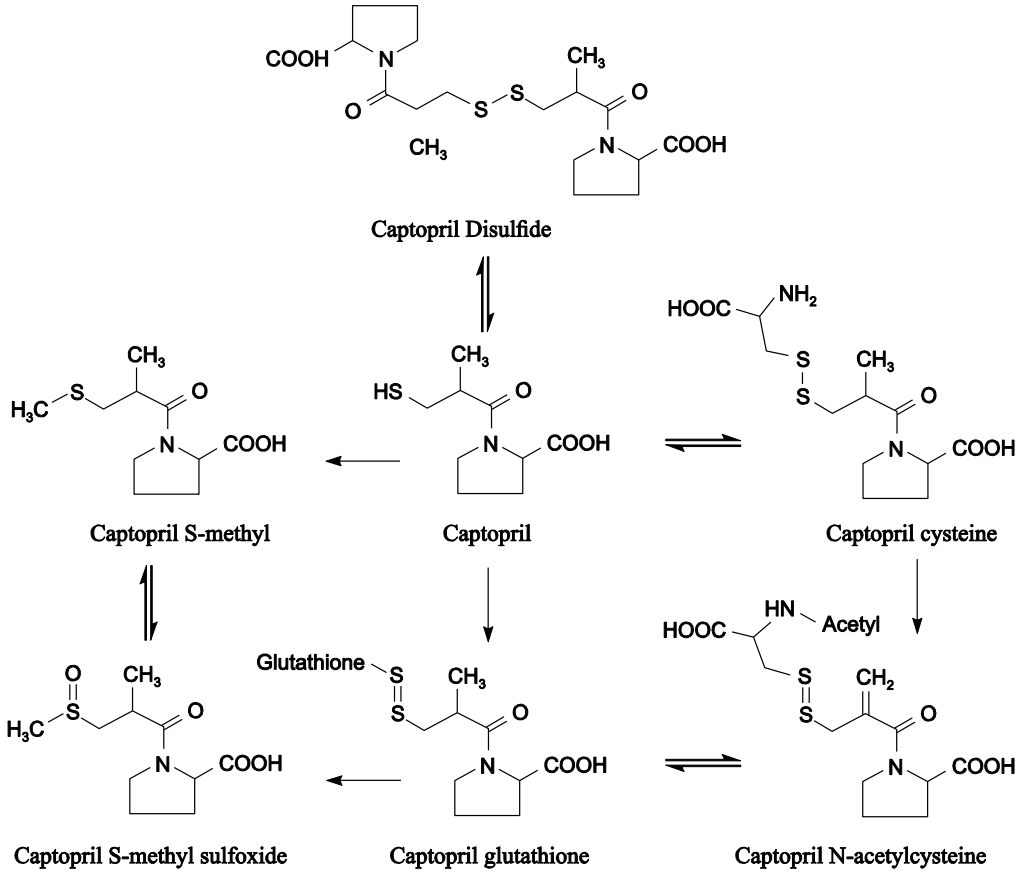

Figure 1.7 *Metabolism of CPT.*

CPT, unlike other ACE inhibitor pro-drugs, does not require biotransformation to produce a therapeutic effect [57]. In a study in rats [58] the oxidised disulfide form of CPT were present in the same or slightly higher proportions than free CPT in the kidney cells. The major metabolites observed were captopril-cysteine, captopril-disulfide and the captopril-disulfide dimer [58] and the metabolites undergo reversible inter-conversion to form CPT, which may contribute to the longer duration of action observed than that anticipated by monitoring unchanged CPT concentration in plasma only. Additional trace metabolites of CPT include captopril S-methyl, captopril S-methyl sulphoxide, captopril glutathione, captopril cysteine and captopril-N-acetylcysteine,which are found at lower levels when compared to the levels of major metabolites [59].

1.7.5 Elimination

CPT and captopril-cysteine are excreted primarily in the urine and approximately 40 % of the administered dose is excreted unchanged in the urine in 24 hours and 35 % as unchanged CPT [58]. The total body clearance of CPT is approximately 0.8 L/kg/hour and the short elimination half-life of CPT is correlated with an increase in creatinine clearance [57], since an increase in GFR results in more creatinine being filtered due to active tubular secretion process in the kidney cells [59]. The elimination half-life of captopril is in the range of 1.6 – 1.9 hour and increases with decreasing renal function [58].

1.8 CONCLUSION

CPT is used for the treatment of hypertension, cardiac failure and diabetic nephropathy and is often prescribed chronically, necessitating appropriate management of therapy. However, the efficacy of CPT doses for paediatric patients has not yet been established and it has been suggested that doses of 0.1 – 1.0 mg/kg/dose [55] be used while titrating against the therapeutic response when administered as an extemporaneous formulation. CPT is an orally active ACE inhibitor that blocks the conversion of AT-I to AT-II and exists as one of four isomers. *S,S*- Captopril is optically active and 100-fold more potent than the other isomers. The sulfhydryl functional group of the *S,S*-captopril binds to zinc on the active site of ACE, resulting in changes in the conformation of the enzyme with significant biological activity. Binding reduces the conversion of AT II and increases plasma renin activity with a subsequent lowering of the diastolic and systolic arterial blood pressure and an antihypertensive effect that lasts for 6 hours.

CPT contains a sulfhydryl functional moiety located at the L-proline side chain. The presence of the sulphur element in CPT gives it a sulphurous odour and facilitates ready conversion to captopril disulfide conjugates, which is a major metabolite eliminated via the kidney, whereas free unbound CPT reflects bioavailability and a decrease in blood pressure. The sulfhydryl moiety is responsible for most of the undesirable adverse effects such as hypersensitivity and taste disturbances, including associated loss of metallic after taste. In addition, macula-papular skin rashes have been observed when CPT powder has been in contact with the skin and membranes, especially in individuals who exhibit a sensitivity to sulphur. Individuals should avoid breathing in CPT powder as it may induce a dry hacking cough due to stimulation of bradykinin synthesis.

CPT is freely soluble in water, isopropanol, chloroform and methanol. The solubility-temperature profile of CPT is linear up to 40 °C and at temperatures ≥ 40 °C CPT exhibits high water solubility. CPT ionises at physiological pH and has a short elimination half-life of between 1.6 and 1.9 hours that requires dosing two or three times daily, which may reduce patient adherence. CPT is weakly acidic, has a pKa of 3.7 and 9.8 and exists as a zwitterion. CPT exhibits excellent stability in the solid state, but undergoes oxygen facilitated first-order degradation in aqueous solution. The instability and BCS classification exhibited by CPT makes it a good candidate for inclusion in a sustained release dosage form manufactured using coated beads.

Patient adherence to medication is important for the successful treatment of hypertension. Most antihypertensive regimens require multiple administrations per day in order to control blood

pressure, often resulting in patient inconvenience. In order to reduce patient inconvenience and the associated challenges in the use of CPT, including taste, stability and odour, the use of drug delivery technologies to produce sustained release dosage forms [60] may improve patient adherence.

The development of sustained release dosage forms that can be administered once or twice daily would be an advantage and may promote patient adherence to therapy. One such an approach is the coating of beads, which provides protection against oxidation and photo-degradation, thereby enhancing the stability and shelf-life of CPT dosage forms. The production of coated CPT beads may overcome the limitations associated with taste and smell by masking the taste and the characteristic sulphur odour. Furthermore, this approach may reduce fluctuations in blood levels of CPT while maintaining therapeutic levels of the API in the systemic circulation. The coated beads dosage can be modified to influence the bioavailability by altering the bead and coating formulation composition, aspects of formulation development that are investigated in this study.

CHAPTER TWO
THE DEVELOPMENT AND VALIDATION OF AN HPLC METHOD FOR THE ANALYSIS OF CAPTOPRIL

2.1 INTRODUCTION

2.1.1 Overview

A quantitative analysis of CPT in different dosage forms have been conducted by means of a number of analytical and detection methods, including normal-phase HPLC [61], anion exchange HPLC with indirect photometric detection [62], gas chromatography (GC) [63, 44], gas chromatography-mass spectrometry (GC-MS) [65, 66], liquid chromatography–mass spectrometry (LC–MS) [67, 68], capillary zone electrophoresis (CZE) [69, 70] spectrophotometry [71, 72] and reversed-phase high performance liquid chromatography (RP-HPLC) [73]. However, the GC methods are limited by the sensitivity and ruggedness of the method for analytical compound identification, whereas thin layer chromatography (TLC) and densito-metric methods [74] have been used for purity determination and quantitative identification of CPT.

Of the analytical techniques employed for the determination of CPT, RP-HPLC is the most extensively used. It is sufficiently sensitive for quantification and characterisation of CPT in biological fluids, specifically blood [73] and urine [65, 75] using fluorometric and ultraviolet-light (UV) detection. RP-HPLC is commonly used for separations and as an analytical technique it is relatively simple, economical and appropriate for quality control analysis in the pharmaceutical industry [76, 77]. *In vitro* release studies coupled with RP-HPLC analysis are used to monitor the amount of API released from the different dosage forms to make sure that these levels are according to the recommendations of Food and Drug Administration (FDA) guidance document(s) on Q2B validation of analytical procedures and methodology [78, 79]. CPT exhibits low UV absorptivity [20] and is an unstable molecule, which makes the assay of CPT dosage forms difficult to perform and accurate quantitation is hindered by the presence of captopril disulphide, a degradation product of the parent molecule [4, 10] that may result in inaccurate quantitation. It is consequently recommended that fresh standards are prepared for analysis on a daily basis or that they are protected by use of antioxidant agents in the sample [80].

RP-HPLC has the potential to eliminate almost all analytical problems [81, 82], including selectivity, sensitivity and dependence on analyst skill and is a powerful and reliable analytical

approach for pharmaceutical analysis. The objective of this study was to develop and validate a linear RP-HPLC method that is simple, selective, sensitive, precise and accurate for the quantitation of CPT using UV detection and that could be applied in formulation development and assessment studies.

2.2 PRINCIPLES OF HPLC

Liquid chromatography (LC) emerged in the early 1960's as an alternative to GC analysis [82] to provide a rapid separation technique with high column efficiency.It has become the primary analytical approach for the analysis of a variety of compounds [81]. LC has been referred to as High Speed Liquid Chromatography (HSLC), High Efficiency Liquid Chromatography (HELC) and High Performance Liquid Chromatography (HPLC) [81] due to its attributes. The attributes include the reusability of the HPLC column without the need for regeneration, reproducible results due to high resolution and a low dependence on operator skill [83]. The major advantage of HPLC for the analysis of compounds has been the ability of the approach to effect a separation with a high degree of selectivity, sensitivity in combination with an ability to effect rapid analysis of dosage forms when compared to other analytical techniques [83, 84].

HPLC is an analytical procedure during which a mixture of compounds can be separated and the quantity of each of the separated components can be ascertained [81] using either normal phase (adsorption) or reversed-phase chromatography. The stationary phase in normal phase chromatography is polar, while the mobile phase is relatively non-polar. This technique is used to separate polar compounds based on the interaction of the compound of interest with the polar stationary phase [24]. For RP-HPLC the stationary phase is non-polar and polar solvents are used to prepare the mobile phase so as to elute analyte(s) of interest [81, 82]. CPT is predominantly retained on the stationary phase of RP-HPLC columns, and the alteration of the mobile phase composition is undertaken until a successful chromatographic separation can be achieved [62, 70]. RP-HPLC was selected as the preferred method of analysis for CPT as it is rugged, provides opportunities for excellent separations, and solvents used for RP-HPLC are generally compatible with UV detectors [84].This compares favourably with other LC methods as summarised in §2.2.4.

The mechanism of retention of a mixture of compounds involve partitioning of the individual compounds based on silano-philic interactions that can either be hydrogen-bonding and/or ionic interactions between the compound and residual ionised silanol groups on the surface(s) of the stationary phase [85-87]. The sample mixture in RP-HPLC is introduced onto the stationary phase

as the mobile phase permeates the column [86, 88] and separation is facilitated by the partition coefficient of the solute(s) between the stationary and mobile phase(s). The average rate at which solutes migrate is dependent on the average time the molecule spends in the mobile phase [89].The rate of solute elution is lower for solutes with a partition ratio factor that favours retention on the stationary phase and is the converse for solutes with a partition ratio factor that favours partitioning into the mobile phase. Ideally the difference(s) in affinity between a stationary and mobile phase results in the components of a mixture separating into different bands located along the length of the column [84]. The analyte moves along and through the stationary phase with the mobile phase due to solvo-phobic or silano-philic mechanisms [85, 86, 88, 90].

Consequently, elution in RP-HPLC is dependent on the physicochemical properties of the analyte, column packing and the composition of the mobile phase [84], especially when an organic modifier or buffer is used. Some physicochemical properties, in particular the pKa and partition coefficient of an analyte, affect the distribution of compounds between the stationary and mobile phases [81, 84, 85]. The organic to aqueous composition ratio of the mobile phase can be modified to effect an appropriate separation of the analyte(s) of interest [89, 91] and reversed-phase column efficiency can be improved by careful consideration of all aspects of the chromatographic separation.

2.2.1 Column selection

The development of a rugged, reproducible analytical method requires that the analyst has an understanding of different column packing materials, selectivity and factors that influence the separation of analyte(s) [92] prior to the selection of a column for use in method development. CPT is a compound that exhibits weakly acidic physicochemical properties [3] and ionises at physiological pH, as described in §1.1.4. CPT has a molecular weight of 217.3 and has a free carboxyl functional group attached to the proline ring [30],which imparts weakly acidic properties to the molecule.It also has an isoelectric point at a pH of 6.8, whereas other ACE inhibitors are amphoteric in nature [93]. The analyst must understand that in order to develop a separation for CPT, the pH of the mobile phase will be a critical factor and the pH selected should also be appropriate to ensure stability for the duration of the analysis.

Column selection of RP-HPLC phases have been characterised by solvo-phobic and silano-philic mechanisms in a hydrophobic-subtraction model [87].The main factors that are purported to

influence a separation in the hydrophobic-subtraction model include hydrophobicity, steric resistance to insertion of bulky solute compounds into a stationary phase, hydrogen-bond acidity contributed by non-ionised silanols, hydrogen-bond basicity from adsorbed water in the stationary phase, and cation-exchange attributed to ionised silanols dependent on the pH of the mobile phase[87].

Luna®-based silica stationary phases are smooth and spherical to provide consistency and even coverage of the bonded phase [76]. The advantage of using Luna® silica columns is that they exhibit sufficient mechanical strength with little likelihood of disruption due to shear forces [76, 94], resulting in column efficiency and long column life. A bonded phase silica Phenomenex® Luna® C_{18} (2) 150 mm x 4.6 mm i.d. (Phenomenex®, Torrance, CA, USA) with a 5 µm particle size stationary phase and 100 Å pore size column was selected for use in the development of an analytical method.

2.2.2 Detection

A highly sensitive method of detection is essential for the development of a rapid, sensitive and reproducible analytical method [84] and it is imperative that an analyst understand the factors that may affect the detection of analyte(s) of interest. The detection is, to a large extent, dependent on the physicochemical properties of the analyte of interest, sensitivity of the detector, amount of API to be analysed and the composition of the formulation(s) assessed [81]. In addition, it is essential to ensure that the analytical method is stability-indicating and is selective for the API(s) of interest [95, 96].

UV/VIS spectrophotometric detection is commonly used for HPLC analysis of CPT that exhibits low UV absorptivity [97] in the range between 0.0001 and 0.15 absorbance units. Solutions of CPT should therefore be diluted and exhibit sink conditions [98] to avoid any deviation from the Beer-Lambert Law. Conventional UV detectors are limited to fixed wavelengths of 210 nm and 355 nm for the analysis of CPT [99], while still exhibiting the necessary sensitivity to detect relevant species at a specific wavelength [100] using mobile phases that are transparent in those wavelength regions [17]. UV/VIS detectors are unable to discriminate between CPT's enantiomers [24, 36]. CPT exhibits low UV absorptivity with a reported λ_{max} of 200 nm and oxidises to form a relatively unstable disulfide molecule [35], making the analysis of dosage forms of CPT difficult. The use of photodiode array detectors (PDA) as rapid scanning spectrometers at these

wavelength(s) [98] results in adequate peak purity that is useful for the identification of an analyte such as CPT.

Modern HPLC systems require rapid scanning spectrometers with lower noise levels at wavelengths below 250 mn while using a large 87 µL flow cell [101] to render them suitable for LC investigations. The demand for more versatile UV detectors for compounds that absorb in the extreme ends of the UV spectrum has been met by the development of PDA detectors [98] with integrated array detectors that improve signal to noise (S/N) ratios by virtue of a multiplex advantage. PDA multi-wavelength detection yields spectra of the analyte(s) of interest that elute in a chromatographic run and allow the spectra to be stored for later analysis [102]. PDA detectors are not limited to detection of analyte(s) at one wavelength, but can monitor complete spectra throughout the chromatogram to aid the identification of analyte(s) and/or other compounds [98], resulting in improved quantitative determination for each sample. PDA detectors provide accurate quantitation of an analyte or solute at an optimum wavelength for each analyte or solute thereby enhancing detection through summation of the outputs of each of the elements in the sample [98, 102].

Prior to HPLC method development, a solution of CPT in MeOH: water (65:35 % v/v), was scanned over the wavelength range of 190 - 300 nm using a dual beam UV-VIS Model GBC 916 spectrophotometer (GBC Scientific Equipment Pty Ltd, Melbourne, Victoria, Australia) as described in §1.2.11. The wavelength of maximum absorption was 200 nm, whichis slightly lower than what has been reported [34]. This can be attributed to the change in solvent composition as MeOH: water (50:50 % v/v) solution was used. PDA detection to monitor complete spectra wavelength in the region of 200 nm was therefore selected for use during HPLC method development and for the *in vitro* analysis of CPT formulations using PDA detection with a low volume of 3 mm^3, 0.005 inches i.d. microbore flow cell,which can reduce S/N levels considerably when compared to results reported by Denton [101], who eliminated mechanical scanning components to facilitate sensitive analysis of low concentrations of CPT.

2.2.3 Mobile phase selection

Mobile phase selection is one of the most important considerations in RP-HPLC to achieve optimum efficiency of an analytical method. The mobile phase in RP-HPLC must be relatively polar to provide reasonable competition for adsorption sites for the analyte(s) of interest [86, 100]

and chromatographic separation depends on the differences in interaction of solutes with the mobile and stationary phases. The selection of and variation of mobile phase components is critical as it can be manipulated to produce changes in the characteristics of the chemical environment that the solute would be exposed to [77]. When a mobile phase is in contact with a stationary phase, the rate at which solutes elute is determined by the overall polarity of the mobile phase, nature of the stationary phase and sample [103], as these parameters affect the time that analyte/sample components permeate through the column to effect a separation.

The theoretical aspects of mobile phase composition on a separation must be carefully considered, as this information can facilitate the development of a separation through knowledge of suppression of ionisation of the analyte(s) of interest [85]. In this regard the optimum pH of the mobile phase must be established as it affects the extent of ionisation and surface characteristics of the silanol functional groups of the surface of the stationary phase [90]. It can alter the retention characteristics of the analyte due to the different types of interaction that can occur between the analyte and the stationary phase. The mobile phase used must be at a constant pH throughout the analysis of ionisable compounds, such as CPT, to ensure that a reproducible and robust analytical method is developed and applied for research, development and quality control purposes. The preferred pH range for a mobile phase is between 2 and 7.5 to allow transmittance of light at or below 220 nm, and to avoid pH extremes when analysing ionisable compounds that exhibit tailing, broad-shaped and asymmetrical peaks during analysis [85]. The initial selection of mobile phase composition for the analysis of CPT was based on methods reported in the literature where pH was adjusted to a suitable level to facilitate UV detection [104].

The HPLC analysis of CPT was performed at an acidic pH [73-75, 92, 51] to ensure that an optimal interaction between CPT and the stationary phase occurred to ensure an appropriate separation. The pH of the mobile phase was adjusted to the required pH to facilitate optimisation of the analytical method. The pH of the mobile phase may affect the retention time and peak shape in RP-HPLC [82], particularly when attempting to separate weakly acidic, basic or amphoteric compounds with ionisable functional groups [85, 92, 112]. If the pH of a mobile phase changes, the polarity of an analyte may change and hence there may be an impact on the retention time of a separation [77].

2.2.4 Challenges of RP-HPLC Analysis

A review of the literature relating to the chromatographic analysis of CPT in pure form and in formulations was conducted prior to development and validation of an HPLC method for CPT in our laboratory. A summary of chromatographic conditions for the analysis of CPT is listed in Table 2.1. The most frequently reported methods for the analysis of CPT were developed for assessing solid oral dosage forms [96, 100, 104, 105], plasma [73] and urine [65, 75].

The analysis of CPT has been achieved using a silica-based stationary phase of 150 mm and 250 mm in length, the most preferred brand was a Phenomenex® C_{18}, 150 mm x 4.6 mm [80, 96, 100]. HPLC with photodiode array (PDA) detection was the preferred method of detection of CPT [73, 75, 96, 100, 104, 105]. The flow rate for the analyses was primarily 1.0 mL/min and the wavelength of detection commonly applied was between 220 - 240 nm [73, 96, 100, 104, 105]. Since CPT is weakly acidic and dissociates in solution, the use of buffers and/or pH modification were considered necessary [72, 93] to effect an adequate separation. Suitable changes can be made to the organic content of the mobile phase to ensure that a desirable peak shape and appropriate retention time and resolution are achieved**.**

Table 2.1 *Summary of published analytical methods for the quantitation of CPT.*

Compound	Sample	Stationary Phase	Mobile Phase	Detection	Internal Standard	Reference
CPT	Plasma	Purospher Star, C_{18} (5µm, 250 x 4.6 mm)	Acetonitrile: water (60:40 v/v) as a mobile phase, adjusting pH to 2.9 using phosphoric acid	UV-230nm	Simvastatin	[73]
CPT	Urine	Zorbax SB C_{18} (5µm, 150 x 4.6 mm)	Acetonitrile: TCA buffer at pH 1.6	UV-335nm	*	[75]
CPT	Pure form	Phenomenex® Luna 5µm (C_{18}) (250 mm x 4.6mm)	Acetonitrile in a ratio of 70:30 % v/v; Phosphate buffer (adjust to pH 3.0)	ECD	Cyclizine	[80]
CPT and Pd(II)	Pure form and tablets	Luna 5µm phenyl-hexyl (250 mm x 4.6mm)	0.025 % w/v of Pd(II) chloride: ACN: MeOH-water containing 10mM Britton-Robinson buffer of pH 4.0 and0.25MKCl solution [1 : 4 : 5 v/v/v]	UV-380nm	Hydrochlorothiazide	[105]
CPT	Tablets	Phenomenex® Luna C_{18} (250 mm x 4.6 mm)	Water: methanol (45:55) v/v maintained at pH 2.5	UV-220nm	Captopril Disulphide	[96]
HCTZ and CPT	Tablets	Beckman Ultrasphere ODS C_{18} 4.6 mm x 150 mm, 5µm	Methanol: water (45:55 % v/v) adjust to 3.8 with 85% ortophosphoric acid	UV-210nm	Phenobarbital	[104]
CPT	Tablets	Partisil SAX, C_{18} 10µm Strong anion Whatman (250 mm x 4.6 mm)	525 mg citric acid. H_2O + 37.7 mg NH_4CIT to 1 L with CH_3OH adjusted to pH 3.30 with 0.1 N HCl	UV 220nm	*	[100]

*Internal standard not mentioned

2.3 STATISTICAL ANALYSIS AS EXPERIMENTAL DESIGN

HPLC method development requires an assessment of the variables or factors at different levels that can be manipulated to enhance the separation of an API and internal standard (IS) in relation to input variable differences. Optimum separation is achieved when variables or factors levels can be located within maximum and minimum levels, depending on the experimental design approach used. This is more efficient than the use of the traditional approach of changing one variable at a time [62, 104] during development, and/or Response Surface Methodology (RSM) as a systematic statistical analysis to evaluate multiple experimental parameters at the same time [106-108].

RSM is a collection of statistical and mathematical approaches that permit elucidation of the factors that have an impact on a response, say Y and the influence on changes in the levels of other control or input factors in an experimental domain [106]. RSM facilitates an understanding of the relationship(s) between one or more measured responses, say Y_1, Y_2 and Y_3 to input factors, or X_1, X_2 and X_3 as its primary purpose [54], using a sequential strategy that results in either first or second order polynomial mathematical relationships. The responses over the domain under investigation are analysed and approximated in accordance with an increase in the complexity of models [109]. Higher polynomial models are pursued only after simple linear polynomial models produce inadequate descriptions of data derived from experimental investigations. RSM was used to establish and study critical factors that can be used to optimise an HPLC method with respect to retention time, asymmetry and other relevant factors relating to the separation being developed.

RSM can be used to identify the challenges of a current method and aims to construct experimental model/s or relationships following the generation of appropriate experimental data for the measured responses that relate to the input factors under investigation [107]. The models generated provide an approximation of the true relationship between the input factors and responses following experiments performed in the region of parameter levels known to effect an adequate separation [106, 108]. RSM and Design of Experiments were used to fit data to response models and to follow which it is further optimised.

The factors to be optimised for the analysis of CPT using HPLC included the MeOH composition, pH of the mobile phase and column temperature. The previously reported chromatographic methods of analysis for CPT were performed in an acidic media [73-75, 80, 92, 104] and it is recommended that such a pH is maintained during separation to suppress silanophilic interactions between CPT and the stationary phase. If the pH changes, molecules may ionise in a mixture [92] and the overall polarity may affect the CPT and Salicylic acid (SCY) solute particle elution through the column, resulting in different retention times and peak shape. The purpose of considering these factors, *viz.* percent MeOH composition, mobile phase pH and column temperature, was to establish an approximate relationship between retention time and asymmetry factor (A_s) so that one can predict response through hypothetical testing of significant input factors or variables.

Central composite designs (CCD) are the most prevalent RSM design used to approximate polynomial models [106, 107] and a CCD methodology with k control variables consists of a 2^k factorial design with six (6) center-points. The CCD approach uses fixed axial points that permit the model to be rotatable with respect to the center point coded 0 to generate quadratic terms that are coded as -1 (minimum) and +1 (maximum) [109-111].

Additional experimental points, say alpha (α) represent new extreme values (low and high) for each factor in the design to represent five levels, *viz.* +α, +1, 0, -1, -α for each factor. The design contains $2^k + 2k + C_o$ experimental runs where 2k is the number of axial points and C_o is the number of repetitions at the center-point of a system with k variables [108, 110]. Three factors were investigated in this study, and therefore $2^3 + (2x3) +6$ or 20 runs were generated.

The value of α depends on the type of CCD and the range of interest for each factor investigated are either rotatable or orthogonal within the design matrix. The axial and α values ensure that the variance of model prediction is constant at all points equidistant from the centre of the design. Repetition of the six centre-points is essential to provide an estimate of the experimental error encountered in the CCD model [55]. A face-centered CCD has only three levels as α values are set to be on the periphery of the design matrix. The use of CCD is advantageous in that there are fewer experimental runs than three level factorial designs [106], hence these can be used as an alternate to three level factorial designs such as Box-Behnken. The presence of –α and +α experimental points provide regions of good predictability at extreme combination(s) of levels of factors not recognised in other model designs [106].

When response data is generated from CCD and RSM experiments, regression analysis is performed to determine coefficients for the response models (β_i, β_j, β_k ……..β_n) and the significance of the coefficient. The second order polynomial regression equation is fitted to the response model shown in Equation 2.1.

$$Y = \beta_0 + \sum_{i=1}^{k} \beta_i X_i + \sum_{i=1}^{k} \sum_{j=i+1}^{k} \beta_{ij} X_{ij} + \sum_{i=1}^{k} \beta_{ii} X_i^2 \qquad \textbf{Equation 2.1}$$

Where,

Y = the predicted response,
k = the number of factors,
X_i=pH of the mobile phase,
X_j =methanol solvent composition in the mobile phase expressed as % v/v
X_k =column temperature
X_{ij}, X_{jk} and X_{ik} are two factor interactions,
β_0 = the y-intercept,
β_i, β_j and β_k are the coefficients for linear effects,
β_{ii}, β_{jj} and β_{kk} are the coefficients for quadratic and/or interaction effects.

RSM using the CCD approach was successfully used to optimise the separation of CPT and SCY to produce an adequate separation. The CCD experimental design was used as an efficient and cost-effective strategy to provide information, including the interactive effects of the factors investigated to ensure that an optimised system was developed more efficiently than if a one-factor-at-a-time (OFAT) approach was used [106]. The CCD approach involves experiments being performed in the region of best-known solutions, generating experimental data, fitting experimental data to a response and optimising the best chromatographic response [106-108]. The three factors investigated were pH (X_1), methanol solvent composition (X_2) and column temperature (X_3). These factors were selected to produce the best analytical signal since they influence the shape and retention of CPT in experimental samples. The response factors included retention time of CPT (Y_1), retention time of IS (Y_2) and A_s of CPT (Y_3).

2.4 EXPERIMENTAL

2.4.1 Reagents and materials

CPT was donated by Protea Chemicals (Midrand, South Africa) and the internal standard (IS) Salicylic Acid (SCY) was purchased from Associated Chemical Enterprises Ltd (Southdale, South Africa) (Batch number 24606/0017). Standard samples of uracil, acetophenone, benzene, toluene and naphthalene (analytical grades) were used to test column efficiency. Cyclizine, carbamazepine, sulphacetamide, nicotinamide, furosemide, chlordiazepine, acetylsalicylic acid, ketoprofen, loratidine and SCY samples were evaluated as potential IS. HPLC-grade methanol (MeOH) and acetonitrile (ACN) were purchased from Romil Ltd (Waterbeach, Cambridge, United Kingdom). HPLC-grade water was prepared using a Milli-RO® 15 water purification system (Millipore Co., Bedford, MA, USA) that consisted of a Super-C® carbon cartridge, two Ion-X® ion-exchange cartridges and an Organex- Q® cartridge. The water was filtered through a 0.22 μm Millipak® 40 stack filter (Millipore Co., Bedford, MA, USA) prior to use. Sodium hydroxide pellets (analytical grade) and ortho-phosphoric acid (85 % w/w) were purchased from Merck Pvt Ltd (Wadeville, South Africa). All chemicals and reagents used were at least analytical grade and were used without further manipulation. Commercially available CPT tablets were purchased from a local pharmacy and included Merck Captopril 50, Adco-Captomax 50, Sandoz Captopril 50, CaptoHexal® 50, and Zapto–50.

2.4.2 Preparation of mobile phase

A mobile phase, consisting of MeOH: water in a ratio of 47:53 % v/v adjusted to pH 3 using 85 % v/v ortho-phosphoric acid, was prepared as described. Appropriate volumes of MeOH and water were separately measured using 1000 mL and 500 mL A-grade measuring cylinders. The solvents were mixed in a 1000 mL Schott® Duran bottle (Schott® Duran GmbH, Wertheim, Germany). The pH of methanol water was adjusted to a pH of 3, using 85 % v/v ortho-phosphoric acid, and monitored with a Crison® pH meter GLP 21 (Crison® Instruments, Johannesburg, South Africa) at 22.5 ˚C. The adjustment of pH following MeOH addition ensured a constant pH during analysis. The mobile phase was prepared on a daily basis and was filtered through a 0.45 μm Millipore® membrane HVLP filter (Millipore®, Bedford, MA, USA) and degassed under a vacuum using an Eyela® Aspirator A-2S vacuum pump (Rikakikai® Co. Ltd, Tokyo, Japan) prior to use.

2.4.3 Preparation of stock solutions

Approximately 10 mg of CPT and SCY respectively were accurately weighed into 100 mL A-grade volumetric flasks, using a Mettler® Model AE 163 analytical balance (Mettler® Inc., Zurich, Switzerland). The mobile phase, prepared as described in §2.4.2, was added to the flasks and made up to volume to make standard stock solutions of 100 µg/mL concentration. The solutions were sonicated using a Branson® B12 sonicator (Branson® Inc., Shelton, Conn, USA) for two minutes to ensure complete dissolution of the powders. The standard stock solutions were diluted in a serial manner with mobile phase to produce CPT solutions of concentrations of 2, 5, 7.5,10, 20, 30, 40, 50 and 60 µg/mL. A 2.5 mL aliquot of the SCY stock solution was pipetted into a 25 mL A-grade volumetric flask and made to volume with the mobile phase to produce a solution with a final concentration of 10 µg/mL. The IS and stock solutions were covered with aluminum foil to protect the solutions from light. The solutions were prepared on a daily basis and covered with aluminum foil and consequently used on that day.

2.4.4 HPLC system

The HPLC system was used for the development, optimisation and validation of the analytical method and the characterisation of CPT content and release profiles during product development and assessment studies. The RP-HPLC system consisted of a Waters® Alliance 2695 Separations module (Waters®, Milford, MA, USA) equipped with a Waters® Alliance 2695 solvent delivery module (Waters®, Milford, MA, USA), Waters® Alliance 2695 online degasser (Waters®, Milford, MA, USA) and a Waters® 2996 photodiode array ultraviolet detector (Waters®, Milford, MA, USA). Data was compiled using Empower Pro data acquisition software (Waters®, Milford, MA, USA).

2.4.5 Column evaluation and specifications

Prior to HPLC method development, chromatographic performance tests were performed to ensure the column quality of Phenomenex® Luna C_{18} (2) column. Column quality or performance was based on calculating the theoretical plate number (N), asymmetry factor (A_s), reproducing retention time and peak of standard solutions.

2.4.5.1 Column efficiency

Column efficiency was assessed by calculating the number of theoretical plates (N) for the column using Equations 2.2 and/or 2.3. The Food and Drug Administration (FDA) [79] recommends the use of columns with at least 2 000 theoretical plates for pharmaceutical applications.

$$N = 16\left(\frac{t_R}{W}\right)^2 \qquad \textbf{Equation 2.2}$$

$$N = 5.54\left(\frac{t_R}{W_{\frac{1}{2}}}\right)^2 \qquad \textbf{Equation 2.3}$$

Where,

N = Number of theoretical plates in a chromatographic column,
t_R = Retention time of the peak,
W = Peak width at baseline determined by the tangent, and
$W_{\frac{1}{2}}$ = Peak width at half of peak height.

As the value for N increases, the resolution for all bands increases and an appropriate separation is achieved. The value for N can be increased with the use of densely packed or long columns, low flow rates, small diameter column-packing particles, low molecular weight sample molecules and mobile phases of low viscosity [97].

A test solution of 10 mg/5mL uracil, 97 µg/100mL acetophenone, 50.70 µg/10mL benzene, 58.14 µg/10mL toluene and 10 mg/10mL naphthalene were used to test column efficiency and separation was achieved using a Phenomenex® Luna C_{18} (2) column and a mobile phase of MeOH: water in a ratio of 50:50 % v/v to reproduce the reported Phenomenex® HPLC column in literature [94]. The column had an N of approximately 9 500, which is > 2 000, and the column was therefore considered appropriate for use for method development and validation.

2.4.5.2 *A_s factor*

The Peak Tailing Factor (*PTF*) or A_s is an important factor for the assessment of band shape of resolved peaks and can be calculated using Equations 2.4 or 2.5. The values for A_s were close to 1.0 and correspond to symmetrical peaks that fall into the FDA [79] recommended range of 0.95 to 1.1.Columns producing A_s values of > 1.2 should not be used [81]. The A_s is calculated using Equation 2.4.

$$A_s = \frac{B}{A} \qquad \textbf{Equation 2.4}$$

Where,

A_s = Peak asymmetry factor,
B = Distance between the middle point and the right side of the peak, and
A = Distance between the middle point and the left side of the peak.

The peak tailing factor *PTF* can be calculated using Equation 2.5.

$$PTF = \left(\frac{A+B}{2A}\right) \qquad \textbf{Equation 2.5}$$

Where,

PTF = Peak tailing factor,
B = Distance between the middle point and the right side of the peak, and
A = Distance between the middle point and the left side of the peak.

The A_s is usually established at 10 % of the full peak height, whereas the *PTF* is calculated at 5 % of the full peak height as depicted in Figure 2.1 [112]. The mean value for A_s calculated for the CPT peak was 0.95, with a % RSD of 1.58 %.The use of Luna C_{18} (2) column was deemed satisfactory. The *PTF* established for the CPT peak was 0.80, with a % RSD of 2.05 %. If the *PTF* is ≤ 2.0 the is considered appropriate for HPLC analysis [79, 97].

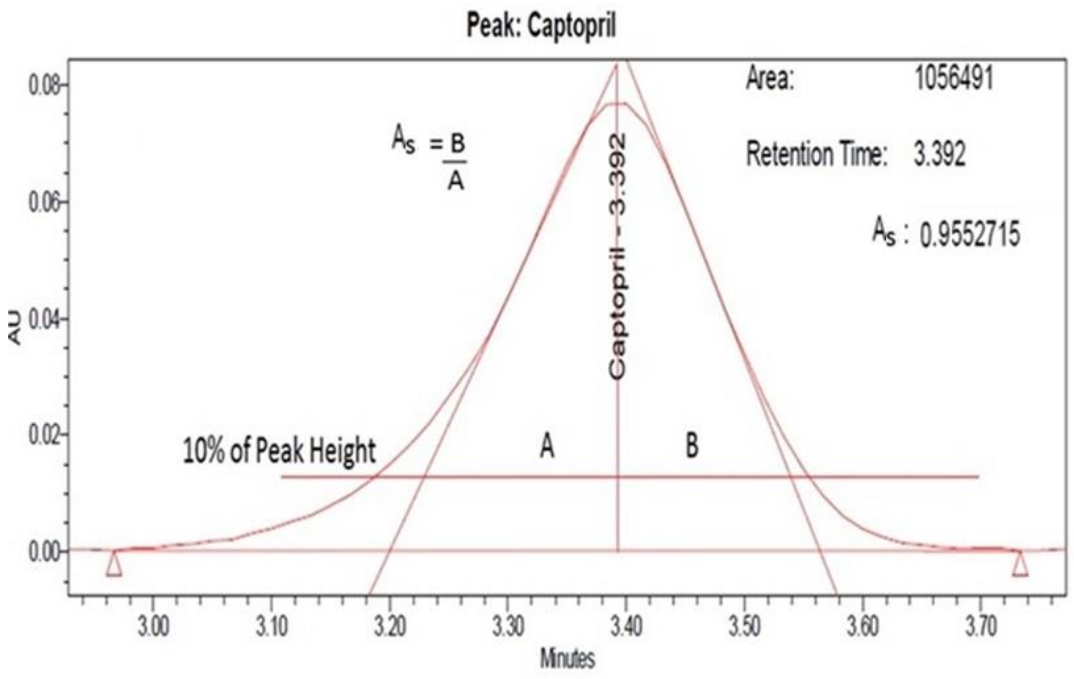

Figure 2.1 *Calculation of peak asymmetry and peak tailing factor.*

2.4.5.3 Resolution factor (R_s)

The R_s is a useful indicator of the degree and quality of a separation between components of a mixture, and it is usually a measure of the extent of separation between two or more peaks of interest [79] and can be calculated using Equation 2.6.

$$R_s = \frac{(R_{t2} - R_{t1})}{\frac{1}{2}(t_{w1} - t_{w2})} \qquad \textbf{Equation 2.6}$$

Where,

R_s = Resolution factor,
R_{t1} = Retention time for first eluting peak,
R_{t2} = Retention time for second eluting peak,
t_{w1} = Width of first eluting peak at the base, and
t_{w2} = Width of second eluting peak at the base.

A value for $R_s > 2.0$ indicates that an appropriate separation has been achieved between peaks, and values ≤ 1.5 suggest that there is poor resolution between peaks and is not acceptable [84]. The values for R_s generated for CPT and SCY were found to be 4.25, with a % RSD of 0.93 %, thereby indicating that appropriate resolution between the two peaks had been achieved.

2.4.6 Choice of internal standard (IS)

The use of an IS in RP-HPLC analyses to improve the performance of the analytical method is often considered [77]. The precision of an RP-HPLC method is dependent on a number of factors, including the accuracy of sample preparation, precision of instruments and the robustness of the method [81, 82]. The IS must be chemically similar to the analyte of interest with almost similar solubility, should be well-resolved from the API and any other peaks that may appear on a chromatogram, should not be present in the original sample, should be similar and mimic analyte behaviour in sample preparation, and should be stable and unreactive with the compound(s) of interest [76, 79, 97, 112].

The response of a detector is monitored by calculating the peak area of a signal generated in response to an analyte and the detector may detect variations to sample concentrations not prepared identically as the technique of the analyst [79, 112]. The use of IS in RP-HPLC compensates for minor variations in the parameters of a separation that affect peak area. These include loss or increase in sample size, fluctuations of injection volume fluctuations, changes in flow rate or sample concentration [79] that may occur during sample manipulation and can hamper the generation of accurate and reproducible data.

The use of an IS improves the accuracy, precision (inter-assay and intra-day) and robustness of quantitation for chromatographic analysis [84] and the same amount of the IS is added to all calibration standards and samples. A number of compounds were evaluated as potential IS and and included cyclizine, carbamazepine, sulphacetamide, nicotinamide, furosemide, chlordiazepine, acetylsalicylic acid, ketoprofen, loratidine and salicylic acid. The chromatographic behaviour of these compounds was assessed using a mobile phase of MeOH: water in a ratio of 47:53 % v/v adjusted to pH 3 using 85 % v/v ortho-phosphoric acid at a flow rate of 1.0 mL/min.The results are summarised in Table 2.2.

Table 2.2 *Selection of IS for CPT using a mobile phase of 47:53 % v/v MeOH: water (pH 3).*

IS	RT (mins)	Peak Shape	Comments
Cyclizine hydrochloride	5.2	Resolved, sharp, shouldering and tailing	Close to API
Carbamazepine	5.4	Asymmetrical	Tailing
Sulphacetamide	5.2	Broad base peak shape	Not resolved
Nicotinamide	5.2 and 8.4	Multiple peaks	Detects IS degradants
Furosemide	4.4	Broad base peak, symmetrical	Close to API
Chlordiazepine	5.1, 5.8 and 8.4	Multiple peaks	Not resolved
Acetylsalicylic acid	7.5	Sharp peak, well-resolved	Degrades in water and mobile phase
Ketoprofen	4.8	Tailing	Close to API
Loratidine	15	Broad base peak shape	Longer retention times
Salicylic acid	8.8	Well-resolved, sharp and symmetrical	Selected for use as IS

SCY was adequately separated from captopril and was selected for use as the IS based on the resolution, retention time and peak shape parameters calculated. The response of the IS was maintained at approximately half the maximum expected concentration of the analyte of interest and the concentration of SCY used was 10 µg/mL,which was added to each sample prior to chromatographic analysis.

2.4.7 Experimental design for HPLC optimisation

The three factors and levels to be evaluated and optimised are summarised in Table 2.3.

Table 2.3 *Experimental factors and levels of input and output variables in CCD.*

Input Factor/Variable	**Level**				
	-1.68	**-1**	**0**	**1**	**+1.68**
X_1= pH	2.5	2.8	3.2	3.6	3.9
X_2= % MeOH composition	33.2	40	50	60	66.8
X_3= Column Temp (ºC)	16.6	20	25	30	33.4
Output Factor/Response	**Output Range**				
Y_1= CPT retention time (mins)	$3 \leq Y_1 \leq 10$				
Y_2= SCY retention time (mins)	$3 \leq Y_2 \leq 7.0$				
Y_3= A_s of CPT	$0.95 \leq Y_3 \leq 1.05$				

The chromatographic factors selected for analysis were based on information from the literature and studies performed to establish the influence of each factor on the peak shape, resolution and retention of CPT. The pH (X_1) investigated was maintained in range 2.8 to 3.6. The minimum and maximum values of the MeOH composition in the mobile phase (X_2) were 40 and 60 % v/v, respectively. The column temperature (X_3) for each experimental run was between 20 to 30 ºC.

Twenty randomised experiments were conducted to minimise bias using the factor levels listed in Table 2.3. The factors were established for the quantitative determination of CPT and are summarised *vide infra* (§2.4.7). The CCD experimental design had 20 runs with 6 centre points and 14 non-centre points. These are summarised in Table 2.4.

The response variables for all model factors were analysed using Design-Expert® version 8.0.4 software (Stat-Ease Inc., Minneapolis, USA). Thecorrelation coefficients (R^2) for the fitting of data to equations providing information on the impact of each factor individually were used to establish best fit data. A number of tools may be used to assess the significance of each factor such as the p-value, normal plot of residuals, contour plots and 3D response surface plots.

Table 2.4 *CCD experiments showing the 20 coded and actual values and factors evaluated.*

			Coded values			Actual values		
			Factor 1	**Factor 2**	**Factor 3**	**Factor 1**	**Factor 2**	**Factor 3**
ID	**Run**	**Type**	**pH**	**% Organic Solvent Composition**	**Column Temperature (°C)**	**pH**	**% Organic Solvent Composition**	**Column Temperature (°C)**
0	**1**	Center	0	0	0	3.2	50	25
3	**2**	Fact	-1	1	-1	2.8	60	20
7	**3**	Fact	-1	1	1	2.8	60	30
2	**4**	Fact	1	-1	-1	3.6	40	20
1	**5**	Fact	-1	-1	-1	2.8	40	20
8	**6**	Fact	1	1	1	3.6	60	30
13	**7**	Axial	0	0	-1.68	3.2	50	16.6
14	**8**	Axial	0	0	1.68	3.2	50	33.4
6	**9**	Fact	1	-1	1	3.6	40	30
12	**10**	Axial	0	1.68	0	3.2	66.8	25
0	**11**	Center	0	0	0	3.2	50	25
4	**12**	Fact	1	1	-1	3.6	60	20
5	**13**	Fact	-1	-1	1	2.8	40	30
0	**14**	Center	0	0	0	3.2	50	25
9	**15**	Axial	-1.68	0	0	2.5	50	25
10	**16**	Axial	1.68	0	0	3.9	50	25
0	**17**	Center	0	0	0	3.2	50	25
0	**18**	Center	0	0	0	3.2	50	25
11	**19**	Axial	0	-1.68	0	3.2	33.2	25
0	**20**	Center	0	0	0	3.2	50	25

2.4.8 Method validation

The validation of an analytical HPLC method is a process that establishes the performance characteristics of an analytical method and ensures that the method is appropriate for its intended purpose and analytical application according to USP compendial methods [113]. The results generated during method validation procedures are analysed by means of statistical testing, including linear regression analysis and the use of percent relative standard (% RSD) [114, 115] to demonstrate the validity of the method within acceptable limits.

The significance of validating the HPLC method is to ensure that reliable, accurate and reproducible results are generated when using the method, even when the analysis is performed by different analysts [114]. The International Conference on Harmonisation (ICH) of Technical Requirements for Registration of Pharmaceutical Products for Human Use recognises linearity, range, accuracy, precision, repeatability, intermediate precision, specificity, limits of quantitation and detection as validation parameters [103]. Statistical testing and associated limits for the validation procedure are provided in the ICH Q2B document [114]. As such, statistical testing permits thorough investigation of the method to establish the limits of different parameters to ensure that the desired outcomes are achieved during analysis. The results of validation studies play an important role in the evaluation and interpretation of stability, *in vitro* dissolution and pharmacokinetic data on application of the method.

Validation studies are performed to ensure that an analytical method maintains appropriate performance characteristics, specificity and demonstrates that the method is fit for purpose to identify the strength, quality, purity and potency of an analyte of interest in a variety of matrices [113]. The degree of validation of an analytical method depends on the purpose of and nature of the change(s) to an analytical method.

The selection of parameters to investigate during validation is based on the rational consideration of specific validation attributes, in this case of CPT and SCY, such as peak shape, retention time and other aspects of the separation that are susceptible to changes to the method parameter/s in relation to the procedures described in the ICH guidelines. A validation procedure must at the very minimum investigate linearity, precision and accuracy. Validation of the proposed HPLC method

was necessary since changes had been made to the method as outlined in §2.4.7 *viz.* pH, column temperature and % content of the organic component of the mobile phase

2.4.8.1 Linearity and range

The ICH [113-115] describes the linearity of an analytical HPLC metebhod as the ability, within a given range, of the method to produce results that are directly proportional to the concentration of API in a series of calibration samples. The linearity of response to concentration must be in accordance with the Beer-Lambert Law [116], that states that the absorbance of solutes in dilute solution is directly proportional to the concentration of solute in that solution.

Linearity is demonstrated over a concentration range with a minimum of five concentrations from different samples produced by serial dilution of a stock solution [116, 117] to provide assurance that accurate results are obtained whenever experiments are performed.An acceptable linearity result is based on an investigation of the correlation coefficient (R^2) data for the calibration curve with R^2 value > 0.99 considered as evidence of an acceptable fit [115].

2.4.8.2 Precision

Precision is the degree of agreement between individual test results when the HPLC method is applied to the analysis of multiple samples from an homogeneous matrix [116]. It is an indication of the degree of random error within an analytical method.The ICH guidelines define precision at three levels, *viz.* repeatability, intermediate precision and reproducibility [114, 115] and recommends that each set of precision data be expressed as standard deviation (SD), % RSD or through a coefficient of variance with an associated confidence interval [113-115, 118].

The SD can be calculated using Equation 2.7.

$$SD = \frac{\sqrt{\sum_{i=1}^{n}(x_i - x)^2}}{n-1} \qquad \textbf{Equation 2.7}$$

Where,

x_i= individual measurements, and
n = number of measurements.

The % RSD can be calculated using Equation 2.8.

$$\% \, RSD = \frac{SD \, x \, 100}{Mean} \qquad \textbf{Equation 2.8}$$

The % RSD may have a limit of 5 % and any value < 5 % would indicate full compliance with the validation criteria for precision under these conditions with reference to USP [113].

2.4.8.2.1 Intra-assay precision (Repeatability)

Repeatability refers to the precision of an HPLC method used under the same operating conditions by an analyst and measured over a short period of time [118]. For an assay method, the limit for % RSD may be < 2 % [113-115, 118]. Repeatability of the proposed HPLC method was determined by interpolation from the calibration curve at three levels covering the specified range *viz.*a low (2 µg/mL), medium (30 µg/mL) and high (50 µg/mL) concentration of the calibration range, with each level analysed in replicates (n=5).

2.4.8.2.2 Intermediate (inter-day) precision

The intermediate precision of an HPLC method is used to evaluate the reliability of the method in an environment different to that used during method development to ensure that the method would produce similar results [117, 118]. The environment or condition difference may require analysis on different days or weeks, use of the method by a different analyst, or use of different instruments [91, 117]. Intermediate precision was established at three (3) concentrations, analysed in triplicate (n=3) to determine mean peak area ratio (MPAR) and the % RSD on three consecutive days.

2.4.8.2.3 Reproducibility

The reproducibility of a method relates to the precision of a method when used in more than one laboratory, *i.e.* it can establish precision between laboratories [103, 116, 117].This is essential when standardising a proposed method for joint research studies or official compendial publications. Reproducibility may be determined by analysing homogeneous lots of samples in different laboratories by different analysts [118]. For the purpose of this research, reproducibility studies were not performed as the proposed HPLC method was only intended for application in the same laboratory, by the same analyst using the same analytical instrumentation.

2.4.8.3 Accuracy

The ICH guidelines define the accuracy of an analytical method as the closeness of an experimental measured value to the true value of a sample [103] and can be established by comparing the amount of an analyte in a sample to that of a standard reference and/or through quantification of the recovery of the analyte of interest. The percent recovery is used to determine the accuracy of the proposed method and is expressed as the amount of analyte of interest reported as a percentage of the theoretical amount in the matrix and for which complete recovery of the analyte is desirable [118]. The percent Bias (% Bias) can also be used to determine the extent of deviation of a result for a sample from the true value for that sample.The closer the percentage recovery from the analysed samples is to 100 %, the lower the % Bias is and the more accurate the analytical method [103, 117, 118]. In general a % Bias < 5 % is acceptable.

2.4.8.4 Specificity

Specificity is defined as the ability of an analytical method to accurately measure and quantify the amount of an analyte in the presence of extraneous components, including impurities [64]. The determination of the specificity of an analytical method is considered one of the most important steps in the development and validation of an HPLC method [103, 116]. If the method lacks the capacity to produce sample responses that are clearly resolved from interference(s), the accuracy of the method is likely to be compromised, as is the accuracy of the overall results.

2.4.8.5 Limits of quantitation (LOQ) and detection (LOD)

The LOQ of an analytical procedure is defined by the ICH as the lowest amount of analyte in a sample that can be quantitatively determined with adequate precision and accuracy [117]. The LOD is defined as the lowest amount of analyte in a sample that can be detected, but not necessarily quantitated as an exact value under defined experimental conditions [117, 118]. With age and continual use the precision of an analyte of PDA UV detectors may vary at low concentrations due a gradual loss of sensitivity of the lamp of the detector. The LOQ and LOD of detectors made by the same manufacturer may also vary due to the noise levels of the detectors [119].

Four different approaches can be used to establish the LOQ and LOD of a proposed method, including visual evaluation of analytical data, determination of the lowest concentration for which

the % RSD ≤ 5 %, plotting standard deviation versus concentration, or the use of a signal-to-noise ratio approach [116].

The use of the signal-to-noise ratio approach can only be applied to analytical procedures that exhibit substantial baseline noise [118].This is determined by comparing signals measured from samples of known low concentration of analyte to that of blank samples. The minimum concentration required to produce a signal-to-noise ratio of 10:1 for the LOQ and between 3:1 to 2:1 for the LOD is established [119].However, the approach is not considered practical, since the noise level on a detector may be variable when the samples are analysed using different detectors.

Determining the LOQ and LOD based on the standard deviation of the response and slope of the regression line entails using the relationship described mathematically in Equations 2.9 and 2.10 respectively.

$$LOQ = \frac{10\sigma}{S} \qquad \textbf{Equation 2.9}$$

$$LOD = \frac{3.3\sigma}{S} \qquad \textbf{Equation 2.10}$$

Where,

σ = standard deviation of the response, and
S = slope of the calibration curve.

2.4.9 Stability studies

Stock solutions containing 10 mg CPT in 100 mL MeOH: water (49:51 % v/v) adjusted to pH 3.27 using 85% v/v ortho-phosphoric acid were prepared as previously described (§ 2.4.3). Solutions containing 100 µg/mL CPT were exposed to different stress conditions and analysed using HPLC with PDA-UV detection to initially yield solutions of approximately 1 mg/mL. Characteristic chromatograms from freshly prepared CPT samples were compared to chromatograms developed following degradation. The ICH guidelines recommend that the analysis of degradation products be investigated in respect of quality of API being investigated and its quantity [10, 41,67, 78, 79, 113-115], and the method can be consequently used to determine any degrading products in formulated dosage forms.

2.4.9.1 Photostability studies

Photostability is an important stress test since a number of compounds degrade in the presence of natural light. The photostability of CPT was tested by exposing a stock solution of CPT (100 µg/mL) to 500 W/m^2 using a Suntest® CPS plus (Atlas, Linsengericht, Germany) for 24 hours. The solutions were then analysed using the validated HPLC method.

2.4.9.2 Temperature stress studies

The effect of temperature on CPT was evaluated and performed over 10 °C increments for accelerated stability studies conducted according to the ICH guidelines [115, 121-123]. To investigate whether CPT degraded at elevated temperatures, five 100 µg/mL CPT solutions were prepared separately and subjected to different temperature conditions that were maintained under reflux conditions in a fume hood. Aliquots of 2.5 mL were collected prior to and during exposure and were diluted with 2.5 mL of a SCY solution and then made up to volume (25 mL) with mobile phase in an A-grade volumetric flask. If no CPT degradation was observed, the experiment was repeated at a higher temperature. Each sample was analysed in triplicate (n=3) using the validated HPLC method.

2.4.9.3 Alkali degradation studies

Alkalicatalysed hydrolytic degradation of a compound or analyte can be performed by refluxing the material in 0.1 M NaOH for eight hours [124]. A 0.1 M NaOH solution was prepared by weighing 0.4 g NaOH pellets that were transferred to a 100 mL A-grade volumetric flask and

dissolved in HPLC grade water. The solution was sonicated for 5 minutes to ensure that the NaOH had dissolved and was then made up to volume with distilled water. Approximately 20 mg of CPT was accurately weighed and transferred into a 20 mL A-grade volumetric flask and made up to volume with 0.1 M NaOH. The sample was refluxed for 8 hours at 50 ± 0.5 °C. Aliquots of 2.5 mL were removed at two hourly intervals and transferred to a 25 mL volumetric flask, after which 2.5 mL of the SCY solution was added and the solution was made up to volume with the mobile phase prior to analysis.

2.4.9.4 Acid degradation studies

Acid degradation studies for a compound or analyte can be performed by refluxing the material in 0.1 M HCl for eight hours [124]. Approximately 20 mg of CPT was weighed and transferred to a 20 mL A-grade volumetric flask and made up to volume with 0.1 M HCl. The sample was refluxed for 8 hours at 50 ± 0.5 °C. Aliquots (2.5 mL) were collected and transferred to an A-grade 25 mL volumetric flask and 2.5 mL of SCY solution was added. The samples were made up to volume with the mobile phase prior to analysis.

2.4.9.5 Oxidation studies

Oxidative degradation studies can be conducted using hydrogen peroxide (H_2O_2) solutions of 3-30% v/v strength [113]. Approximately 20 mg CPT was weighed into a 20 mL A-grade volumetric flask and dissolved in 2 mL of a 30 % v/v H_2O_2 solution that was made up to volume with water to produce a 3 % v/v H_2O_2 solution. Aliquots (2.5 mL) were removed every 2 hours and were transferred into a 25 mL volumetric flask. 2.5 mL SCY solution was added, after which the samples were made up to volume with mobile phase prior to analysis.

2.4.10 Assay of commercially available captopril formulations

Each commercially available formulation was assayed and the average CPT content and % recovery with respect to the label claim calculated.The data are summarised in Table 2.15. Twenty tablets were weighed and the average tablet weight was determined. The tablets were then pulverised and a portion of the powder equivalent to the weight of 50 mg of CPT was accurately weighed and dissolved in 100 mL of mobile phase prepared as described in §2.4.2. The solution was sonicated for 20 minutes using a Branson® B12 ultrasonic bath (Branson® Inc., Shelton, Conn,

USA). The resultant mixture was filtered through a 0.45 µm Millipore® membrane HVLP filter (Millipore®, Bedford, MA, USA) and 1 mL aliquots of the solution were transferred into a 25 mL A-grade volumetric flask containing 2.5 mL of SCY solution prepared as described in §2.4.3. The samples were made up to volume with mobile phase prior to analysis.

2.5 RESULTS AND DISCUSSION

2.5.1 Effect of pH

The effect of pH on the retention characteristics of CPT and SCY was investigated over the pH range 2.8 to 3.6 using a mobile phase composition of 50 % v/v MeOH: water. The results of pH effects on retention time are depicted in Figure 2.2. The retention times of SCY increased significantly with an increase in pH. A pH of 3 was selected as the pH of the mobile phase, since the retention time for CPT and SCY peaks were at least three minutes and not more than 10 minutes. The results obtained are similar to published [73, 75, 80] reports that show that CPT is retained over a pH range of 2.5 to pH 3.3.

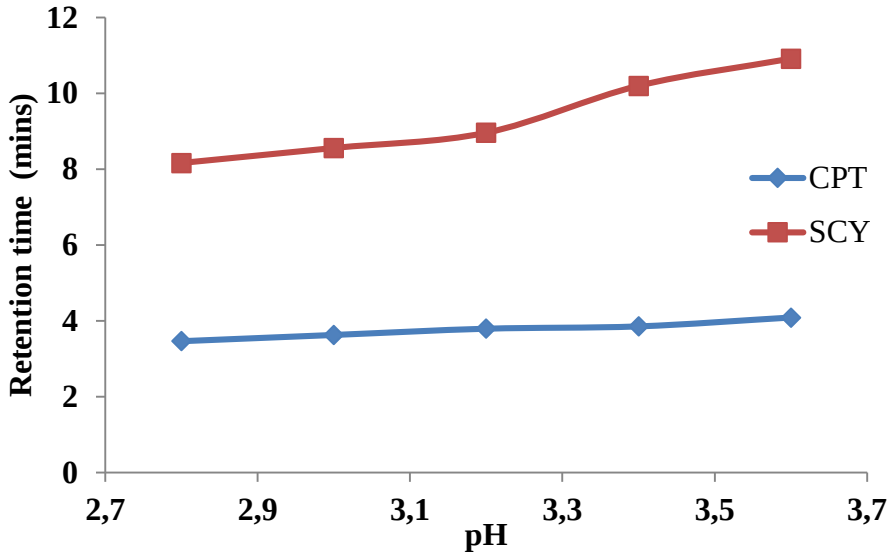

Figure 2.2 *The effect of pH on retention time of CPT and SCY.*

It was important to establish the optimum pH of the mobile phase as it affects the extent of ionisation. The surface characteristics of the silanol functional groups on the surface of the stationary phase [90] may alter the retention characteristics of the analyte due to the different types of interaction that can occur between the analyte and the stationary phase. Furthermore, analysis at a constant pH ensures a reproducible and robust analytical method that can be applied for qualitative and quantitative analysis of CPT formulations.

2.5.2 Central composite design

Twenty experiments were conducted in a randomised manner to minimise bias using the factor levels described in §2.4.7.A summary of the experiments and the response are summarised in Table 2.5.

Table 2.5 *Summary of CCD experiments and responses.*

ID	Run	pH	Solvent Composition (%)	Column Temperature (°C)	Retention Time, CPT(min)	Retention Time, SCY(min)	A_s CPT
0	**1**	3.2	50	25	3.31	7.63	1.00
3	**2**	2.8	60	20	2.48	4.74	0.98
7	**3**	2.8	60	30	2.41	4.31	1.01
2	**4**	3.6	40	20	5.33	11.37	1.06
1	**5**	2.8	40	20	4.99	14.71	0.96
8	**6**	3.6	60	30	2.45	4.16	0.98
13	**7**	3.2	50	16.6	3.36	7.96	0.99
14	**8**	3.2	50	33.4	3.19	6.95	1.01
6	**9**	3.6	40	30	4.85	9.51	0.98
12	**10**	3.2	66.8	25	2.48	4.59	1.04
0	**11**	3.2	50	25	3.31	7.62	0.99
4	**12**	3.6	60	20	2.52	4.43	0.97
5	**13**	2.8	40	30	4.82	12.61	0.95
0	**14**	3.2	50	25	3.31	7.61	1.00
9	**15**	2.5	50	25	3.16	7.34	0.99
10	**16**	3.9	50	25	3.12	5.93	0.98
0	**17**	3.2	50	25	3.31	7.62	1.00
0	**18**	3.2	50	25	3.31	7.63	1.00
11	**19**	3.2	33.2	25	5.02	12.06	0.99
0	**20**	3.2	50	25	3.31	7.63	1.00

Design-Expert® 8.0.4 software was used to validate the responses observed in experimental studies. Analysis of Variance (ANOVA) was used during the development and optimisation of this HPLC method to identify the best analytical end-point. The target retention times were between three and ten minutes. The evaluation of CPT retention time is discussed in detail since SCY was used as an IS. The statistical test was performed and the Fisher F-ratio and p-values were calculated and are listed in Table 2.6.

Table 2.6 *ANOVA data for Response Surface Quadratic Model for retention time.*

Source	Sum of Squares	Df	Mean Square	F Value	p-value Prob > F	
Model	16.1	9	1.79	14.13	0.0001	Significant
A-pH	0.011	1	0.011	0.085	0.7769	
B-Organic solvent composition (% v/v)	15.19	1	15.19	119.97	< 0.0001	Significant
C-Column Temperature (ºC)	0.085	1	0.085	0.67	0.4323	
AB	0.011	1	0.011	0.083	0.7791	
AC	0.012	1	0.012	0.095	0.7644	
BC	0.033	1	0.033	0.26	0.6233	
A^2	1.83E-03	1	1.83E-03	0.014	0.9068	
B^2	0.74	1	0.74	5.86	0.036	Significant
C^2	0.05	1	0.05	0.4	0.5432	
Residual	1.27	0.13	10			
Lack of Fit	1.27	5	0.25			
Pure Error	0	5	0			
Cor Total	17.37	19				

Parameter	Value
Std. Dev.	0.36
Mean	3.5
C.V. %	10.16
PRESS	9.62
R^2	0.9271
Adjusted R^2	0.8615
Predicted R^2	0.4462
Adequate Precision	14.099

The p-value is most commonly used to assess the significance of a particular response with respect to variance of all terms included in a 95 % confidence interval [106]. A low p-value is indicative of a significant effect and it provides a baseline for determining the relative effect of each variable tested with respect to a desired response. The model for retention time was considered significant with a p-value of 0.0001 < 0.05 following use of ANOVA analysis. The p-values listed in Table 2.6 reveals that the MeOH solvent composition contributes significantly to the model.

The F-value of 14.13 implies that the model is significant. P-values < 0.05 indicate model terms are significant, and in this case the % v/v MeOH content in the mobile phase and B^2 are significant model terms that have an impact on retention time. Values > 0.10 indicate that the model terms are not significant. The R^2 value of 0.9271is close to 1 and denotes a high degree of correlation between the observed and predicted values, as depicted in Figure 2.3.

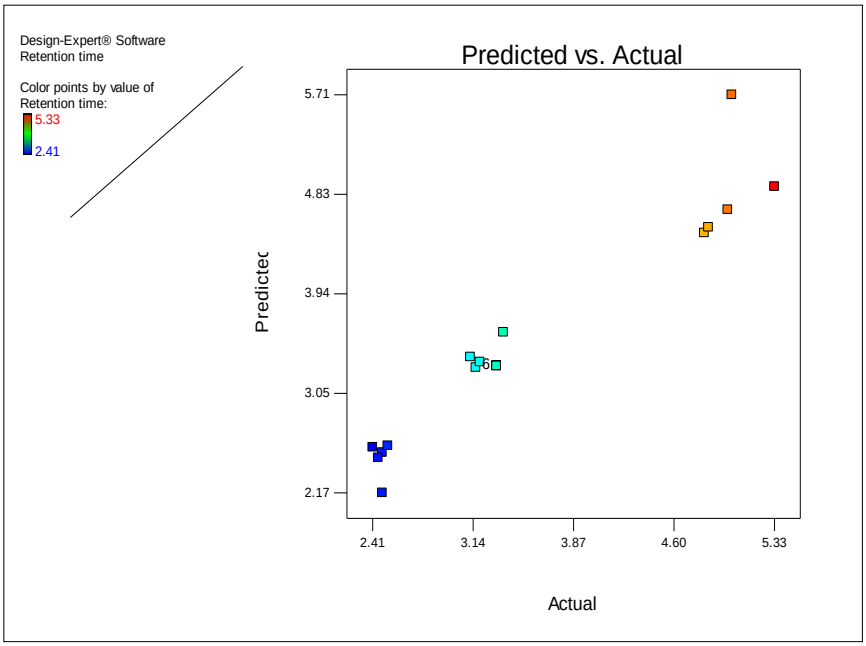

Figure 2.3 *Plot of actual versus predicted response for retention time.*

The coefficient of variance (CV) indicates the degree of precision with which experiments were conducted and reliability is indicated by a low CV. A CV of 10.16 was calculated for the experiments performed for the optimisation of an HPLC method, indicating the data are reliable. The predicted R^2 of 0.4462 is not as close to the adjusted R^2 of 0.8615 as one might normally expect. Adequate precision is used to compare the signal-to-noise ratio measurements of experimental results and predicted points [107].The model had an adequate precision of 14.099, which is > 4, indicating satisfactory model discrimination. Furthermore, the model is significant and can be used to navigate the design space despite the presence of greater numbers of insignificant than significant terms. To further improve the model, model reduction can be performed, but it was not considered necessary for this model.

The model can be used to predict the retention time of CPT and the limits described by the results of these experiments. The normal probability plot of residuals for retention time is shown in Figure 2.4.

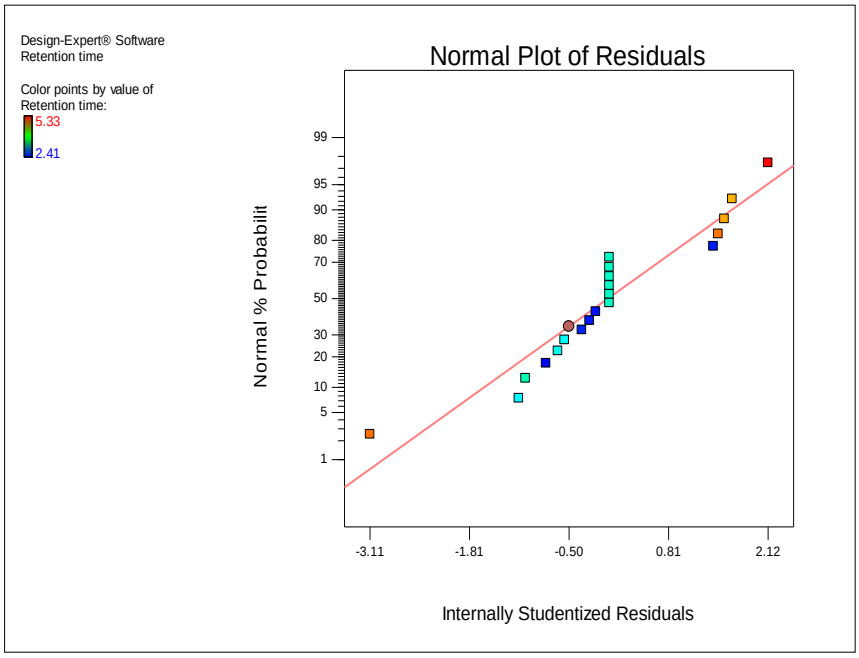

Figure 2.4 *Normal probability plot of residual for retention time.*

The normal probability plot of residuals reveals that the residuals fall mostly on a straight line, indicating that the errors are normally distributed, and thereby further supporting the assertion that the data fits the proposed model adequately. The proposed model in this case provides an adequate approximation of the optimised process for retention time and provides a means to check the desired responses to the model.

2.5.3 Response surface plots for retention time.

A quadratic polynomial equation was developed and the coefficients of the response for retention time of CPT revealed that optimum conditions existed. The combined effects of the independent variables *viz*. pH, MeOH content and column temperature are depicted in Equation 2.11.

Y_1 (Retention time) = + 3.299 + 0.028pH - 1.054MeOH composition - 0.079Column temperature - 0.036pH*MeOH composition- 0.038 pH*Column temperature+ 0.063 MeOH composition*Column temperature+ 0.011 pH^2 +0.226 MeOH $composition^2$ + 0.058$Column\ temperature^2$ **Equation 2.11**

The sign and magnitude of the coefficient provide an indication of the influence of specific or interactive factors on the overall response. A positive sign is indicative of a synergistic effect, whereas a negative sign indicates an antagonistic effect.

One of the most effective ways to visualise the changes in the response of a system as a consequence of an increase or decrease in one or more of the input factors, is to study the interactive effects, if any, using two-dimensional contour and three-dimensional response surface plots [109]. The contour and response surface plots for retention time are depicted in Figures 2.5 – 2.6. The retention time of CPT decreased with an increase in MeOH content when the pH and column temperature were held constant (Figure 2.5A). The response surface plot depicted in Figure 2.5B shows the relationship in 3D.

A B

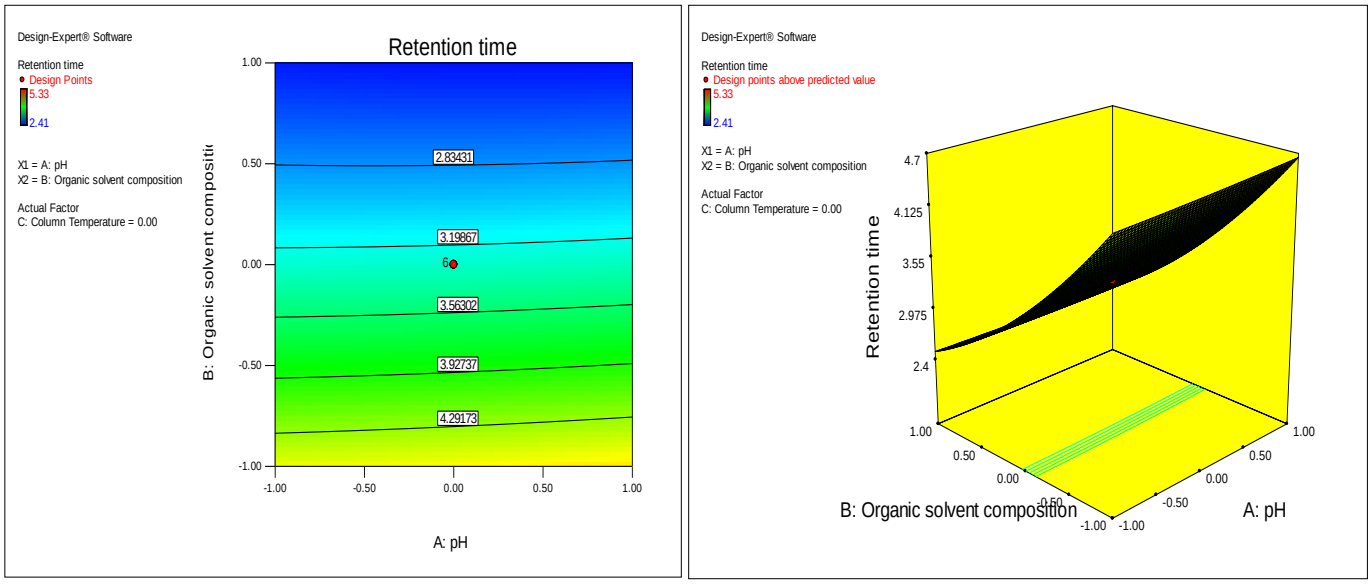

Figure 2.5A) *Contour plot for retention time as a function of pH and MeOH content.* ***B)*** *Response surface plot for retention time as a function of pH and MeOH content.*

An increase in MeOH content resulted in a decrease in the retention time of CPT, which was almost linearand that can be attributed to the partitioning of the CPT molecule due to a silanophilic retention mechanism involving hydrogen bonding and/or ionic interaction between CPT and the residual ionised silanol groups on the surface of the stationary phase [83, 87, 90]. Partitioning affects the separation of CPT between a stationary and mobile phase and the average rate at which CPT migrates through the column is a function of this relationship.

The retention time for CPT decreased with an increase in MeOH content, while maintaining the column temperature in a nearly linear relationship as depicted in Figure 2.6 A and the 3D plot in Figure 2.6 B.

A. B.

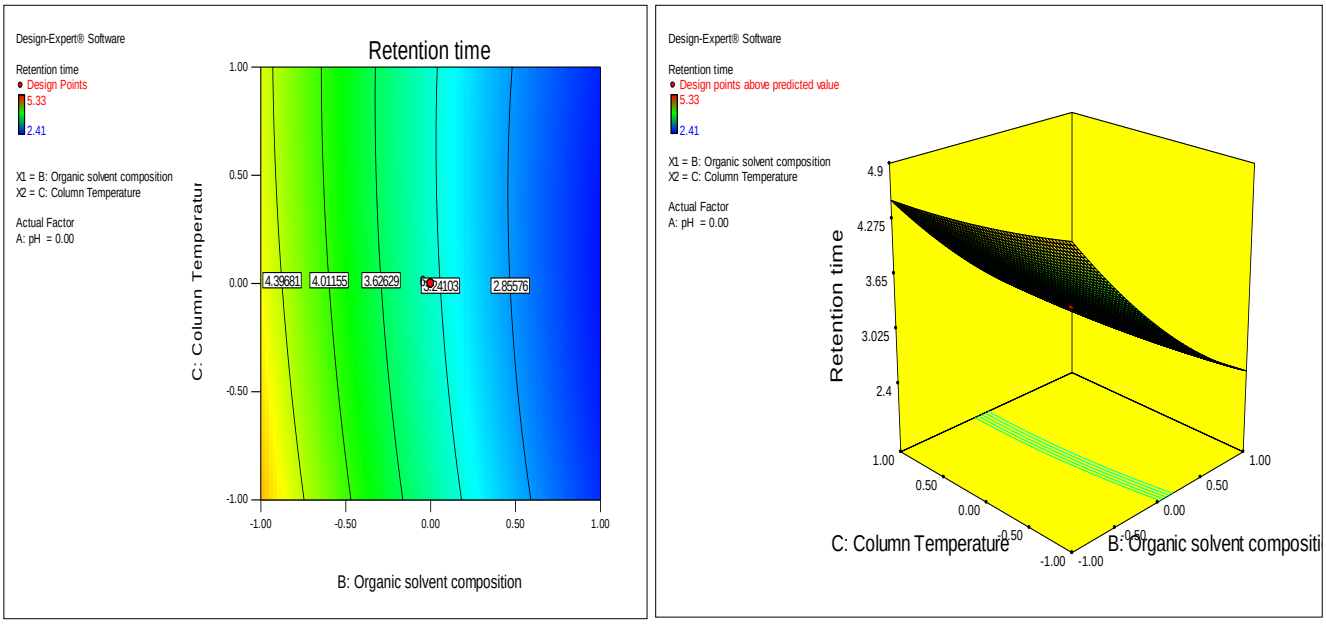

Figure 2.6A) *Contour plot for retention time as a function of MeOH content and columntemperature.* ***B)*** *Response surface plot for retention time as a function of MeOH content and column temperature.*

An increase in the pH of the mobile phase did not produce a significant change in the retention time of CPT at constant column temperature.This may be due to the evaluation of the range of pH from 2.8 to 3.6, which was investigated. It is therefore essential to use a mobile phase of constant pH throughout analysis to ensure that the method behaves in a reproducible and robust manner to prevent different types of interactions between CPT and the stationary phase that may alter the overall retention characteristics of the CPT.

As deducted from Equation 2.11 and the contour and response surface plots, the MeOH content and column temperature have an antagonistic effect on CPT retention time, as depicted in Figure 2.7 A and B, despite MeOH content having the greatest effect with a magnitude of 1.054. Increasing MeOH content therefore decreases CPT retention time, whereas increasing column temperature increases CPT retention time.

A. B.

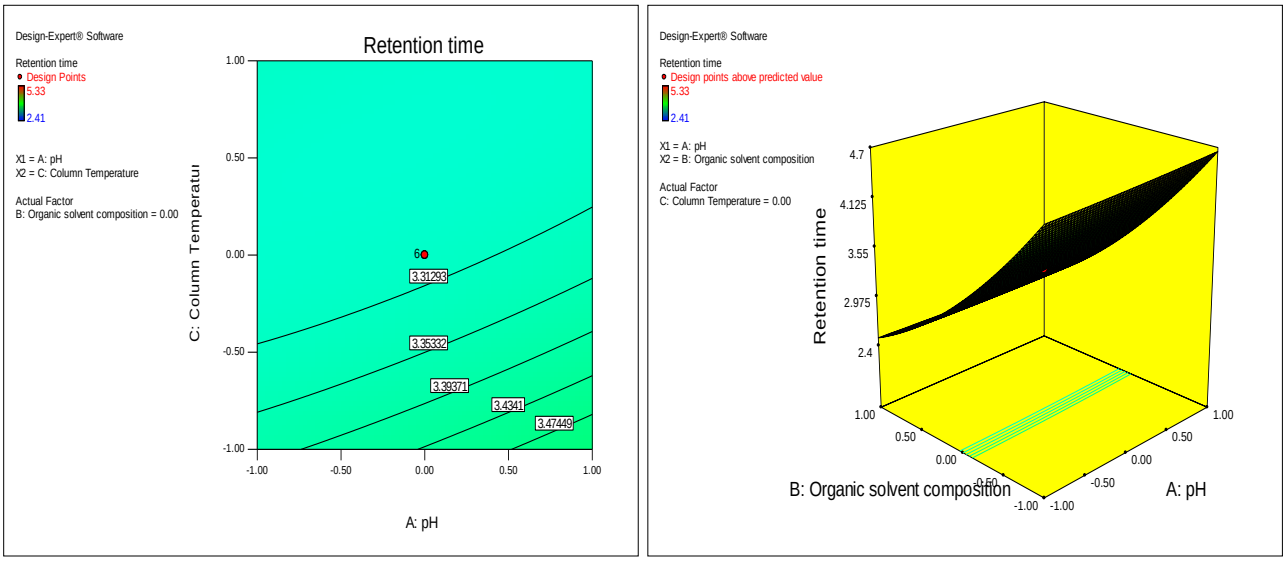

Figure 2.7A) *Contour plots for the retention time as a function of pH and column temperature.* ***B)*** *Response surface plots for the retention time as a function of pH and MeOH composition in the mobile phase.*

2.5.4 Effect on asymmetry factor (A_s)

The mathematical relationship can be described by a quadratic polynomial equation for the A_s measured, as depicted in Equation 2.12.

$Y_2(A_s)$ = + 1.00 + 5.36E-003pH + 5.425E-003MeOH composition -1.198E-003Column temperature - 0.021pH* MeOH composition- 0.011pH*Column temperature+ 0.016MeOHcomposition*Column temperature- 7.64E-003pH ^{2} + 2.97E-003MeOH composition ^{2} - 2.33E-003Column temperature ^{2}

Equation 2.12

The data generated reveal that there is linear contribution of X_1, X_2 and X_3 that was not significant for the A_s for CPT as indicated by the low magnitude of the coefficients of the model terms in the equation.The interactive terms X_1X_2 and X_1X_3 reveal a significant and antagonistic effect on the A_s for CPT. Both interactive model terms that were significant revealed that the mobile phase pH was a common factor and has an effect on peak shape, particularly for compounds such as CPT that can be associated with how ionisable functional groups elute differently to unionised compounds [82, 83, 85, 95, 112].

ANOVA data for A_s revealed that the model was significant with an F-value of 3.17.Significant model terms included the interactive effects of pH-MeOH content and pH-column temperature with p-values < 0.05.The data are summarised in Table 2.7.

Table 2.7 *Analysis of variance table for Response Surface Quadratic Model for A_s.*

Source	Sum of Squares	df	Mean Square	F Value	p-value Prob > F	
Model	8.65E-03	9	9.61E-04	3.17	0.0434	Significant
X_1-pH	3.92E-04	1	3.92E-04	1.29	0.282	
X_2-Organic Solvent Composition (% v/v)	4.02E-04	1	4.02E-04	1.33	0.2764	
X_3-Column Temperature (°C)	1.96E-05	1	1.96E-05	0.065	0.8044	
X_1X_2	3.61E-03	1	3.61E-03	11.91	0.0062	Significant
X_1X_3	1.01E-03	1	2.11E-03	6.97	0.0248	Significant
X_2X_3	2.11E-03	1	1.01E-03	3.34	0.0976	
X_1^2	8.41E-04	1	8.41E-04	2.77	0.1269	
X_2^2	1.27E-04	1	1.27E-04	0.42	0.532	
X_3^2	7.85E-05	1	7.85E-05	0.26	0.622	
Residual	3.03E-03	10	3.03E-04			
Lack of Fit	2.95E-03	5	5.90E-04	35.39	0.0007	Significant
Pure Error	8.33E-05	5	1.67E-05			
Cor Total	0.012	19				

Parameter	Value
Std. Dev.	0.017
Mean	0.99
C.V. %	1.75
PRESS	0.023
R^2	0.741
Adjusted R^2	0.507
Predicted R^2	-0.968
Adequate Precision	7.156

The p-value for the model was 0.0434, indicating that the model for A_s is significant. The lack of fit F-value of 35.39 implies that the model is significant and a negative predicted R^2 of 0.9678 implies that the overall mean is a better predictor of the response for A_s than the current model. The adjusted R^2 value is useful for comparing models with different numbers of terms and is often used when model reduction is necessary. An adequate precision ratio of 7.156 that is > 4 indicates adequate discrimination of the model.The model can therefore be used to navigate the design space for this parameter.

The contour plot depicted in Figure 2.8 A exhibits a non-linear relationship for pH and % MeOH content.The relevant 3D response surface plot is depicted in Figure 2.8 B.

A. s B.

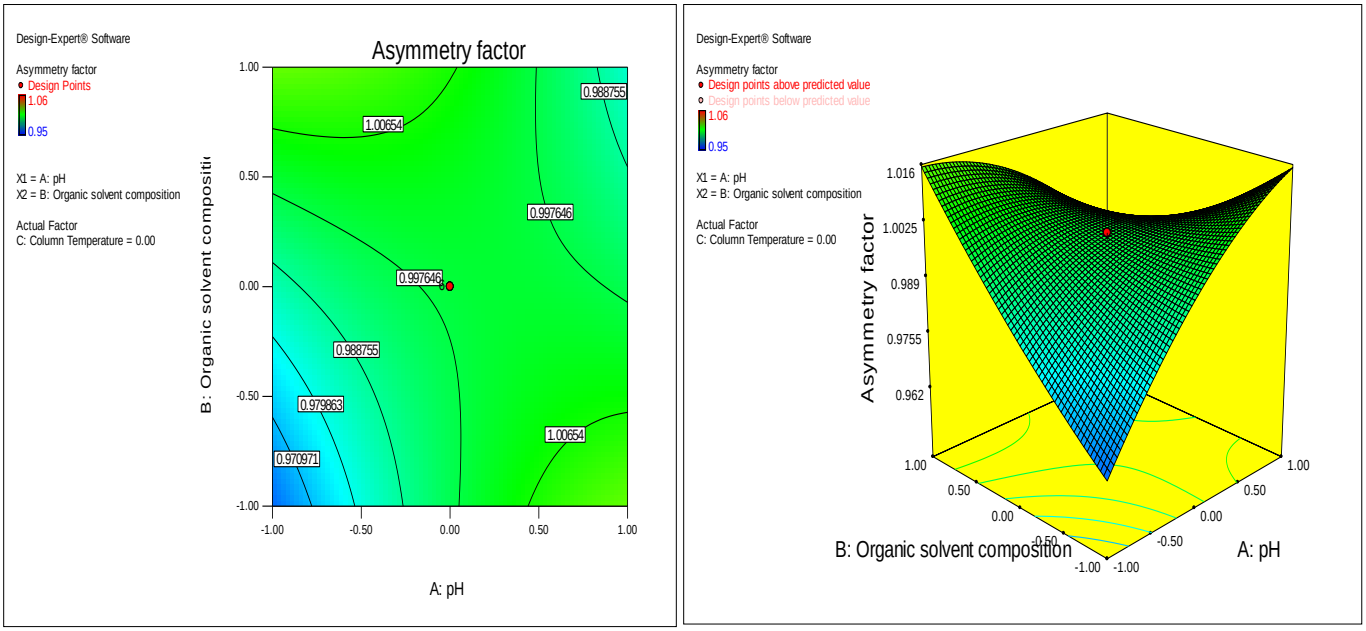

Figure 2.8 A) *Contour plot for A_s as a function of pH and MeOH content.* ***B)*** *Response surface plot for A_s as a function of pH and MeOH content.*

2.5.5 Optimised HPLC conditions

All experiments were performed in a randomised manner to minimise the effects of uncontrolled factors that may introduce bias to the responses. The solutions that were obtained for the optimised chromatographic conditions that produced a separation with the shortest retention time and an A_s of 1 were a mobile phase pH (X_1) of 3.27, % MeOH content (X_2) of 49 % v/v and a column temperature (X_3) of 22.5 ºC.

An HPLC method for the analysis of CPT using ECD detection optimised by using CCD has been reported [80]. However, there are no reports in which the chromatographic conditions for a CPT separation using UV detection have been optimised. The optimised chromatographic conditions selected for the quantitation of CPT are summarised in Table 2.8 and a typical chromatogram of the separation is depicted in Figure 2.9. These method parameters were selected for validation and future analytical studies.

Table 2.8 *Summary of optimised chromatographic conditions for the analysis of CPT.*

Column	Phenomenex® 5µm Luna C_{18} (2) , 150 mm x 4.6 mm i.d.
Mobile Phase	49 % v/v methanol adjusted to pH 3.27 using 85 % v/v ortho-phosphoric acid
Flow Rate	1.0 mL/min
Retention Time	CPT = 3.5 ± 0.5 minutes, SCY = 6.8 ± 0.3 minutes
Column Pressure	1 925 ± 50 psi
Column Temperature	22.5 °C
Injection Volume	10 µL
Wavelength	200 nm
Bandwidth	1.2 nm
Detector	Waters® 2996 Photodiode Array Detector
Pump and Injector	Waters® 2690 Separations Module, Alliance
Data Capture	Waters Empower™ Software

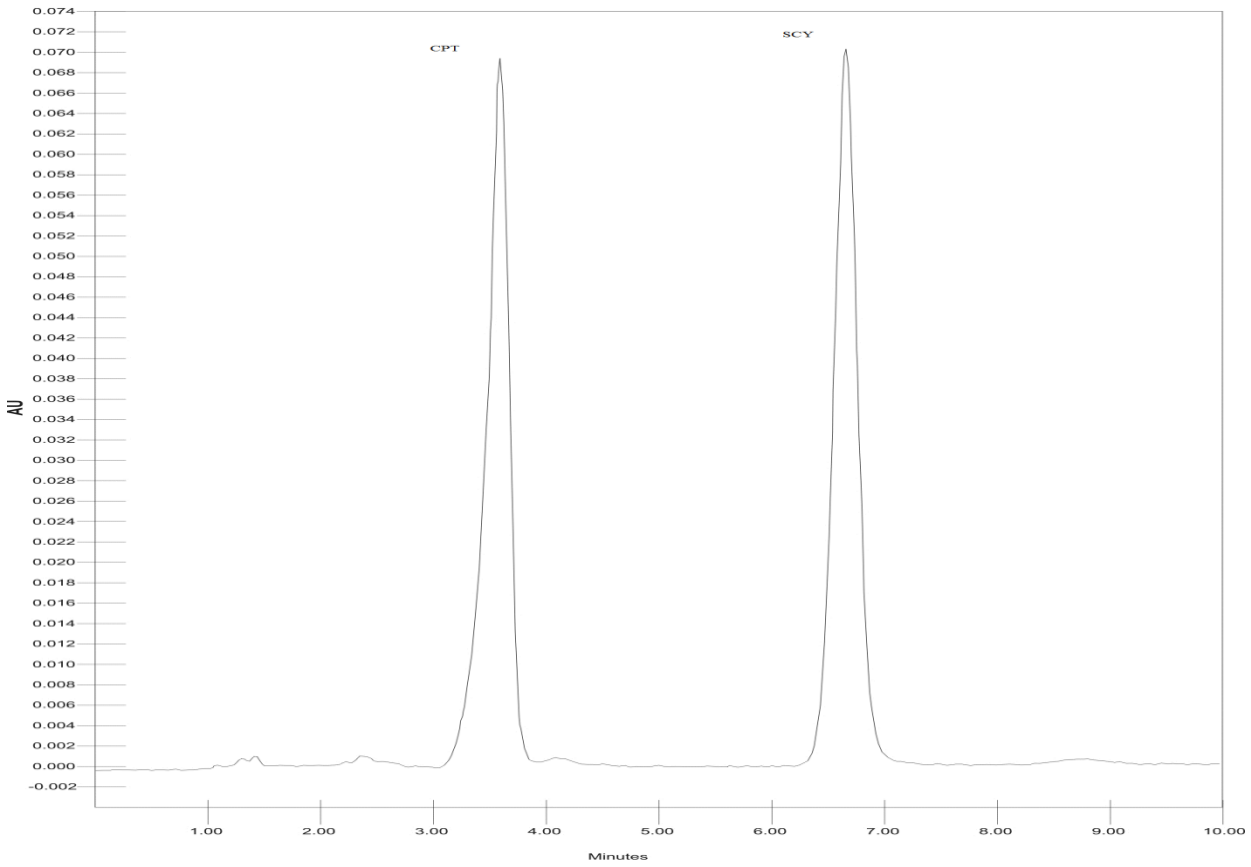

Figure 2.9 *Typical chromatogram for CPT analysis using optimised conditions.*

2.5.6 Specificity

Specificity was assessed comparing chromatograms developed from an analysis of a standard solution of CPT and IS to those developed from the analysis of commercially available CPT tablets.The resultant chromatogram is depicted in Figure 2.10. It shows that the peaks are adequately resolved, suggesting that the proposed HPLC method can be considered specifically for the analysis of CPT.

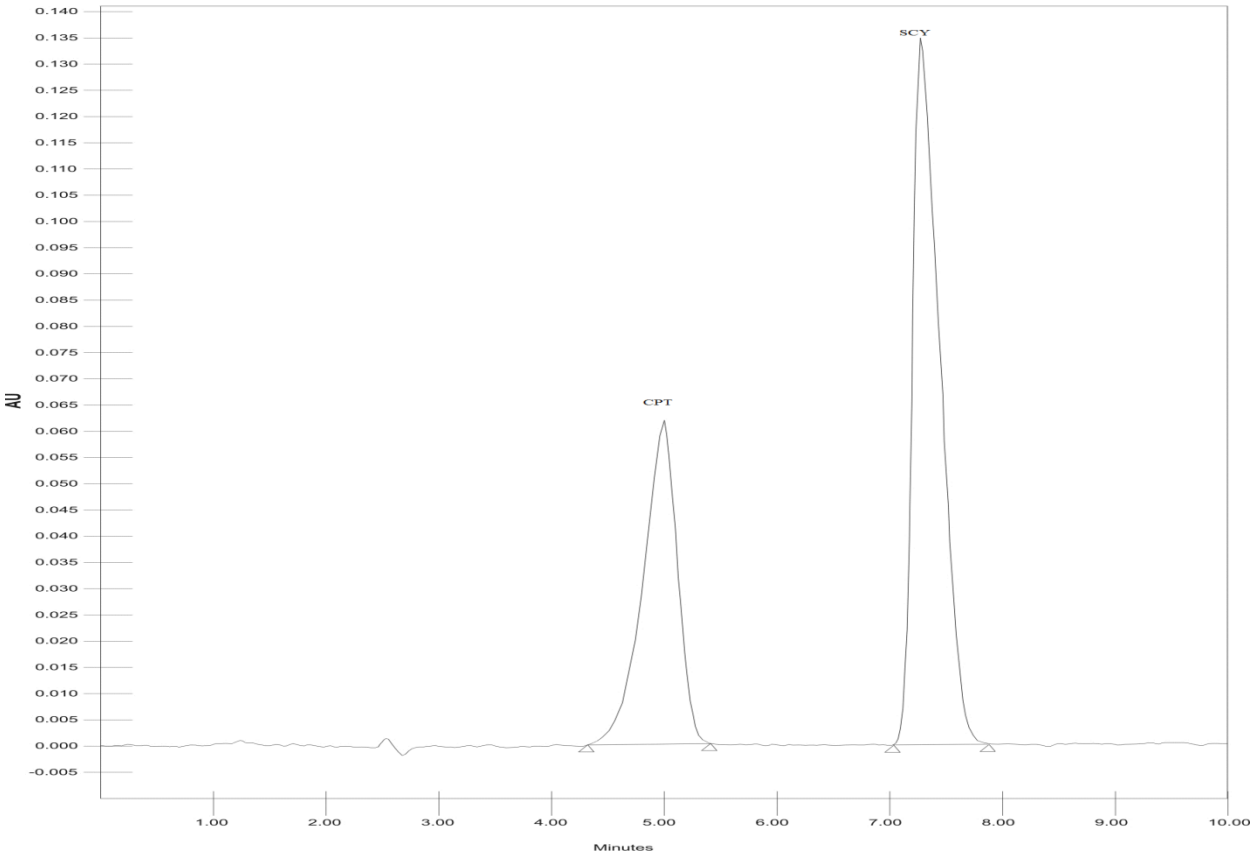

Figure 2.10 *Typical chromatogram from the analysis of a commercial CPT product.*

2.5.7 Validation of the optimised analytical method

2.5.7.1 Linearity

The linearity of the method was established over the concentration range of 2 – 60 µg/mL to correspond to the conditions that would be used during *in vitro* dissolution testing of CPT dosage forms. The selection of 2 µg/mL was based on establishing the LOQ, as described in §2.5.7.4. The calibration standards were prepared as described in § 2.4.2 and linearity was established in the manner described in § 2.4.8.2. A calibration curve was constructed by plotting the peak area ratio of CPT and SCY versus concentration and is depicted in Figure 2.11.

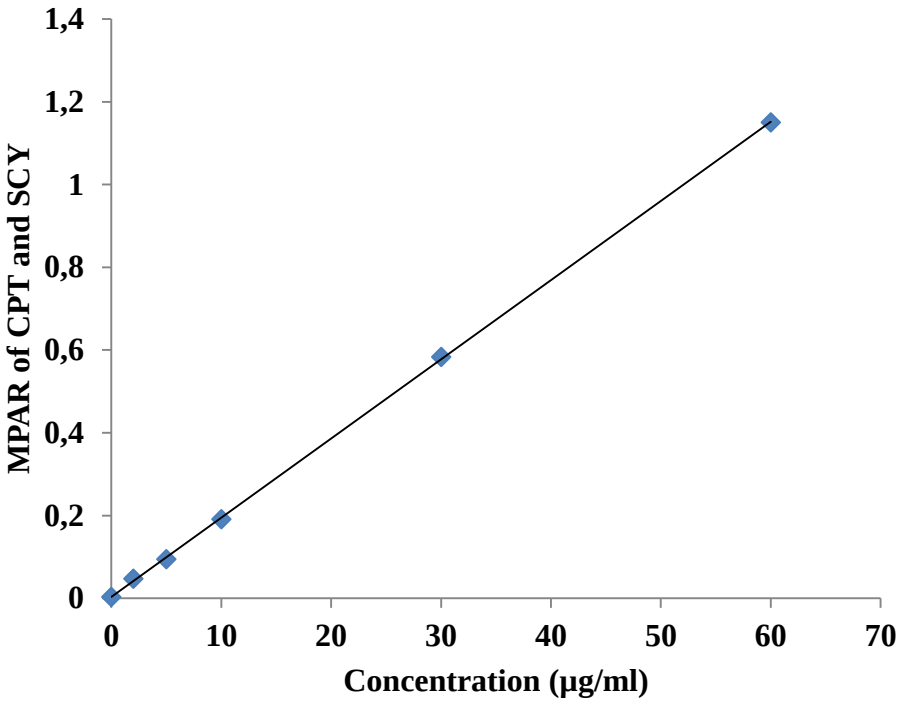

Figure 2.11 *Calibration curve for CPT over the concentration range 2 – 60 µg/mL.*

The calibration curve depicted in Figure 2.11 is linear with an equation for the line, $y = 0.0191x + 0.0035$ and an R^2 value = 0.9999. If the response factor at each concentration is equal or similar at the different concentration levels, the points should form a straight line with a slope of zero to indicate a higher degree of linearity [116]. The average response factor was 0.0196 ± 0.00378 and the responses obtained for most concentrations were within one (1) standard deviation of each other, as depicted in Figure 2.12. The equation for the line was $y = 0.00009x + 0.0193$ and the slope of the response factor has a value near zero. The R^2 value of 0.0038 indicates that the relationship is indeed linear.

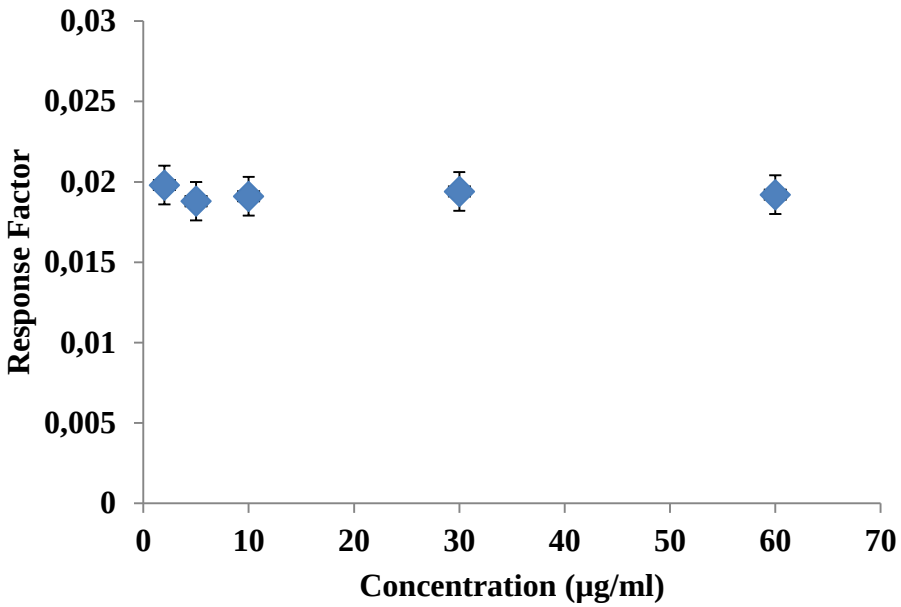

Figure 2.12 *Response factor curve for CPT over the concentration range 2- 60 µg/mL.*

2.5.7.2 Precision

Intra-assay and inter-day precision were performed over the concentration range 2- 60 µg/mL as described in §2.4.8.2.1 and §2.4.8.2.2 respectively.

2.5.7.2.1 Intra-assay precision (Repeatability)

The repeatability of the optimised method was determined at three concentration levels, *viz.* 2 µg/mL, 30 µg/mL and 50 µg/mL (n = 5) and the results of these studies are summarised in Table 2.9.

Table 2.9 *Results of intra-assay precision studies over the concentration range 2-60 µg/mL.*

Concentration (µg/mL)	MPAR (n=5)	Standard Deviation (SD)	%RSD
2	1.03	0.00291	0.279
30	0.517	0.00457	0.882
50	0.0443	0.000351	0.793

The data summarised in Table 2.9 reveal low % RSD values of < 5 % for all samples analysed in precision studies.This indicates that the analytical method for CPT was precise in terms of the repeatability criterion.

2.5.7.*2.2* *Inter-day precision (Intermediate precision)*

Intermediate precision was assessed over a period of three consecutive days and was expressed as coefficient of variation (% RSD) of the peak area ratios of the calibration standards (n = 5). The data summarised in Table 2.10 reveal that the % RSD values for all samples were ≤ 5 %, indicating that the analytical method conforms to the requirements for intermediate precision.

Table 2.10 *Results of inter-day precision for CPT over the concentration range 2-60 µg/mL.*

Concentration (µg/mL)	Day1		Day 2		Day 3	
	MPAR (n=5)	%RSD	MPAR (n=5)	%RSD	MPAR (n=5)	%RSD
2	0.0404	1.39	0.0319	0.916	0.0461	0.825
30	0.526	0.219	0.531	0.132	0.546	0.336
50	1.04	0.237	1.03	0.107	1.03	0.474

2.5.7.3 Accuracy

The accuracy of the method was established as described in § 2.4.8.3 at three (3) concentration levels, *viz.*7.5 µg/mL, 20 µg/mL and 40 µg/mL (n = 5) and the results are summarised in Table 2.11 and list the % recovery, % RSD and % Bias. The data reveals that the analytical method is accurate for the analysis of CPT as all % RSD and % Bias are ≤ 5 %.

Table 2.11 *Results of accuracy studies for CPT over the concentration range 2-60 µg/mL.*

Theoretical Concentration (µg/mL)	Actual Concentration µg/mL (n=5)	% RECOVERY	% RSD	% BIAS
7.5	7.51	100.1	1.01	0.124
20	19.3	96.9	0.342	-3.04
40	40.1	100.1	0.315	0.186

2.5.7.4 LOQ

For the purposes of this research, the approach that recommends that the % RSD following analysis of replicate samples of the lowest concentration of the calibration curve should be< 5 % was used to identify the LOQ. Samples of known low concentration were injected (n=5) and the lowest concentration that produced precision data with a % RSD < 5 % was selected as the LOQ. Results for the LOQ studies are summarised in Table 2.12.

Table 2.12 *LOQ data for CPT.*

Concentration (µg/mL)	MPAR (n=5)	SD	% RSD
1	0.0443	0.00569	12.8
2	0.0627	0.00257	4.11
3	0.0726	0.00317	4.37
4	0.188	0.00356	1.88
5	0.265	0.00384	1.44

The LOQ was established at a concentration of 2 µg/mL by using the described approach, and this sample was used as the lowest calibration point.

2.5.7.5 LOD

As noted in § 2.4.8.5, the LOD was calculated as a third of the concentration of the LOQ and was established as a concentration of 0.6 µg/mL.

2.5.7.6 Stress studies

The assay of CPT solutions following exposure to different stress conditions are summarised in Table 2.13.

Table 2.13 *Percent recovery of CPT following exposure of solutions to stress conditions.*

	Stress condition				
Time/hrs	**500W/m^2**	**Neutral, 80 °C**	**30 % v/v H_2O_2**	**0.1M HCl**	**0.1M NaOH**
0	98.4±1.03	97.5± 0.672	98.6±0.774	97.2±2.17	98.5± 0.873
2	69.1±2.96	56.8±3.88	45.4±6.03	59.7±2.72	58.5±2.26
4	58.2±4.39	54.9±1.04	12.2±5.11	59.3±2.39	0
6	56.2±8.09	54.1±1.67	2.74±2.54	58.5±2.26	0
8	56.4±1.36	53.7± 2.58	1.08± 0.18	56.8±3.13	0

2.5.7.6.1 Photo-stability studies

The results of percent recovery from the assays investigated under photolytic conditions reveal a decrease to 56.4 ± 1.36 % following exposure to 500 W/m^2 after 12 hours. The chromatogram depicted in Figure 2.13 showsthe peak area ratio of CPT following exposure after 4 hours and Figure 2.13 after 12 hours.

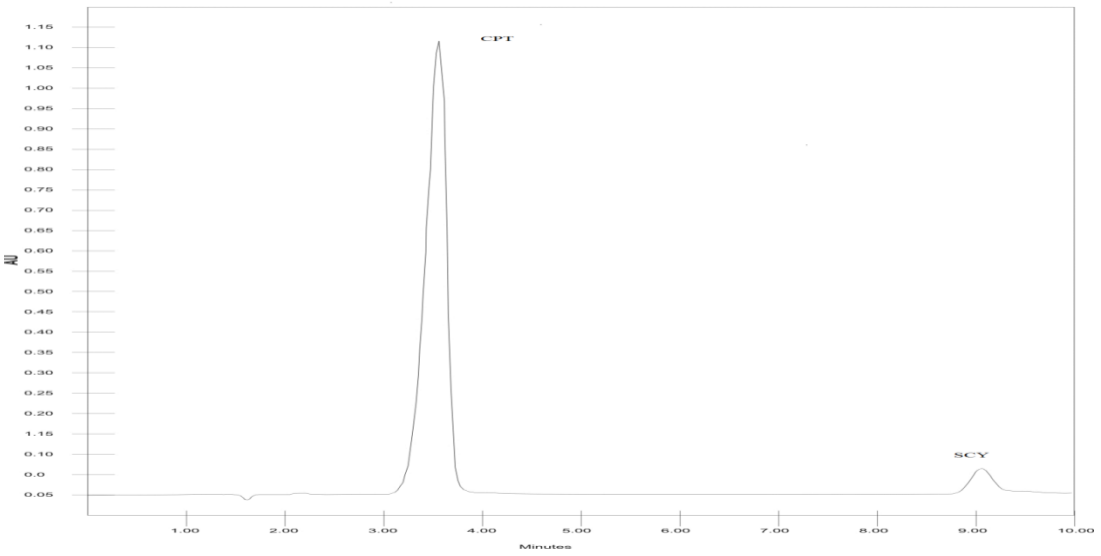

Figure 2.13 *Chromatogram of CPT following photolytic degradation of CPT when exposed to 500 W/m^2 light for 4 hrs.*

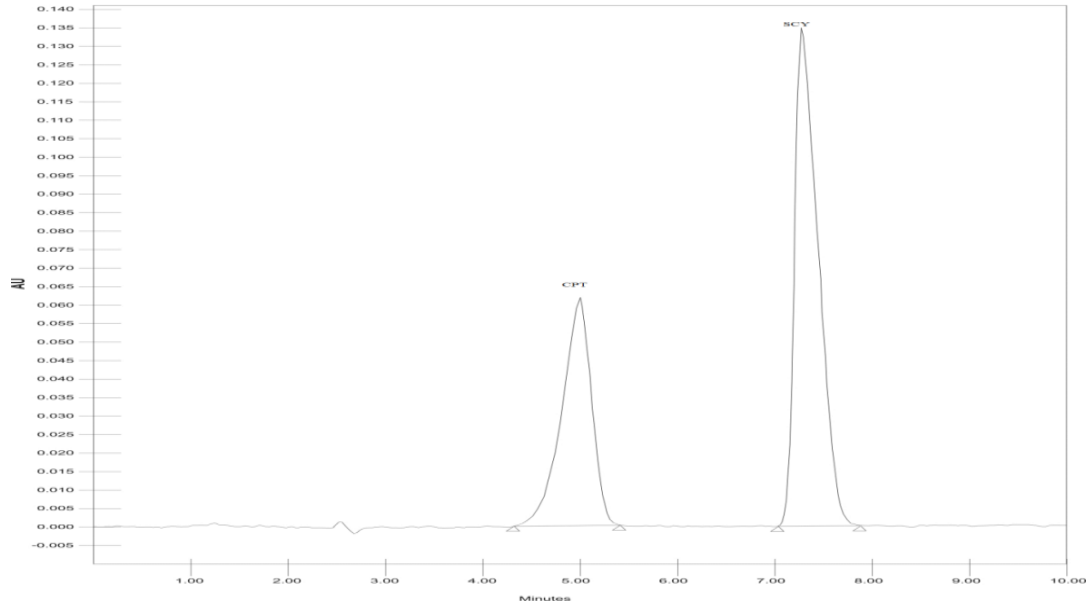

Figure 2.14 *Chromatogram following photolytic degradation of CPT on exposure to 500 W/m2 light for 12 hrs.*

No clear mechanism of photo-degradation has been reported, but Khalaf [120] suggests that a free radicle scavenging mechanism that uses the captodative centers of the CPT are implicated in the photochemical reactions of the molecule. As a result of photolytic degradation, coated formulations may be considered appropriate so as to protect CPT from rapid degradation on

exposure to light and moisture. CPT beads in yellow opaque hard gelatin capsules may further protect CPT from light to ensure long-term stability on prolonged storage as an enhancement to the dosage form development. A packaging recommendation may include packing gelatin capsules in either blister packs or plastic amber bottles.

2.5.7.6.2 Temperature stress studies

All CPT stored at temperatures < 80 °C were considered stable, since no extra peaks were observed. However, at a temperature of 80 °C, one peak, fully resolved at 2.5 minutes, was observed in each CPT sample.The data are summarised in Table 2.14.

Table 2.14 *The effect of different temperatures on CPT stability.*

Temperature (°C)	Time (hrs)	Observations (n=3)	Comments
50	8	CPT peak was resolved at 3.5 min. No extra peak	No degradation
60	8	CPT peak was resolved at 3.5 min. No extra peak	No degradation
70	8	CPT peak was resolved at 3.5 min. No extra peak	No degradation
80	8	CPT peak was resolved at 3.5 min. Extra peak at 2.5 min	Possible degradation
90	8	CPT peak was resolved at 3.5 min. Extra peaks at 2.7 min and 5.1 min	Possible degradation

Two peaks were observed at 2.7 minutes and 5.1 minutes for samples exposed to a temperature of 90 °C, indicating possible degradation products of CPT (denoted A and B) in the chromatogram depicted in Figure 2.15.

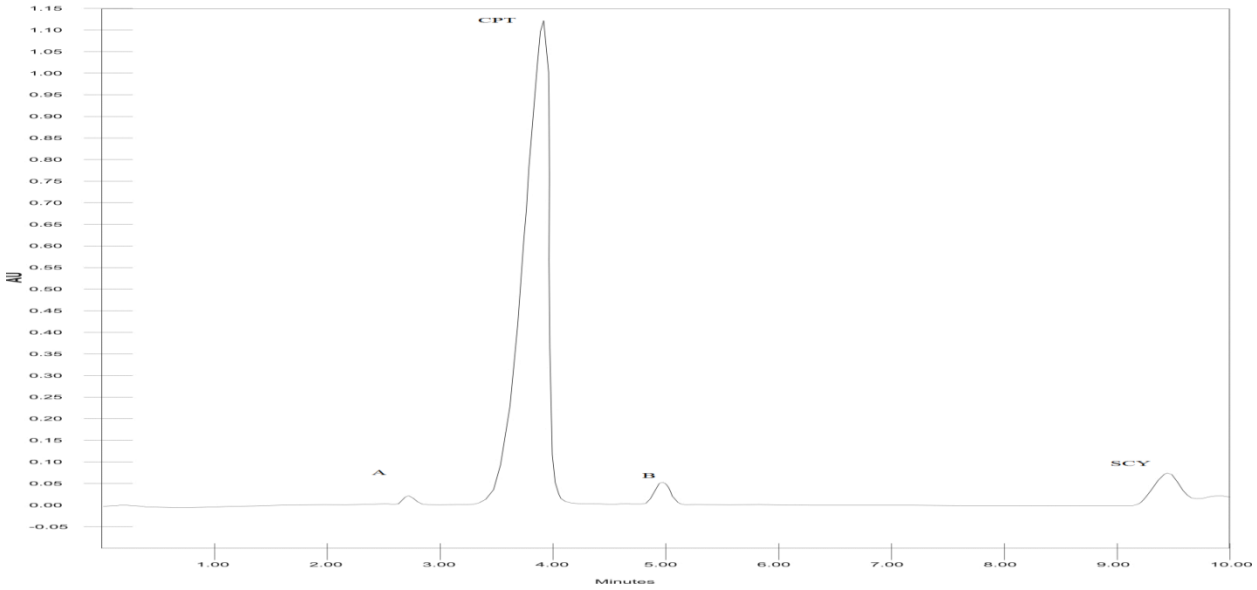

Figure 2.15 *Chromatogram of CPT following exposure to a temperature of 90 °C depicting possible degradation products A and B.*

An increase in temperature by 10 °C increases the rate of vibrations, providing energy to cleave the amide link and the carboxyl functional group attached to the proline backbone of the CPT molecule [32]. During the course of these experiments, it was noted that a characteristic strong pungent sulfurous odour was present.This suggests that degradation of the sulfhydryl functional group had occurred. The results reveal that CPT is susceptible to degradation at elevated temperatures and it is therefore essential to consider using low temperature conditions when manufacturing CPT coated beads to control and/or minimise the rate of degradation of the compound. Furthermore, it is important to ensure that any degradation product formed does not interfere in the analysis of CPT to facilitate accurate results during formulation, manufacturing and process development studies.

2.5.7.6.3 Alkali degradation studies

The chromatogram depicted in Figure 2.16 reveals that CPT is highly unstable in alkali conditions. The extent of degradation of CPT under these conditions was determined and the results reveal that 58.54 ± 2.26 % of CPT remains after exposure to alkali conditions for two (2) hours, as shown in Table 2.13. The degradation can be attributed to the weakly acidic nature of CPT and can be attributed to a carboxyl-mediated neutralisation reaction by sodium hydroxide, resulting in a reduction in the overall amount of CPT detected by the analytical method.

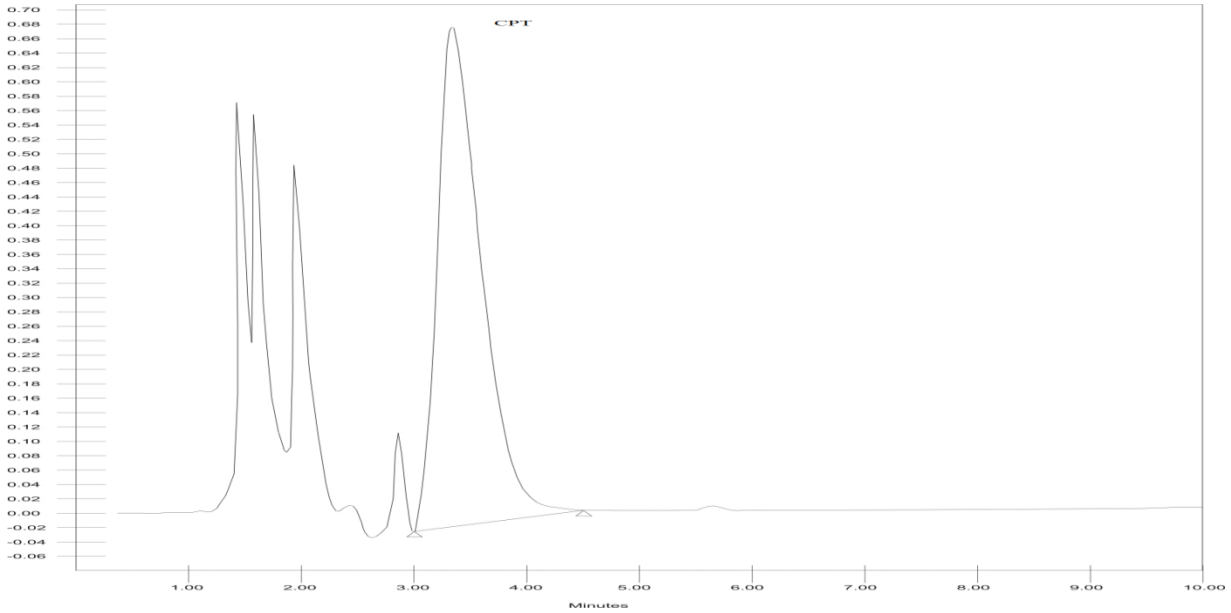

Figure 2.16 *Chromatogram following exposure of CPT to 0.1 N NaOH for 2hrs.*

2.5.7.6.4 Acid degradation studies

The assay of CPT solutions following exposure to acidic conditions revealed a significant decrease in CPT to 56.82 ± 3.13 % 8 hours as shown in Table 2.13. The chromatogram that depicts acid degradation is shown in Figure 2.17. The decrease in CPT has been suggested [123] to be a result of thiol-mediated degradation and therefore a constant pH will be necessary to enhance the stability of CPT in aqueous solution. CPT is sensitive to acid and alkali hydrolysis and must therefore be protected from these extreme conditions to ensure long-term storage stability.

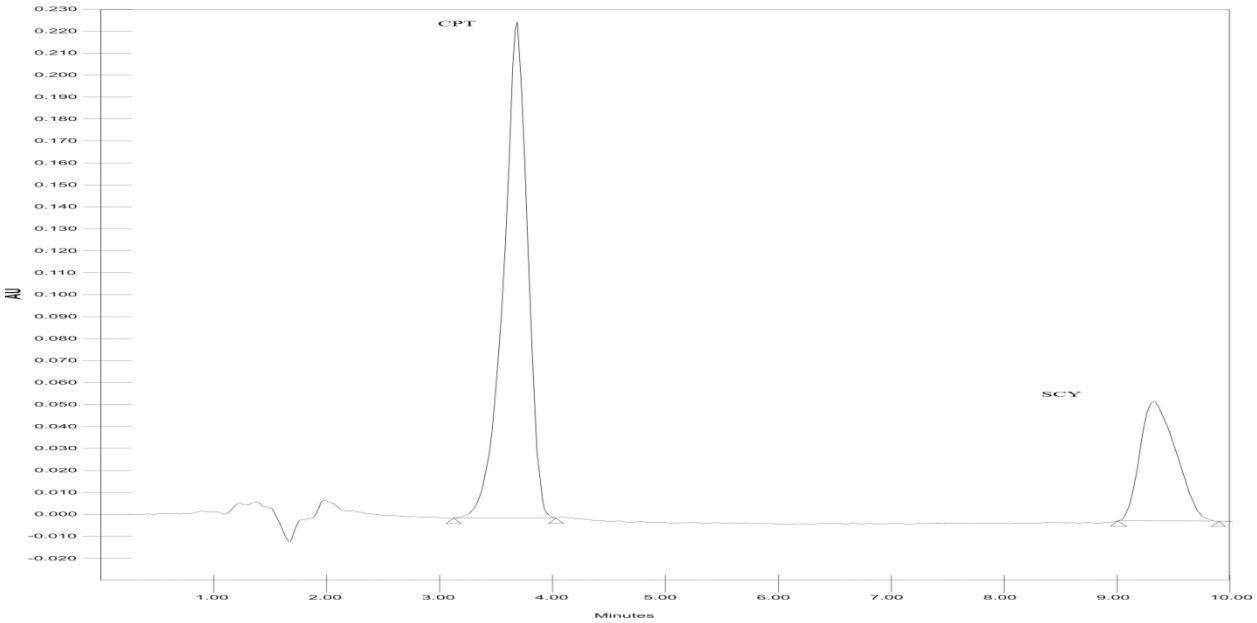

Figure 2.17 *Chromatogram of CPT following exposure to 0.1 N HCl for 8hrs.*

2.5.7.6.5 Oxidative degradation studies

CPT was found to degrade to 58.54 ± 2.26 % of the starting concentration following exposure to 30 % v/v H_2O_2 with refluxing for two (2) hours. It was completely degraded after four (4) hours. The data are summarised in Table 2.13. A chromatogram of CPT following exposure to H_2O_2 is depicted in Figure 2.18 and reveals the presence of many unknown peaks, suggesting the presence of degradation products of CPT.These peaks interfere with that of CPT. Captopril disulphide forms a dimer and it has been widely reported to form following exposure to oxidative conditions [10, 96, 122].

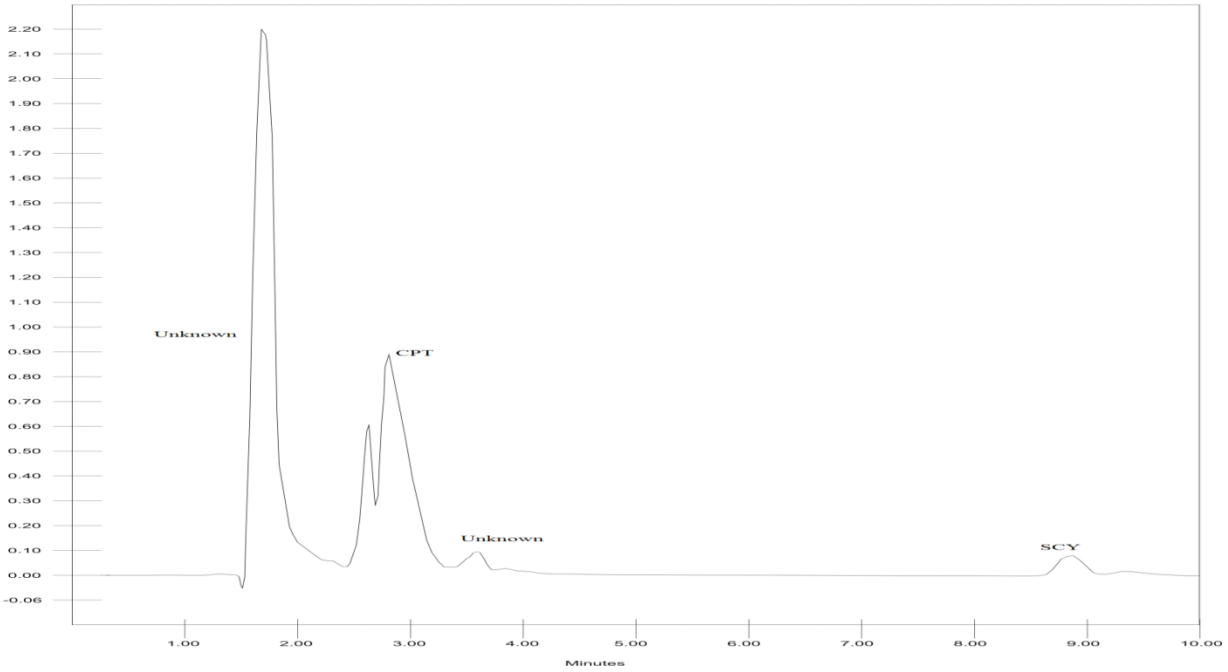

Figure 2.18 *Chromatogram of CPT following to 3 % v/v H_2O_2 for 2hrs.*

2.5.8 Assay of commercially available captopril formulations

The assay of the commercially available CPT tablets in South Africa was performed using the HPLC method that was developed, validated and is reported in this study. Commercially available CPT products were purchased from a local pharmacy and included MERCK CAPTOPRIL® 50, ADCO-CAPTOMAX® 50, Sandoz® Captopril 50, CaptoHexal® 50 and ZAPTO – 50®.

No interfering peaks were observed in the resultant chromatograms, indicating that there was no interference from the excipients used to manufacture the tablets. The assay results ranged between 91.1 and 102.0 % CPT as shown in Table 2.15, which is within the limits of 90 – 110 % of label claim for CPT recommended by USP 29 [34]. The results show that the RP-HPLC method developed for the analysis of CPT in commercial formulations is selective and rugged and can be used in the analysis of developed formulations.

Table 2.15 *Assay results following analysis of commercially available CPT products.*

Product	Label Claim (mg)	Sample	Concentration Added (µg/mL)	Concentration Found (µg/mL)	%RSD	%Recovery
MERCK CAPTOPRIL® 50,	50	1	50.3	51.3	2.53	102
		2	50.2	49.3	1.13	98.2
		3	50.2	48.9	0.491	97.4
ADCO-CAPTOMAX® 50,	50	1	50.0	49.2	1.57	98.4
		2	50.0	50.3	1.08	101
		3	50.1	50.1	0.426	100
Sandoz® Captopril 50,	50	1	50.1	45.9	2.45	91.7
		2	50.1	45.6	0.267	91.1
		3	50.1	45.5	0.529	90.8
CaptoHexal® 50,	50	1	50.0	50.1	0.469	100
		2	50.1	50.1	0.594	100
		3	50.0	49.8	0.266	99.6
ZAPTO - 50®	50	1	50.2	49.3	0.615	98.1
		2	50.3	49.5	0.648	98.3
		3	50.1	49.3	0.538	98.2

2.6 CONCLUSION

A simple, precise, accurate, selective and rapid RP-HPLC method with UV detection at 200 nm has been developed and validated for the *in vitro* quantitation of CPT. The method was optimised by manipulating the mobile phase composition, modification of mobile phase pH and adjustment of temperature to establish the appropriate chromatographic conditions for the separation and analysis of CPT using SCY as the IS.

Modification of pH is important in the separation of ionisable molecules as the pH of the mobile phase affects the distribution of charge entities and impacts the interaction of CPT and SCY with the mobile and stationary phases, thereby affecting the separation of the analytes specifically impacting the resolution and retention time. A pH of 3.27 revealed the best-shaped peaks, with reasonable retention times that did not interfere with the solvent front. This resulted in analysis times of no more than 10 minutes for each sample.

The CPT and SCY peaks were well-separated with retention times of approximately 3.5 ± 0.5 minutes and 6.8 ± 0.3 minutes for CPT, and 3.7 minutes and 9.0 minutes for SCY respectively. Consequently, the proposed method has a relatively short analytical run time of 7.5 minutes and permits multiple sample analysis in a short space of time.The method is therefore appropriate for use in quality control laboratories.

The method was validated in terms of linearity, accuracy, precision, selectivity, LOQ and LOD in accordance with ICH reproducibility [61, 62], FDA [79] and USP guidelines [113]. The coefficient of determination obtained from linearity studies (R^2) was 0.9999, ensuring that the interpolation of data over the concentration range 2 – 60 µg/mL was reliable and accurate. The precision of the method ranged between 0.279 – 0.882 % RSD, indicating that it was reproducible and that day-to-day variation of the response would be minimal. The validated method was found to be linear, precise and had acceptable accuracy for the analysis of CPT in its pure form and in pharmaceutical dosage forms.It revealed no interference from excipients used in the tablet dosage forms.

The method reported herein is an improvement on the majority of those reported in literature, since the PDA detector is a fast scan spectrometer with a low S/N ratio and has the ability to scan a wide wavelength range with enhanced sensitivity and peak purity as compared to conventional UV detectors. This method has a short analysis time and uses a simple mobile phase composition that suggests that it is cheaper to implement than previously reported methods. The developed method is therefore deemed appropriate for use in the analysis of pure CPT, commercial formulations and assessment of *in vitro* release of CPT from test formulations.

A CCD was successfully used to optimise the chromatographic conditions for the quantitation of CPT. The CCD approach required 20 experimental runs, which is fewer when compared to the traditional experimental approach of changing one factor at a time, thereby saving reagent costs and development time. Furthermore, the CCD approach permitted an investigation of the interactive effects of input factors *viz.* pH, MeOH content and column temperature on the responses, retention time to yield well-resolved and symmetrical peaks for CPT and SCY. The MeOH content had the greater impact on the retention time of CPT can be attributed to the impact of composition on the retention mechanism. An increase in the amount of MeOH in the mobile phase increased the overall polarity of the solvent, resulting in an overall decrease in the retention time of CPT due to a decrease in the interaction of CPT with silanol functional groups of the stationary phase it elutes through the column.

A stability-indicating RP-HPLC method for the *in vitro* quantitation of CPT has been developed, validated and can be used for the analysis of commercially available CPT dosage forms. The method is an improvement on the method in the USP monograph for CPT [60]. CPT was found to degrade completely in 0.1 M NaCl after four hours, and in 30 % v/v H_2O_2 1.08± 0.18 % was found after 8 hours. The results of assays investigated under photolytic conditions reveal a decrease to 56.4 ± 1.36 % following exposure to 500 W/m^2 after 12 hours, suggesting photochemical reactions. As a result of photolytic degradation, coated formulations may be considered appropriate to protect CPT from rapid degradation on exposure to light. Stress studies revealed the presence of degradation products following exposure to neutral hydrolytic conditions at an elevated temperature of 80 °C for two (2) hours with 53.7± 2.58 % assayed after 8 hours. The peaks for the degradation products interfered with the peak for CPT and are suspected to be captopril disulphide dimer that has been widely reported [8, 70]. CPT beads in yellow opaque hard gelatin capsules as

formulation development may further protect CPT from light to ensure long-term stability on prolonged storage in bottled or blister packages. The validated method was specific and is stability-indicating when evaluating the results of forced degradation studies. The method is simple, sensitive, selective, precise and accurate and can therefore be applied in formulation development studies of CPT containing dosage forms.

CHAPTER THREE
PREFORMULATION STUDIES FOR SUSTAINED RELEASE BEAD FORMULATIONS

3.1 INTRODUCTION

Active Pharmaceutical Ingredients (API) are routinely tested during preformulation studies to establish their physical and chemical stability to ensure bioavailability [125]. Preformulation studies of an API does not attempt to determine whether the molecule would perform to an acceptable level following formulation [125, 126], which is established through extensive *in vitro* performance testing of test products. Preformulation studies combined with formulation optimisation is necessary to fully elucidate the compatibility of an API with excipients, particularly if that API is off patent and/or to counter generic competition [127] to provide data and information with regard to manufacturing technology prior to initiating plans for formulation development activities. The ever-increasing demand and expectation for high quality and safe medicines has resulted in the development of new API characterised by high assay values and lower impurity content [126, 128]. The quality of medicines depends in part on the characteristics of the API, the production process and the quality of the excipients used. The formulation testing routine is complex, time consuming and expensive and advanced technologies should be used to ensure the successful characterisation of a medicine to ensure improved potency, selectivity with a decrease in side effects and toxicity [125, 126, 128].

Prior to dosage form development, it is crucial that some fundamental physical and chemical properties of an API molecule and of the API powder are elucidated [127]. The information, to some degree, dictates subsequent processes and methodologies to be used in formulation and product development studies. The significance of powder flowability and cohesive interaction between particles has been well documented in the production of pharmaceutical dosage forms, including beads [129-131]. The preformulation phase has been suggested [126, 128] to have a significant influence on the ultimate safety, efficacy, stability and regulatory compliance of the API and medicine. Preformulation generally includes a study of the physico-chemical properties of an API and excipients, including an assessment of their relevance in a final formulation, the chemical and physical stability of the API and relevant excipients, impurity profiling of the API,

including content of synthetic and degradation products and the chemical compatibility of the API with potential excipients [125, 126, 128].

Appropriate preformulation studies help formulation scientists to achieve the desired performance attributes of a final formulation. A change in particle size and shape with regular measurement of these parameters can lead to improved process and product understanding [132], particularly when batch to batch variability exists. It is therefore important to understand and elucidate differences between current and past batches for product development and/or quality control purposes. To improve quality control and current Good Manufacturing Practices (cGMP) for pharmaceutical products, the FDA has recommended that a Process Analytical Technology (PAT) initiative [133] be undertaken during preformulation studies to understand the impact of differences in particle shape and size on product performance. The PAT initiative provides greater efficiency in formulation and dosage form manufacture, limits the waste of raw materials and lowers the cost of production in a climate of growing economic challenges [133]. Furthermore, the PAT initiative encourages the selective analysis of API prior to and following manufacture in relation to product quality, particle size, polymorphic form and blend uniformity. With these fundamentals in mind, the PAT approach allows formulation scientists an opportunity to identify and control parameters specific to the manufacture of a final product of the desired quality.

Most API incorporated into commercial formulations are pure chemical compounds that are either crystalline or amorphous in the solid state [8]. Preformulation studies were undertaken and analysed in terms of the physiochemical properties reported in §1.1 and §1.4 as part of a systematic process for the development of sustained release (SR) CPT beads. The potential excipients for inclusion in the SR bead dosage form were investigated to establish the impact they may have on the successful development of SR CPT beads. Powder rheology and thermal analysis approaches were used to investigate the properties and compatibility of CPT and potential excipients.

Commonly used techniques to assess the flowability of powders that are used in pharmaceutical industry include the measurement of the angle of repose (AOR), bulk and tapped density determination [125, 128, 134, 135] used to calculate Carr's Index (CI) and the Hausner ratio (HR) [134, 136]. This is exemplified in Figure 3.1. The potential interaction between CPT and hydroxypropylmethyl cellulose (HPMC) (Methocel®K100M and Methocel®E4M), microcrystalline cellulose (MCC) (Avicel® PH102), methacrylic acid copolymer (Eudragit® RS PO) and talc was investigated. TGA was used to characterise CPT, while each of the identified ingredients was exposed and characterised alone and in 1:1 mixtures using DSC and IR in an effort to establish if CPT underwent physical or chemical modification in powder blends.

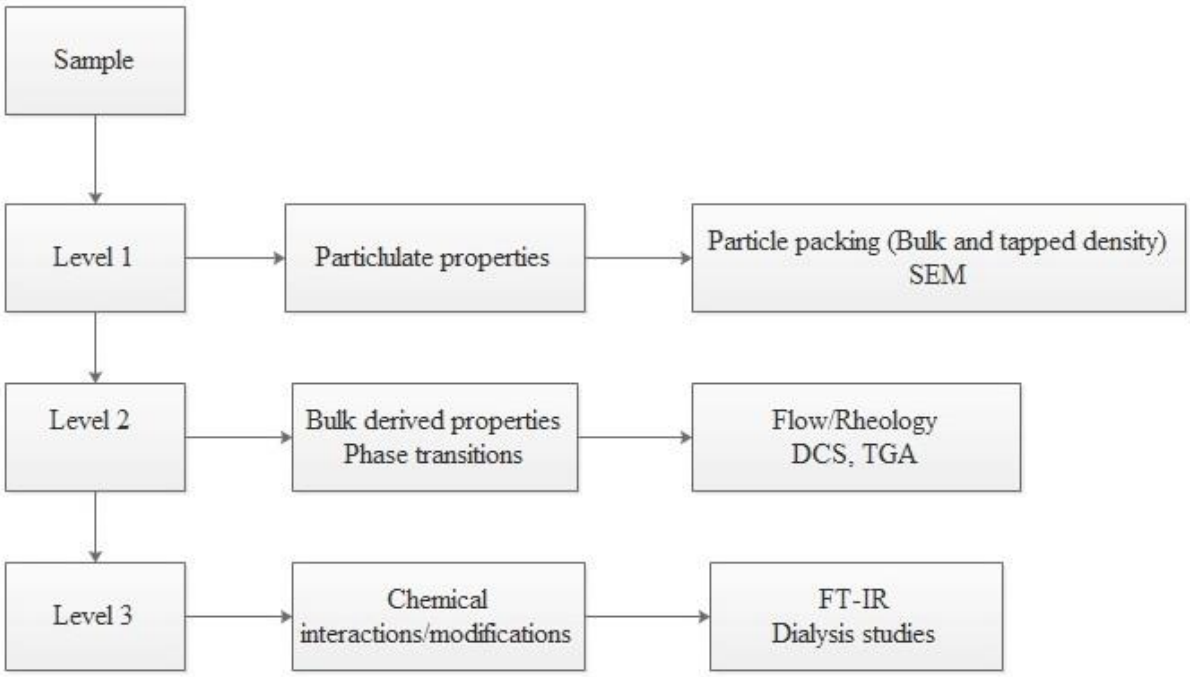

Figure 3.1 *Flow diagram showing testing procedures for pharmaceutical excipients adapted from [127].*

3.2 MATERIALS

3.2.1 Materials/Excipients

All materials and/or excipients used in this study are generally regarded as safe and have GRAS status. The materials used are also listed in the FDA Indicative Ingredients Guide for general inclusion in oral formulations [137].

3.2.1.1 Microcrystalline cellulose (MCC)

MCC is partially depolarised cellulose and occurs as a white crystalline powder with different particle sizes available in a variety of grades with a wide range of properties and uses [137]. MCC is traditionally used as a diluent in solid oral formulations manufactured using wet granulation. In recent years, MCC has been commonly used as an excipient in extrusion-spheronisation processes [138]. Avicel® PH 102 (FMC BioPolymer, Philadelphia, PA, USA) has a mean particle size of 100 μm and a moisture content of ≤ 5 %. It has a bulk and tapped density of 0.29 g/cm^3 and 0.45 g/cm^3 respectively and was used as a diluent and spheronising aid [137] as the rheological properties of an MCC based wet mass are suitable for effective extrusion and spheronisation [16]. MCC has good binding properties and provides cohesiveness to the wet mass whilst exhibiting an ability to adsorb and retain a large quantity of water and/or granulating fluid due to a large surface area and high internal porosity [139] improving the plasticity of the wet mass and enhancing spheronisation [140, 141].

Two models have been proposed to explain the behaviour of MCC during extrusion/ spheronisation process. In the first model MCC is characterised as a molecular sponge that is able to retain water and/or granulating fluid [140]. During the extrusion process the sponge is compressed and the granulating fluid is squeezed out of the internal structures and it acts as a lubricant. Following extrusion, the volume of the sponge increases and it appears dry and brittle, facilitating the breakage of the extrudate during the initial stages of spheronisation. During the spheronisation process the sponge densifies in a mass transfer phenomenon in which water facilitates the spheronisation of the beads [140].

In the second model during wet granulation and extrusion in the presence of water, MCC particles are broken down into smaller units and in some cases to single crystals of colloidal, sized according to a crystallite-gel model [142]. The resulting crystalline materials are porous and form a gel-like network that immobilises the granulation liquid. At a specific water content which relates to a particular gel strength, extrusion and spheronisation becomes possible [142].

A wide range of granulating fluid content and the processing parameters can be used to produce beads of acceptable quality. MCC-based beads have been manufactured [143] with smooth surface properties and optimum sphericity so as to be suitable for subsequent coating to sustain drug release.

3.2.1.2 Hydroxypropyl methylcellulose (HPMC)

HPMC is a non-ionic, non-toxic polymer that has been used for the manufacture of oral formulations [146]. HPMC is widely used as a binder and has been extensively reported [131, 147] as a sustained release matrix-forming excipient. HPMC is available in a variety of grades, depending on the degree of substitution and average molecular weight of the components of the polymer [146].

The use of water as granulation liquid is not appropriate for formulations with HPMC concentrations > 60 % since hig concentrations of HPMC pose problems with elasticity of wet mass to form tacky mass that can hinder further spheronisation of beads [146 - 148]. Beads containing MCC and HPMC possess fairly smooth surfaces and low friability [148, 149]. Furthermore, HPMC-based beads adsorb water and form a gel-like structure that is classified as a swelling-controlled release system with two factors that affect the rate of API release [149]. The factors include the rate of aqueous medium infiltration into the matrix and the rate of formation of a partially hydrated gel layer at the surface of the bead on contact of the polymer and gastric fluids [146]. As a result, a swelling and eroding front are observed in uncoated beads, whereas in coated systems hydrostatic pressure build-up and cracking of coating layer becomes the primary mechanism of API release [150, 151] as compared to osmotic pumping.

3.2.1.3 Methacrylic acid

Methacrylic acid and an acrylic or methacrylic ester are polymerised to produce a methacrylic acid copolymer [146]. There are three types of methacrylic acid copolymers, namely Type A or Eudragit® L, Eudragit® RL, Type B or Eudragit® S, Eudragit® RS and Type C or Eudragit® L 30 D-55. All types of methacrylic acid copolymer have a molecular mass in excess of 100 000 units, but the types vary in respect of methacrylic acid ester content and viscosity in solution [146]. Eudragit® RS PO consists of polyethylacrylate, methylmethacrylate and trimethylammonioethyl methacrylate chloride in a ratio of 1:2:0.1 [146].

Eudragit® RS PO has approximately 5 % quaternary ammonium functional groups that make it a water-insoluble polymer. The presence of insoluble quaternary ammonium functional groups provide fewer pores and channels for effective drug diffusion, resulting in a lower rate of API release [152] with a significant pH-independent permeability, resulting in sustained release. Eudragit® RS PO was used to manufacture sustained release matrix systems of CPT in these studies, as it is considered a biologically safe excipient [146].

3.2.1.4 Talc

Talc exists as a naturally hydrated magnesium silicate that exhibits batch-to-batch variability dependent on the geographical source of the material [146]. Talc is a white to greyish-white fine powder that is used in oral dosage formulations as a glidant to improve the flow properties of powder blends [23], thereby ensuring content uniformity between different batches of beads.

3.2.1.5 Surelease®

Water is the most common granulation fluid used in extrusion and spheronisation as it functions as a binder during wet massing, provides sufficient plasticity to the extrudate, and facilitates successful rounding during spheronisation, in addition to relative ease of acquisition [135]. Surelease® E-7-19010 clear (Colorcon, West Point, PA, USA) is an aqueous dispersion of ethylcellulose that can be diluted to different concentrations and was used as a binder during wet massing in this study. The dispersion has been used to retard drug release from monolithic matrix SR formulations [145, 153, 154].

Beads intended to sustain the release of an API are regularly coated with water insoluble polymers such ethylcellulose [129, 143, 153-155]. Several commercially available coating mixtures such as Surelease® and Aquacoat® are available for coating pharmaceutical dosage forms and can be used to achieve control of API release. Aqueous dispersions of Surelease® and Aquacoat® have a significant advantage over organic solvent-based coating mixtures, particularly in respect of environmental, safety and economic considerations [145].

Ethylcellulose film coats permit modification of drug release, can mask unpleasant taste and odours such as that of CPT and can improve the overall stability of formulations. However, the main use of ethylcellulose is as a hydrophilic controlled release coating [153, 155, 156].

Ethylcellulose is an odourless, tasteless material that exhibits a high degree of light and heat stability to a temperature of at least 135 °C, which is the melting point of the material [146]. The high melting point, indicative of its high glass transition temperature that is associated with ethylcellulose based polymeric materials, makes them ideal for coating and subsequent curing. The composition of film coating mixtures and the coating technique used can affect the properties of the membranes formed, including their permeability, mechanical resistance and drug dissolution retarding properties [155]. A 25 % w/w Surelease® E-7-19010 clear dispersion diluted to different concentrations was used to coat the CPT beads manufactured in this study. The mechanism of film formation from aqueous dispersions is complex, since the polymer is present as discrete particles suspended in an aqueous medium. The ethylcellulose particles must aggregate, deform and ultimately coalesce when sprayed onto the surface of the beads [145, 157]. The coalescence process is intensely affected by the glass transition temperature of the polymer. A plasticiser was added to the aqueous dispersion to lower the glass transition temperature of the polymer and to facilitate coalescence of polymer particles. Surelease® E-7-19010 clear, unlike Aquacoat® dispersions, contains dibutyl sebacate as a plasticiser and the dispersion is stabilised with oleic acid and ammonium hydroxide. Surelease® also contains fumed silica that acts as an anti-tacking agent during coating with the pseudolatex film [155, 158, 159]. The major limitation of many aqueous coating formulations is the risk of premature permeation of API through the film [158, 159]. This is attributed to an increased permeability of the film coating or the water solubility of the API to be delivered.

3.2.2 Physicochemical properties of API

3.2.2.1 Particle size and shape

Preformulation studies of particulate solids in which the dimensions of the API and relevant excipients are elucidated are gaining significance in the process of achieving an efficient production process of efficacious dosage forms [162]. Particle size and shape can impact product performance and regular measurement of these parameters can lead to improved process and product understanding [128, 134], as they may impact bioavailability and/or stability of API intended for sustained release use.

The shape of power particles is an important consideration in preformulation studies as it may influence critical powder properties such as flowability, compatibility, content uniformity and dissolution rate of the API [126, 134]. The flow properties of powders are fundamental to quality control of raw materials and the establishment of product and content uniformity [163] and particle shape can influence blending, wet granulation and other manufacturing procedures, including extrusion and spheronisation as described in §4.2.2 and consequently the content uniformity of a final dosage form [135]. Irregularly shaped particles generally contribute to poor flow of materials, whereas spherical particles tend to exhibit good flowability. A wide particle size distribution may result in segregation and ultimately non-uniformity of dosage forms [136, 164]. It is therefore vital to understand differences in particle size distribution and shape of raw materials for product development and quality control purposes.

Subtle variations in particle size, shape and source of raw material exhibit differences that affect the final product performance and appearance and can be elucidated in quality control testing [164]. The morphology of powder particles may have a significant bearing on particle size distribution of powders independent of whether the particles are spherical, cuboidal, flake-like, pyramidal, flaky, granular, rod- or needle-like, block-shaped, sponge-like and fibrous in nature [128,134, 136].

One of the methods for determining particle size is the use of sieve stacks [128, 134] that involve passing API or excipient powder passed through standard sized sieves. The method described in United States Pharmacopoeia 29 and National Formulary 24 (USP-29 NF-24) [165] to measure particle size was used to characterise the materials in this study. The sieve stack included sieves

of 0.315, 0.80, 1.25 and 2.0 mm (Mesh DIN 4188, 1977 Pruf-Sieb, Germany) stacked in descending order of aperture size. Approximately 10 g of Methocel® K100M, Methocel® E4M, Avicel® PH102, Eudragit® RS PO and talc were placed in the top sieve and were sieved manually for 5 minutes. The powder was collected on each sieve and was weighed to determine the percent (w/w) of each size retained to determine the size distribution of the materials.

3.2.3 Powder rheology

3.2.3.*1* *Angle of repose (AOR)*

The flowability of individual powders and blends thereof was determined following the measurement of the AOR. When establishing the AOR the powder under investigation is poured through a funnel stack to form a cone in order to form an angle between the base and free surface, after which the powder flows down the surface of the cone until the gravitational forces balance inter-particulate forces associated with overcoming frictional force [126, 128, 134], at which point powder flow ceases. The particles form a conical shape and the angle between the surface on which the powder resides and the free surface of the powder is known as the AOR [126, 128]. The AOR is indicative of the cohesion between the particles of the powder and is therefore an indirect measure of flowability. The relationship between the AOR and powder flow properties are summarised in Table 3.1 and values of the AOR of < 25° are indicative of good powder flow [166]. Rough and irregularly surfaced particles have high values for the AOR indicating poor powder flow [166] that can be improved through the addition of a glidant.

Table 3.1 *Relationship between AOR and powder flow.*

Angle of Repose (°)	**Flow**
< 25	Excellent
25 – 30	Good
30 – 40	Satisfactory
>40	Very poor

3.2.3.*2* *Bulk density*

The bulk density of a powder is determined after a well distributed powder is allowed to settle in a container under the influence of gravity [127, 134] and can be calculated using Equation 3.1.

$$\rho_{bulk} = \frac{Weight\ of\ powder\ mass\ (g)}{Volume\ occupied\ by\ powder\ mass\ (ml)} \qquad \textbf{Equation 3.1}$$

The powder volume includes air voids located between the particles of that powder. The size and shape of the container influences the tendency of particles to adhere to each other and the density of a powder [164]. The bulk density of a powder is an important parameter, as it is often used to establish the size of the blender to be used for the manufacture of a specific batch of tablets or beads [166].

3.2.3.*3* *Tapped density*

The tapped density of a powder is calculated using Equation 3.2. It is the ratio of the total mass of a powder to volume occupied by an aerated powder after it has been compacted or tapped for a specified period of time [164].

$$\rho_{tapped} = \frac{Weight\ of\ powder\ mass\ (g)}{Volume\ occupied\ after\ being\ tapped\ (ml)} \qquad \textbf{Equation 3.2}$$

Tapping of the powder facilitates the removal of small air voids trapped between the particles of a powder blend. The structure of a cohesive powder will collapse on tapping, resulting in a weakly flowing powder [136].

3.2.3.*4* *Carr's Index (CI)*

The bulk and tapped density of a material is used to calculate CI, which provides an indication of the compressibility of a powder. The CI is useful for evaluating sustained release and/or controlled release blends [134, 167]. The CI was calculated using Equation 3.3 and interpreted using the compressibility index summarised in Table 3.2.

$$CI = \left[\frac{\rho_{tapped} - \rho_{bulk}}{\rho_{tapped}}\right] \times 100 \qquad \textbf{Equation 3.3}$$

Where,

CI = Carr's Index,
ρ_{tapped} = tapped density, and
ρ_{bulk} = bulk density.

A low value for CI is indicative of excellent powder flow properties and is associated with low cohesiveness a powder blend [166], whereas value for the CI > 40% is indicative of extremely poor flow that may be improved by addition of a lubricant and/or glidant material.

Table 3.2 *Interpretation of Carr's Index.*

Carr's Index (%)	Type of Flow
5-12	Excellent
12-18	Good
18-23	Satisfactory
23-35	Poor
35-38	Very Poor
>40	Extremely Poor

3.2.3.*5* *Hausner Ratio (HR)*

The HR is also used to provide an indication of the flow properties of a powder and is useful for the evaluation of sustained and/or controlled release powder blends [136]. The HR is calculated using Equation 3.4 and the data can be interpreted using the information summarised in Table 3.3.

$$HR = \frac{\rho_{tapped}}{\rho_{bulk}} \qquad \textbf{Equation 3.4}$$

Where,

ρ_{tapped} = tapped density and
ρ_{bulk} = bulk density.

The addition of a glidant improves the flow properties of powders and powder mixtures exhibiting HR value between 1.25 and 1.5. Values of HR < 1.25 are indicative of good flow properties associated with low cohesiveness of powder particles in a blend [134, 167].

Table 3.3 *Interpretation of Hausner ratio.*

Hausner Ratio (HR)	Flow
1.00 – 1.11	Excellent
1.12 – 1.18	Good
1.19 – 1.25	Fair
1.26 – 1.34	Satisfactory
1.35 – 1.45	Poor
> 1.46	Very poor

3.2.4 Powder blend homogeneity

The blending of solids and semisolids is an important step in the production of pharmaceutical products, including the manufacture of beads [168]. The homogeneity of blends, otherwise known as blend uniformity analysis (BUA) is vital to produce high quality products that exhibit uniformity of content [165, 168]. The object of performing BUA studies is to achieve a uniform powder blend to manufacture CPT beads. As recommended by the FDA [169], blend uniformity testing is performed on dosage forms that contain < 50 mg API per dosage unit. If there is no content uniformity for a sample of a powder blend, the product may be recalled due to sub- or super-potent results [169]. Typical mixing practices involve blending of materials for a predetermined time, after which samples are removed from the blender and analysed using a validated HPLC or ultraviolet (UV) spectroscopic method to establish the concentration of active ingredients [168, 170]. The API content and % RSD is established and compared to known values to determine whether the blend is homogeneous [168]. If the blends are homogenous they are released for further processing. In this study, the powder mix was wet massed using the process described in §4.2.2.3.

The BUA method recommended by the FDA [169] to evaluate blend uniformity within a powder mix may result in sampling errors associated with removal of samples from the blend. If there is particle size variability between the excipients used the segregation of particles can be of concern, as inconsistency in the blend may result [170, 171]. BUA has a number of limitations in that the procedure is time consuming and it requires the use of a limited number of sample sites, making full characterisation of blend homogeneity difficult [171].

3.2.5 Drug excipient compatibility

In the pharmaceutical industry the solid state properties of an API plays a crucial role, especially in the development of dosage forms as they may affect therapeutic efficacy, toxicity, bioavailability, processing and stability [172]. Thermal analysis techniques provide an extremely sensitive measure of heat transfer on a comprehensive scale and permit the determination of the presence of a pure sample and/or drug interactions following mixing of an API with excipients [172]. The combined use different thermal analytical techniques provide specific information that facilitates rapid interpretation of the experimental data to establish if incompatibilities may exist [173, 174]. Thermal analysis of a substance and/or its reaction products subjects the material to a controlled temperature programme and measures changes in behaviour as a function of temperature [173]. Thermal analysis makes use of techniques such as thermogravimetry (TGA), derivative thermogravimetry (DTG), differential thermal analysis (DTA) and differential scanning calorimetry (DSC).

Thermal methods of analysis are widely used for the characterisation of solid API and excipients and these techniques are established for quality control, stability, drug-excipients interaction, polymorphism and purity studies of raw materials and pharmaceutical products [173, 175]. The use of thermal analysis for the identification of drug-excipient incompatibility is important in formulation development as the data provide assistance in the selection of appropriate excipients to produce stable dosage forms [162].

3.2.5.*1* *Thermogravimetric analysis*

Thermogravimetric analysis (TGA) is a technique in which the change in sample mass is determined as a function of temperature, $\frac{d\Delta m}{d\Delta T}$ and/or time, $\frac{d\Delta m}{d\Delta t}$ while the sample is subjected to a controlled temperature programme [176]. In differential thermogravimetry (DTG), the difference in temperature between the sample and reference is monitored as a function of time and/or time. Either approach results in the generation of a first derivative TGA curve with a series of peaks rather than a stepwise curve [176]. The presence of a plateau in the TG curves corresponds to a plateau in the DTG curve, since $\frac{d\Delta m}{d\Delta t} = 0$. A maximum in the DTG curve is obtained when the TGA curve has an inflection point when mass loss is rapid [162, 176]. TGA is used to improve product quality through establishing stability using isothermal and non-isothermal kinetic methods

[32, 176] and it is also used to assess the compatibility of an API with commonly used pharmaceutical excipients.

3.2.5.*2* *Differential Scanning Calorimetry (DSC)*

DSC is widely used [177, 178] to characterise properties of materials such as melting point, glass transition and purity of amorphous and crystalline compounds. The use of DSC also permits the acquisition of information relating to polymorphism and associated characteristics [178, 179]. DSC measures the difference in heat required to maintain a sample and a reference at the same temperature as they are heated and subsequently cooled. Any difference seen in the energy input to the sample and reference corresponds to a thermal event in the sample [178]. Empty aluminium, tin, zinc or indium pans are used as the reference as they are inert and can withstand elevated temperatures [176]. If an endothermic reaction occurs, the rate of heat flow during a phase transition results in heat energy being absorbed by the sample resulting in a positive rate of change of heat flow [177, 178].

While DSC cannot be used to determine the chemical nature of a sample undergoing testing the results of testing can be used to determine if samples have different thermal properties and thus are likely to be different e.g. starting material and product of a chemical reaction [179]. DSC was used to determine drug-excipient compatibility in 1:1 binary mixtures following analysis of CPT alone.

3.2.5.*3* *IR Spectroscopy*

Transitions in the vibrational energy levels of an API or powder blend can be experimentally monitored as a consequence of absorption in the IR region of the light spectrum and IR spectroscopy with Fourier Transform IR (FT-IR) capability is used for the physical characterisation of mixtures of powders in the solid state [33, 180, 181]. IR spectroscopy is a critical tool for the study of API-excipient interactions as the technique permits easy elucidation of structural attributes as it is sensitive to molecular vibration as a result of chemical or physical factors [180]. Molecular vibrations are characterised according to the energy associated with the functional groups present in an API molecule within the range of 650 – 4000 cm^{-1} [163]. FT-IR spectra were used to generate information relating to the chemical and physical reactions of API-

excipient blends. To minimise incorrect conclusions the spectrum of CPT alone was used for comparison with those generated from analysis of binary mixtures of CPT and potential excipients.

3.3 METHODS

3.3.1 Scanning Electron Microscope (SEM)

The particle shape and surface morphology of powders were investigated using a VEGA LMU© Scanning Electron Microscope (Tescan, Czechoslovakia Republic). A small amount of CPT (Protea chemicals, Midrand, South Africa), Avicel® PH102 (FMC International, Wallingstown, Cork, Ireland), Methocel® K100M Premium (Colorcon® Ltd., Dartford, Kent, United Kingdom), Methocel® E4M (Colorcon® Ltd., Dartford, Kent, United Kingdom), Eudragit® RS PO (Evonik Industries, Pharma Polymers, Darmstadt, Germany) and talc (Aspen Pharmacare, South Africa) were dusted onto double-sided carbon tape mounted on a separate disc carrier (3 mm height, 10 mm diameter) and were sputter coated under vacuum (0.25 Torr) with gold for 30 minutes (Balzers Union Ltd., Balzers, Lichtenstein). The samples were then visualised using SEM at an accelerated voltage of 20 kV.

3.3.2 Angle of repose (AOR)

The AOR was measured using a funnel method. The stationary AOR for each powder was performed by placing 10 g of material in a funnel with orifice and base diameters of 1.0 and 5.0 cm respectively. The tip of the funnel orifice was set at a fixed height of 30 cm above a horizontal surface and the powders were allowed to flow under the force of gravity. The AOR (n=3) was calculated using Equation 3.5 and reported as an average.

$$\tan\theta = \frac{h}{r} \qquad \textbf{Equation 3.5}$$

Where,

h= height of the pile of powder, and
r = radius of the base of the cone.

The preliminary formulations listed in Table 3.4 obtained from changing one factor approach were assessed for their flow and powder densities prior to formulation.

Table 3.4 *Formulation composition of powder blends used in preliminary studies.*

Formulation	*CPT	*MCC	*HPMC K100M	*HPMC E4M	*Eudragit® RS PO	*Talc
F1	20	77.5				2.5
F2	20	65	12.5			2.5
F3	20	65		12.5		2.5
F4	20	65			12.5	2.5
F5	20	57.5	10	10		2.5
F6	20	57.5	10		10	2.5
F7	20	57.5		10	10	2.5
F8	20	47.5	20	10		2.5
F9	20	47.5	20		10	2.5
F10	20	47.5		20	10	2.5
F11	20	47.5	10	20		2.5
F12	20	47.5	10		20	2.5
F13	20	42.5	10	10	10	2.5
F14 (CPT-001)	20	40	15	7.5	15	2.5

* % w/w content

3.3.3 Powder density

The FDA [163] recommends that all powders must be sieved to disrupt agglomerates that may have accumulated during packing and storage. The sieving process must be undertaken gently to avoid alteration in the nature of the powders under investigation. The powders analysed included CPT, MCC, HPMC K100M, HPMC E4M, Eudragit® RS PO and talc. Approximately 10 g of each powder was transferred into separate 100 mL graduated measuring cylinders and the bulk density was established as described in §3.2.3.2. The tapped density of each powder was determined with the aid of a Model SVM 203 tapped density tested (Erweka GmbH, Heueastamm, Germany), operated at a rate of 200 taps per minute for two (2) minutes. Following two minutes of agitation, the volume of the tapped powder was noted and the tapped density calculated as described in §3.2.3.3. The HR and CI were calculated using Equations 3.3 and 3.4. The measurement of bulk density, tapped density, CI and HR were measure in replicates (n=3) and the average recorded.

3.3.4 Powder blend homogeneity

A Kenwood Multi-Pro FP580 planetary mixer (Kenwood Ltd., Maraisburg, South Africa) was used to blend the powder mixtures. Prior to loading powders into the blender, all powders were passed through a sieve of 0.80 mm (Mesh DIN 4188, 1977 Pruf-Sieb, Germany). The blender was filled to approximately 50% v/v of the working capacity with 200 g of the powder mixture, which is within the acceptable range of filling of blenders [184].

Blending was continued for 30 minutes and 1g samples were withdrawn at 2, 5, 10, 15, 20, 25 and 30 minutes from six different locations in the powder bed using a stainless steel laboratory spatula in Figure 3.2.

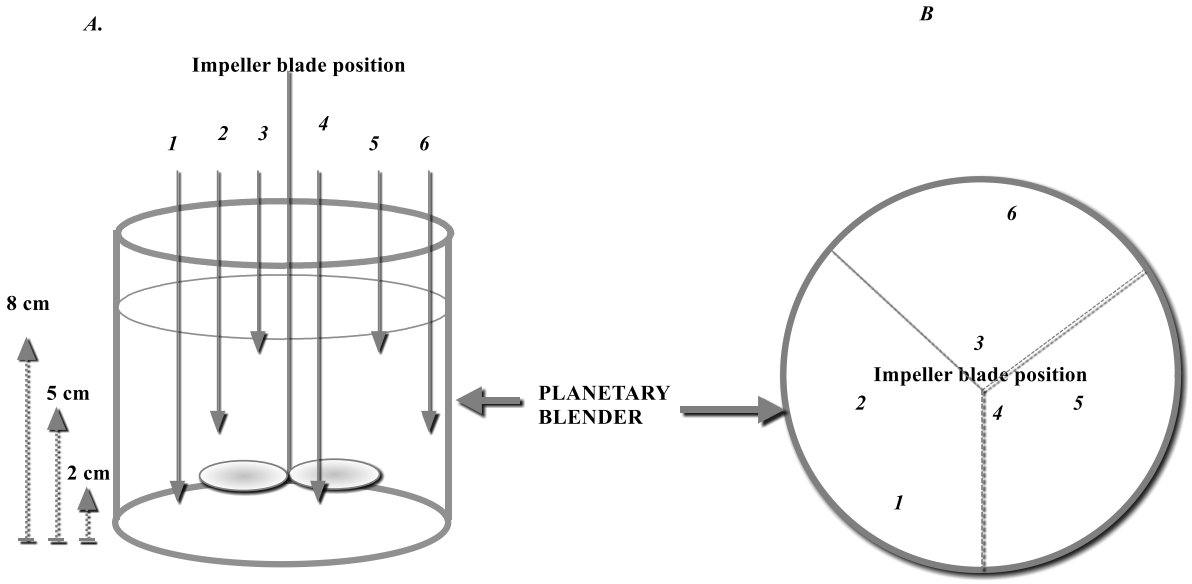

Figure 3.2 A) *Lateral and* ***B)*** *aerial view showing six positions of BUA sampling adapted with slight modifications from El-Hagrasy et al. [170.*

The powder was transferred to a 100 mL A-grade volumetric flask and dissolved in a MeOH: water mixture (49:51 % v/v) adjusted to pH 3.27 using 85 % v/v ortho-phosphoric acid and then sonicated for 5 minutes using a Model B-12 Ultrasonic bath (Branson Cleaning Equipment Co., Shelton, Connecticut, USA). Approximately 5.0 mL of each solution was filtered through a 0.45 µm Durapore® membrane HVLP filters (Millipore Corporation, Ireland) and 2.5 mL of the filtered solution was transferred into a 25 mL A-grade volumetric flask containing 2.5 mL of IS solution.

The sample was made up to volume with mobile phase and analysed using the validated HPLC method described in §2.5.5.

3.3.5 Thermogravimetric Analysis (TGA)

Approximately 4 mg of CPT and/or 1:1 binary mixtures with excipients were placed in platinum crucibles. TGA experiments were performed using a Model TGA 7 PerkinElmer Thermogravimetric Analyser (PerkinElmer Inc., Massachusetts, USA) fitted with a platinum sample holder. Pyris™ Manager Software (PerkinElmer Inc., Massachusetts, USA) was used for data analysis. Measurements were performed in triplicate for each sample under a nitrogen atmosphere at flow rate of 25 mL/min using a heating rate of 10 °C/min over the temperature range 25 – 600 °C.

3.3.6 Differential Scanning Calorimetry (DSC)

CPT, individual excipients and 1:1 CPT excipient mixtures were mixed and passed through 0.80 mm mesh sieve (DIN 4188, 1977 Pruf-Sieb, Germany) before being placed directly into aluminium pans prior to analysis. The DSC was calibrated with Indium (m.p. = 156.6 °C; ΔH_{fus}= 28.54 J/g) prior to analysis. Approximately 3 mg of CPT, excipients or binary mixtures of CPT and excipients were placed into aluminium pans and then sealed. The sealed pans were placed directly onto the hot stage of the DSC instrument. DSC thermograms curves were generated using a Model DSC-7 PerkinElmer Differential Scanning Calorimeter (PerkinElmer Inc., Massachusetts, USA). Pyris™ Manager Software (PerkinElmer Inc., Massachusetts, USA) was used to analyse the thermograms. The temperature of the DSC was monitored using a central processor and a controlled heating rate of 10 °C/min was used for analysis over the temperature range of 25 - 200 °C. The conditions for the analysis were a compromise between speed of analysis and heating rate to facilitate acquisition of enthalpy changes in the sample. Each thermogram was acquired at 10 scans per revolution of 4 cm^{-1}. All DSC analyses of samples were performed in triplicate under a nitrogen atmosphere purged at flow rate of 20 mL/min.

3.3.7 IR Absorption Spectroscopy

The IR absorption spectra of CPT, individual excipients and binary mixtures were generated using a Spectrum 100 FT-IR ATR Spectrophotometer (PerkinElmer®Inc., Beaconsfield, United Kingdom). Binary mixtures were prepared by weighing 0.5 g of each material using a Mettler AG 135 top loading balance (Mettler Instruments, Zurich, Switzerland) and gently blended in a mortar and pestle. A small amount of the powder mixture was placed on a diamond crystal and analysed over the wavenumber range, 4000 – 650 cm^{-1} at a revolution of 4 cm^{-1}.

3.3.8 Dialysis studies

Dialysis studies were performed to establish if possible interactions between a negatively charged component of a coating material and the positively charged CPT may alter the release characteristic of CPT across a semi-permeable membrane [161]. A potential interaction between the cationic drug, metoclopramide and anionic ammonium oleate was investigated using dialysis studies. The results revealed that in slower rates of metoclopramide-ammonium oleate, precipitate were observed compared to the release of the anionic drug, diclofenac [161]. The interaction of verapamil, which is a positively charged API with a negatively charged component of Surelease E-7-19010®, was also investigated. The verapamil release decreased at a high pH [186]. The decrease in verapamil release was due to the interaction of the dissociated polymer-carboxylic groups with basic tertiary amines of verapamil [186, 187]. The possible interaction of CPT and ammonium oleate in Surelease E-7-19010® was investigated.

To investigate any potential interaction between CPT and ammonium oleate a component of Surelease® E-7-19010 (Colorcon® Ltd., Orpington, Kent, United Kingdom), a dialysis study was performed. Approximately 970 mg of a 25% w/w ammonia solution was added to 4 g of oleic acid to form ammonium oleate based on an equimolar interaction. The blend was mixed thoroughly with a magnetic stirrer (Silverson, Bucks, UK) at 400 rpm and left in a fume hood for 24 hours at 22.5 ˚C. Approximately 500 mg of the ammonium oleate was dissolved in 50 mL water and 1 mL aliquots of this solution were transferred to 5 mL A-grade beakers and approximately 50 mg of CPT was accurately weighed using a Mettler AG 135 top loading balance (Mettler Instruments, Zurich, Switzerland) and added to the solution.

A 25 cm length of SpectraPor® 4 dialysis tubing (size 4, diameter 15.9 mm, molecular weight cut-off 12,000–14,000 Da) (Spectrum Medical Industries Inc., Los Angeles, California, USA) was placed into distilled water for one hour prior to dialysis. A SpectraPor® closure was tied at one end of the tube and approximately 5 mL of the sample solutions was placed into the tubing. The beaker was washed with the aid of an additional 5 mL of deionised water in a two-step process to ensure complete removal of the contents of the beaker into the dialysis tubing. The effective length of the tubing was 4.5 cm. Reference dialysis tubes were prepared, but contained a 50 mg/mL CPT solution in water. The filled dialysis tubes attached to capsule sinkers were immersed in 900 mL distilled water maintained at 37 °C and stirred with a paddle. There was a 25 mm distance between the paddle and the inside bottom of the vessel at 50 rpm using USP Apparatus 2 (Hanson SR8PLUS equipped with AutoPlus™ Maximiser and AutoPlus™ MulitFill, Hanson Research Corp, Chatsworth, California, USA). The amount of CPT released by dialysis from the tubes was determined using the HPLC method described in §2.5.5. The experiment was conducted in triplicate and sample aliquots were withdrawn every 1 hour for 12 hours and are reported as an average.

3.4 RESULTS AND DISCUSSION

3.4.1 SEM

The particle and surface morphology of CPT and excipients were analysed following SEM imaging as described in §3.3.1. The information obtained from SEM was essential to provide preliminary information in respect of the potential flow and compressibility properties of excipients and powder blends. SEM analysis was considered appropriate since SEM provides a high resolution imaging capability, is relatively simple to use [182] and permits the rapid generation of suitable images. SEM also permits analysis of the surface texture of particles in a high depth of field [182] and facilitates detailed characterisation of particle surface morphology.

Knowledge of the particles' surface texture is essential as it can influence surface area and the adherence of a powders or raw material to other particles within a powder blend [134]. SEM images of CPT and potential raw materials for bead formulations are depicted in Figure 3.3.

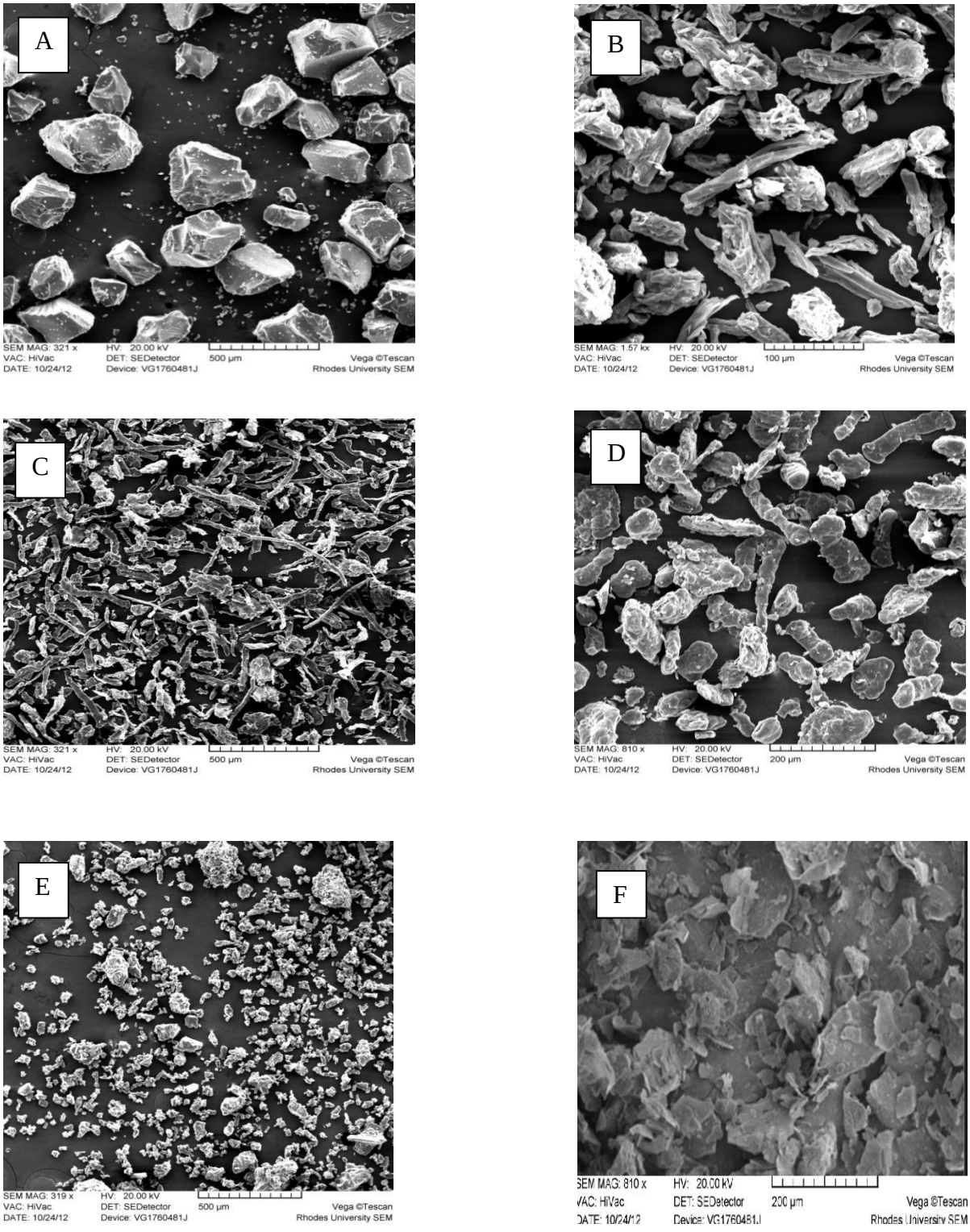

Figure 3.3 A) *Typical SEM image of CPT.* ***B)*** *Typical SEM image of MCC.* ***C)****Typical SEM image of Methocel® HPMC K100M.* ***D)*** *Typical SEM image of Methocel® HPMC E4M.****E)*** *Typical SEM image of Eudragit® RS PO.* ***F)*** *Typical SEM image of talc.*

The SEM image depicted in Figure 3.3 A reveal the solid state appearance of CPT. The particle size ranged between 10 and 30 µm in length along one side of the crystals and they form irregular flat aggregates, suggesting that CPT would exhibit poor flow properties. These particles may consequently form aggregates of approximately 100 µm diameter on storage prior to sieving.

SEM images of MCC revealed the presence of irregular, elongated crystals as depicted in Figure 3.3 B. MCC particles vary in size depending on the source of the MCC. However, most grades exhibit porous particles [146]. To make a final assessment on the flow properties, supplementary testing will be required to describe the flow properties of powder blends. The variable particle size of MCC indicates that it may be necessary to sieve the material when manufacturing a dosage form to ensure final product particle size uniformity.

A SEM micrograph of Methocel® HPMC K100M is shown in Figure 3.3 C and that of Methocel® HPMC E4M in Figure 3.3 D. Methocel® HPMC K100M has longer cylindrical fiber-shaped particles, whereas Methocel® E4M is an irregularly shaped granular material. The Eudragit® RS PO particles depicted in Figure 3.3 E were crystalline and on close examination, most of the powder particles had rough edges. Eudragit® RS PO particles showed a high degree of sphericity and the presence of nonporous particles with rough edges are indicative of poor flow properties. Approximately 70% of the Eudragit® RS PO particles were fine powders with a low potential for segregation. The SEM image of talc depicted in Figure 3.3 F revealed the presence of a flake-like crystalline powder with smooth surface morphology. Most of the talc flakes were in the size range of 5 – 50 µm and were irregularly shaped. They may subsequently agglomerate on storage. The presence of agglomerates highlights the necessity to sieve all powders prior to manufacture.

3.4.2 Powder density

The bulk and tapped density of the API and excipients used in formulation development studies were established and used to calculate CI and HR to assess the compressibility of the materials. A summary of these results are listed in Table 3.5 for the individual powders.

Table 3.5 *Summary of preformulation powder densities of CPT and excipients.*

Property	Bulk Density (g/mL)	Tapped Density (g/mL)	CI (%)	HR	AOR (°)
CPT	0.46±0.12	0.57±0.19	18.9±2.09	1.23±0.03	36.9±2.8
MCC	0.35±0.03	0.44±0.25	21.3±3.88	1.27±0.06	34.7±2.1
	0.34*	0.45**			
K100M	0.31±0.04	0.44±0.33	29.2±4.35	1.41±0.09	39.4±1.7
	0.34*	0.56**			
E4M	0.43±0.16	0.59±0.23	26.1±1.47	1.35±0.02	30.3±0.8
	0.34*	0.56**			
RS PO	0.59±0.25	0.75±0.39	21.5±4.82	1.27±0.08	22.5±1.1
	0.39*	0.42**			
Talc	0.52±0.09	0.66±0.81	21.4±4.98	1.27±0.08	35.9±0.2

*Reference bulk density [42].
** Reference tapped density [42].

The bulk and tapped densities of CPT and excipients were used to calculate CI and HR as described in §3.2.3.4 and §3.2.3.5. According to the classification of CI described in Table 3.2 CPT, MCC and Eudragit® RS PO exhibit satisfactory flow properties. HPMC K100M and HPMC E4M exhibit poor flow properties since the HR values were 1.41 and 1.35 respectively. Both are > 1.25, indicating that the materials exhibit poor flow properties. It is therefore important to assess the flowability of excipients before and after blending to ensure that the powder flows adequately prior to wet massing, extrusion and spheronisation. The data revealed that a formulation that includes a glidant will exhibit enhanced flow properties when compared to flow if powders alone. The experimental data are in close agreement with literature that addresses bulk and tapped density as depicted in Table 3.4. This suggests that the excipients have adequate physicochemical properties for extrusion and spheronisation.

MCC is an ideal excipient in most bead formulations as it exhibits a high degree of porosity [164] and the porous surfaces provide sites for fine particles of API to be distributed homogenously through the powder blend. The powder blends of different formulations were manufactured to determine the bulk density, tapped density, CI, HR and AOR for each product and a summary of the results are listed in Table 3.6.

Table 3.6 *Micromeritic properties of CPT powder blends.*

Formulation	Density (g/mL)		CI (%)	HR	AOR (°)
	Bulk Density	**Tapped Density**			
F1	0.69±0.08	0.99±0.04	30.31±1.01	1.43±0.34	30.34±4.25
F2	0.72±0.01	0.99±0.17	27.27±3.05	1.38±0.41	25.28±3.78
F3	0.69±0.04	0.83±0.25	16.86±2.34	1.20±0.28	33.67±3.69
F4	0.64±0.03	0.78±0.33	17.94±1.76	1.21±0.43	27.11±1.28
F5	0.73±0.06	0.92±0.21	20.65±3.10	1.26±0.39	29.23±2.07
F6	0.61±0.15	0.87±0.13	29.88±2.87	1.42±0.18	25.32±3.15
F7	0.69±0.27	0.90±0.34	23.33±3.42	1.30±0.26	26.05±2.11
F8	0.73±0.21	0.88±0.16	17.04±3.96	1.21±0.53	29.86±1.57
F9	0.77±0.39	0.96±0.29	19.79±2.40	1.25±0.22	32.56±2.33
F10	0.68±0.11	0.87±0.14	21.83±2.07	1.27±0.35	27.75±1.63
F11	0.71±0.26	0.96±0.39	26.04±3.71	1.35±0.12	28.73±2.58
F12	0.64±0.24	0.89±0.22	28.08±1.24	1.39±0.36	30.17±4.66
F13	0.58±0.13	0.76±0.19	23.68±2.96	1.31±0.29	27.06±1.46
F14 (CPT-001)	0.59±0.28	0.69±0.28	14.49±1.67	1.16±0.18	29.56±2.89

The results of bulk and tapped density testing ranged between 0.58 ± 0.13 g/mL to 0.77 ± 0.39 g/mL and 0.69 ± 0.28 g/mL to 0.99 ± 0.17 g/mL respectively. Increasing the molecular weight of HPMC resulted in a decrease in bulk density. These results are in agreement with those reported by Efentakis and Vlachou [183], who concluded that bulk density of blends increased when the molecular weight of the polymer used in the blends is decreased.

The results for CI and HR indicate satisfactory to poor flow properties for powder blends of the different formulations. The results support evidence that significantly improved flow properties can be achieved if talc is included in the different blends. The micromeritic properties indicate that the powder blends exhibit satisfactory flow properties that would facilitate the production of products that exhibit uniform content. Therefore a blending process was considered feasible to manufacture powder blends prior to wet massing, extrusion and spheronisation.

3.4.3 AOR

There is an empirical relationship between AOR and flowability of powders that is depicted in Table 3.1. The AOR of individual excipient powders are listed in Table 3.4 and that of powder blends are summarised in Table 3.5 and ranged between 22.5 ± 1.1° to 39.4 ± 1.7° and 25.28 ± 3.78° to 32.56 ± 2.33° respectively. The results reveal that CPT and all excipients investigated have satisfactory or poor flow properties that are confirmed by the CI and HR results. The AOR for all batches except F1, F9 and F12 exhibited good flow properties. These results support the fact that a glidant may be necessary in the formulation to promote adequate flow properties of the powder blends to enable the production of homogenous dosage forms. Talc is a glidant and improves the flow properties of powder blends by dispersing between particles to reduce surface irregularity and therefore decrease inter-particulate friction [134, 146]. The flowability results suggest that batch CPT-001 has the best flow properties, since the CI was 14.49 %, the HR of 1.16 and an AOR of 29.56°.

3.4.4 Powder blend homogeneity

The results of blend homogeneity testing conducted for 30 minutes blending for Batch CPT-001 are summarised in Table 3.7. The content of powder blend at six different positions within the mixer was determined using the validated HPLC method described in §2.5.5.

Table 3.7 *Blend homogeneity of batch CPT-001 blending.*

Blending Time (mins)	Position of Sample	Theoretical Content (mg)	Actual Content (mg)	% Content	% RSD
2	**1**	50	121.61	243.21	10.32
	2	50	170.61	341.23	9.68
	3	50	49.81	99.61	4.18
	4	50	79.89	159.78	2.11
	5	50	112.96	225.92	15.79
	6	50	137.71	275.42	4.11
5	**1**	50	95.05	190.1	6.12
	2	50	43.52	87.05	3.58
	3	50	35.92	71.84	3.92
	4	50	100.37	200.75	5.55
	5	50	101.35	202.70	2.87
	6	50	129.56	259.13	3.06
10	**1**	50	84.40	168.80	3.11
	2	50	48.14	96.28	2.92
	3	50	40.15	80.31	3.85
	4	50	69.04	138.08	4.16
	5	50	43.53	87.07	4.33
	6	50	112.96	225.92	4.24
15	**1**	50	52.57	105.14	0.98
	2	50	46.79	93.59	2.01
	3	50	69.04	138.08	1.32
	4	50	53.11	106.22	1.04
	5	50	52.57	105.14	0.35
	6	50	51.83	103.66	0.78

Table 3.7 *Blend homogeneity of batch CPT-001 blending.*

Blending Time (mins)	Position of Sample	Theoretical Content (mg)	Actual Content (mg)	% Content	% RSD
20	**1**	50	52.01	104.01	0.32
	2	50	51.02	102.03	0.22
	3	50	51.03	102.05	0.21
	4	50	52.37	104.75	0.54
	5	50	52.01	104.01	0.22
	6	50	51.98	103.97	0.28
25	**1**	50	53.91	107.83	0.37
	2	50	50.57	101.14	0.28
	3	50	51.87	103.74	0.19
	4	50	51.88	103.76	0.41
	5	50	50.53	101.07	0.22
	6	50	53.92	107.83	0.03
30	**1**	50	50.49	100.98	0.35
	2	50	50.11	100.21	0.99
	3	50	50.53	101.07	0.85
	4	50	51.73	103.47	0.62
	5	50	49.81	99.61	0.51
	6	50	50.85	101.71	0.73

The results reveal that the content varied within the powder blend between 102.03 ± 0.22 % and 104.75 ± 0.54 % at 20 minutes. The variability is likely due to the difficulty in withdrawal of samples using a spatula for sample collection at time intervals ≤ 15 minutes. A change in the insertion angle using a sample probe may minimise variation in API content. The potency and percent RSD for the blends at different positions at different times are depicted in Figure 3.4.

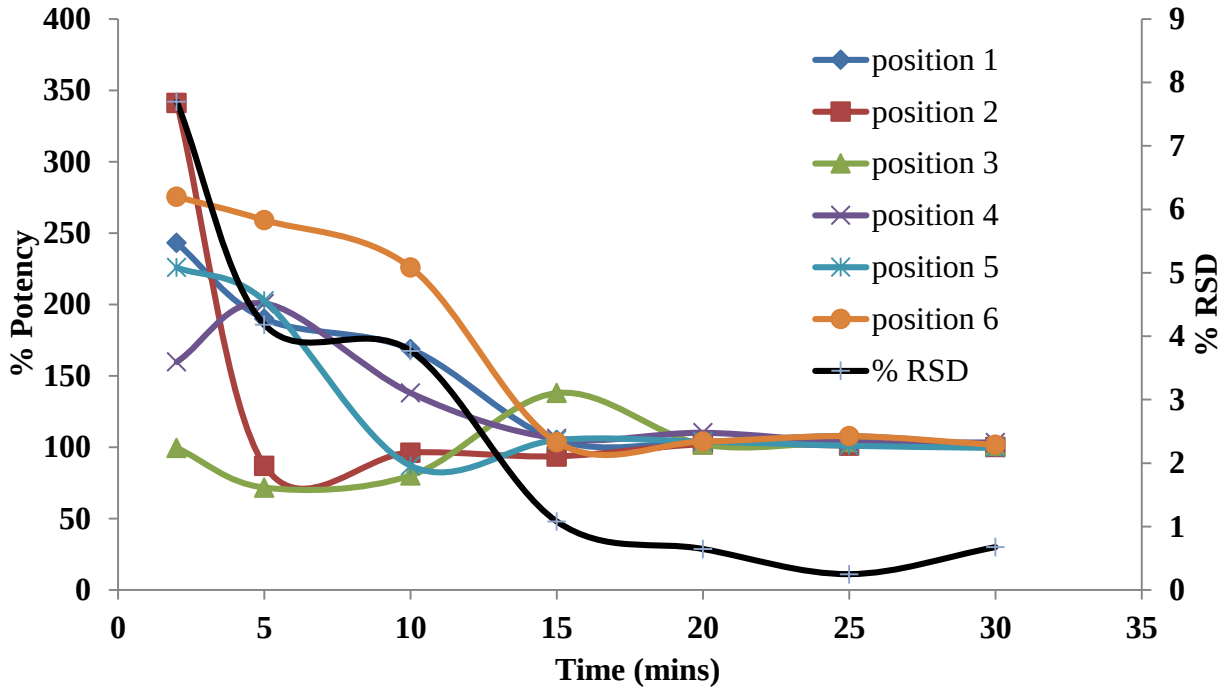

Figure 3.4 *Potency and % RSD results for powder blend homogeneity at different positions in the mixer.*

The results reveal that the potency varied between 100 % and 350 % over the first 10 minutes of blending and the difference can be attributed to the fact that CPT was loaded into the blender from position 1 resulting in an initial high assay value that side of the blender when compared to the assay of a sample from position 3. On prolonged blending the potency values equilibrated to an acceptable % RSD of < 1 % after 20 minutes of blending. The end point determination for blending was based on the mean and standard deviation (SD) acceptance criteria stated in the PDA technical report No. 25 [184] that calls for all samples to be between 90 and 110 % of the label claim and the % RSD to be ≤ 5 % at that point. These results indicate the importance of identifying an exact time end point for the blending process to avoid subsequent loss of homogeneity when mixing is unnecessarily long.

3.4.5 TGA

TGA of CPT performed under nitrogen revealed that CPT is stable up to a temperature of approximately 180 °C, after which a three-step decomposition occurs as depicted in Figure 3.5.

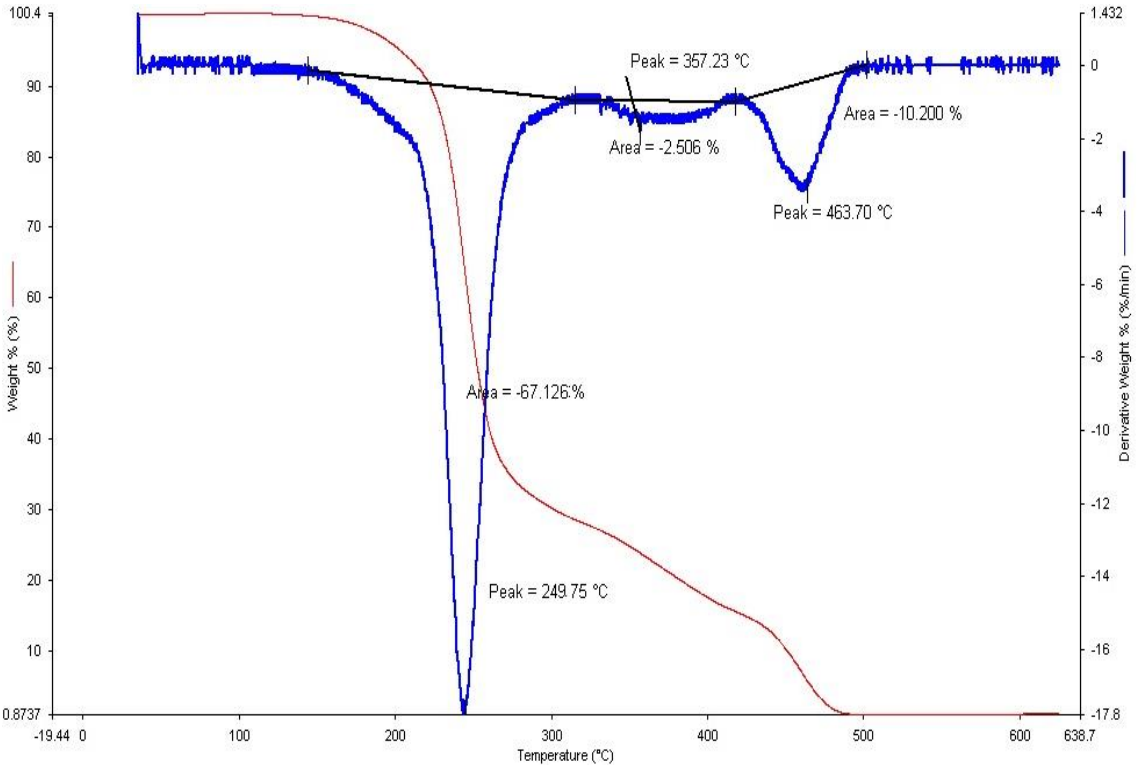

Figure 3.5 *TGA thermogram of CPT generated at a constant heating rate of 10 °C/min.*

CPT decomposes in the temperature range 160 °C - 450 °C [32]. The TGA thermogram depicted in Figure 3.5 revealed that CPT degraded in a similar three-step decomposition process over the temperature range 180 °C - 470 °C. The first significant decomposition of CPT relates to 67 % weight loss observed from the initial 4 mg analysed. The decomposition commences at 180 °C, which is suggestive of the elimination or degradation of the cyanide (C-N) bond present in the CPT molecule [32] and the curve is almost symmetrical about 249.75 °C in the first phase of decomposition. The second step of decomposition commences at 320 °C and ceases at 390 °C and corresponds to a 2.5 % loss of weight. The last step of decomposition commences at 400 °C and the maximum rate of decomposition occurs at 463.7 °C.

The first noticeable phenomenon at 106 °C on the TGA thermogram corresponds to melting point of CPT. The maximum signal with respect to the rate of change $\frac{d\Delta m}{d\Delta T}$ occurs at 249.75 °C and is a sharp peak representing the primary decomposition of CPT between 25 °C and 600 °C. The weight change during decomposition is depicted in an overlay on the DTG curve. A small quantity of carbon residue and characteristic sulphurous odour as a consequence of CPT combustion was evident at the end of the experiment.

3.4.6 DSC

The DSC thermograms for CPT and 1:1 binary mixtures of CPT with excipient are depicted in Figures 3.6 – 3.11. The thermograms are typical examples of derivative heat flow curves with respect to temperature. The DSC thermogram of pure CPT depicted in Figure 3.6 reveals a sharp endothermic event between 105 and 115 °C and a melting temperature range of 106 – 109 °C. The thermal transition (T_{peak}) at 110.93 °C with a T_{onset} at 107.61 °C corresponds to the presence of the α form of CPT, which melts at 106 °C, and the ΔH_{fusion} of – 24.92 J/g is in reasonable agreement to reported values [66].

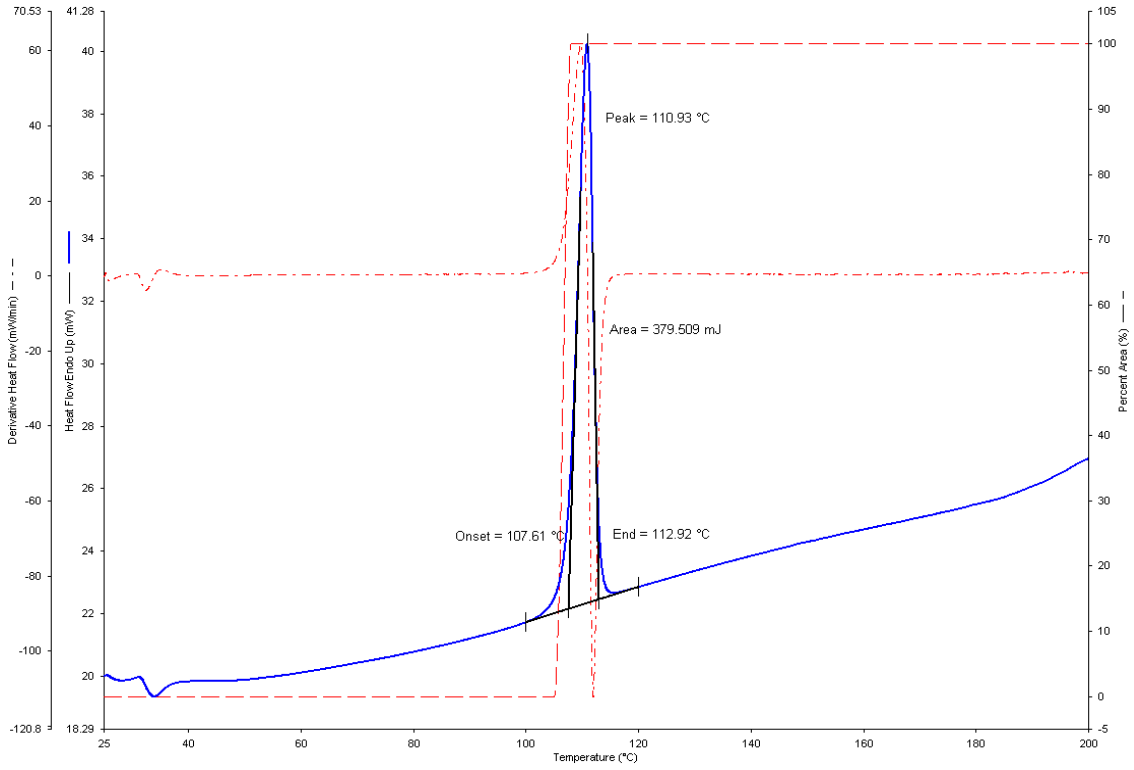

Figure 3.6 *Typical DSC thermogram for CPT determined at a heating rate of 10 °C/min.*

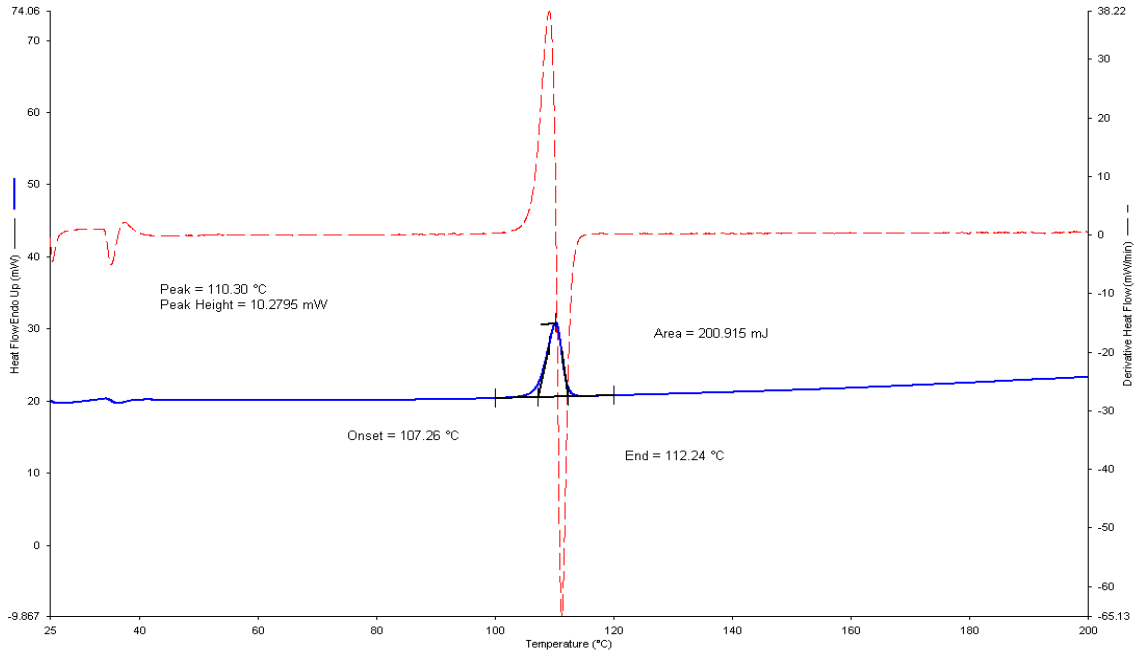

Figure 3.7 *Typical DSC thermogram for a 1:1 mixture of CPT and MCC determined at a heating rate of 10 °C/min.*

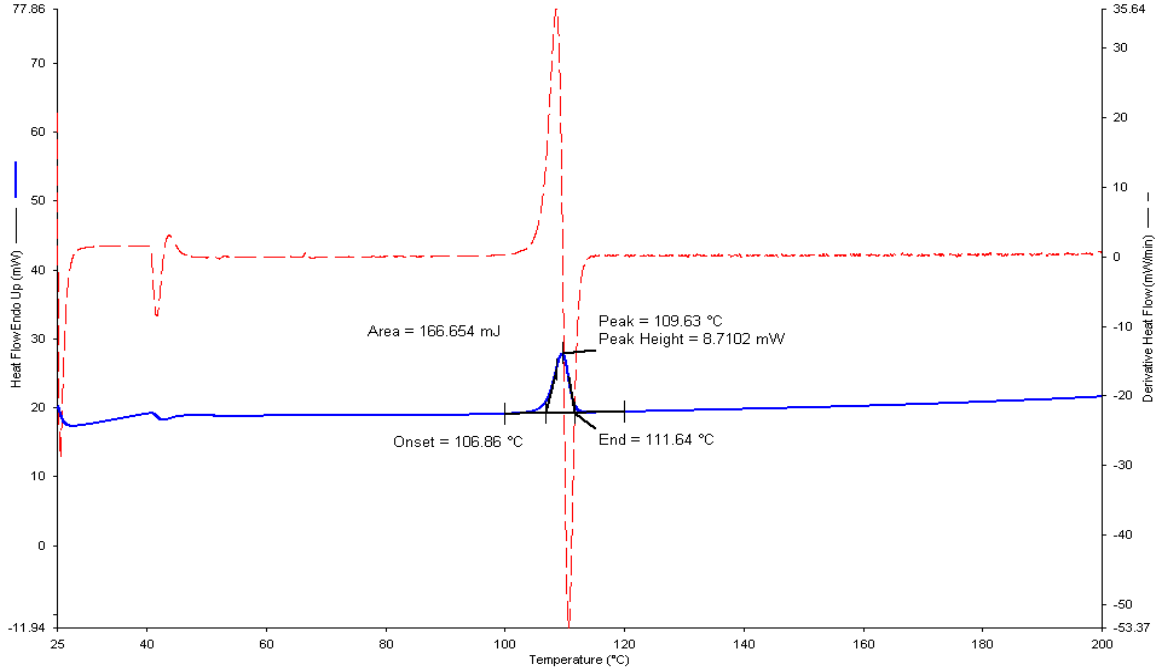

Figure 3.8 *Typical DSC thermogram for a 1:1 mixture of CPT and HPMC K100M determined at a heating rate of 10°C/min.*

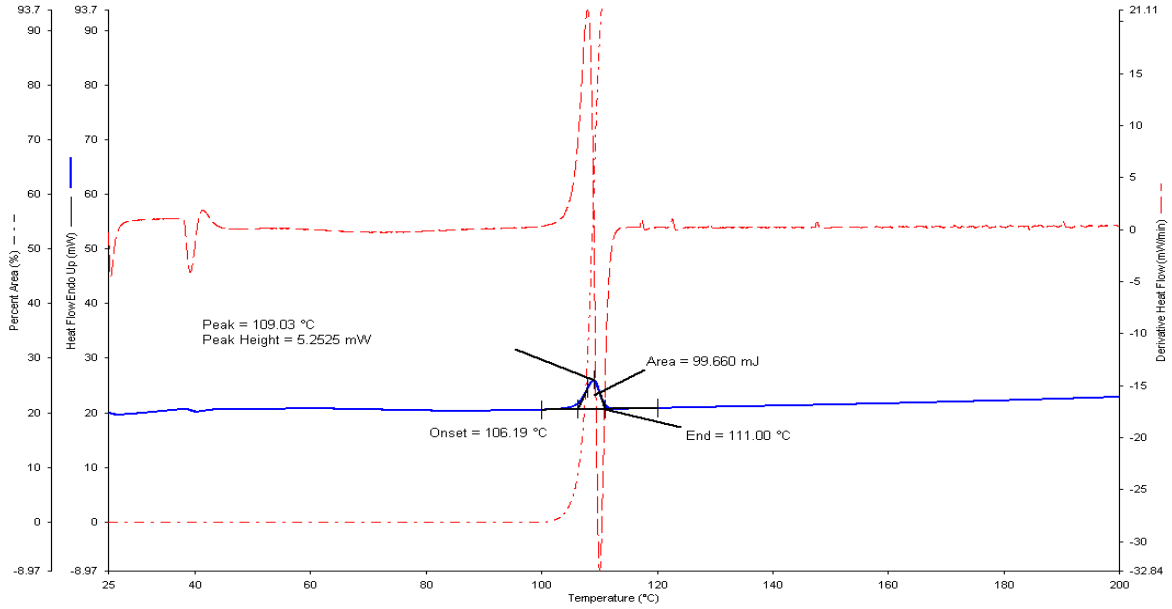

Figure 3.9 *Typical DSC thermogram for a 1:1 mixture of CPT and HPMC E4M determined at a heating rate of 10 °C/min.*

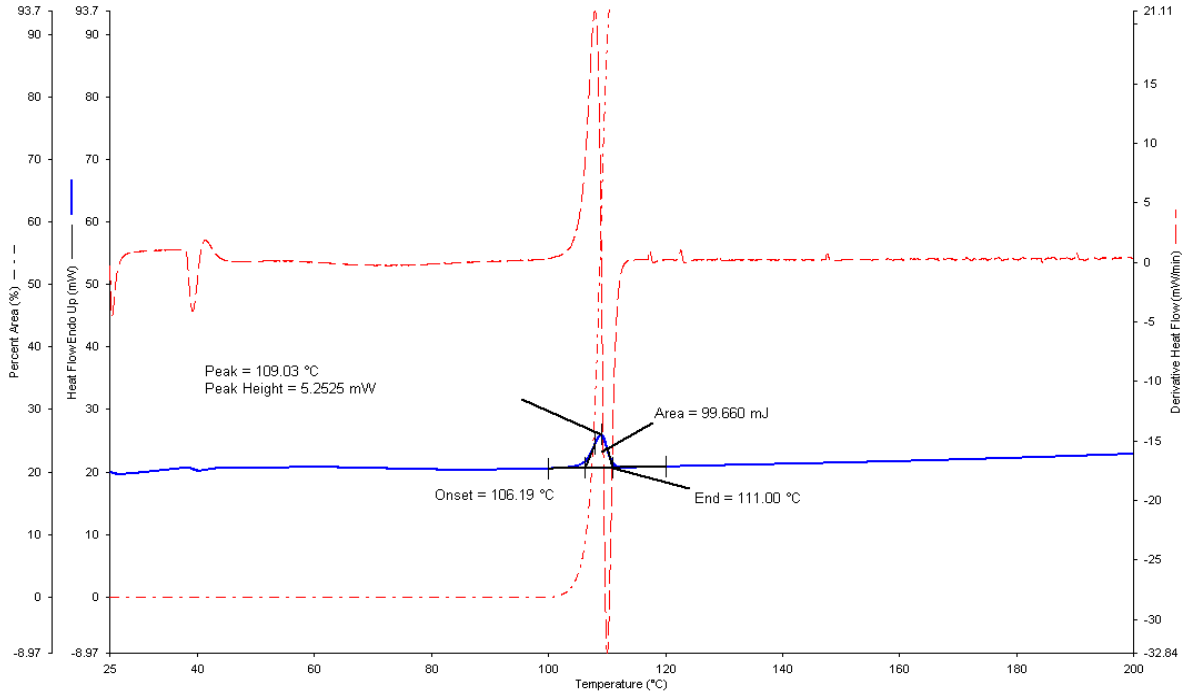

Figure 3.10 *Typical DSC thermogram for a 1:1 mixture of CPT and Eudragit® RS PO determined at a heating rate of 10 °C/min.*

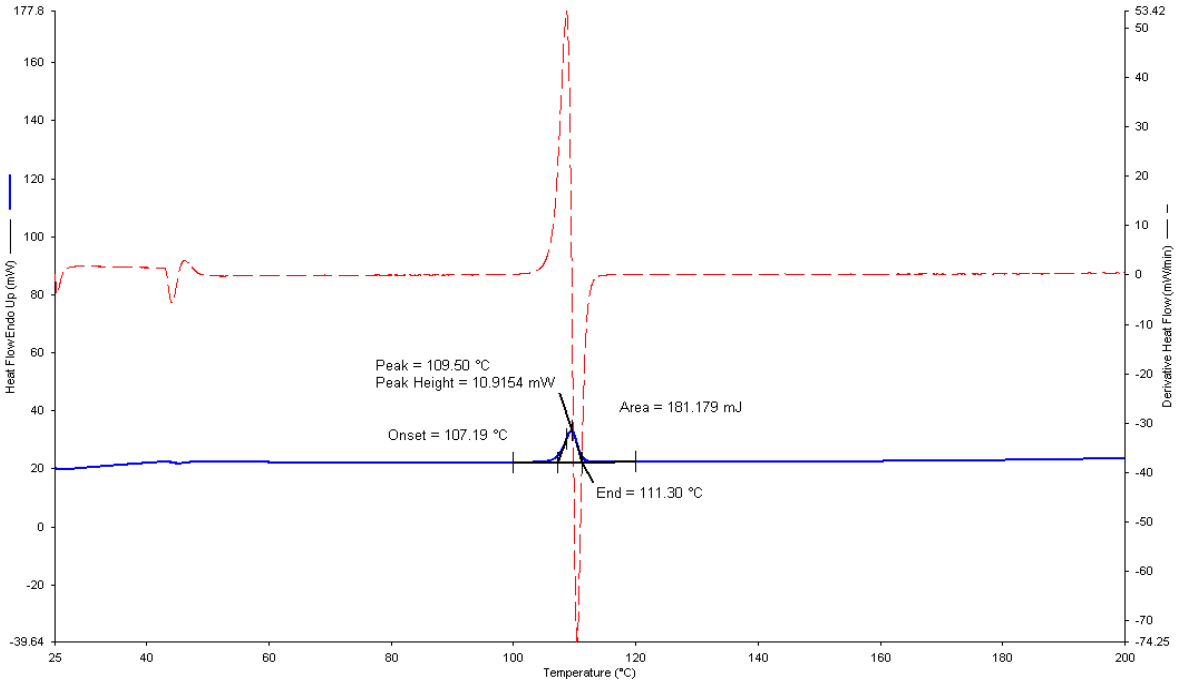

Figure 3.11 *Typical DSC thermogram for a 1:1 mixture of CPT and talc determined at a heating rate of 10 °C/min.*

The selection of acceptable excipients for a formulation is primarily based on the physico-chemical properties and compatibility of the API with potential excipients. The process of selecting excipients is integral in formulation development, particularly for generic pharmaceutical dosage forms. The majority of the thermograms for binary mixtures of CPT and potential excipients mixtures showed the melting endotherm for CPT, which was wider. It fluctuated between a slightly lower or higher temperature for a T_{peak} of 110.93 °C that was observed for pure CPT. However, the endotherms were, unchanged and this can be considered as an absence of incompatibility interactions between CPT and the excipients tested. The slight changes in the melting endotherm for CPT may be due to the mixing of CPT and excipients, which lower the purity of the API, and may not necessarily, indicate that a possible incompatibility exists.

The DSC curves for 1:1 mixtures of CPT and Avicel® PH 102, Methocel®K100M, Methocel® E4M, Eudragit® RS PO and talc showed an endothermic peak in the range 106 – 111 °C, which is characteristic of the melting point of CPT and the ΔH_{fusion} are summarised in Table 3.8. The results are in agreement with the thermoanalytical curves of the physical mixtures with a slight displacement of the melting endotherm for CPT.

Table 3.8 *Thermoanalytical data for CPT and 1:1 binary mixtures.*

	DSC		
Sample	**T_{onset} (°C)**	**T_{peak} (°C)**	**ΔH_{fusion} (J/g)**
API			
CPT	107.61	110.93	24.92
Binary Mixture			
CPT: MCC	107.26	110.30	50.23
CPT: HPMC K100M	106.86	109.63	41.67
CPT: HPMC E4M	106.19	109.03	24.92
CPT: Eudragit® RS PO	105.62	109.07	17.32
CPT: Talc	107.19	109.50	45.29

One of the advantages of using DSC as an analytical tool is that it permits rapid evaluation of potential interactions with a small number of samples [177, 178]. Although there is wide spread recognition that the presence of a physical or chemical interaction does not necessarily point to an incompatibility, it is generally established that any alterations observed in a DSC thermogram is proof that an interaction may exist [179]. Stability studies may be necessary to confirm the fact that no incompatibilities exist. The high temperatures that are used for TGA are not used in most manufacturing processes, and as all procedures during extrusion-spheronisation are performed at ambient temperatures and the subsequent coating procedure for CPT beads at slightly elevated temperatures, incompatibility reactions were not considered likely under these conditions. Performing TGA at high temperatures increases the temperature of reaction kinetics, which may alter the physicochemical properties of samples under investigation. To establish whether an incompatibility exists, additional techniques such as TGA, FT-IR and other stability studies must be performed to supplement DSC data.

3.4.7 IR Spectroscopy

IR absorption spectroscopy was used to confirm the identification of CPT with the presence of characteristic absorption and to evaluate 1:1 binary mixtures of CPT and excipients. The IR studies revealed that all characteristics bands of CPT were present in all spectra generated with some spectra showing a slight shift in some of the bands. The spectra are depcited in Figures 3.12 to 3.17.

The IR bands for CPT and assigned wave number are summarised in Table 3.9 and the fingerprint IR spectrum for CPT is depicted in Figure 3.12.

Table 3.9 *Summary of IR band assignment for CPT.*

Wave Number (cm^{-1})	Functional Group
800	-C-C- stretching vibration
1300	-C-H/-CH_3 bending/ symmetric vibration
1450	-C-H stretching/ asymmetric vibration
1500	-C-N amide band
1580	-C=C- stretching
1750	-COOH (-C=O)
2600	-SH stretching vibration
2980	-CH_3 stretching vibration (symmetric)
3400	-OH functional group

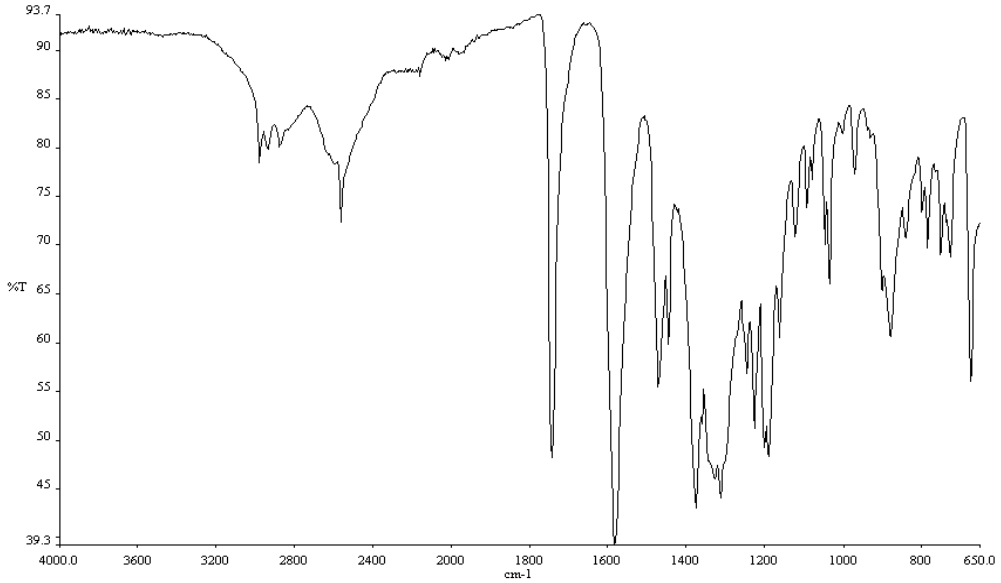

Figure 3.12 *FT-IR fingerprint spectrum for pure CPT.*

The FT-IR spectrum for pure CPT depicted in Figure 3.12 reveals characteristic bands at 2980 cm^{-1} assigned to a CH_3 stretch and a band at 2877 cm^{-1} assigned to the CH_2 stretch that represents alkane groups. The broad peak at 2565 cm^{-1} correspond to the SH stretch mode that is characteristic of mercaptans [3]. The peaks at wave numbers of 1744 cm^{-1} and 1588 cm^{-1} were assigned to the C=O stretch vibration of the carboxylic acid and amide bands, respectively. The peaks at wave numbers of 1227 cm^{-1} and 1246 cm^{-1} correspond to the C-H and/or C-H_3 stretching. The spectrum for CPT was similar to that reported [3]. The FT-IR spectra of 1:1 binary mixtures of CPT and excipients are depicted in Figures 3.13 – 3.17.

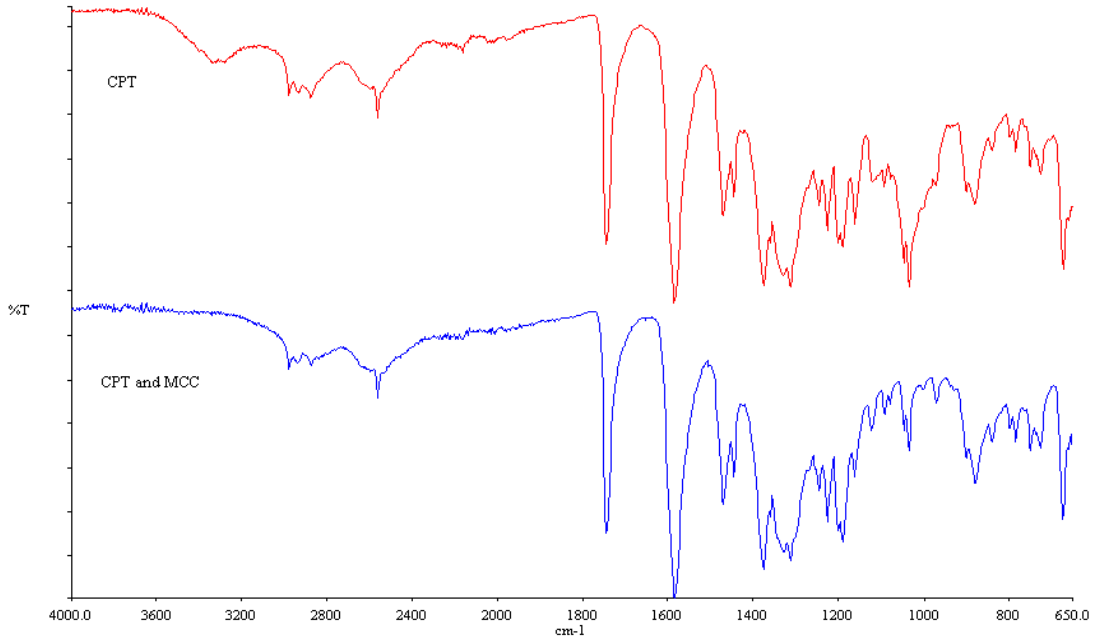

Figure 3.13 *FT-IR spectrum of a 1:1 binary mixture of CPT and MCC.*

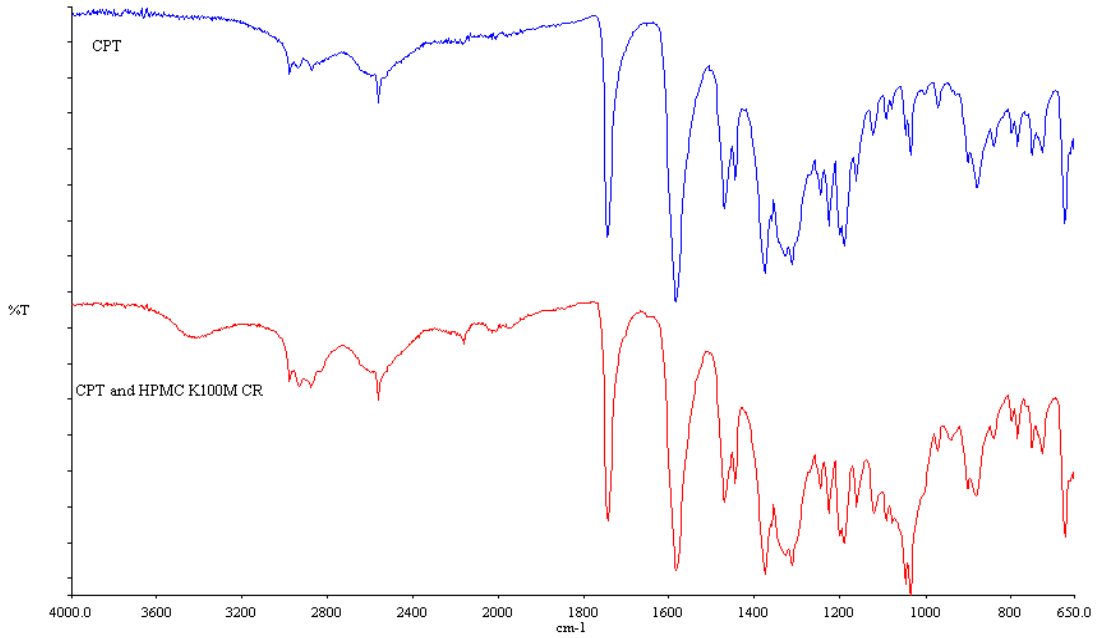

Figure 3.14 *FT-IR spectrum of a 1:1 binary mixture of CPT and HPMC K100M.*

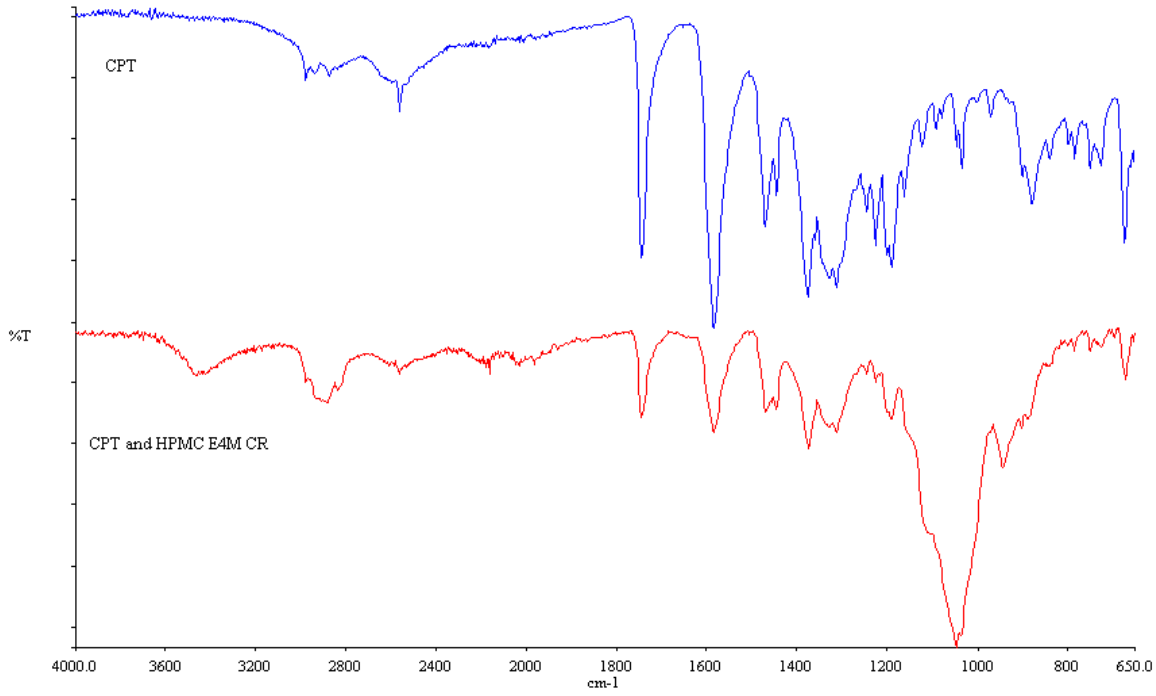

Figure 3.15 *FT-IR spectrum of a 1:1 binary mixture of CPT and HPMC E4M.*

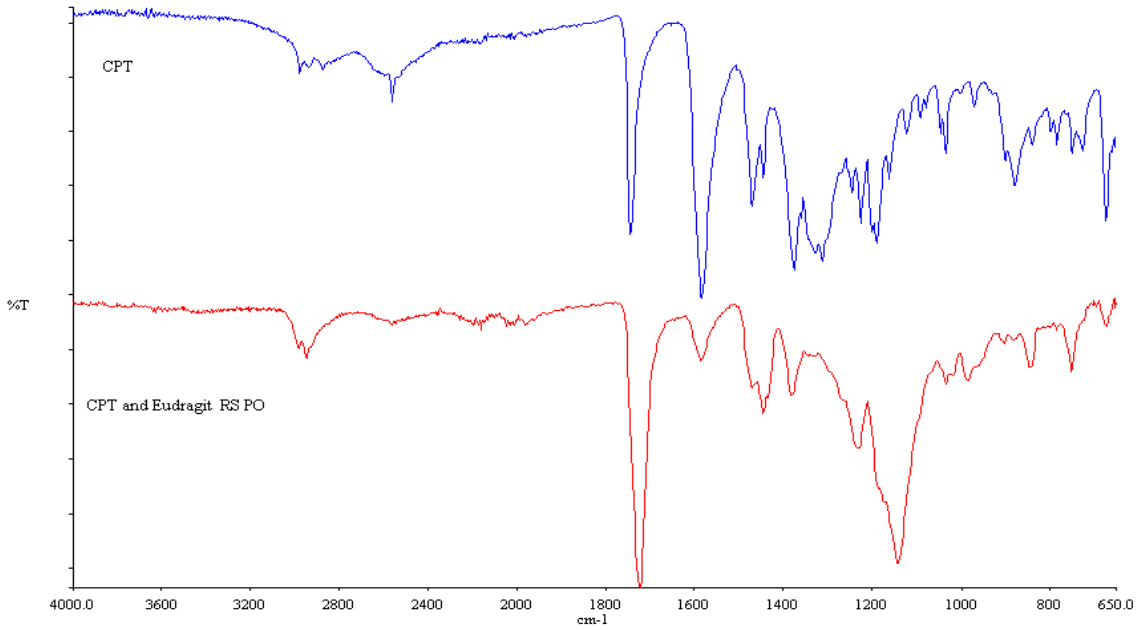

Figure 3.16 *FT-IR spectrum of a 1:1 binary mixture of CPT and Eudragit® RS PO.*

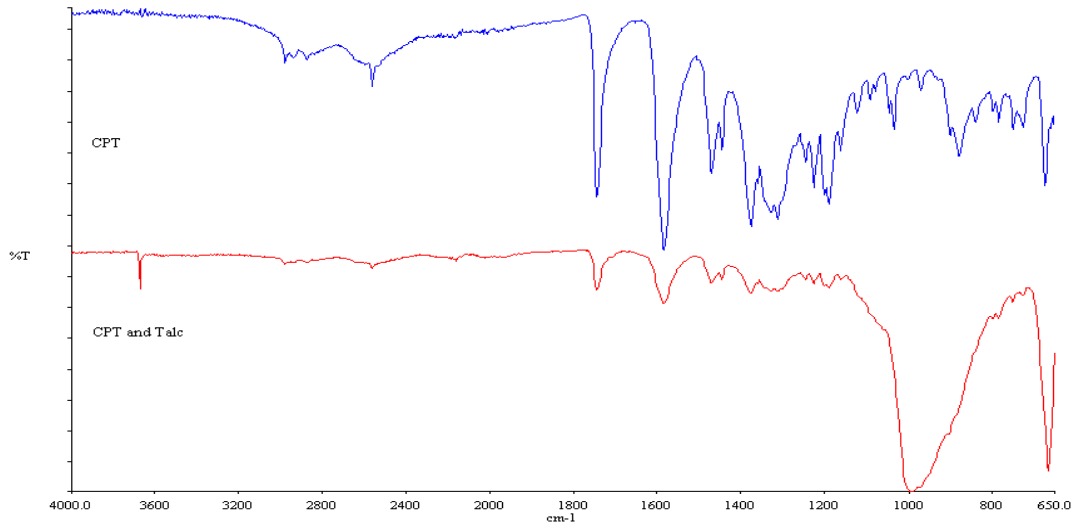

Figure 3.17 *FT-IR spectrum of a 1:1 binary mixture of CPT and Talc.*

The spectra of binary mixtures of CPT and MCC, HPMC K100M, HPMC E4M and Eudragit® RS PO indicate that all characteristic bands for CPT and the respective excipients and/or polymers were present, except for the spectrum for a mixture with talc. However, a slight shift in the bands was observed for most binary mixtures, which may be attributed to the lower purity of CPT when diluted with excipients and therefore may not necessarily indicate that possible incompatibilities exist. The lower intensity of the CPT bands is likely to be a consequence of a dilution effect. The FT-IR spectra for a 1:1 binary mixture of CPT-talc is depicted in Figure 3.17 and reveal a very weak

intensity for the characteristic bands of CPT and very prominent bands for talc. The OH stretch vibration due to magnesium hydroxide ($Mg(OH)_2$) is visible at a wave number of 3677 cm^{-1}. The broad peak at approximately 990 cm^{-1} is due to a Si-O-Si bond vibration and the peak observed at 665 cm^{-1} is attributed to Mg-O-Si vibrations. The weak intensity of bands at wavenumbers 2980 cm^{-1},2600 cm^{-1}, 1750 $cm^{-1}$and 1500 cm^{-1} represent symmetric CH_3 stretch vibrations, SH stretch vibration, COOH (-C=O) and C-N amide bands that are functional groups present in the CPT molecule. It can therefore be concluded that there is a possibility of interaction between CPT and talc, but the results obtained with FT-IR are not confirmed by the DSC thermograms. Further stability studies would be necessary to establish whether an incompatibility did truly exist.

3.4.8 Dialysis

The release of CPT in the presence and absence of ammonium oleate was similar as depicted in Figure 3.18 with resultant f_2 values of 87.7 calculated using Equation 5.2.

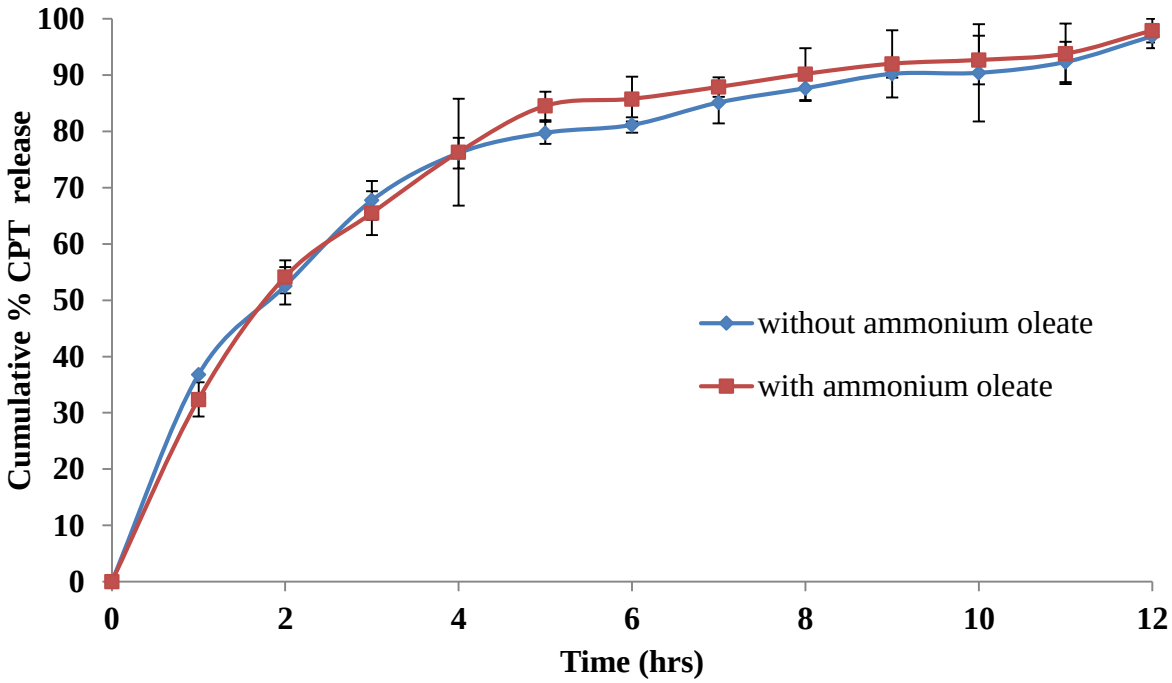

Figure 3.18 *CPT release of CPT in the absence and presence of ammonium oleate.*

The error bars at the time intervals of 2, 3, 4, 7, 8, 9, 10, 11 and 12 hours overlapped, suggesting that the release profiles for CPT in the presence and absence of ammonium oleate were similar. The similarity in the release profiles suggests that no interaction exists between CPT and ammonium oleate and it is clear that CPT permeation across a coating layer consisting of Surelease E-7-19010® may occur slowly, and given that Surelease E-7-19010® is an optimally plasticised ethylcellulose dispersion blended with oleic acid and dibutyl sebacate [157, 158], the ethylcellulose is completely emulsified in ammonium water during the manufacturing process. Ammonium oleate is an unstable compound that is formed *in situ* by reaction of oleic acid with ammonia and the complex degrades easily on heating [161] to allow the formation of an oleate ion in solution with evaporation of the ammonia gas. Anionic oleate ions did not appear to interact with CPT in these studies as depicted by similar release profiles in the presence and absence of ammonium oleate.

When CPT was added to the ammonium oleate solution, a milky white solution with no precipitates was formed, whereas a clear solution was formed when CPT was mixed with water in the control sample. The passage of CPT from the solution that contained ammonium oleate through the dialysis bag was rapid and little difference was observed when this profile was compared to the release profile of CPT from water. The absence of precipitates may account for the rapid release since precipitates tend to retard API release profile as dissolution must occur prior to diffusion.

3.5 CONCLUSION

The preformulation phase of research is critical in establishing the properties of an API and potential excipients that will permit suitable risk assessment for the development of desirable characteristics of coated bead containing dosage forms. To ensure the development of a quality formulation, parameters of selected excipients such as powder flow and interaction between CPT and selected excipients that are used in the early stages of formulation development studies of SR beads, must be undertaken and analysed. Decisions made on the information generated during preformulation are a strategic step in the subsequent development of CPT containing bead dosage forms.

SEM analysis was used due to ease of operation and high resolution of the images to generate SEM micrographs. SEM images revealed that particle size and shape may play an important role in the selection of excipients and that certain excipients may need to be sieved prior to blending to produce homogenous blends that exhibit content uniformity. The bulk and tapped densities of CPT, potential excipients and powder blends used for different formulations were established and the results were used to calculate CI and HR. The results reveal satisfactory flow properties and some excipients and powder blend mixtures exhibited poor flow properties and therefore the inclusion of talc is likely to be necessary to ensure a successful blending and wet granulation process to produce a high quality homogenous bead dosage form if HPMC K100M and HPMC E4M are to be included in extruded and spheronised beads. Following the addition of talc, most powder blends had values for the AOR, CI and HR within a range to indicate satisfactory and good flow properties, suggesting that the use of talc would ensure the materials are suitable for blending and wet granulation prior to extrusion-spheronisation.

The DSC thermograms for all CPT-excipient mixtures revealed that the melting endotherm either widened or fluctuated around the T_{peak} for pure CPT of 110.93 °C. The binary mixtures exhibited a characteristic endotherm at 109.03 °C in all thermograms and therefore the absence of incompatibility between CPT and the excipients tested is likely. Slight changes in endotherm values may be due to the dilution of CPT and it might not necessarily indicate possible incompatibilities. The use of DSC and TGA as thermal analytical techniques provide crucial information with respect to the existence of polymorphic forms of an API, as well as the compatibility of an API with excipients [174, 177-180, 188]. It allows the formulation scientist to correlate structural changes with thermal events to ascertain which excipients are suitable for formulation development studies. The high temperatures to which the binary mixtures would be exposed are not the same as those

used for the production processes used for extrusion-spheronisation and coating of beads. However, they provide the formulation scientist an opportunity to identify the impact of potential thermal changes arising from variation of manufacturing process on product quality. The results of these investigations reveal that the excipients investigated were compatible with CPT and provided important information in respect of the stability of CPT alone and in combination with excipients that could be used during manufacturing.

FT-IR studies established that there is a possibility of interaction between CPT and talc. However, despite the limitations of FT-IR analysis these data provide insight into to thermal and molecular changes to understand potential interactions. The results of FT-IR were not confirmed by DSC and suggest that the presence of talc reduced the purity of CPT, resulting in a low intensity signal for the characteristic bands of CPT. Based on the preliminary studies of flow properties, SEM, TGA, DSC and FT-IR, HPMC Methocel® K100M, HPMC Methocel® E4M, MCC Avicel® PH102, Methacrylic acid copolymer (Eudragit® RS PO) and talc were selected for formulation development studies of CPT coated beads.

The release profile for CPT was investigated in the absence and presence of ammonium oleate and it was concluded that the anionic oleate did not interact with CPT as shown by the similar release profile produced in the presence and absence of ammonium oleate. These data provide insight into the lack of interactions between CPT and Surelease® E-7-19010 when processing CPT beads.

DSC and FT-IR analysis have been examined to investigate possible CPT-excipient interactions. All excipients appeared to be compatible with CPT and were therefore used for formulation development studies. The dialysis studies have been detrimental to reveal potential interaction between CPT and Surelease® E-7-19010.

CHAPTER FOUR
FORMULATION DEVELOPMENT AND CHARACTERIZATION OF CAPTOPRIL BEADS MANUFACTURED BY EXTRUSION-SPHERONISATION

4.1 INTRODUCTION

Worldwide, research, development and sales of drug-delivery systems [189] has been refined due to a demand for highly effective medicines at low cost. To meet this demand many existing medicines that are currently in use are being reformulated and placed in delivery technologies that add value to therapeutic approaches [190]. The manufacture of controlled and targeted drug delivery systems in the pharmaceutical technology domain include the development of sustained release (SR) dosage multi-particulate dosage forms [189, 190] as an option to meet the demand to achieve a desired plasma concentration over a prolonged period of time to optimise therapy for a specific API, as fluctuations in blood levels are a common cause of therapeutic failure.

Multi-particulate delivery systems such as beads are predominantly oral dosage forms [189] in which the API is located in many small independent subunits that, combined,deliver the recommended dose. The subunits systems may be coated and subsequently placed in a hard capsule [142, 152, 155, 191, 192,] or compressed into a tablet [159]. CPT is a class III compound [3] that exhibits permeability rate-limited absorption across the epithelial cells of the GIT resulting in high variability in the rate and extent of absorption. CPT is solvated rapidly and therefore the rate of CPT release from dosage forms is rapid and absorption can be controlled by the rate of release from coated multi-particulate bead technologies [193]. For molecules such as CPT, it is possible to predict *in vivo* performance from *in vitro* dissolution studies as a surrogate approach to assessing whether a technology will be successful and an added advantage of this approach is that the number of human studies required duringformulation development can be minimised [193].

Individual beads in a multi-particulate systems may be divided into fractions according to their size, coating level, release characteristics and API payload [194], offering a range of possibilities for drug product development. Multi-particulate delivery systems offer several benefits over traditional single-unit dosage forms including a lower incidence of gastrointestinal irritation,[195] since a decrease in the local concentration of API is achieved inthe GIT following oral administration of bead dosage forms. Furthermore, lower individual variability in plasma concentrations are observed when compared to tablets [155, 159] as there is a reduced risk of dose dumping that is characteristic

from technologies containing water soluble molecules [195]. In addition, bioavailability may be improved and the use of discrete units offers a simple solution to minimising potential API/API or API/excipient interactions [155, 158].

4.2 BEADS AS A MULTI-PARTICULATE DOSAGE FORMS

Beads are agglomerates of powder or granules of API and excipients [190] that are small, free-flowing, spherical or semi-spherical solid units. Beads intended for oral administration should be near spherical and have a smooth surface if they are to be subsequently film-coated. The particle size range of beads should be as narrow as possible and an ideal size range is between 600 and 1200 μm diameter [194]. The beads should have as high a payload of API as possible to ensure that the final dosage form is as small as possible [196].

Benefits of beads as dosage forms include their free flowing and packing nature, which facilitates reproducible capsule filling and content uniformity of dose units within a batch [194, 196]. The ideal shape, smooth surface morphology, narrow size distribution, low friability and low surface-to-volume ratio facilitate the film coating process of the individual units [196, 197, 198]. Each bead is a single reservoir and any imperfection in the coating will affect the release of a small fraction of the payload [192] that is in contrast to extreme dose dumping that may be observed from single unit technologies.

The potential side effects of an API can be reduced without affecting bioavailability, since the beads disperse freely throughout the GIT and absorption is maximized without peak plasma level fluctuations resulting in improved safety and efficacy [196, 197, 199]. Local irritation as a consequence of high local concentrations of API associated with single unit dosage forms are avoided due to the dispersion of API minimising irritant effects to the gastric mucosa [195]. An advantage of using multiple-unit dosage forms as SR dosage form relates to *in vivo* behaviour, particularly the dispersion pattern along the GIT [196].

4.2.1 Extrusion and spheronisation

Several methods can be used to manufacture beads, the most popular of which is a solution/suspension layering approach [194]. Powder layering [196, 200, 201], direct pelletisation using high shear mixers and conventional or rotary fluid-bed granulators [196, 197] and extrusion–spheronisation [129,144, 192, 202, 203, 204, 205] are alternate approaches to manufacture beads. The challenges associated with the agglomeration process have been reported [201, 202, 205] in general and suggest that the powder layering technique is difficult. Agglomeration occurs and different powder components are layered to produce different sized granules that may compromise the quality of finished products [201]. Extrusion-spheronisation is considered a feasible method for the manufacture of uniform spherical beads that overcome agglomeration challenges and a schematic of the process is depicted in Figure 4.1 to highlight process variable parameters that can be investigated.

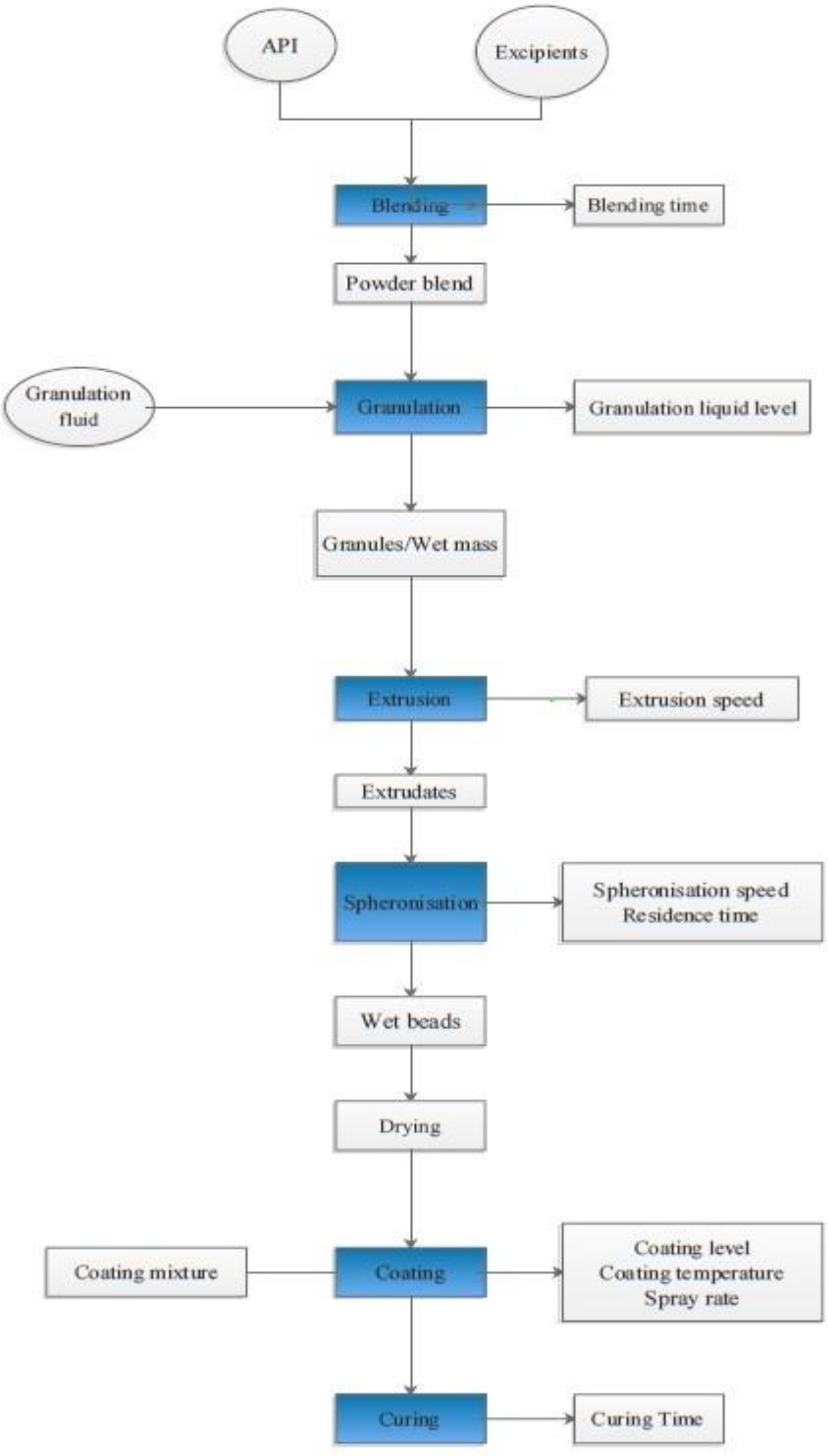

Figure 4.1 *Schematic representation of an extrusion-spheronisation procedure highlighting key process parameters adapted [171].*

The initial step of the process involves mixing and/or blending of API and excipients, followed by wet massing using an appropriate granulating fluid in sufficient quantities. The granulation step can be performed in batch-type processors such as conventional planetary mixers, vertical or horizontal high-shear and sigma-blade mixers [194, 199].

The type and amount of the granulation fluid is an important factor to consider in an extrusion-spheronisation process and for a specific formulation a relatively small volume and concentration is usually appropriate for the agglomeration process [199] to wet mass the powders sufficiently, while retaining the necessary plasticity and cohesiveness that isessential to yield spherical beads of narrow size distribution. Insufficient moisture addition results in the generation of fine powders and dumb-bell shaped beads, whereas excess moisture promote bead agglomeration and results in a wide size distribution of the beads [138]. If the amount of granulating fluid is within an acceptable range for extrusion and spheronisation, beads of acceptable sphericity, narrow size distribution, reduced friability, improved surface properties and prolonged API release may be produced [144, 191, 205, 206].

Extrusion of the wet powder mass leads to the formation of an intermediate spaghetti-like product, which is subsequently spheronised to yield beads [144, 202, 205]. A sieve and basket extruder was used to extrude the wet mass as it uses a gravity feed mechanism to transport the wet mass towards the die [199]. Most spheronisers are designed based on a revolving grooved plate driven by a variable-speed unit located at the base of a smooth-walled drum [205]. The introduction of cross-hatched disc plates has increased the capacity of the spheronisation process and was therefore selected for use throughout this study. The transition of extrudate into spherical beads occurs during several stages via one of two mechanisms or models. The first model suggest that during spheronisation afterbreakage of the extrudate, cylinders are initially rounded at the edge, after which dumb-bell like granules are formed that ultimately produce spherical beads [137] and this process is depicted in Figure 4.2.

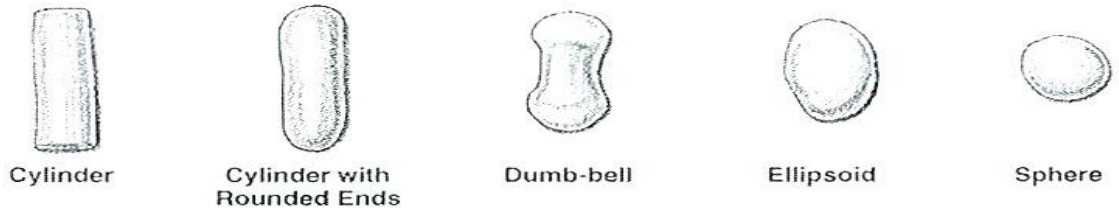

Figure 4.2 *Schematic representation of bead formation stages during spheronisation according to a model proposed by Rowe [137]***.**

The second model [207] suggests that during spheronisation, cylinders of extrudate are rounded at the edges and the cylinder is bent, after which dumb-bell shaped particles that break into two parts with a cavity on their flat side are formed and with further process arerounded into spheres as depicted in Figure 4.3.

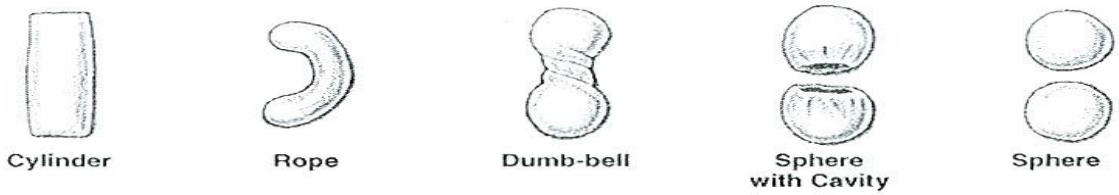

Figure 4.3 *Schematic representation of bead formation stages during spheronisation according to the models proposed by Baert and Remon [207].*

The principal mechanism of bead formation depends on formulation composition and granulation fluid level and spheronisation process parameters influence whether the spheronisation step will result in beads that are dumb-bells or spherical beads with a narrow size distribution [208-211]. The resultant beads are dried in a fluidised bed dryer and screened to achieve the required size distribution [144, 202, 205]. Recent research has been dedicated to investigate the influence of formulation variables on extrusion-spheronisation [144, 191, 192] and since these steps are related the quality of the resultant beads is highly dependent on process and formulation factors.

4.2.2 Coating of beads

CPT is unstable in light, acid, alkali and oxidative conditions, and therefore to enhance the chemical stability of the API, and aqueous film coating should be applied to dosage forms [160]. There are a number of challenges associated with the aqueous film coating process, including difficulty in accurately establishing a coating end-point [160], achieving the target weight gain and satisfactory content uniformity [145, 155] or coating efficiency. Aqueous dispersions of Surelease® and

Aquacoat® have a significant advantage over organic solvent-based coating mixtures since aqueous dispersions are environmentally safer and considerably cheaper [145]. Coating efficiency is described as the ratio of the amount of coating material deposited on the surface of a bead and the amount of material delivered. The use of Würster or bottom-spray coating equipment provides excellent coat uniformity and efficiency [212-214] and is suitable for the manufacture of coated CPT beads using ethylcellulose dispersion.

The Würster spraying process uses the energy and controls of the fluid bed dryer to create pneumatic mass transport inside a Würster insert [213] and requires the use of a perforated bottom screen coupled with an air distribution plate that results in a fluid-like motion of particles in a conical product chamber. Most of the processed air is guided through the center of the cylindrical Würster insert and produces a venturi effect that sucks product from outside the partition past a spray nozzle mounted centrally at the bottom of product chamber [213]. The inlet temperature evaporates excess moisture and the dry product then passes through the coating zone, during which time additional coating material is deposited on the surface of the bead [214]. The short distance between the coating mixture and particles during the coating process minimises drying and contributes to coat uniformity and efficiency and the uniform residence time of all particles in the coating zone results in the deposition of homogenous coats [214]. Pneumatic mass flow is characterised by high kinetic energy that permits moist particles to separate resulting in coat deposition on individual particles [213, 214]. The deposition of a uniform layer of an aqueous coating dispersion on beads is therefore dependent on several key process parameters and the main impact on the coating processes are summarised in Table 4.1.

Table 4.1 *Key process parameters and their impact on the coating process.*

Parameter	Impact
Spray rate of suspension	Agglomeration
Atomising airflow	Spray drying, agglomeration, yield
Inlet air temperature	Agglomeration, spray drying, yield
Bed temperature	Agglomeration, spray drying, yield
Inlet airflow	Overwetting, pellets in filter
Inlet air moisture content	Overwetting

The maximum spray rate is limited by the viscosity and tackiness of the coating dispersion, drying capacity and droplet size in the fluidised bed system and exceeding an appropriate spray rate may result in irreversible agglomeration of coated beads, since more liquid is pumped into the coating chamber that subsequently cools the air in the chamber resulting in lower particle bed temperatures [212]. The atomisation pressure is an important parameter that has an impact on the size distribution of droplets and the spray drying process that occurs when excessive atomisation airflow pressure is used whereas agglomeration tends to occur at lower atomisation pressures [215]. An elevated inlet air temperature may lead to agglomeration as the coat may soften and become tacky. However, an elevated temperature is necessary to evaporate the aqueous coating dispersion. The inlet airflow patterns determine particle flow in the fluidised bed and a high air volume may trap beads in the outlet filter whereas low airflow volumes may result in over wet beads [212, 214, 215]. The key parameters are related and take into account process conditions that are necessary to produce a high quality coating with high efficiency. Different formulation and processing parameters must be used to optimise CPT release patterns, i.e. coating level, coating mixture composition, curing time and temperature, but must be considered in conjunction with a target coating efficiency.

4.2.3 Curing

There are two stages in the process of coalescence of polymers from aqueous dispersions in the coating process [214] and these involve evaporation of water to form a dry, continuous film that gradually coalesces through a process of curing [216] as depicted in Figure 4.4.

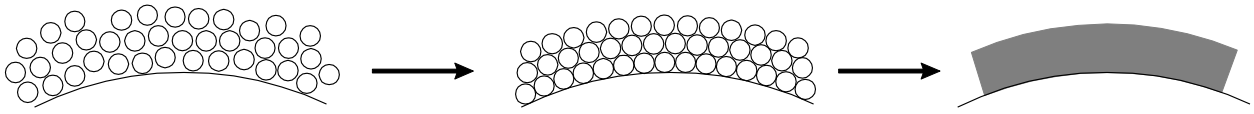

Figure 4.4 *Schematic representation of the curing process depicting coalescence of insoluble polymers as water evaporates.*

Curing of film forming polymer coats occurs when individual polymer particles fuse completely to form a homogeneous, continuous film when water evaporates from interstitial spaces from the deposited [216]. It is not possible to assume that film formation is complete following coating and it isnecessary to ensure complete film formation occurs through period of curing. Curing is dependent on the time and temperature of post-coating exposure and results in additional

evaporation of water due to capillary pressure effects within the interstitial spaces of the coating layer [217]. A curing step is therefore suggested when polymers with high glass transition temperatures, such as ethylcellulose [217] are used to coat dosage forms.

4.2.4 Aims

The objective of this study was to develop a SR CPT coated bead technology using Response Surface Methodology (RSM) to screen and optimise formulation and process parameters critical for the manufacture of beads by extrusion-spheronisation. The coated beads were futher assessed for their quality attributes.

4.3 EXPERIMENTAL

4.3.1 Manufacture of CPT beads

The manufacture of CPT beads is a multiple-step production process with a minimum of five unit operations that include powder blending, wet massing, extrusion, spheronisation and drying [138, 205, 206]. Overly an extrusion and spheronisation process with subsequent coating was selected and used to manufacture all bead formulations. Extrusion, spheronisation and coating processes were undertaken using different types of equipment, which is a disadvantage in terms of equipment expense, time, labour and space. Each of the multiple-step production pocess is a distinct process that requires control of a number of process parameters to produce beads of appropriate quality and a schematic of the process is depicted in Figure 4.5.

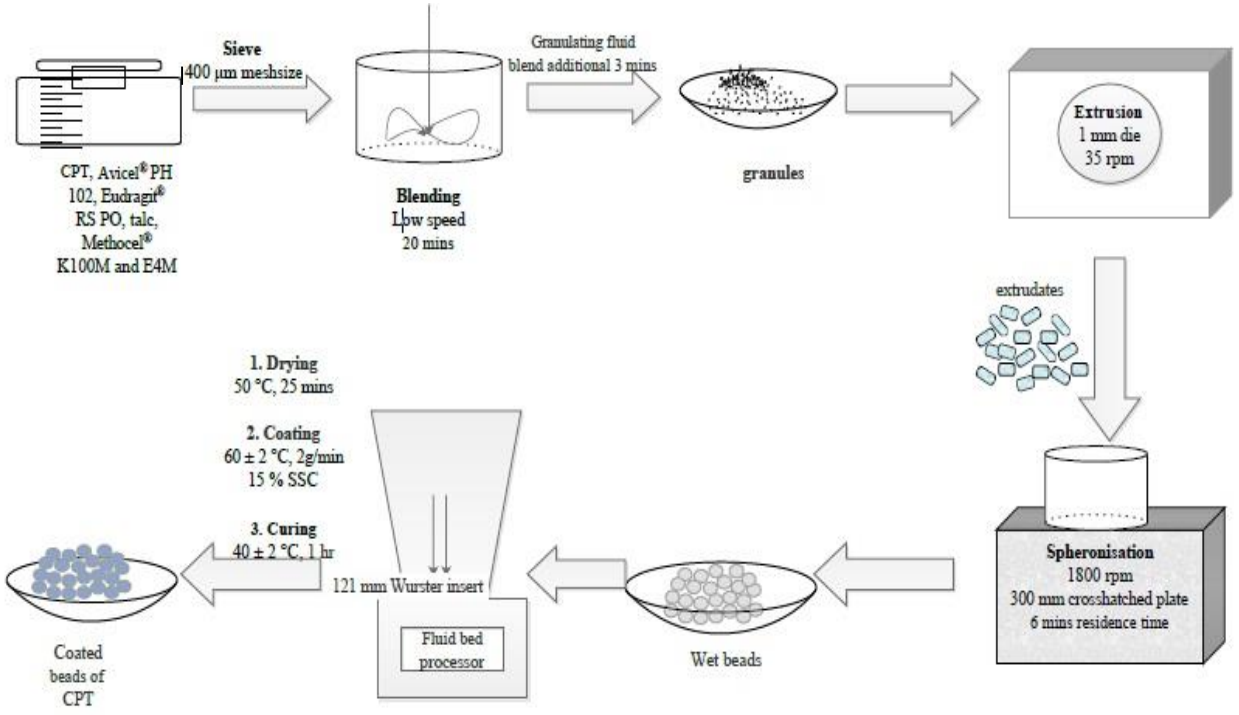

Figure 4.5 *Schematic representation of the manufacturing process for CPT beads coated.*

4.3.1.1 Sieving

CPT (Protea chemicals, Midrand, South Africa) and excipients such as Methocel® K100M and Methocel® HPMC E4M (Dow Chemical Company, Midland, MI, USA), Avicel® PH102 (FMC BioPolymer, Philadelphia, PA, USA), Eudragit® RS PO (Evonik Industries, Pharma Polymers, Darmstadt, Germany) and talc (Aspen Pharmacare, South Africa) were sieved througha 1400 µm mesh prior to processing. Sieving is important to produce powders of uniform particle size to achieve homogeneity of the product during blending and wet massing.

4.3.1.2 Blending

Appropriate quantities of sieved powders were weighed using a Mettler AG 135 top loading balance (Mettler Instruments, Zurich, Switzerland) and were transferred to a Kenwood Multi-Pro FP580 planetary mixer (Kenwood Ltd. Maraisburg, South Africa) and blended for 20 minutes at low speed using the procedure described in §3.2.4. The use of a planetary mixer was preferred for small-scale production of 200 g blends for this study.

4.3.1.3 Granulation

Surelease® E-7-19010 clear (Colorcon, West Point, PA, USA) is a 25 % w/w aqueous dispersion of ethylcellulose that was diluted prior to use as the granulating liquid. The diluted dispersion was prepared by accurately weighing the correct amount of a 25 % w/w Surelease® E-7-19010 clear dispersion on a top loading balance (Mettler Toledo Inc., Columbus, OH, USA) and then diluted using HPLC grade water to total solid content of 5 %, 10 %, 15 % and 20 % w/w (SSC) for batches CPT-003 to CPT-006. The dilute SSC dispersion was gradually sprayed onto the powder blend manually and the minimum volume of SSC dispersion required to achieve suitable consistency of the wet powder mass was subjectively assessed. The powder blend was mixed at low speed using a planetary mixer for an additional 3 - 6 minutes after the addition of minimum quantity of fluid. The effect of different solid content was investigated with respect to the physical properties and dissolution profiles of the beads. Assays performed for CPT-003 beads were made with 5 % w/w SSC granulating fluid, while CPT-004- CPT-006 where manufactured using 10 %, 15 % and 20 % w/w SSC, respectively. To ensure uniform granulation fluid distribution during wet granulation, the material was repeatedly scraped from the walls of the mixing bowl during wet massing.

4.3.1.4 Extrusion

The powder mass obtained following the addition of granulating fluid was transferred into the gravimetric powder feeder of a Model 20 Caleva® extruder (Schlueter, Neustadt am Ruebenberge, Germany) fitted with co-rotating impellers. The extruder was equipped with a screen with an aperture pore sized of 1 mm diameter. The granules were gravity fed into the extruder to produce equal length pieces of extrudate. During the extrusion process the impeller speed, temperature and humidity were monitored and recorded. The effect of extrusion speed was investigated using CPT-001 composition on % yield and sphericity.

4.3.1.5 Spheronisation

Batches of approximately 200 g of extrudate were transferred to a Caleva® MBS 250 spheroniser (Schlueter, Neustadt am Ruebenberge, Germany) immediately following extrusion and spheronised for between 3 and 6 minutes. The apparatus was equipped with a 300 mm diameter crosshatched friction plate and different speeds and residence times were used to produce spheronised wet beads. Beads were harvested at different time intervals during CPT-001 and their shapes were reviewed using SEM to elucidate the bead formation stages according to models proposed by Rowe[137] and

Baert and Remon[207]. The effect of spheronisation speed was investigated on % yield and sphericity.

4.3.1.6 Drying

The beads were dried using a fluid bed drier (STREA-1^{TM} Classic Fluid Bed Processor, GEA, Maryland, USA). The inlet air temperature was set at 50 °C and an atomising airflow rate of 115 m^3/hr was used for 25 minutes. The desired size fractions were collected by sieving the dried beads using a set of standard sieves with nominal screen sizes of 1.25 mm, 0.80 mm and 0.3125 mm (Mesh DIN 4188, 1977 Pruf-Sieb, Germany).

4.3.1.7 Coating of beads

4.3.1.7.1 *Preparation of coating mixture*

Surelease® E-7-19010 was diluted to 15 % w/v solids prior to use as a coating suspension by using distilled water and stirred with a magnetic stirrer (Silverson, Bucks, UK) at 400 rpm for at least 2 hours to stabilise the aqueous pseudolatex dispersion prior to use. The coating dispersion was passed through a 0.80 mm sieve to remove large agglomerates prior to use.

4.3.1.7.2 *Coating process*

The dried beads in the size range 0.80 mm to 1.25 mm were coated using a bottom-spray fluid-bed coating apparatus fitted with a 121 mm Würster insert (STREA-1^{TM} Classic Fluid Bed Processor, GEA, Maryland, USA) and an air perforated distributor plate. Prior to coating the beads were pre-heated to between 58 and 60 °C and a coating dispersion prepared as described in §4.3.1.7.1 was sprayed at a rate of 2.0 - 5.0 g/min, through a 1.2 mm nozzle with an atomising airflow pressure in the range of 115 m^3/hr to 130 m^3/hr. The inlet air temperature was set at 60 ± 2 °C and the outlet temperature target temperature was 50 ± 2 °C. Batches of CPT beads were coated to a target weight gain of a 20 % w/w. Following coating the beads were cured at a product temperature of between 40 °C and 60 °C for 1 hour to facilitate complete film formation.

4.3.1.8 Capsule filling process

Coated beads were encapsulated in opaque yellow size 1 hard gelatin capsules to protect the product from direct light and moisture. The use of capsules provided a carrier system for the CPT coated beads. The capsules were hand-filled with weighed 250 mg quantity of coated beads equivalent to 50 mg CPT. The manual hand-filling process of weighed coated CPT beads was suitable for these studies, although automated filling would be necessary if the product were to be manufactured on a large scale.

4.3.2 Evaluation of coated CPT beads

4.3.2.1 Yield

The yield was calculated as the average fraction (n=3) of coated beads retained between 0.80 and 1.25 mm and was presented as a percentage of the total bead weight retained after coating.

4.3.2.2 Scanning electron microscopy (SEM)

The shape and surface morphology of the coated beads were investigated using SEM (VEGA LMU© Scanning Electron Microscope, Tescan, Czechoslovakia Republic) and Secondary Electron Imaging (SEI) (Jeol JXA 8230 Superprobe, Electron Probe Micro-Analyser, JEOL Ltd, Tokyo, Japan). Images of 960 x 1280 pixels were produced using a scan/freeze time of 38.4 seconds. Prior to the micrographs production samples were sputter-coated with gold (Balzers Union Ltd, Balzers, Lichtenstein) for 30 minutes under 0.25 Torr vacuum pressure.The sputter coating was performed in multiple steps to avoid partial melting of the coating prior to SEM and SEI analysis. The samples were viewed at an accelerated voltage of between 15 and 20 kV and a probe current of 20 nA.

4.3.2.3 Aspect ratio (AR) and Sphericity

The shape of coated beads was determined using the SEM image analysis approach described in §4.3.2.2. The area (A), perimeter (p), minimum and maximum diameter (d_{min} and d_{max}) for each coated bead particle were assessed. The aspect ratio (AR) and sphericity were derived from the data and the AR was used to evaluate the shape of individual beads. The AR was calculated using Equation 4.1.

$$Aspect\ Ratio\ (AR) = \frac{d_{max}}{d_{90}} \qquad \textbf{Equation 4.1}$$

Where,

d_{max} =maximum Feret diameter of individual beads and
d_{90} =Feret diameter perpendicular to d_{max}.

The Feret diameter of beads was measured using several different orientations to obtain maximum and minimum values. The sphericity index for each batch was established by evaluating SEM images of 10 beads and calculated using Equation 4.2.The sphericity or roundness is defined as the ratio of the perimeter of a circle with an area equivalent to that of the bead image.

$$Sphericity = \frac{p^2}{4\pi A} \qquad \textbf{Equation 4.2}$$

Where,

p = perimeter and
A= area of the bead.

For a perfectly spherical shape the sphericity would be 1 and values for sphericity ≥ 1.80 indicate non-spherical or dumb-bell shaped particles.

4.3.2.4 Density

The bulk density was determined by pouring 20 g of beads into a 100 mL grade A graduated glass cylinder that was held at an angle of 45 ° during filling. The cylinder was returned to a vertical position and the volume occupied by the materials was recorded. The value for bulk density was the quotient of the weight and volume occupied as described by Equation 3.1. The tapped density of each batch of beads was determined with the aid of a Model SVM 203 tapped density tester (Erweka GmbH, Heueastamm, Germany) operated at a rate of 200 taps per minute for two minutes. The volume of the tapped beads was recorded after agitation and tapped density was calculated using Equation 3.2 as described in §3.2.3.3. The HR and CI of the beads were calculated using Equations 3.3 and 3.4. The measurement of each bulk density, tapped density, CI and HR was performed in triplicate. The AOR and flow properties of the beads were measured using the funnel method, and 50 g of beads were allowed to flow through a funnel orifice of 1.0 cm. The AOR (n=3) was calculated using Equation 3.5.

4.3.2.5 Friability

An acceptable friability value is essential for beads prior to and following coating to withstand shear stress during further processing or testing. The friability was determined (n=3) using an Erweka friabilator (Erweka GmbH, Heueastamm, Germany) into which 10 g of beads and 200 glass beads of 6 mm diameter were rotated at 25 rpm for 3 minutes [198]. After rotation the materials were passed through a 180 mm sieve and the friability was calculated as the quotient of the geometric mean bead size after testing and comparison to the values before testing. Friability values < 1 % indicate the acceptance criterion following coating process.

4.3.2.6 Differential Scanning Calorimetry (DSC)

The thermal characteristics of an optimised formulation for CPT beads were elucidated using a DSC-7 PerkinElmer Differential Scanning Calorimeter (PerkinElmer Inc., AG, USA). DSC scans were conducted at a controlled heating rate of 10 °C/min over the temperature range 25 - 200 °C. Samples with an initial weight of approximately 3 mg were sealed in an aluminium pan prior to heating. Pyris™ Manager Software was used to analyse the resultant thermograms. An empty aluminium pan was used as the reference. Each thermogram generated during the heating process was acquired at 10 scans per revolution of 4 cm^{-1}. All DSC analyses were performed in triplicate in an inert N_2 atmosphere supplied at a flow rate of 20 mL/min.

4.3.2.7 Infrared (IR) absorption spectroscopy

The IR absorption spectrum of the coated beads was generated using a Spectrum 100 FT-IR ATR Spectrophotometer (PerkinElmer Inc., Massachusetts, USA). The spectra were acquired from samples of coated beads pulverised using a mortar and pestle. An aliquot of the resultant powder was placed on a diamond crystal and analysed over the range 4000 cm^{-1} to 650 cm^{-1} at a resolution of 4 cm^{-1}.

4.3.2.8 Assay of CPT coated beads

Approximately 250 mg of each batch of coated beads were accurately weighed using Mettler balance (Mettler Toledo Inc., Columbus, OH, USA). The weighed beads were ground to a fine powder using a pestle and mortar. The pulverised powders were quantitatively transferred into an A-grade beaker and dissolved in 100 mL of MeOH: water adjusted to pH 3.27 using 85 % v/v ortho-phosphoric acid (49:51 % v/v). The solution was sonicated for 5 minutes using a Model B-12

Ultrasonic bath (Branson Cleaning Equipment Co., Shelton, Connecticut, USA). A 5.0 mL aliquot of each sample was filtered through a 0.45 µm HVLP Durapore® membrane filter (Millipore Corporation, Ireland) and a 2.5 mL aliquot of the filtered solution was transferred into a 25 mL A-grade volumetric flask containing 2.5 mL of an IS solution. The samples were made up to volume with mobile phase and analysed using the validated HPLC method described in §2.5.5.

4.3.2.9 Dissolution testing

Dissolution testing is used as quality control test for solid oral dosage forms and is integral to quality assurance as *in vitro* performance may reflect *in vivo* release and highlight potential bioavailability concerns [42]. Bioequivalence studies are used in the approval stages of dosage forms for market authorisation and a major objective of dissolution testing is focused on establishing *in vitro-in vivo* correlations where possible to assess whether dissolution testing can be used as a substitute approach for bioequivalence studies [218]. The rotating basket (USP Apparatus 1) and paddle (USP Apparatus 2) are robust, adequately standardised and require simple manipulation when performing dissolution studies [218, 219]. Experimental difficulties may arise when a change in pH or a change in sink conditions is required due to the single container nature of the basket and paddle apparatus and the use of the reciprocating cylinder (USP Apparatus 3). Bio-Dis® has offered an alternative to the use of USP Apparatus 1 and 2 and is gaining significance in testing extended-release dosage forms as the media and test conditions can mimic pH conditions in the GIT [218, 219].

Approximately 250 mg of coated beads were filled into opaque yellow size 1 capsules and were tested using Apparatus 3. A VanKel® Bio-Dis® (VanKel® Industries, New Jeysey, USA) was used for dissolution testing of CPT bead batches. The temperature of the USP Apparatus 3 was controlled with a digital controlled water circulation/heater (VanKel® Industries, New Jersey, USA) that was set at 37 ± 0.5 °C. The dosage forms were tested in 200 mL phosphate buffers of different pH and the actual conditions are summarised in Table 4.2. Phosphate buffer (50 mM) was prepared by pipetting 3.4 mL 85 % v/v ortho-phosphoric acid into a 1L volumetric flask and made up to volume with HPLC grade water. The pH of the phosphate buffer was adjusted to a pH of 1.6, 3.4, 4.6, 6.8 and 7.2 using 0.1 M NaOH. The pH was measured using a Model GLP 21 Crison pH meter (Crison Instruments, Johannesburg, South Africa) and 200 mL of buffered solution was transferred into dissolution vessels for each test.

Table 4.2 *Dissolution conditions for USP Apparatus 3.*

Parameter	**Value**		
Dissolution Medium	200 mL of 50 mM phosphate buffer		
Dissolution Time	**Row**	**pH**	**Time in Medium**
	1	1.6	1
	2	3.4	1
	3	4.6	2
	4	6.8	2
	5	6.8	2
	6	7.2	4
Temperature	37.0 ± 0.5 ºC		
Initial Volume	200 mL		
Basket Dip Speed	10 dpm		
Screen Size	177 µm (Mesh Size 78)		
Filter Size	0.45 µm		
Volume Removed	2.5 mL		

Dissolution testing was performed at 10 dpm rate and samples of 2.5 mL were withdrawn and filtered through a 0.45 µm HVLP Durapore® membrane. Samples were collected after 1, 2, 4, 6, 8 and 12 hours exposure to the different media and CPT release was monitored using the validated HPLC method described in §2.5.5.

4.3.2.10 Coating efficiency

The coated beads were weighed and the final yield established to assess coating efficiency. The coating efficiency was calculated as the ratio of the actual weight of coated beads to theoretical weight of coated beads and expressed as a percentage. Coating efficiency was therefore used as an indicator of the coating end point and is described in Equation 4.3. The closer the coating efficiency to 100 %, the more efficient the coating process is in uniformly coated beads.

$$Coating\ Efficiency\ (\%) = \frac{a}{b} \times 100\ \% \qquad \textbf{Equation 4.3}$$

Where,

a= actual weight of coated beads and
b= theoretical weight of coated beads.

4.3.3 Statistical Analysis

4.3.3.1 Experimental design

The use of experimental design approached is gaining recognition in the development of pharmaceutical formulations as more than one of the variables influence quality attributes of dosage forms that can be evaluated at the same time [106, 107]. The variables, also called factors, can be qualitative or quantitative, whereas the responses are preferred to be within predetermined ranges to achieve the desired quality attributes of a final product [109]. The use of RSM has an advantage over the conventional one-factor-at-a-time (OFAT) approach, since the best possible solution can be generated in minimum time with fewer resources [107]. However, as the number of input variables increases, this approach is time and resource consuming [106, 107]. The use of statistical design aids the simultaneous evaluation of important factors and possible interactions between them that may affect the production and performance of formulations [220]. Properly designed experiments assure the production of products with high quality attributes [107, 220].

4.3.3.2 Plackett-Burman Design

The Plackett-Burman experimental approach allows formulation scientists to ascertain key formulation factors and process variables [106] required to produce, in this case, coated CPT beads with the desired quality attributes following extrusion-spheronisation and subsequent coating. The desired quality attributes can be set at maximum or minimum levels and the model constructed is crucial to provide an approximate true relationship between the input factors and responses that are monitored [106]. When considering the production of coated CPT beads a number formulation and process variables must be assessed to minimise production challenges, such as agglomeration in extrusion-spheronisation [201] or identifying the coating end-point to consistently achieve 100 % coating efficiency for example [160]. A Plackett-Burman approach was used as it permits screening of a large number of significant factors in a two level design with equal allocation of weighting [221] while using a small number experiments with a balance in the design matrix by variation of all factors, thereby making the design complete and efficient from resource perspective whilst gaining a wealth of information [222].

Crucial process and formulation factors deemed necessary for the development of coated beads were identified from preliminarily studies and these data are summarised in Table 4.3. These input parameters were used for the Plackett-Burman design that permitted a study of n factors in n+1 runs with each factor weighted at low and high settings that correspond to coded values of -1 and +1 value [222] and the factors are simultaneously varied at different levels computationally [223]. Each factor is tested the same number of times at the coded values [222, 223] to create an equal allocation for each factor.There is consequently a balance between each and every pair of factors assessed throughout the design and the responses had set constraints summarised in Table 4.3 to accept or reject the models generated.

Table 4.3 *Range and levels of independent input variables used for the Plackett-Burman design.*

	Levels	
Input Factor	**-1**	**+1**
X_1=MCC (%)	40.0	50.0
X_2=K100M (%)	15	25
X_3=E4M (%)	15	25
X_4=RS PO (%)	7.5	15
X_5=Extrusion Speed (rpm)	15	35
X_6=Spheronisation Speed (rpm)	1200	1800
X_7=Residence Time (min)	3	6
X_8=Coating Temp (°C)	60	90
X_9=Atomizing Airflow Rate (m^3/h)	115	130
X_{10}=Spray Rate (g/min)	2	5
X_{11}=Curing Temp (°C)	40	60
Output Response	**Constraints**	
Y_1=Yield (%)	$60 \leq Y_1 \leq 95$	
Y_2=AOR (˚)	$Y_2 \leq 30$	
Y_3=Friability (%)	$Y_3 \leq 1$	
Y_4=AR	$0.80 \leq Y_4 \leq 1.20$	
Y_5=Sphericity	$0.80 \leq Y_5 \leq 1.20$	
Y_6=Cumulative % CPT released at 2 hours	$20 \leq Y_6 \leq 30$	
Y_7=Cumulative % CPT released at 6 hours	$50 \leq Y_7 \leq 60$	
Y_8=Cumulative % CPT released at 12 hours	$80 \leq Y_8 \leq 100$	
Y_9=Coating Efficiency (%)	$80 \leq Y_9 \leq 100$	

Accordingly, a Plackett-Burman design that required 12 design points was selected CPT-013 to CPT-024. This reduced the number of experimental runs to a manageable level to permit the evaluation of all significant factors likely to affect the ultimate quality of the CPT beads. The effects of the different responses are computed mathematically using Equation 4.4.

$$Y = \beta_0 + \sum \beta_i X_{i(i=1,2,3,4,\ldots,k)}$$ **Equation 4.4**

Where,

Y = predicted response,
B_0 = y-intercept,
B_{i-k} = linear regression coefficients for interaction effects,
X_{i-k} = experimental factors with k being the number of variables [107].

Eleven independent variables in twelve combinations were organised into a Plackett-Burman design matrix as depicted in Table 4.4. The response variables for all model formulation and process factors were analysed using Design-Expert® 8.0.4 software (Stat-Ease Inc., Minneapolis, USA). The R^2 coefficients obtained for the analysis provides information about the impact of each individual factor on the response measured. The tools used to help access the significance of each factor included the use of p-values, normal plots, 2D contour plots or 3D response surface plots and Pareto charts.

Table 4.4 *Plackett-Burman experimental design matrix representing the actual values for 11 independent variables.*

Run	Factor 1	Factor 2	Factor 3	Factor 4	Factor 5	Factor 6	Factor 7	Factor 8	Factor 9	Factor 10	Factor 11
	MCC (%)	K100M (%)	E4M (%)	RS PO (%)	Extrusion Speed (rpm)	Spheronisation Speed (rpm)	Residence Time (min)	Coating Temp (°C)	Atomising AFR (m^3/h)	Spray Rate (g/min)	Curing Temp (°C)
CPT-013	40.0	15	15	7.5	15	1200	3	60	115	2	40
CPT-014	50.0	15	25	15	35	1200	3	60	130	2	60
CPT-015	50.0	25	15	15	35	1800	3	60	115	5	40
CPT-016	50.0	25	25	7.5	15	1200	6	60	130	5	40
CPT017	40.0	25	25	15	15	1200	3	90	115	5	60
CPT-018	40.0	15	15	15	15	1800	6	60	130	5	60
CPT-019	50.0	15	15	7.5	35	1200	6	90	115	5	60
CPT-020	40.0	15	25	7.5	35	1800	3	90	130	5	40
CPT-021	40.0	25	15	15	35	1200	6	90	130	2	40
CPT-022	50.0	15	25	15	15	1800	6	90	115	2	40
CPT-023	40.0	25	25	7.5	35	1800	6	60	115	2	60
CPT-024	50.0	25	15	7.5	15	1800	3	90	130	2	60

4.4 RESULTS AND DISCUSSION

4.4.1 Process variables

The effect of extrusion speeds of 15, 25 and 35 rpm on yield and sphericity was performed in triplicate to CPT-001 reference formulation composition. CPT-001 comprised of 20 % CPT payload, 40 % MCC, 15 % Methocel® K100M, 7.5 % Methocel® E4M, 15 % Eudragit® RS PO and 2.5 % talc. The results are summarised in Table 4.5.

Table 4.5 *Effect of extrusion speed on yield and sphericity.*

	Extrusion Speed (rpm)		
	15	**25**	**35**
%Yield	76.91±3.46	88.39±4.18	80.84±3.85
Sphericity	1.19±0.68	1.21±0.52	1.18±0.44

The results reveal that the sphericity value was almost identical when the extrusion speed was increased and these results are consistent with previously reported data [203] in which extrusion speed was found not to have a significant effect on the shape, size and size distribution of beads. The effect of spheronisation speeds on yield and sphericity was performed in triplicate to to CPT-001 formulation composition and the results are summarised in Table 4.6.

Table 4.6 *Effect of spheronisation speed on yield and sphericity.*

	Spheronisation Speed (rpm)				
	600	**900**	**1200**	**1500**	**1800**
% Yield	54.87±5.97	66.71±6.99	74.87±7.02	72.93±6.72	79.12±5.07
Sphericity	2.08±0.79	1.96±0.48	1.46±0.57	1.27±0.38	1.24±0.35

The results show that the sphericity value is approaching 1 with an increase in spheronisation speed with a constant 6 minute residence time. Lower spheronisation speeds led to the production of dumb-bell shaped beads due to low energy input. However, at higher spheronisation speeds sufficient energy to convert extrudates into spherical beads was generated.

The SEM pictogram depicted in Figure 4.6 A reveals that during spheronisation cylindrical extrudates of CPT-001 are rounded at the edges to form dumb-bell like units harvested at 3 minutes. Increasing the residence time of these materials produces spherical beads as depicted in Figure 4.6 B harvested at 6 minutes. Therefore this formulation produces beads as suggested in the model developed by Rowe [137].

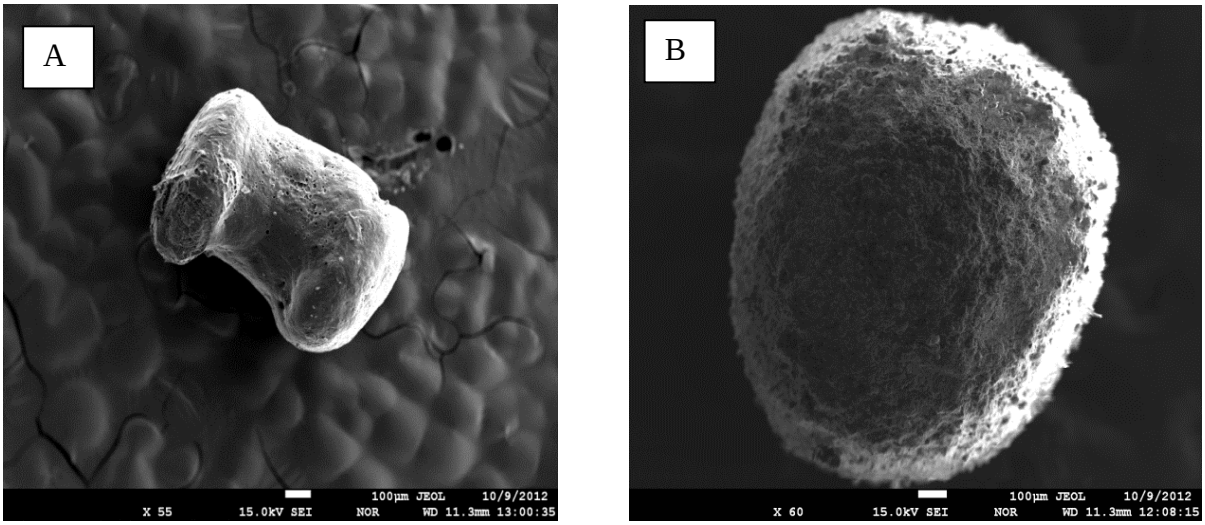

Figure 4.6 *SEM images showing dumb-bell like beads harvested at 3 minutes* ***(A)*** *and spherical beads after spheronisation* ***(B)*** *harvested at 6 minutes.*

A relatively short residence time of approximately six (6) minutes was sufficient to produce a maximum yield of beads with acceptable sphericity and longer residence times of > 10 minutes did not appear to improve the sphericity of bead and resulted in a wide bead size distribution and agglomeration.

The lack thereof of SR commercial formulations in South Africa prompted the development of bead dosage form to modulate CPT release to provide a SR effect. The intent of formulation CPT-001 considered as the reference product was to provide guidance to manufacture coated CPT beads with the desired quality attributes following extrusion-spheronisation and coating. The use of batch CPT-001 as a reference product was intended to minimise wastage of excipients particularly and to screen formulation and process variables investigated using a Plackett-Burman experimental design. The SR effect and quality attributes were assessed against the guidelines stipulated in the USP for SR effects [218]. Amounts of excipients in CPT-001 were blended for 20 minutes and 10

% SSC used to granulate the powders. The granules are extruded at 25 rpm extrusion speed and spheronised at 1500 rpm for 6 minutes residence time. Wet beads are dried in a fluidized bed processor for 25 minutes and coated using 15 % SSC dispersions at a rate of 2 g/min. The coating temperature is 40 ˚C and cured at 40 ˚C for 1 hour. *In vitro* CPT release of CPT-001 reference bead dosage form using the USP Apparatus 3 system in triplicate (n=3) generated the release profile Figure 4.7.

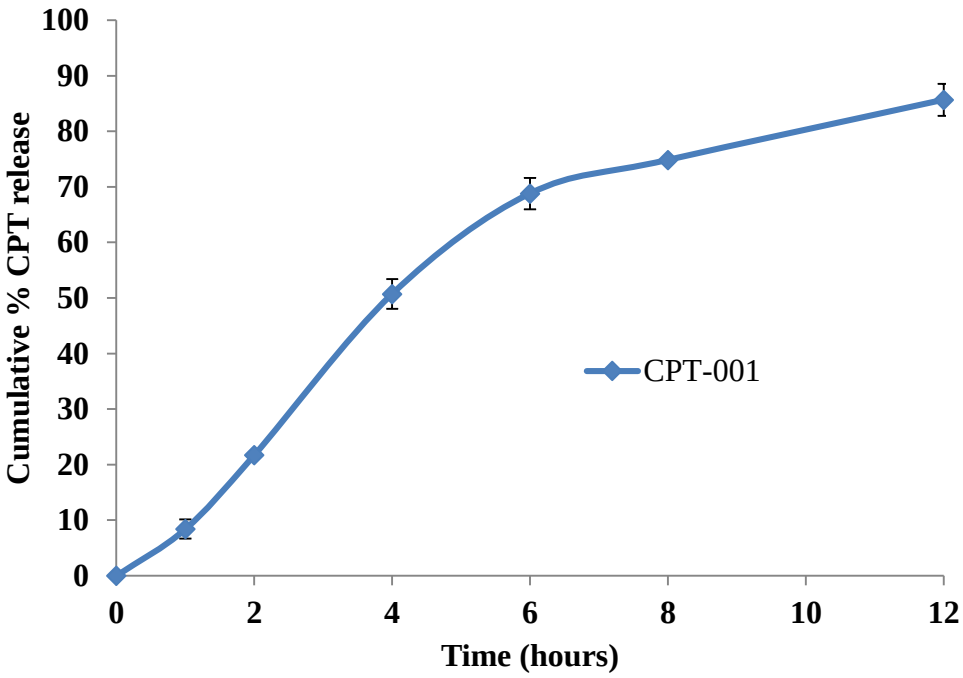

Figure 4.7 *In vitro dissolution profiles of CPT release from CPT-001.*

The *in vitro* release profile of reference CPT-001 depicted in Figure 4.7 reveal 21.7 % of CPT release at 2 hours, 68.8 % release at 6 hours and 85.6 % released at 12 hours. It is evident that CPT-001 comply with USP pharmacopeia [218] which stipulates that a dissolution profile for modified and SR formulations should exhibit at least 20 - 30 % of an API in 2 hours, at least 50 % in the middle percentile range and at least 80 % after 12 hours. The reference formulation was used for statistical comparison to evaluate the release profiles of CPT from experimental runs and optimized batches.

4.4.2 Plackett–Burman design

The outputs monitored for the Plackett-Burman experimental design were percent yield, AOR, friability, AR, sphericity, coating efficiency and percent CPT released at 2, 6 and 12 hrs. The results are summarised in Table 4.7. All batches of CPT beads were manufactured to have a 20 % w/w payload with a fixed concentration SSC (10% w/w) added as appropriate and coated with a 15 % w/w SSC to a target weight gain of 20 %. Talc was used to improve the flow properties of the beads due to the cohesive nature of the tacky wet mass and was added to the formulation prior to extrusion. The significance of the each response was tested using the ANOVA function of Design-Expert® 8.0.4 software program (Stat-Ease Inc., Minneapolis, USA) and the resultant responses are summarised in Table 4.8. The significant response models included yield, AR, sphericity, coating efficiency and cumulative percent CPT release at 2 and 12 hrs.

Table 4.7 *Responses observed using a Plackett-Burman experimental design.*

Run	Y_1	Y_2	Y_3	Y_4	Y_5	Y_6	Y_7	Y_8	Y_9
	Yield (%)	**AOR (°)**	**Friability (%)**	**AR**	**Sphericity**	**Cumulative % CPT released at 2hrs**	**Cumulative % CPT released at 6hrs**	**Cumulative % CPT released at 12hrs**	**Coating Efficiency (%)**
CPT-013	70.41	28.5	0.79	1.27	1.43	45.4	72.1	88.8	82.4
CPT-014	91.38	25.1	1.31	1.23	1.41	43.5	67.2	88.3	97.9
CPT-015	75.13	29.5	0.92	1.02	1.17	38.8	82.8	95.6	86.1
CPT-016	74.39	30.5	0.86	1.22	1.29	33.0	72.9	84.9	89.1
CPT-017	74.41	26.7	0.99	1.04	1.14	19.4	59.7	78.4	78.7
CPT-018	87.69	28.3	0.53	0.91	1.29	24.5	70.2	86.5	90.7
CPT-019	81.86	21.3	0.89	0.81	1.31	30.5	69.5	92.8	76.4
CPT-020	69.21	32.1	0.92	1.08	1.17	34.6	69.9	93.4	92.1
CPT-021	85.85	28.3	0.43	0.91	1.27	40.0	69.2	86.5	98.6
CPT-022	84.78	31.1	0.52	0.98	1.01	51.1	81.2	99.7	84.6
CPT-023	81.85	30.3	0.56	1.01	0.98	24.6	70.2	89.7	83.1
CPT-024	83.81	29.4	0.43	1.06	1.18	28.5	75.4	98.2	98.4

Table 4.8 *ANOVA: Model fit summary for coated beads.*

Source	Y_1	Y_2	Y_3	Y_4	Y_5	Y_6	Y_7	Y_8	Y_9
	Yield (%)	**AOR (°)**	**Friability (%)**	**AR**	**Sphericity**	**Cumulative % CPT released at 2hrs**	**Cumulative % CPT released at 6hrs**	**Cumulative % CPT released at 12hrs**	**Coating Efficiency (%)**
Model	0.028	0.108	0.149	0.031	0.046	0.033	0.092	0.027	0.014
SS*	562	95.2	0.799	0.214	0.215	1004	401	562	635
SP**	Significant	Not Significant	Not Significant	Significant	Significant	Significant	Not Significant	Significant	Significant

*Sum of Squares, ** Significance of parameter

4.4.2.1 Yield

The percentage yield of coated beads achieved using an experimental design approach ranged between 69.21 and 91.38 %. The use of sieving to evaluate production efficiency was simple, cost effective and rapid, despite the potential of screen skewing to alter bead shapes. Usually a process yield > 80 % is acceptable with values greater than 95 % most preferred. However, lower yields of 60 % are acceptable for establishing cost-effective production of coated beads and is indicative of the successful application of extrusion-spheronisation. The range of 60 – 95 % yield was observed in the experimental desgn. ANOVA responses for the percent yield are summarised in Table 4.9.

Table 4.9 *ANOVA data for % yield.*

Source	**Sum of Squares**	**p-value (Prob > F)**	
Model	561.82	0.0279	Significant
X_1-MCC	40.08	0.0271	Significant
X_2-K100M	8.15	0.0597	
X_3-E4M	6.35	0.0676	
X_4-RS PO	118.5	0.0157	Significant
X_5-Extrusion Speed	7.99	0.0603	
X_6-Spheronisation Speed	1.45	0.1397	
X_7-Residence Time	85.71	0.0185	Significant
X_9-AFR	47.56	0.0248	Significant
X_{10}-Spray Rate	104.37	0.0167	Significant
X_{11}-Curing Temp	141.66	0.0144	Significant
Residual	0.072	1	0.072
Cor Total	561.89	11	
Std. Dev.	0.27	**R^2**	0.9999
Mean	80.06	**Adj R^2**	0.9986
C.V. %	0.34	**Pred R^2**	0.9815
PRESS	10.38	**Adeq Precision**	85.649

These results suggest that the main effects of model process optimization can be used to fit data from the design matrix, as indicated by a p value of < 0.05. The predicted R^2 value of 0.9815 was in reasonable agreement with the adjusted R^2 value of 0.9986, with eleven degrees of freedom. The linear model terms for % w/w MCC (X_1), % Eudragit® RSPO (X_4) residence time (X_7), AFR (X_9), spray rate (X_{10}) and curing time (X_{11}) were significant. The adequate precision was > 4 and the R^2 of 0.9999 indicating that the data can be described adequately by a linear mathematical model and can be used to navigate this design space.

These results were further supported by evaluation of the predicted versus actual normal probability plot, with most points distributed in a straight line as depicted in Figure 4.8.

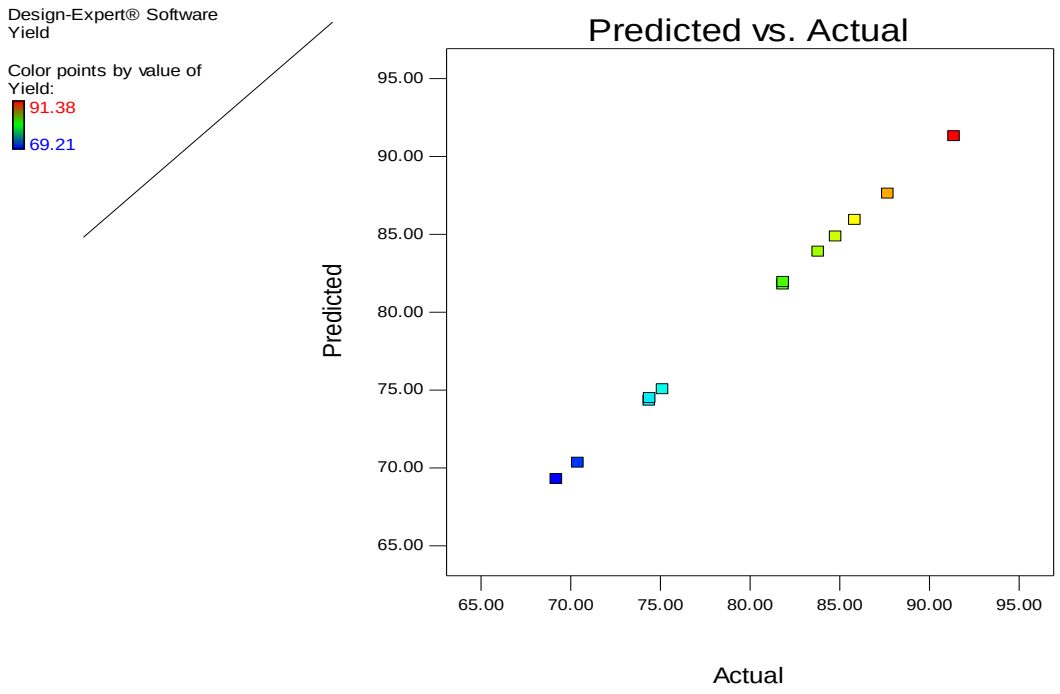

Figure 4.8 *Actual responses versus predicted response plot for % yield.*

The linear regression equation for the % yield in terms of the actual factors can be described using Equations 4.5:

Yield = + 80.06 + 1.83*MCC - 0.82*K100M - 0.73*E4M + 3.14* Eudragit® RSPO + 0.82* Extrusion speed + 0.35*Spheronisation Speed + 2.67*Residence time + 1.99*Atomising air flow rate - 2.95*Spray rate + 3.44*Curing temp **Equation 4.5**

The contour and 3D-surface response plots for percent yield as a function of Methocel® K100M and Methocel® E4M content are depicted in Figures 4.9 A and B. The plots show relatively high percent yield > 84 % for all batches manufactured. Formulations in which the higher molecular weight HPMC K100M at high levels led to the formation of wet sticky mass and the extrudate had a "shark skin" morphology, which resulted in the production of fines and consequently a decrease in the yield of beads in the desired size range. The wet mass had tendency to adhere to walls and/or friction plate of the extruder leading to agglomeration into particles of large and unacceptable size.

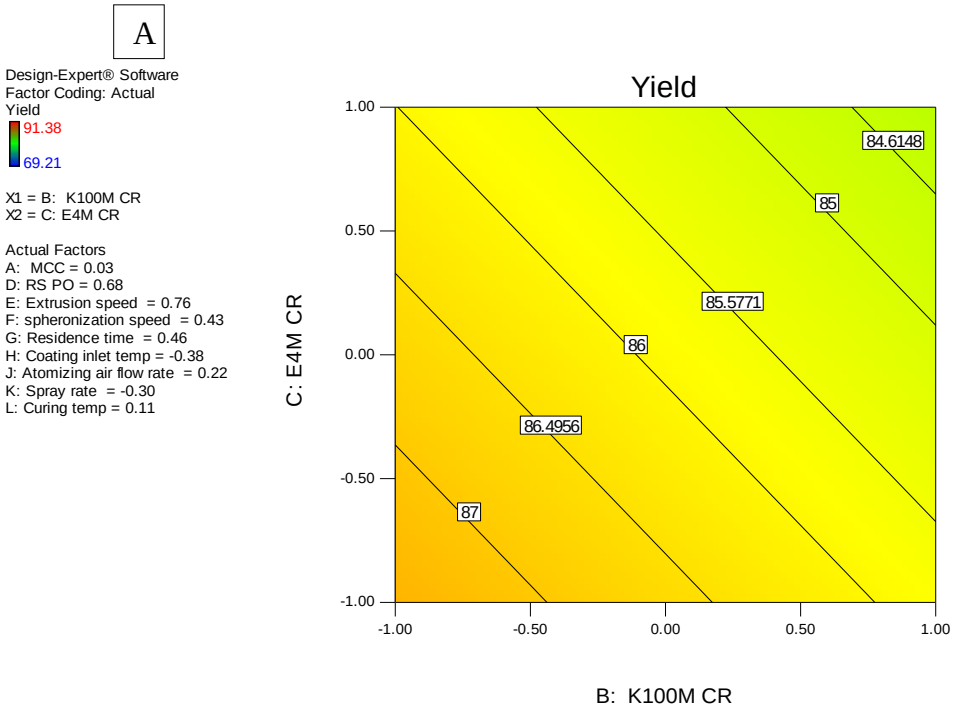

Figure 4.9 A) *Contour plots showing the effect of Methocel® K100M and E4M on the % yield (Y_1).*

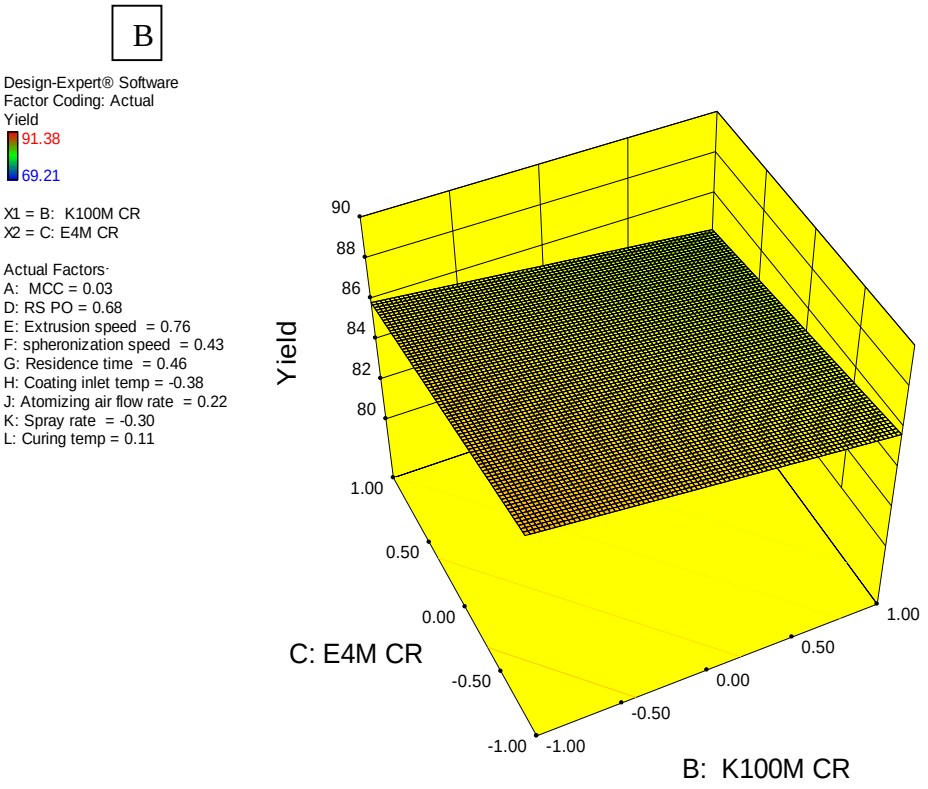

Figure 4.9 B) *Response surface plot depicting the effect of Methocel® K100M and E4M on the % yield (Y_1).*

The response surface plot of percent yield as a function of spheronisation speed and residence time is depicted in Figure 4.10. An increase in the speed of spheronisation while maintaining a constant residence time resulted in an increase in the yield whereas longer residence times resulted in a decreased yield. Longer residence times tended to increase particle-to-particle interactions, resulting in the formation of agglomerates and oversized beads that consequently decrease the yield of beads of the target size. Cohesive and destructive forces are involved in the spheronisation process and an increase in residence time limits bead growth and results in a decrease in the average bead diameter, as indicated by the decrease in yield of beads in the desired range [152].

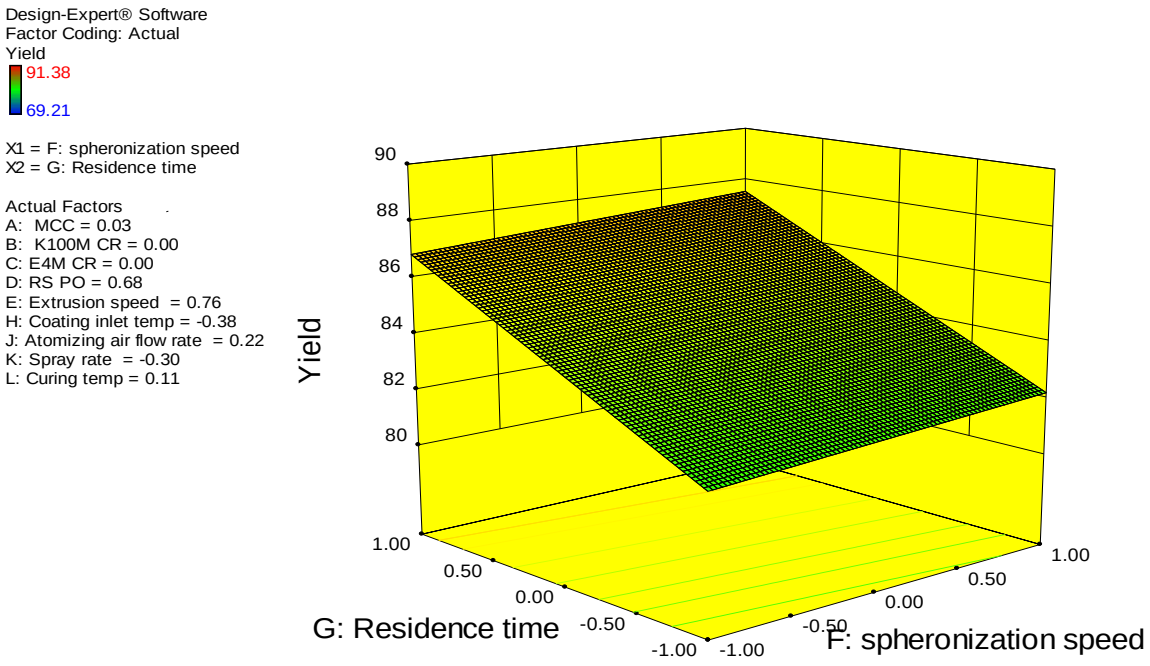

Figure 4.10 *Response surface plot showing effect of spheronisation speed and residence time on % yield (Y_1).*

4.4.2.2 Scanning Electron Microscopy (SEM)

SEM images permits the visualisation of changes in the characteristics of the beads, including parameters such as shape and texture, as experimental conditions are varied. SEM illustrates the presence of discrete, spherical or oval beads that appear to have rough surface prior to coating as depicted in Figure 4.11 A.

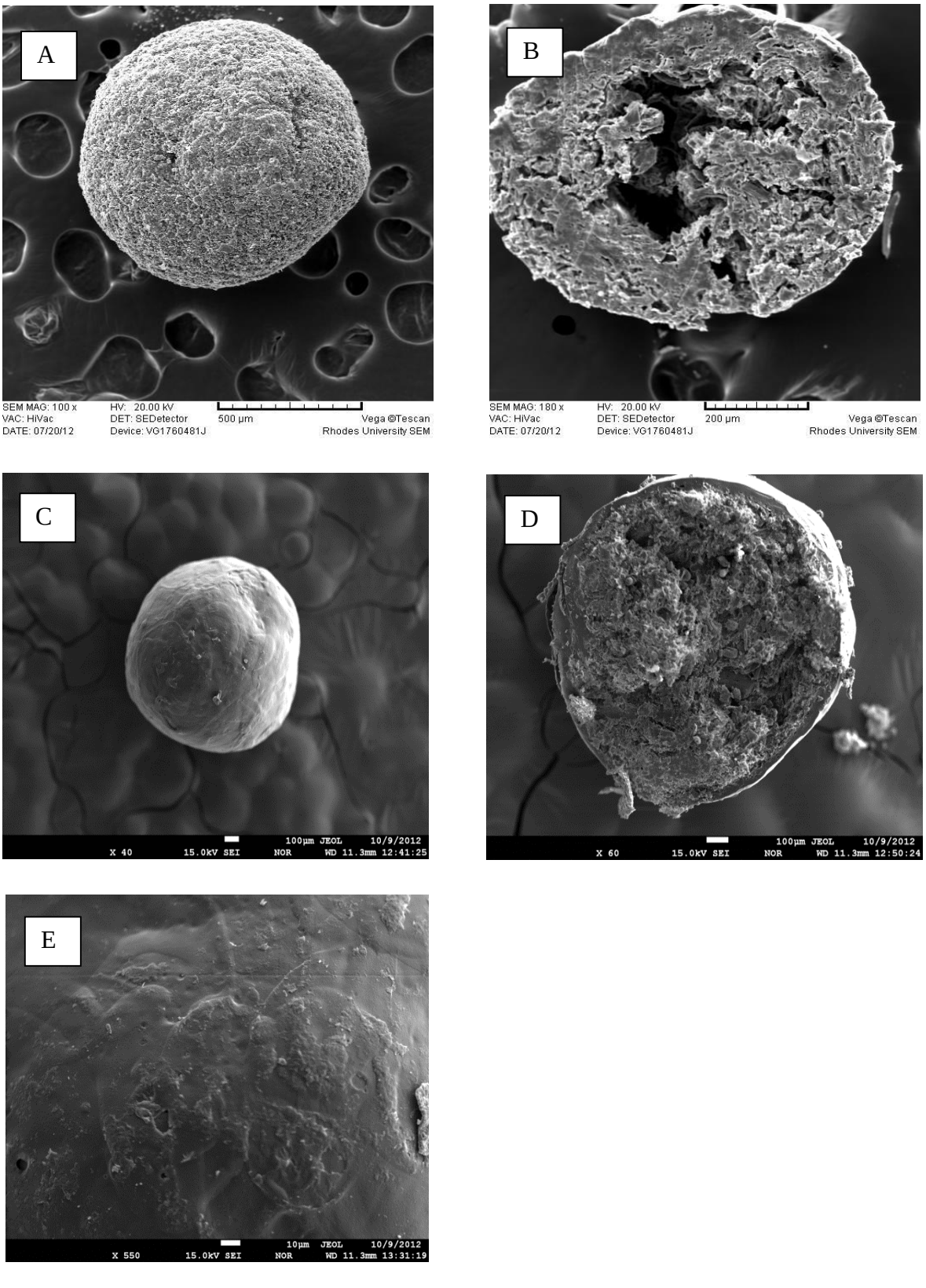

Figure 4.11 *SEM images showing an uncoated bead* ***(A),*** *a cross-section of an uncoated bead* ***(B),*** *a coated bead* ***(C),*** *a cross-section of a coated bead* ***(D)*** *and a magnified coated surface of a bead* ***(E).***

The cross-section of an uncoated CPT bead depicted in Figure 4.11 B reveals that the bead is spherical in shape and has visible pores with a compact matrix around the peripheral regions. The quality of the coating layer inspected using SEM image shown in Figure 4.11 C reveals the presence of a smooth coat. The use of the 121 mm Würster insert in a fluidised bed dryer facilitated the uniform deposition of the coat resulting in beads with a smooth surface. The cross-section of a coated bead depicted in Figure 4.11 D permits visualisation of the porosity difference between the core and the coat. The cross-section of the coated bead reveals the core and polymer coating layer are uniform and the coat is likely to control CPT release. The coating layer formed by coalescence of ethylcellulose in the presence of a plasticiser and stabiliser results in the formation of a compact film that is less friable with fewer when compared to the uncoated beads. At higher magnification the coating layer depicted in Figure 4.11 E is clearly shown to have fewer pores and smooth surface with a limited number of irregularities.

4.4.2.3 Aspect Ratio (AR)

The shape of the beads was evaluated using the AR and sphericity. The determination of the AR requires the measurement of the Feret diameter of beads from all possible orientations from an image of that bead, unlike establishing sphericity that ultimately compares the shape of the bead to a circle [203]. Bead shape in multi-particulate dosage forms is critical to ensure uniformity of coating and filling processes. The value for AR for all batches ranged between from 0.81 - 1.27 as summarised in Table 4.7, indicating that minor deviations occurred when the process parameters were altered, despite the beads being visually assessed as spherical.

ANOVA data for the AR indicate that the model was significant with a p-value < 0.05 and a reasonably good correlation adjusted R^2 value of 0.9983, which was in close agreement with the predicted R^2 value of 0.9776 as summarised in Table 4.10.

Table 4.10 *ANOVA data for Aspect Ratio and Sphericity.*

Aspect Ratio				Sphericity			
Source	**Sum of Squares**	**p-value**		**Source**	**Sum of Squares**	**p-value**	
Model	0.21	0.0307	Significant	**Model**	0.22	0.0459	Significant
X_1-MCC	8.33E-04	0.1257		**X_1-MCC**	6.75E-04	0.2048	
X_3-E4M	0.028	0.0219	Significant	**X_2-K100M**	0.029	0.0323	Significant
X_4-RS PO	0.011	0.0353	Significant	**X_3-E4M**	0.035	0.0294	Significant
X_5-Extrusion Speed	0.015	0.0303	Significant	**X_4-RS PO**	4.08E-04	0.2578	
X_6 -Spheronisation Speed	0.015	0.0303	Significant	**X_5-Extrusion Speed**	7.50E-05	0.5000	
X_7-Residence Time	0.062	0.0148	Significant	**X_6-Spheronisation Speed**	0.092	0.0182	Significant
X_8-Coating Inlet Temp	0.051	0.0163	Significant	**X_7-Residence Time**	0.01	0.0544	
X_9-AFR	6.53E-03	0.0454	Significant	**X_8-Coating Inlet Temp**	0.02	0.0389	Significant
X_{10}-Spray Rate	0.012	0.0335	Significant	**X_9-AFR**	0.027	0.0335	Significant
X_{11}-Curing Temp	0.015	0.0303	Significant	**X_{10}-Spray Rate**	6.75E-04	0.2048	Significant
Residual	3.33E-05	1	3.33E-05	**Residual**	7.50E-05	1	7.50E-05
Cor Total	0.21	11		**Cor Total**	0.22	11	
Std. Dev.	5.77E-03	**R^2**	0.9998	**Std. Dev.**	8.66E-03	**R^2**	0.9997
Mean	1.05	**Adj R^2**	0.9983	**Mean**	1.22	**Adj R^2**	0.9962
C.V. %	0.55	**Pred R^2**	0.9776	**C.V. %**	0.71	**Pred R^2**	0.9498
PRESS	4.80E-03	**Adeq Precision**	83.217	**PRESS**	0.011	**Adeq Precision**	53.669

The model can therefore be used to describe the data and optimise the manufacture of coated beads containing CPT. The composition of Methocel® E4M, Eudragit® RSPO, extrusion speed, spheronisation speed, residence time, inlet temperature during coating, AFR, spray rate and curing time were significant model terms. The linear regression equation for AR in terms of actual factors is listed as Equation 4.6:

Aspect Ratio = +1.05 +8.33E-003*MCC +0.048*E4M -0.030* Eudragit® RS PO -0.035*Extrusion speed -0.035*Spheronisation speed -0.072*Residence time -0.065*Coating inlet temperature +0.023*Atomising air flow rate -0.032*Spray rate -0.035*Curing temperature

Equation 4.6

A Pareto bar chart (Figure 4.12) was used to rank independent, but related factors in decreasing order of significance in respect of the AR. The principle developed by Pareto [223] permits separation of significant from trivial terms that may influence a response. In this case the purpose was to improve the AR. The parameter that has the greatest effect on the AR was residence time and all spheronisation process parameters had some influence on bead shape and the AR.

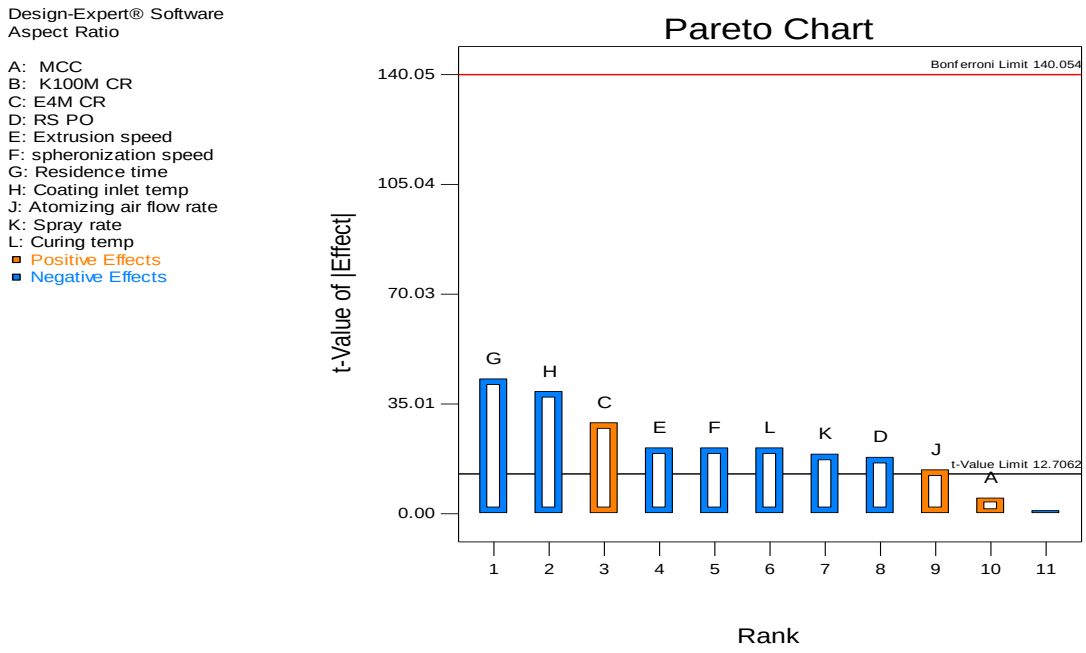

Figure 4.12 *Pareto chart showing the impact and rank of independent terms in respect of AR.*

The response surface plot of AR in terms of spheronisation and residence time is depicted in Figure 4.13. An increase in the spheronisation speed resulted in more spherical shaped beads. This was due to higher energy resulting in fragmentation of extrudate through interaction with the frictional plate, subsequently rounding the fragments into beads through particle to spheroniser wall and particle-to-particle interactions.

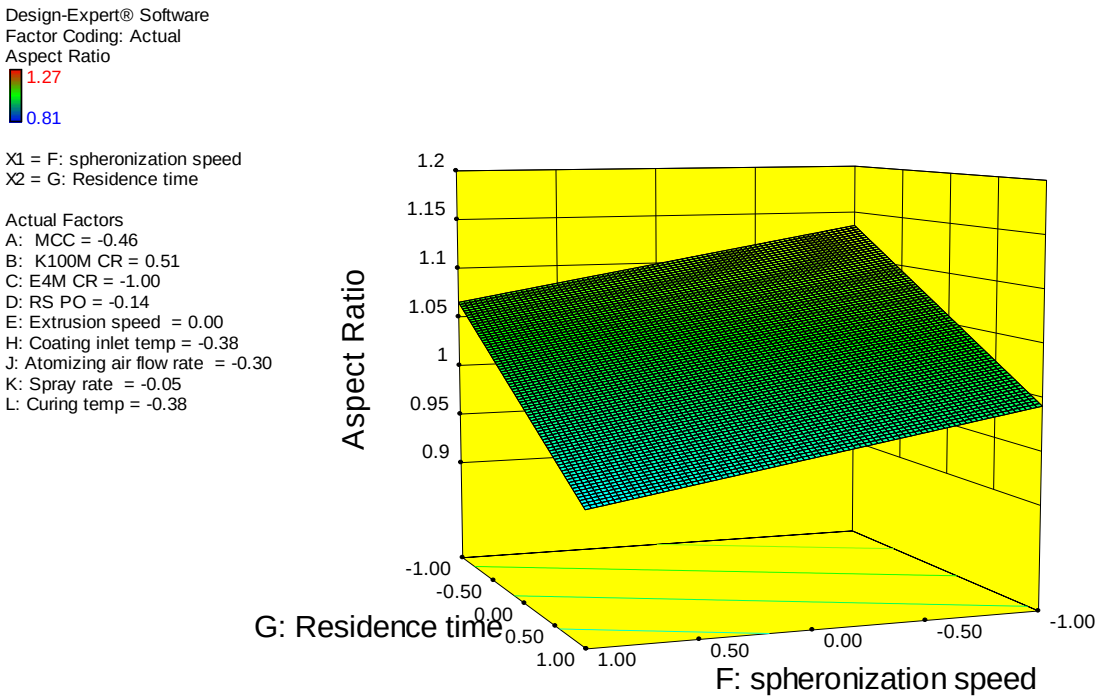

Figure 4.13 *Response surface plot showing effect of spheronisation speed and residence time on AR.*

4.4.2.4 Sphericity

The sphericity parameter compares the perimeter of beads to that of a circle of equivalent area [203] and the more irregular the shape of the bead, the longer is its perimeter and the lower the sphericity value for that bead. The sphericity values for the bead manufactured in these studies range from 0.98 to 1.43 and the data are summarised in Table 4.7. The results suggest that beads from most batches were spherical, and values for sphericity > 1.80 indicate the presence of a dumbbell shaped product.

The model design was checked for appropriateness using sequential sum of squares, correlation values and press statistic (Table 4.10). ANOVA data for the linear model for sphericity suggest that the model is significant and correlated well with the adjusted R^2 of 0.9962. The Methocel® K100M and Methocel® E4M composition, spheronisation speed, inlet coating temperature and AFR had a significant influence of the sphericity of the beads.

The regression equation for beads sphericity in terms of the actual factors is summarised in Equations 4.7:

Sphericity = + 1.22 + 7.500E-003*MCC - 0.049*K100M - 0.054*E4M - 5.833E-003* Eudragit® RS PO - 2.500E-003*Extrusion speed - 0.087*Spheronisation speed - 0.029* Residence time - 0.041*Coating inlet temperature + 0.047*Atomising air flow rate +7.500E-003*Spray rate

Equation 4.7

A contour plot revealing the impact of Methocel® K100M composition and and spheronisation speed on sphericity is depicted in Figure 4.14.

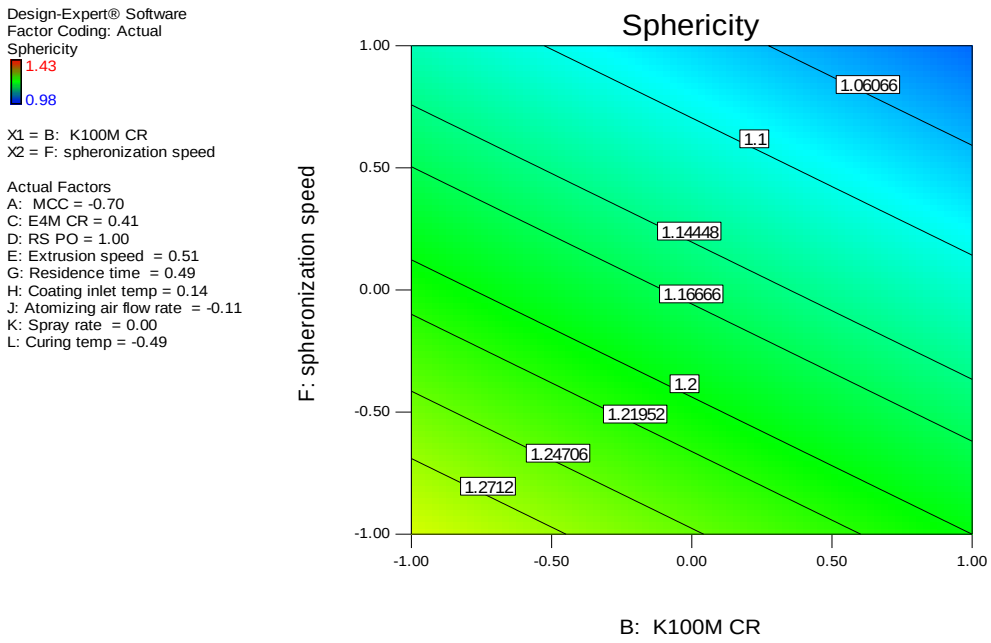

Figure 4.14 *Contour plot showing effect of Methocel® K100M and spheronisation speed on sphericity.*

A contour plot depicting the impact of Methocel® E4M and spheronisation speed on sphericity is depicted in Figure 4.15.

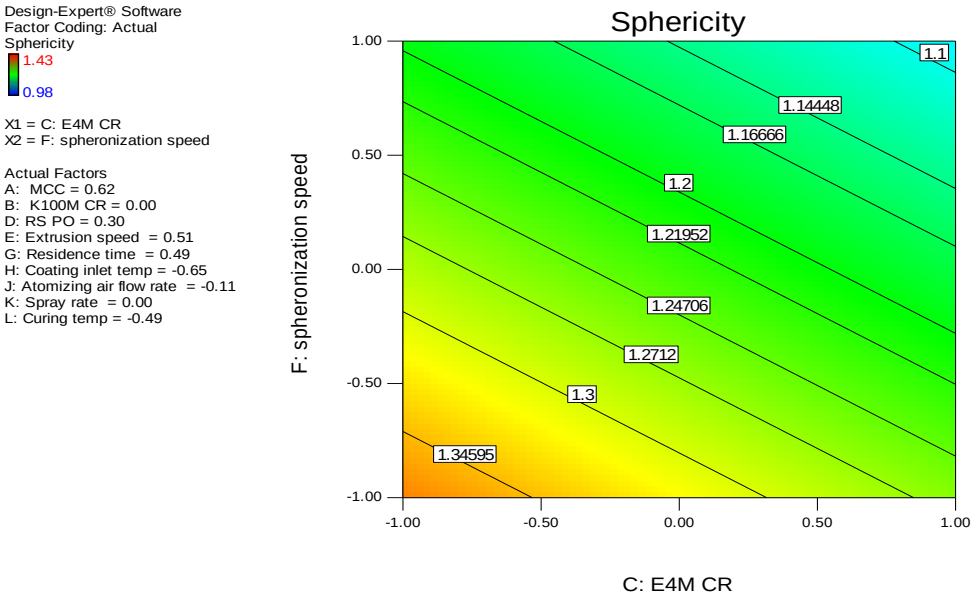

Figure 4.15 *Contour plot showing effect of Methocel® E4M and spheronisation speed on sphericity.*

Increasing the amount of either Methocel® K100M or E4M at a constant spheronisation speed resulted in a decrease in the overall sphericity of the beads. Increased amounts of HPMC resulted in an increase in the tackiness of the wet mass and produced rough and irregular shaped beads that exhibited a characteristic "shark skin" extrudate prior to spheronisation that causes beads to break unevenly during spheronisation. An increase in the spheronisation speed did not necessarily increase mechanical forces to a sufficient level to facilitate fracture and eventual rounding of the extrudate.

4.4.2.5 Dissolution test

4.4.2.5.1 Effect of different levels of granulating fluid

During spheronisation moisture from the granulating fluid migrates towards the surface of the particles and provides additional plasticity capacity to round the beads [137]. The strength of agglomerates during wet massing depends on the liquid saturation level in a uniformly blended powder mixture and that strength can be increased following the addition of more adhesive and viscous binders such as ethylcellulose that form solid bridges due to capillary effects during the granulation process [207]. During the drying phase in which solvent(s) is/are completely removed via evaporation the mechanical strength of the bead is primarily due to the formation of solid bridges between the particles [137, 207].

To investigate the effect of different amounts of granulation fluid on CPT content an assay for CPT content in beads was undertaken and the results are summarised in Table 4.11. The assay results indicate that the percent CPT recovered from 250 mg of the coated CPT beads theoretically equivalent to 50 mg of CPT.The actual amount recovered is approximately equal to the predicted label claim. The low standard deviations indicate the CPT is uniformly distributed in the batches tested and provide an indication that dose uniformity is likely.

Table 4.11 *Content uniformity of CPT beads manufactured to different granulation level.*

Sample Number	% SSC	Theoretical Amount of CPT present per 250mg beads (mg)	*Analysed Amount of CPT (mg)	*SD ±	% Recovery
CPT-003	**5**	50	49.1	2.47	98.2
CPT-004	**10**	50	49.2	0.641	98.4
CPT-005	**15**	50	48.7	0.408	97.4
CPT-006	**20**	50	49.4	0.832	98.8

*Mean and SD is for six determinations.

The release profiles of CPT from coated beads using purified water (control- CPT-002) and different levels of SSC as the granulating fluid using the dissolution conditions described in §4.3.2.9 are depicted in Figure 4.16.

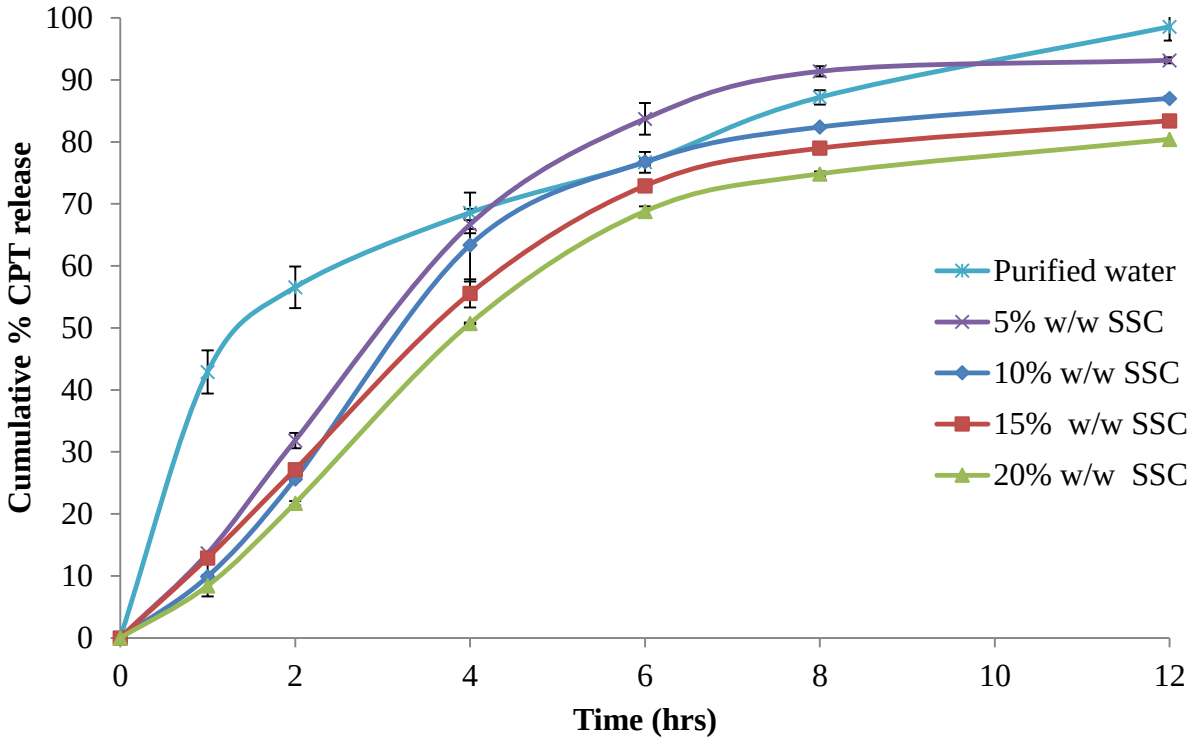

Figure 4.16 *Release profiles of CPT from beads granulated with purified water (control) and different levels of SSC.*

The percent CPT released in batch manufactured using purified water released 55 % within the first two hours of testing. This shows the burst effect usually associated with high water solubility compounds and that can diffuse rapidly across the matrix and through pores in the coating and dissolve immediately once in contact with the dissolution medium prior to formation of an extensive gel layer. The initial burst release appears to be followed by slow release of CPT for the balance of the test period. In order to reduce the burst effect and develop a SR system for a water soluble drug, such as CPT, Surelease® coatings or inclusion as a binder may suppress the initial burst effect. Surelease® contains ethylcellulose dispersions with the aqueous solvent completely removed via evaporation during the curing process to form a thin film membrane around the bead core formed with solid bridges of ethylcellulose particles. Furthermore, the presence of film membrane around the bead core may enhance the stability of the bead formulation, since CPT degrades in water to form captopril disulphide.

MCC facilitates the extrusion of granulations with minimal resistance and limited heat due to friction resulting in the formation of even fragments of extrudate that can easily be spheronised. In addition since MCC exhibits good wetting properties and readily liberates granulating fluid that can be used as a lubricant during the spheronisation process [129, 142, 202]. The use of Surelease® dispersion as granulating fluid can therefore result in polymer deposition, increased cohesiveness and the production of fewer fines.

Increasing the amount of SSC from 5 % w/w to 20 % w/w resulted in a decrease in the rate of CPT release. Moreover, the cumulative amount of CPT released was considerably lower at higher levels of SSC. The releaseof CPT from formulation with a lower level of SSC was more variable, as depicted in Figure 4.16. At lower SSC levels, the amount of ethylcellulose present is less, and this creates a less homogenous dispersion of the polymer in the granules resulting in pockets of more erodible materials that create erratic release. At higher SSC levels, the degree of homogeneous dispersions increase and the release rates depend not only on the solubility, but also on the polymer/dissolution medium partition coefficient [161].

4.4.2.5.2 Dissolution testing of bead formulations

The percent CPT release after 2 and 12 hours were selected as dependent variables since the p value for these parameters were < 0.05 and therefore these terms reflect that the model is significant and can be used to navigate the design space. The USP pharmacopeia [218] stipulates that a dissolution profile for modified and sustained release formulations should exhibit at least 20 - 30 % of an API in 2 hours, at least 50 %in the middle percentile range and at least 80 %after 12 hours. These limits were used for the purposes of assessing CPT release at 2, 6 and 12 hours.

The pH of the dissolution media was based on physiological pH of sites located along the GITand the duration exposure of dosage forms to each pH was based on published transit times through the GIT [218, 219]. USP Apparatus 3 is useful for assessment of bead type modified release dosage forms since information on multi-unit dosage performance at three time points are readily obtained. This permits the characterisation of *in vitro* release with a change of dissolution medium [218]. Multiple time point data is essential for approval purposes in relation to assessment of the percent released at all times to futher permit evaluation of dose dumping characteristics [219].

The dissolution profiles of CPT beads generated for each batch manufactured for the experimental design are depicted in Figures 4.17 and 4.18. The impact of different input factor combinations resulted in different release profiles for CPT. The cumulative percent CPT released at 2 hours (Y_6) ranged from 24.5 % to 51.1 % and 12 hours (Y_8) ranged from 78.4 % - 99.7 %.

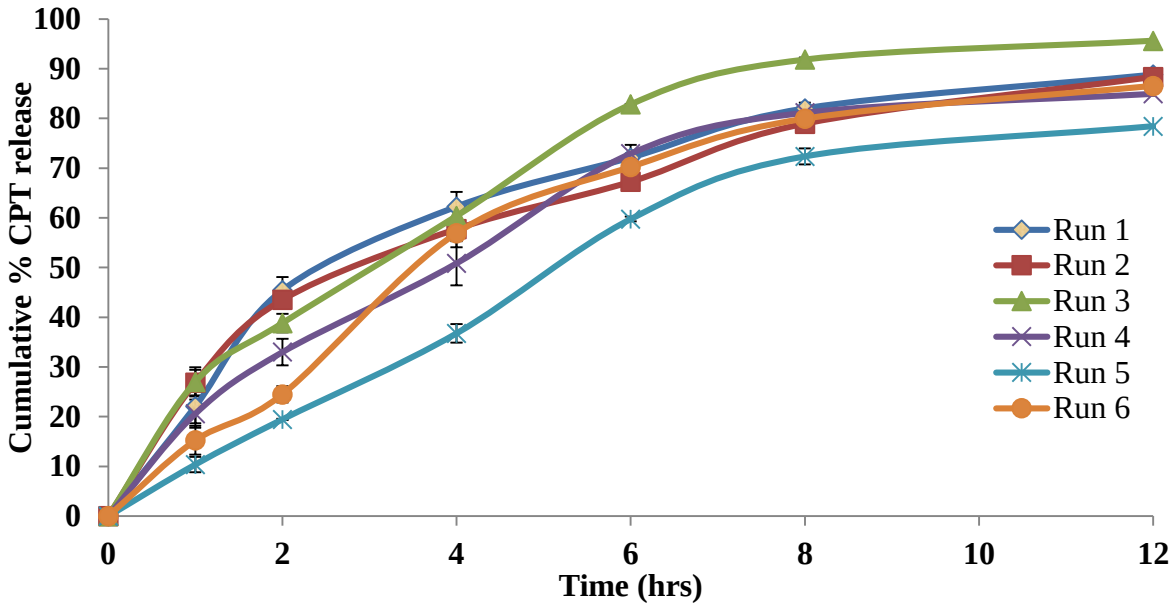

Figure 4.17 *Dissolution profiles of CPT for batches 1–6 (CPT-013-CPT-018).*

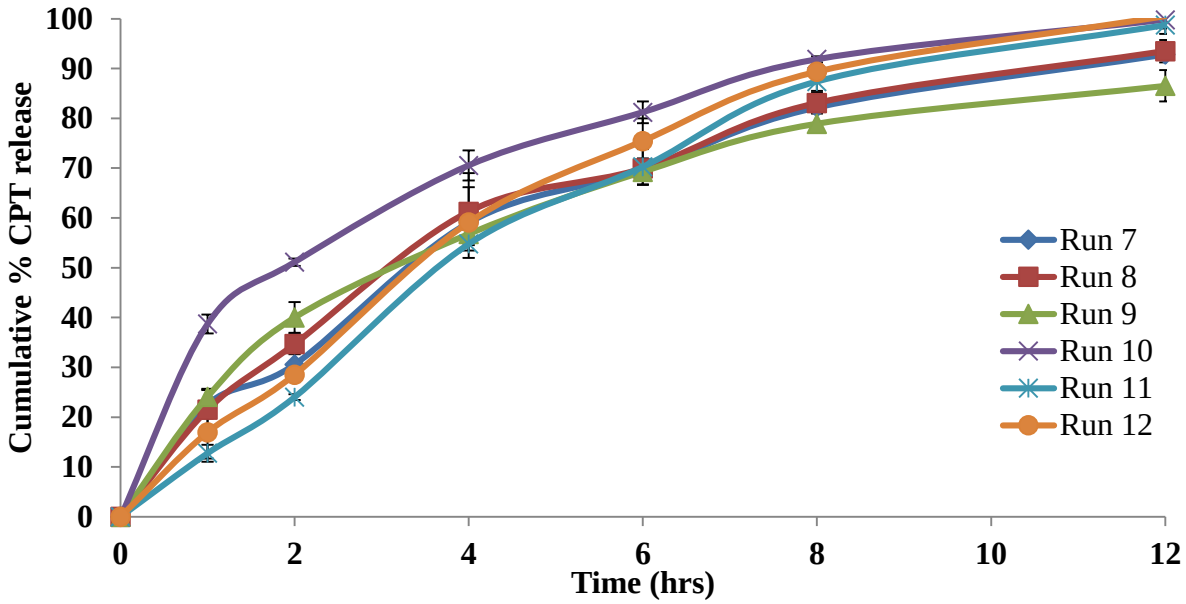

Figure 4.18 *Dissolution profiles of CPT for batches 7–12 (CPT-019-CPT-024).*

4.4.2.5.3 Percent drug release at second hour

ANOVA data obtained for CPT release at 2 hours revealed a p value of 0.0336, suggesting that the model was significant to fit the Plackett-Burman design space.The results of modelling are summarised in Table 4.12.

Table 4.12 *ANOVA of percent CPT released at 2 and 12 hours.*

2nd hour				**12th hour**			
Source	**Sum of Squares**	**p-value**		**Source**	**Sum of Squares**	**p-value**	
Model	1004.2	0.0336	Significant	**Model**	561.82	0.0279	Significant
X_1–MCC	113.47	0.0259	Significant	**X_1-MCC**	40.08	0.0270	Significant
X_2-K100M	171.01	0.0211	Significant	**X_2-K100M**	8.15	0.0203	Significant
X_4-RS PO	35.71	0.0461	Significant	**X_3-E4M**	6.35	0.0144	Significant
X_5-Extrusion Speed	8.50	0.0939		**X_4-RS PO**	118.5	0.0157	Significant
X_6-Spheronisation Speed	7.84	0.0977		**X_5-Extrusion Speed**	7.99	0.0676	
X_7-Residence Time	3.52	0.1444		**X_6-Spheronisation Speed**	1.45	0.1397	
X_8-Coating Inlet Temp	2.71	0.1638		**X_7-Residence Time**	85.71	0.0597	
X_9-AFR	2.71	0.1638		**X_9-AFR**	47.56	0.0248	Significant
X_{10}-Spray Rate	227.94	0.0183	Significant	**X_{10}-Spray Rate**	104.37	0.0167	Significant
X_{11}-Curing Temp	430.8	0.0133	Significant	**X_{11}-Curing Temp**	141.66	0. 0354	Significant
Residual	0.19	1	0.19	**Residual**	0.072	1	0.072
Cor Total	1004.39	11		**Cor Total**	561.89	11	
Std. Dev.	0.43	**R^2**	0.9998	**Std. Dev.**	0.45	**R^2**	0.9985
Mean	34.49	**Adj R^2**	0.9979	**Mean**	71.69	**Adj R^2**	0.9945
C.V. %	1.26	**Pred R^2**	0.9731	**C.V. %**	0.63	**Pred R^2**	0.9761
PRESS	27	**Adeq Precision**	76.463	**PRESS**	9.85	**Adeq Precision**	60.019

A value of probability < 0.05 indicates that the model terms were significant. In this case the composition of MCC, Methocel® K100M and Eudragit® RS PO, spray rate and curing temperature were established as significant model terms. The equation for the percent CPT released at 2 hours in real terms is listed in Equation 4.8:

Cumulative % CPT Released at 2 hours (Y_6) = + 34.49 + 3.08*MCC - 3.77*K100M + 1.73* Eudragit® RS PO + 0.84*Extrusion speed - 0.81*Spheronisation speed -0.54*Residence time - 0.48* Coating inlet temperature - 0.48*Atomizing air flow rate - 4.36*Spray rate - 5.99*Curing temperature **Equations 4.8**

The initial burst effect characteristic of SR dosage forms manufactured with water soluble compounds can be controlled by manipulation of the content of different grades of HPMC and application of a coat to the beads. The formulation composition and coating process parameters were investigated in an attempt to reduce the burst effect for CPT. The effect of release modifying polymers content on CPT released at 2 hours is illustrated as a contour plot in Figure 4.19. The percent CPT released decreases with an increase from 15 - 25 % w/w HPMC K100M with the content of HPMC E4M is constant. In contrast changing the amount of HPMC E4M in the formulation has no impact on CPT release suggesting that only HPMC K100M may reduce the extent of burst release of CPT due to the increased viscosity of the higher grade HPMC polymer.

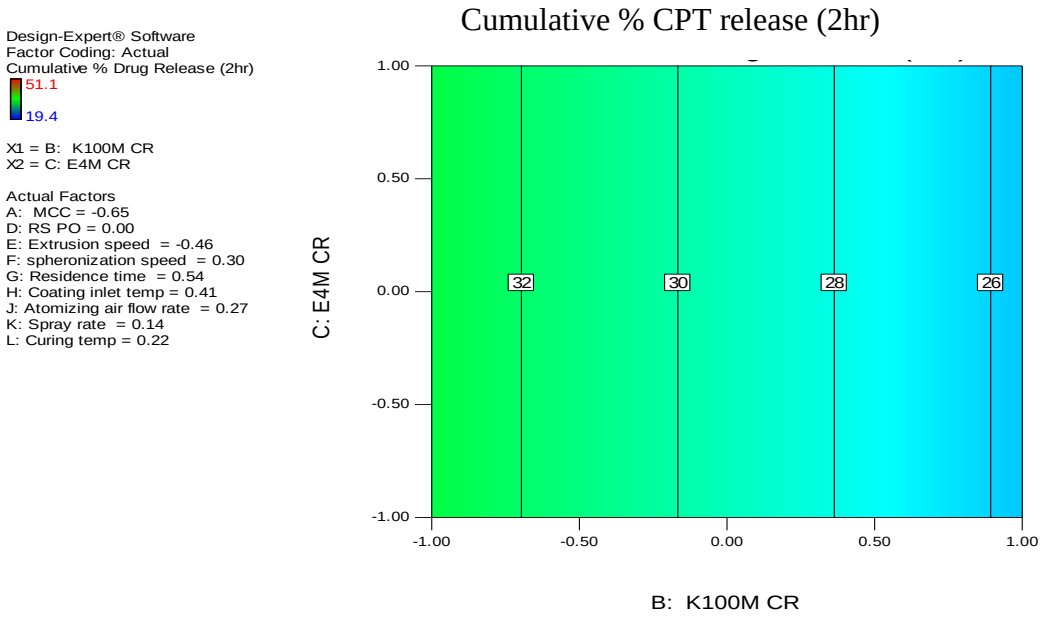

Figure 4.19 *Contour plot depicting the effect of Methocel® K100M and Methocel® E4M on CPT release at 2 hours.*

The rate-limiting step for CPT release at 2 hours is the rate of dissolution medium into the core of the bead across the ethylcellulose coat and polymer composition of the bead. The contour plot depicted in Figure 4.20 depicts influence of coating parameters in controlling the initial burst effect. An increase in the spray rate decreased the amount of CPT released at 2 hours, possibly as a result of the increased spray rate producing smaller droplets of the coating dispersion and their subsequent deposition on the surface of the bead. Surface deposition of small droplets sprayed rapidly is associated with the production of thicker coats that may retard liberation [157]. The application Surelease® onto the surface of the beads retards CPT release and prevents the initial burst effect of CPT due to the presence of this permeable film.

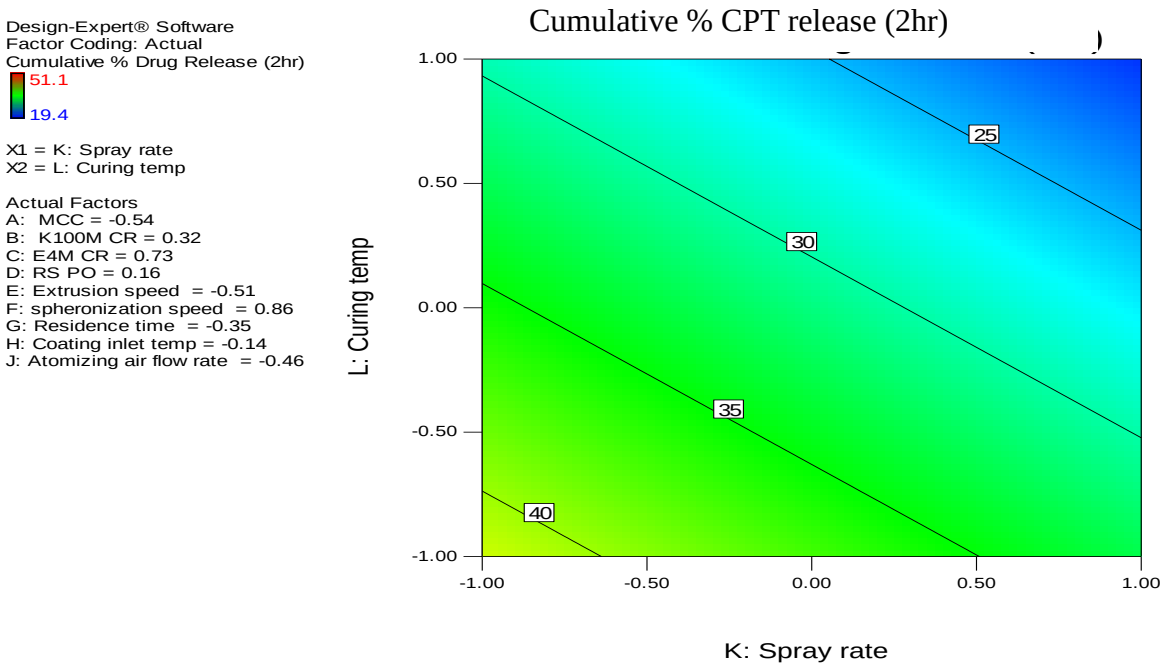

Figure 4.20 *Contour plot depicting the effect of spray rate and curing temperature on cumulative percent CPT released at 2 hours.*

4.4.2.5.4 Percent CPT released at 12 hours

Model adequacy was assessed for the percentage CPT released at 12 hours and the model had a p value of 0.0279, indicating that the model was significant and that the data can be navigatedin the design space. The data are summarised in Table 4.12. The model generated significant terms with p values > 0.05 for the amount of MCC, HPMC K100M, HPMC E4M, Eudragit® RS PO and the process parameters AFR, spray rate and curing time.

The equation for percent CPT released at 12 hours in specific terms is described in Equations 4.9:

Cumulative % CPT released at 12 hours (Y_8) = + 66.22 – 1.58*MCC - 13.38*K100M – 19.36*E4M – 1.12*Eudragit® RS PO + 2.61*Extrusion speed + 2.78*Spheronisation speed + 0.86*Residence time - 0.86*Atomizing air flow rate + 0.04*Spray rate + 0.76*Curing temperature **Equations 4.9**

The contour plot depicted in Figure 4.21 reflects that the products comply with an acceptance criterion of 80 % CPT release at 12 hours. As the composition of HPMC K100M and HPMC E4M is increased, the rate of CPT release retarded, possibly due to an increase in the diffusion path length for CPT within the hydrated matrix within the beads. HPMC is a non-ionic polymer hydrates rapidly to form a viscous gel layer to produce swelling-controlled release systems. In the dissolution media the matrix materials within the coated beads hydrate and the rate limiting step for release at 12 hours is the rate of formation of a partially hydrated gel layer at the surface of the bead between the ethylcellulose coat and core materials. Consequently, the highly viscous gel forms a matrix that retards the release of the entrapped CPT.

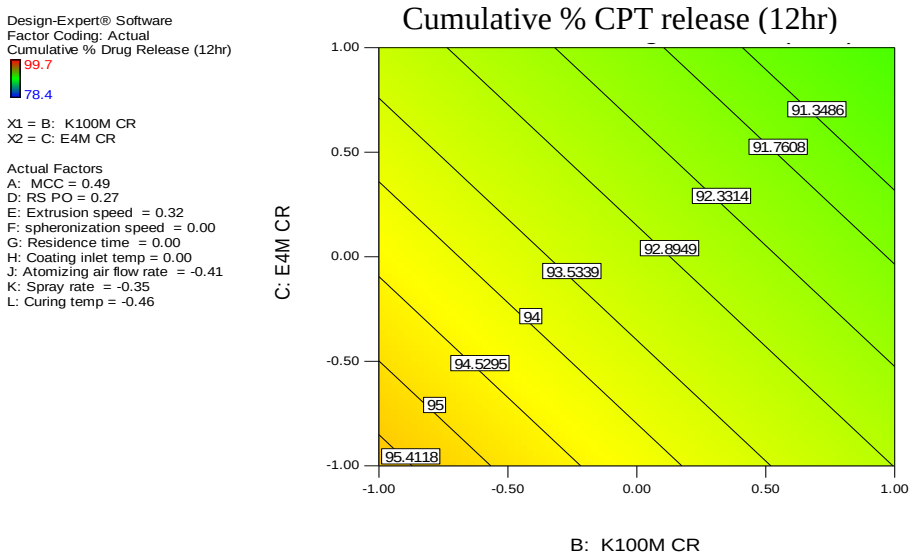

Figure 4.21 *Contour plot depicting the effect of Methocel® K100M and E4M on cumulative percent CPT released after 12 hours.*

An increase in the amount of Eudragit® RS PO from 7.5 to 15 % w/w in the formulation resulted in a decrease in the cumulative percentage CPT released at 12 hours (Figure 4.22). The impact of this polymer may be due to the presence of insoluble quaternary ammonium functional groups that are less porous than other polymers, reducing effective CPT diffusion resulting in slower release.

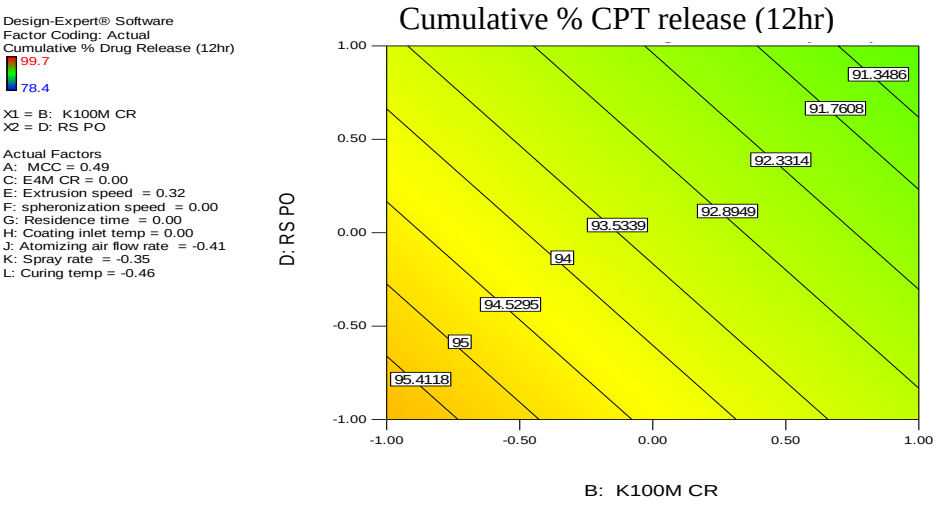

Figure 4.22 *Contour plot depicting the effect of Methocel® K100M and Eudragit® RS PO on cumulative percent CPT released at 12 hours.*

4.4.2.6 Coating

4.4.2.6.1 Effect of different coating levels

The release profiles of CPT from uncoated beads exhibited a burst effect and to ensure that sustained release was possible, preliminary studies were undertaken to evaluate the effect of different coating levels on release. The CPT beads were coated to 15 %, 20 % and 25 % weight gain (CPT-007 – CPT-009) and the resultant dissolution profiles are depicted in Figure 4.23. Uncoated CPT beads released CPT rapidly with at least 50 % of the dose released within the first two hours of testing. The addition of an ethylcellulose coat and increasing the level from 15 to 25 % resulted in reductions in the rate and extent of CPT release since an increase in the level of coating creates a larger physical barrier between the core bead, reducing water penetration and delaying water uptake and producing a slow rate of release of CPT. Beads coated to a target 20 % weight gain release approximately 27 % CPT at 2 hours, which is within the range set for a modified release profile that is recommended in the USP [218, 219].

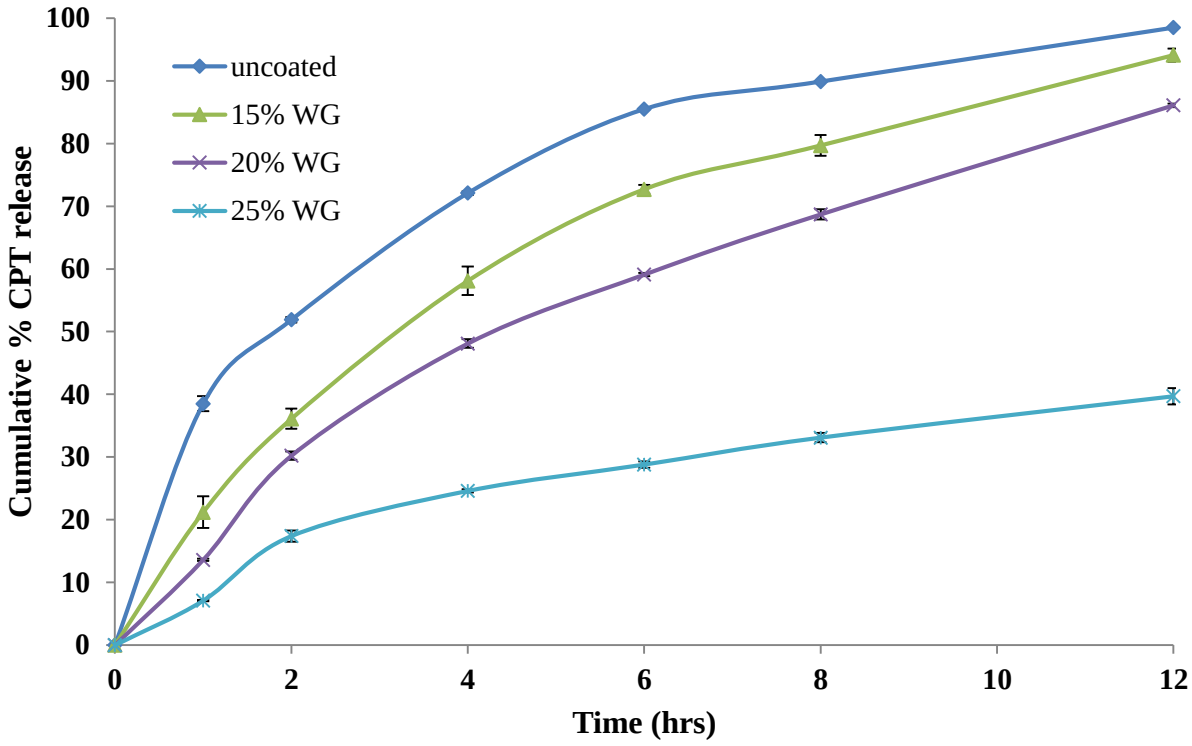

Figure 4.23 *Effect of different levels of coating level on CPT release.*

4.4.2.6.2 Curing

During coating processes coating materials are deposited on the surface of beads and the efficiency of the process is a function of inlet temperature, which initiates evaporation of the carrier solvent, the atomising air flow rate that modulates pneumatic mass transport within the chamber and the spray rate the coating dispersion. The release rate of CPT from beads coated at 60 ºC and cured at 40 ºC for 0 (CPT-010), 1 (CPT-011) and 2 hours (CPT-012) are depicted in Figure 4.24 and these results indicate that the amount of CPT released decreases as the duration of curing increases, and is due to improved coalescence of coating polymer on the surface of the beads during the curing process.

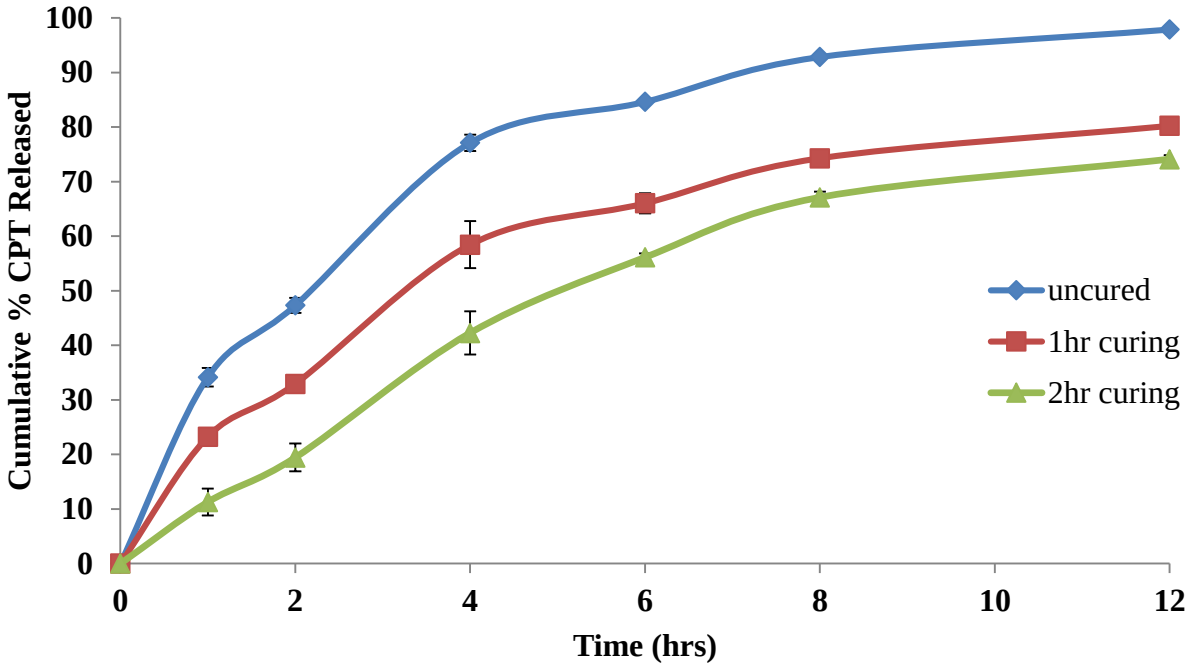

Figure 4.24 *Effects of curing time on CPT release.*

The formation of film coats is often only completed after completion of a curing process in which complete coalescence of the coating polymers on the substrate eventually leads to the development of a smooth and homogeneous coat [35]. An increase in the curing time therefore facilitates complete coalescence of the membrane through evaporation of the aqueous phase via capillary forces, resulting in the formation of a less permeable membrane that reduces CPT release or water uptake.

4.4.2.6.3 Coating efficiency

Coating operations are complex procedures in which the efficiency of the process may be affected by many factors. The efficiency of the coating process was evaluated by assessing the physical appearance of the coated beads and the weight gained relative to the theoretical weight gain. The coating efficiency of all 12 batches ranged between 76.4 % and 98.6 % as the data are summarised in Table 4.7. Of the individual input process variables, the AFR and spray rate had a more significant effect on coating process as illustrated, in the Pareto chart depicted in Figure 4.25.

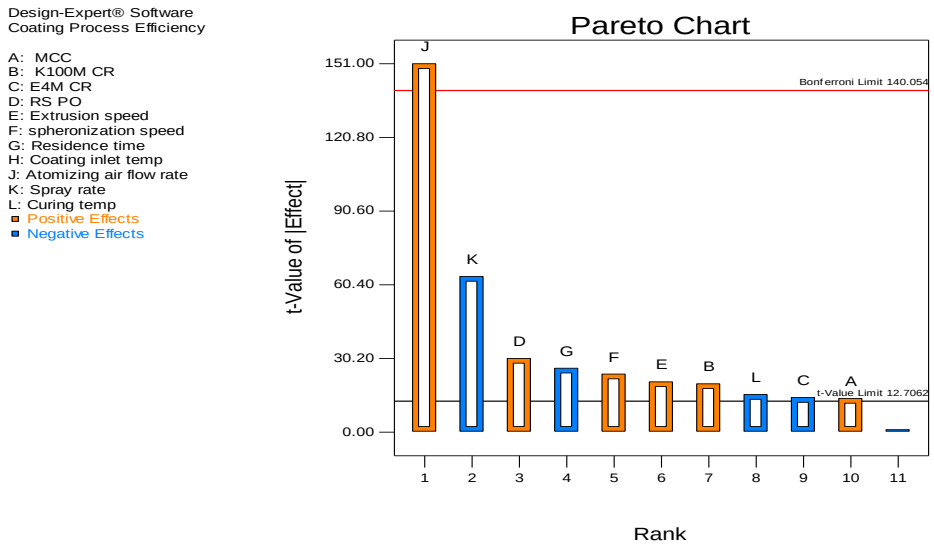

Figure 4.25 *Pareto chart depicting the significance and rank of independent terms on coating efficiency.*

The results of ANOVA analysis for coating efficiency are listed in Table 4.13 and the model was found to be significant with a predicted R^2 value of 0.9953, which was in close agreement to the adjusted R^2 value of 0.9996.

Table 4.13 *ANOVA data for coating efficiency.*

Source	**Sum of Squares**	**p-value**	
Model	635.04	0.0141	Significant
X_1-MCC	3.97	0.0461	Significant
X_2-K100M	8.17	0.0321	Significant
X_3-E4M	4.2	0.0448	Significant
X_4-RS PO	19	0.0211	Significant
X_5-Extrusion Speed	8.84	0.0309	Significant
X_6-Spheronisation Speed	11.8	0.0267	Significant
X_7-Residence Time	14.3	0.0243	Significant
X_9-AFR	475.02	0.0042	Significant
X_{10}-Spray Rate	84.8	0.0100	Significant
X_{11}-Curing Temp	4.94	0.0413	Significant
Residual	0.021	1	0.021
Cor Total	635.06	11	
Std. Dev.	0.14	**R^2**	1
Mean	88.18	**Adj R^2**	0.9996
C.V. %	0.16	**Pred R^2**	0.9953
PRESS	3	**Adeq Precision**	160.645

All individual input variables were significant to coating efficiency and the regression equation for efficiency in actual values is described in Equation 4.10:

Coating Efficiency = + 88.18 + 0.58*MCC + 0.83*HPMC K100M - 0.59*HPMC E4M + 1.26* Eudragit® RS PO + 0.86*Extrusion speed + 0.99*Spheronisation speed - 1.09*Residence time + 6.29*Atomizing air flow rate - 2.66*Spray rate - 0.64*Curing temperature **Equation 4.10**

An interaction plot for coating efficiency is depicted in Figure 4.26 and reveals that high AFR are important for better coating efficiency. Coating efficiency was more affected by spraying than environmentally related coating variables, such as inlet air temperature. Higher AFR are associated with continuous pneumatic mass transport of air within the coating chamber and consequently results in an increased evaporative capacity in the coating unit, ensuring complete delivery of the coating dispersion to the product bed, thereby eliminating over wetting and agglomeration of beads [157, 158].

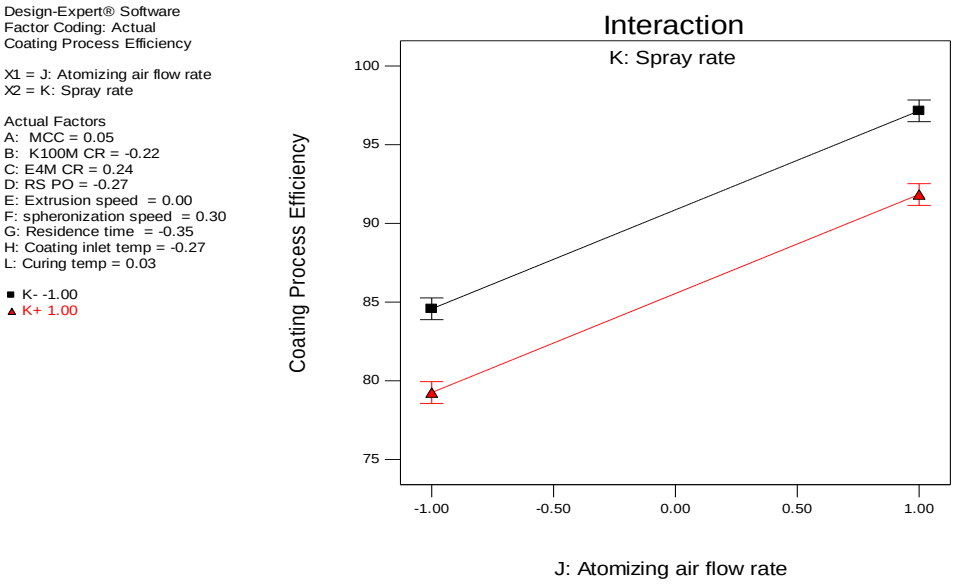

Figure 4.26 *Interaction diagram depicting the effect of spray rate and AFR on coating efficiency.*

An increase in the spray rate resulted in a decrease in coating efficiency, since spray rate affects droplet size distribution and subsequently droplet spreading and these data are depicted in Figure 4.27. An increase in the spray rate results in smaller droplets that move with increased velocity

and momentum that promotes the extent of droplet spreading [157]. The increased spray rate therefore affects the rate of droplet drying and may reduce the degree of coalescence. The use of low spray rate results in the formation of large droplets that could overwet beads and consequently agglomeration.

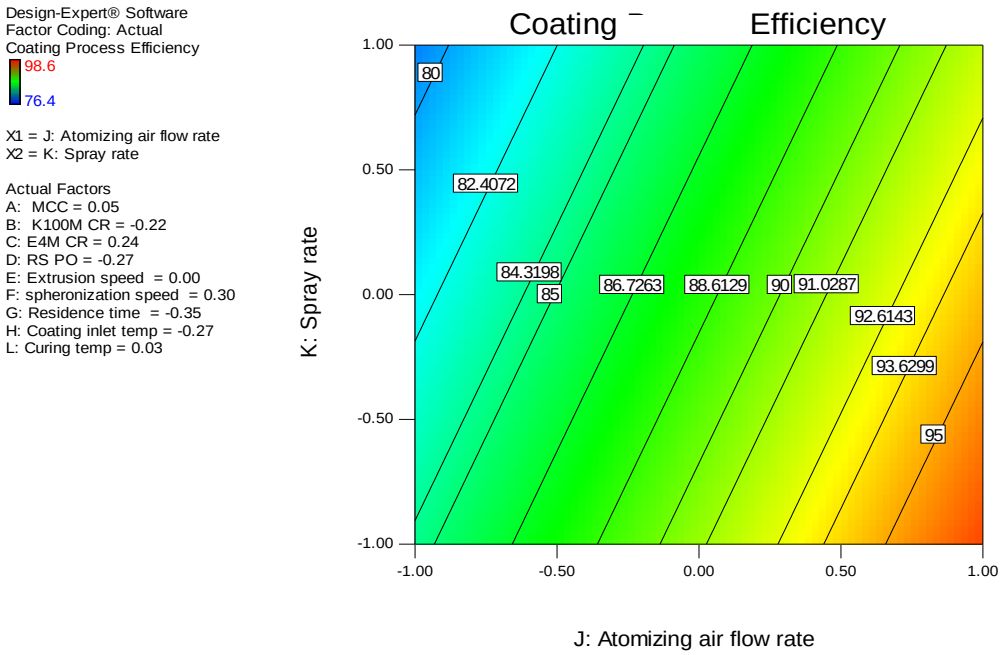

Figure 4.27 *Contour plot depicting impact of AFR and spray rate on coating efficiency.*

Increasing the curing temperature decreases the coating efficiency as depicted in the contour plot in Figure 4.28 in which the impact of spray rate and curing temperature on coating efficiency is highlighted. The curing temperature affects evaporation during drying and can have an effect on the uniformity of coating polymer deposition. High temperatures during curing process result in an increase in the rate of water evaporation from coating dispersions and excessively high temperatures result in premature drying of the sprayed dispersion, thereby affecting coating efficiency as the temperature may not impede film formation and sufficient coalescence of droplets on the bead surface may be impossible. At low rates of evaporation, polymer particles are able to move freely facilitating droplet coalescence prior to drying thereby improving film integrity.

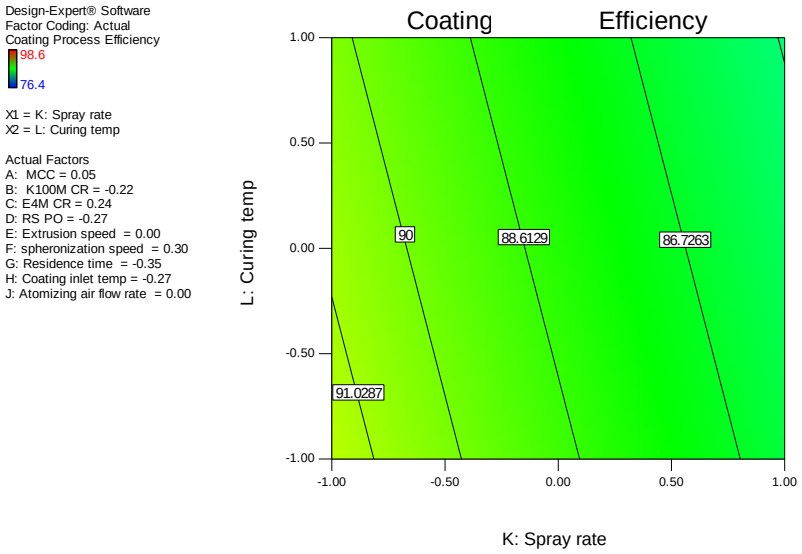

Figure 4.28 *Contour plot depicting impact of spray rate and curing temperature on coating efficiency.*

4.4.2.7 Density

The bulk and tapped density of the beads manufactured using experimental design was established for beads retained in the size range 0.80 mm to 1.25 mm. In addition the CI and HR were calculated. A summary of the results of this assessment is listed in Table 4.14.

Table 4.14 *Powder densities of coated CPT beads.*

Run	Bulk Density (g/mL)	Tapped Density (g/mL)	HR	CI	Friability (%)
CPT-013	0.667±0.002	0.729±0.016	1.09	0.084	0.79±0.52
CPT-014	0.652±0.036	0.721±0.007	1.10	0.095	1.31±0.79
CPT-015	0.631±0.003	0.709±0.014	1.12	0.110	0.92±0.28
CPT-016	0.626±0.004	0.693±0.031	1.11	0.097	0.86±0.21
CPT-017	0.670±0.007	0.705±0.011	1.05	0.051	0.99±0.87
CPT-018	0.594±0.007	0.663±0.024	1.11	0.103	0.52±0.25
CPT-019	0.626±0.005	0.716±0.042	1.14	0.125	0.89±0.39
CPT-020	0.615±0.001	0.666±0.016	1.08	0.076	0.92±0.65
CPT-021	0.683±0.013	0.721±0.002	1.05	0.051	0.43±0.05
CPT-022	0.683±0.039	0.761±0.051	1.11	0.101	0.52±0.05
CPT-023	0.665±0.002	0.727±0.016	1.09	0.083	0.56±0.31
CPT-024	0.629±0.002	0.719±0.002	1.14	0.125	1.28±0.68

The bulk and tapped densities of CPT coated beads were used to calculate CI and HR as described in §3.2.3.4 and §3.2.3.5. According to the data listed in Table 3.2, which summarizes CI for powder flow, all batches of CPT beads exhibited satisfactory to good flow properties. The values for HR for all batches were < 1.25 indicating the beads exhibited good flow properties. Coated beads containing HPMC K100M exhibited higher bulk densities than those with lower levels of the polymer, possibly due to particle size of the beads. The slightly higher densities of coated beads may in part be attributed to dense packing of the polymers in voids between the MCC micro fibrils. Difference in flow properties may affect the potency of the finished capsule products and ultimately content uniformity.

4.4.3 Optimisation Process

Based on the acceptance criteria and the desirability factor data derived using Design-Expert® 8.0.4 (Stat-Ease Inc., Minneapolis, USA) revealed a possibility of sixteen optimised formulation compositions with desirability values between 0.95 and 1.00. A desirability value close to 1 was considered the target and therefore the most favourable composition and this is summarised in Table 4.15. Three batches of beads manufactured using this formulation were manufactured and assessed.

Table 4.15 *Composition and process parameters for the manufacture of the optimal formulation.*

Independant Factor	Value
MCC (%)	41.2
HPMC K100M (%)	23.1
HPMC E4M (%)	24.95
Eudragit® RS PO (%)	8.4
Extrusion Speed (rpm)	35
Spheronisation Speed (rpm)	1800
Residence Time (min)	5.6
Coating Temp (°C)	63.6
Atomising Airflow rate (m^3/h)	116.8
Spray Rate (g/min)	2.02
Desirable Dependant Response	**Target**
Yield (%)	60 - 100
AOR (˚)	≤ 30
Friability (%)	≤1
AR	0.80 - 1.20
Sphericity	0.80 - 1.20
Cumulative % CPT released at 2 hours	20 – 30
Cumulative % CPT released at 6 hours	50 – 60
Cumulative % CPT released at 12 hours	80 – 100
Coating Efficiency (%)	80 – 100

4.4.4 Validation of optimised model

The physical evaluation and micromeritic properties of beds manufactured (n=3) using the formulation and process parameters are listed in Table 4.15 and summarised in Table 4.16 and were within predefined limits.

Table 4.16 *Micromeritic properties of CPT beads in optimized batches.*

Response	CPT-025	CPT-026	CPT-027
Yield (%)	84.5±4.87	85.2±5.18	85.4±4.63
AOR (°)	28.3±0.89	28.6±1.05	28.5±0.93
Friability (%)	0.78±0.33	0.84±0.47	0.82±0.26
AR	1.04±0.09	1.05±0.12	1.04±0.04
Sphericity	1.03±0.16	1.02±0.06	1.05±0.09
Cumulative % CPT released at 2hrs	24.5±1.66	29.1±3.06	25.8±1.52
Cumulative % CPT released at 6hrs	70.2±2.43	72.4±0.56	70.5±1.98
Cumulative % CPT released at 12hrs	86.7±3.06	90.5±7.34	87.3±2.06
Coating Efficiency (%)	91.2± 2.85	90.8±3.53	91.5±2.95

The batches manufactured using the optimised formulation (CPT-025 – CPT-027) exhibited good flow properties, sphericity and released CPT in a sustained manner (Figure 4.29). The prediction error varied between -1.44 % and +0.78 %, which was considered reasonable and of low magnitude and the R^2 value of 0.9996 is indicative of a high degree of reproducibility.

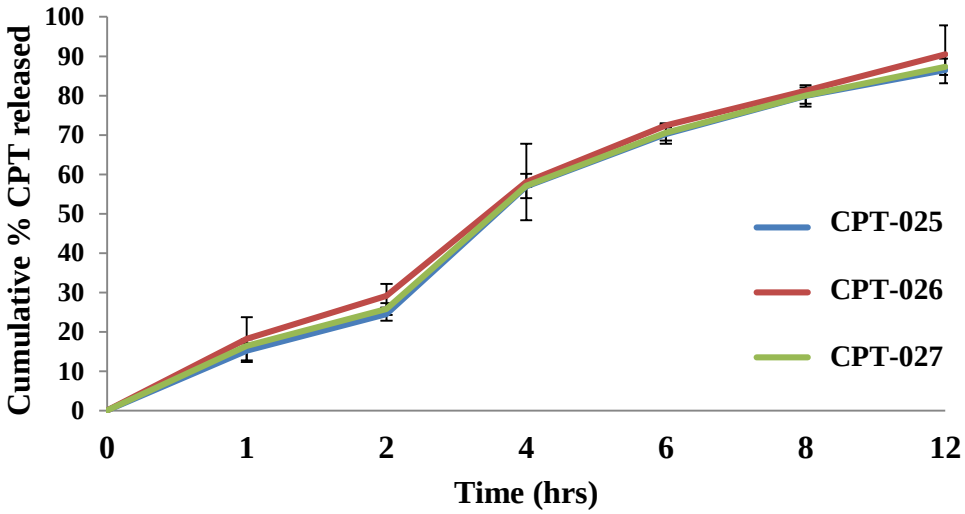

Figure 4.29 *Dissolution profiles of CPT release from the optimized batches CPT-025–CPT-027.*

A SEM image of a coated bead from anoptimised batch manufactured using optimal conditions is depicted in Figure 4.30 and reveals a smooth surfaced, spherical shaped bead indicating the success of the optimisation procedure used to facilitate formulation development and process optimisation studies.

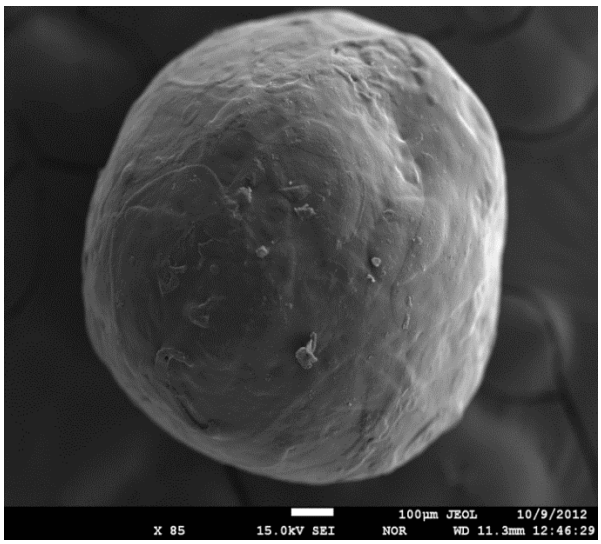

Figure 4.30 *SEM image depicted a coated CPT bead from an optimized batch.*

The reproducibility of the manufacturing process was evaluated using ANOVA and the cumulative percent CPT released at two and twelve hours for the three batches manufactured using the optimised conditions and the statistical data were 0.0267 and 0.173 with confirmation that the difference was not significant at an error probability of p = 0.05. The sphericity for batches (CPT-025 –CPT-027) were 1.03 ± 0.16, 1.02 ± 0.06 and 1.05 ± 0.09 and therefore the batches of coated beads can be considered spherical with moderate surface irregularity that would not adversely impact capsule filling.

4.4.5 DSC

The DSC thermograms for powder obtained following pulverisation of the coated CPT beads is illustrated in Figure 4.31 and the curve reveals the presence of a sharp endothermic event between 102 °C and 112 °C with a melting temperature range between 106 and 109 °C that is characteristic of the endothermic melting event for pure CPT.

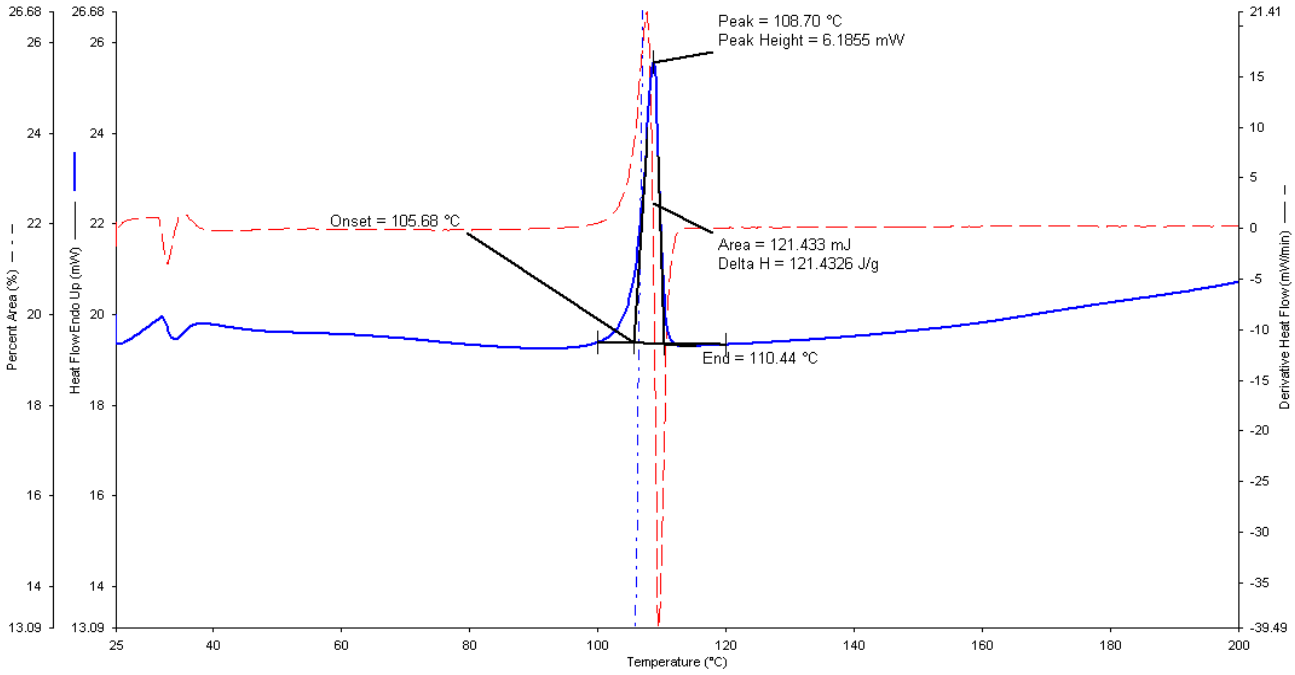

Figure 4.31 *Typical DSC thermogram for optimized coated CPT determined at a heating rate of 10 °C/min.*

The thermal transition at a T_{peak} of 108.70 °C with a T_{onset} of 105.68 °C were slightly lower for the coated beads when compared to that of pure CPT and reported in §3.4.6. The slight change in the melting endotherms of the ground beads may be due to the mixing of CPT and the excipients, which lowers the purity of CPT and does not necessarily indicate that a possible incompatibility

exists. The ΔH_{fusion} of – 40.5 J /g was lower than previously reported data [185] and the endotherms were unchanged which is generally considered as an indication that no potential incompatibility exists.

4.4.6 IR spectroscopy

The IR absorption spectrum of a sample from an optimised batch is depicted in Figure 4.32 and reveals all relevant absorption bands for CPT are present although a slight shift was observed at 1 744 cm^{-1} that is assigned to a C=O stretching vibration of a carboxylic acid, 2980 cm^{-1} assigned to CH3 stretching and 1 246 cm^{-1} that corresponded to C-H and/or C-H_3 bending. The slight shift in the bands observed may be attributed to an artificial reduction in purity of CPT due to sample preparation and doesnot necessarily indicate that possible incompatibilities exist.

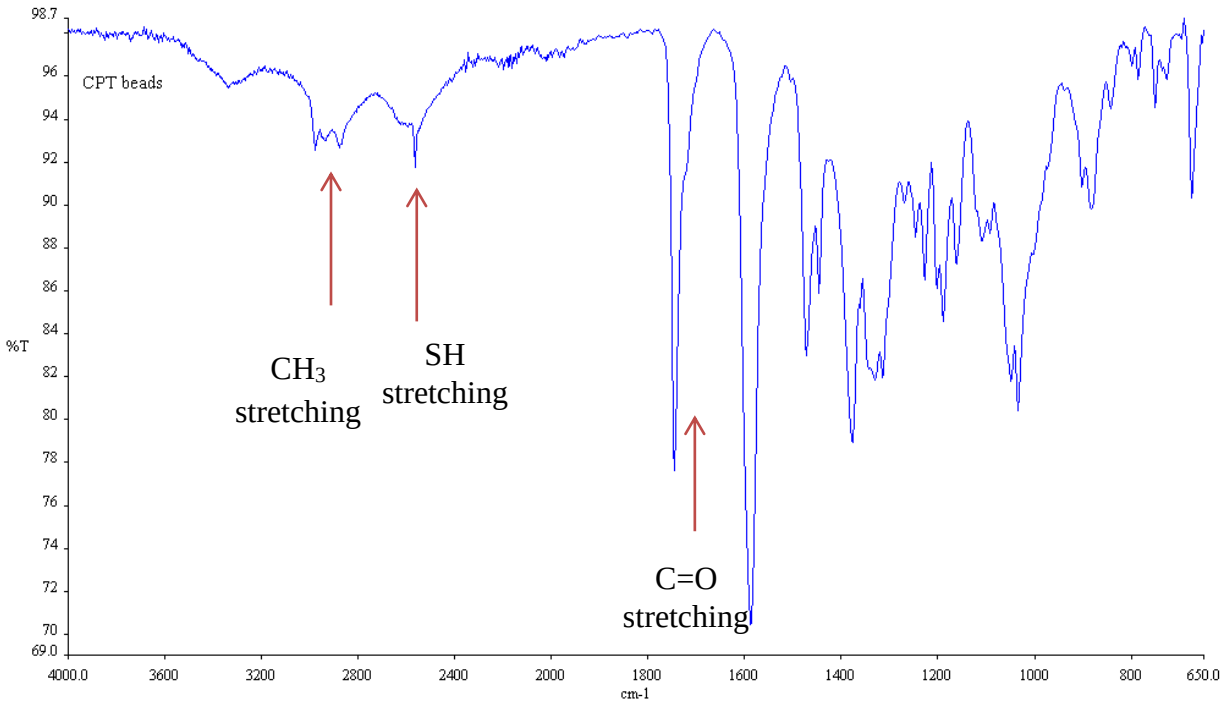

Figure 4.32 *FT-IR spectrum of pulverised coated beads.*

4.5 CONCLUSION

Coated CPT SR beads with the potential for further optimisation have been developed and manufactured using extrusion-spheronisation. The coated beads were manufactured and met all desired quality attributes in respect of micromeritic and flow properties, content uniformity and friability. Different rates of CPT release were achieved by altering the amount of SSC in the granulation and coating stages of manufacture. In addition, release retarding polymers of HPMC and methacrylic acid co-polymers were included to modulate release that was further assessed through concurrent screening and optimisation with manufacturing and coating process parameters.

An increase in the amount of granulating fluid from 5 % w/w to 20 % w/w resulted in a decrease in the extent of CPT. SR of CPT was achieved by the use of Surelease® as a granulating fluid that suppressed the burst effect. At lower SSC levels the amount of ethylcellulose present is low thereby creating a less homogenous dispersion of the polymer in the granules, resulting in pockets of more erodible materials that consequently result in erratic release. At high SSC levels, the homogeneity of the dispersion increases and the release rates depend on the solubility and polymer/dissolution medium partition coefficient.

SEM images of extrudate revealed cylindrical extrudate that were rounded at the edges initially during spheronisation and an increase in residence time in the spheroniser produced spherical beads [137]. Low spheronisation speeds led to formation of dumb-bell shaped particles due to low energy input, resulting in incompletely rounded beads whereas at higher energy input levels the extrudate is converted into spherical beads. A short residence times of approximately 6 minutes in the spheroniser was sufficient to produce beads at maximum yield levels with an acceptable degree of sphericity. Longer residence times resulted in the production of agglomerates and oversized beads due to increased particle-particle interactions with a decrease in the yield of beads of the desired size. An increase in coating level from 15 % w/w to 25 % w/w resulted in a decrease in the rate of release of CPT, since the higher coating level increased the physical barrier between the core of the bead and the dissolution medium thereby retarding the release of CPT.

A Plackett-Burman design was preferred as it permitted the screening of a larger number of formulation and process factors in a two level equal allocation design with size-run efficiency in order to establish a balance and to ensure that the design was complete and efficient. Eleven independent formulation and process variables were investigated in an attempt to produce a SR dosage form with desirable quality attributes and was achieved by altering formulation composition, extrusion-spheronisation variables and coating parameters. ANOVA data revealed that several significant response models were achieved, specifically for yield, AR, sphericity, coating efficiency and cumulative percent CPT released at 2 and 12 hours.

The SR beads exhibited good quality attributes with adequate flow characteristics and an acceptable yield. The yield of coated beads ranged between 69.21 and 91.38 %. Formulations in which higher molecular weight HPMC was used in increased concentrations resulted in the formation of a sticky wet mass and extrudate with a shark skin appearance that resulted in the production of excessive fines and a decrease in the yield of beads.

CPT release at two hours was significantly affected by the burst effect phenomenon. Consequently, the rate of aqueous dissolution medium infiltration into the matrix through the coating layer on the beads was considered a rate-limiting step in CPT release from beads. The application of a permeable film of Surelease® onto the surface of the bead established a barrier that complemented the activity of the hydrophilic matrix in preventing rapid dissolution and retarded the release of CPT from the beads. An increase in the spray rate resulted in a decrease in CPT release at two hours. An increase in curing temperature facilitated complete coalescence of the coating membrane through evaporation of the aqueous phase through capillary forces, resulting in a less permeable membrane coat. The film coat therefore reduces aqueous medium infiltration and CPT diffusion from the core of the beads through the coating layer into the dissolution medium.

The model generated for CPT release at 12 hours revealed that the amount of MCC, HPMC K100M, HPMC E4M and Eudragit® RS PO, the AFR, spray rate and curing time were significant in controlling the release of CPT. An increase in the amount of the higher molecular weight and more viscous HPMC K100M entrapped CPT more efficiently in the matrix resulting in slow rate of CPT release. The rate-limiting step of release is the rate of water transport across the coating and the rate of formation of a partially hydrated gel layer within the bead surface on contact with the dissolution medium. An increase in Eudragit® RS PO content from 7.5 % w/w to 15 % w/w

increased the amount of insoluble quaternary ammonium functional groups in the bead matrices resulting in slow release of CPT. The presence of HPMC [149, 150, 151] and Eudragit® RS PO [152] in the CPT bead and change in release characteristics has been reported and is a well-known phenomenon [147, 148].

The coating efficiency for all 12 batches ranged between 76.4 % and 98.6 %. The AFR and spray rate had a more pronounced effect on coating efficiency than any other of the process variables investigated. A high AFR modulated the delivery of the coating dispersion to the product bed and eliminate over wetting and associated agglomeration of the product being coated.

Following preliminary investigations and optimised formulation composition and manufacturing process conditions were identified. Three batches of the optimised formulation (Batches CPT-025 – CPT-027) were manufactured and the quality attributes assessed and compared. Comparison of the observed responses to the theoretical or anticipated responses resulted in a reasonable prediction error ranging between -1.44 % and +0.78 % and was considered of low magnitude and the R^2 of 0.9996 is an indication of the reproducibility of the method.

The use of experimental design was a successfully applied to the development of SR CPT beads that can be used for twice-daily dosing of this ACE inhibitor. All batches of beads that were manufactured exhibited satisfactory to good flow properties and demonstrated SR profiles over 12 hours that met the USP criterion for SR dosage forms [218]. The SR technology may prove useful for the treatment of hypertension in paediatric and adult patients.

Spherical CPT beads with a smooth surface are also unlikely to pose a challenge during hand-filling of capsules. The use of coated beads in hard gelatin capsules may be a solution to the challenges posed when treating paediatric patients and may facilitate adherence to pharmacotherapy, as different doses can be easily achieved when compounding extemporaneous CPT formulations. The distribution of coated beads in food and filling in smaller sized capsules that are easy for children to swallow as an advantage.The bead formulations can be further investigated using mathematical modelling in order to develop and optimise scale-up production with RSM approaches such as CCD or Box- Behnken design. In addition, the stability of the beads and scale-up product must be investigated to assess the shelf life and long-term compatibility of this technology.

CHAPTER FIVE
KINETIC MODELLING OF CPT RELEASE FROM COATED BEADS

5.1 INTRODUCTION

Investigations into controlled drug delivery technologies is the most rapidly advancing area in pharmaceutical sciences since coated beads offer advantages in respect of improved safety, stability and efficacy [226]. Evaluation of controlled drug delivery systems requires the use of mathematical models to predict delivery technology performance. Mathematical modelling permits elucidation of information relating to drug release mechanisms, which can be manipulated by the formulation scientist to design and control drug release from delivery systems [150, 227-229]. Coated matrix systems intended to produce a SR effect have been effectively used to control the release of an API [150, 227-231].

Models that have been used to describe API release were either empirical [227, 232] or mathematically [150, 200, 233, 234] derived. Several published reports summarise the release models of API from coated formulations [230-232] and focus on the use of a semi-permeable membrane film coats as a vital factor affecting the mechanism of API release. The focus has been on models that describe osmotic pumping mechanisms for the release of API from coated formulations or beads in which cracks develop in the coat due to the hydrostatic pressure build-up in the core [227].

Mechanistic models have also been studied [227] in an effort to understand release mechanisms of API from coated, swelling and dissolving matrix systems, whereas empirical models are used to describe the manner in which beads develop cracks in the coat due to the osmotic and hydrostaticpressure build-up. The selection of suitable mathematical models to elucidate drug release mechanisms depends on the nature of API [235], type of excipients [226, 236], core composition and coating system [227, 231, 237]. Experimental characterisation of dosage forms can also facilitate discrimination of model parameters specifically in the case of hydrostatic pressure build-up and/or in swelling systems [238, 239].

API release from coated formulations follow an osmotic pumping mechanism since the film coat is semi-permeable to dissolved API [240, 241]. It is therefore fundamental to understand the principles of diffusion and/or osmotic pumping to supplement empirical conclusions in understanding drug delivery. Several reports [226, 229, 241] indicate that it is vital to understand API release from the core dosage form following comprehensive analysis of that API, excipients and the characteristics of polymers to design polymeric matrix formulations intended for SR delivery of compounds.

Mathematical models take into account solute transport processes and structural characteristics of polymer/s that may facilitate understanding of potential transport mechanisms of API within and out of delivery systems [240]. Consequently, there is a need to develop adequate mathematical theories specific to coated SR systems to elucidate chemical and physical processes associated with the coating of beads that have been manufactured using extrusion and spheronisation. The objective of kinetic modelling in these studies was to model changes in the release kinetics of CPT from a coated oral delivery system of different polymer compositions in the core, granulation fluid levels and coating levels.

5.2 DRUG RELEASE FROM COATED BEADS

The level and composition of the coating system and polymer compositions of the core of beads provide the impetus and control for API release from coated systems [231, 241]. Drug release models can be classified as empirical or mechanistic [233] and a review of mechanistic model approaches that have been used to describe API release from coated systems is presented here[154, 231, 237]. Mechanistic models are used to describe drug release facilitated by osmotic pumping and diffusion or cracking due to hydrostatic pressure build-up inside the coated beads.

5.2.1 Hydrostatic pressure

The hydrostatic pressure model [154] is suitable to describe the manner in which coated systems that consist of a solid core surrounded by a porous semi-permeable membrane release API. The main processes that occur in such coated systems involve the influx of a solvent driven by the difference in osmotic pressure between the core and medium the core is in, followed by dissolution of the API followed by release via diffusion [15]. It is likely that the beads will swell due to solvent accumulation after uptake followed by the hydrostatic pressure build-up inside the coated bead,

resulting in stress fracturing or cracking of the coating [18, 20] if no pores or cavities are present in the coating.

In order to evaluate CPT release using models it is essential to understand the suitability and accuracy of the model and the application of the model for prediction and description of API release. In this context the release of CPT, a highly water soluble and poorly permeable molecule in an HPMC based matrix that it coated with ethylcellulose coating as described in §4.4.3, will be a function of its physicochemical properties and the mechanism of release is complex. Initially there is an osmotic gradient between the core and external medium due to the high water solubility of CPT. This becomes a driving force for the influx of the dissolution medium into the technology, resulting in hydration and swelling of the polymer and dissolution of the CPT as illustrated in Figure 5.1. As the polymer swells there is an increase in the pressure on the interior of the bead, which coated with the semi-permeable membrane.

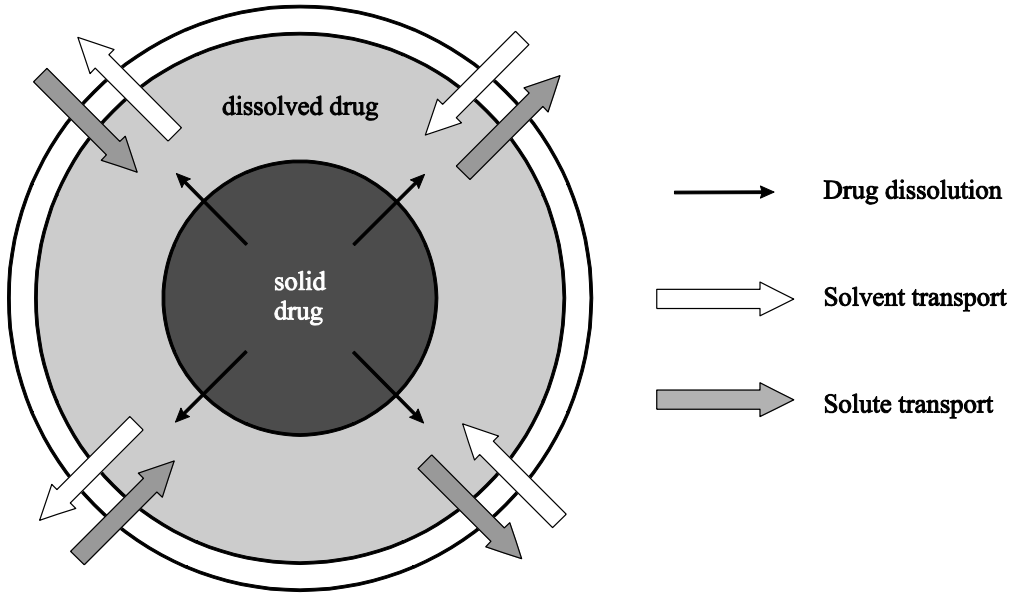

Figure 5.1 *Schematic representation of API release process from a bead coated with a semi-permeable membrane and facilitated by hydrostatic pressure build up and diffusion [240].*

5.3 STATISTICAL COMPARISON AND MATHEMATICAL MODELLING OF API RELEASE PROFILES

Several approaches have been used to compare API release profiles for the characterisation of the kinetics of release from different dosage forms [228, 229, 243-247]. The methods of assessment of *in vitro* release profiles are model-dependent [154], statistical [243] and model-independent [248] approaches be used to establish pharmaceutical equivalence of technologies. These methods can be used for the evaluation and comparison of dissolution profiles generated following *in vitro* dissolution testing of prototype dosage forms. Furthermore, the statistical methods can be used to compare the different formulations under investigation under the same experimental conditions in addition to providing a tool, albeit with limited application, for dissolution data for the same formulation tested under different conditions.

5.3.1 Model-independent methods

Model-independent methods do not allow for assumptions regarding the shape of the curves under investigation [228, 245-247] when a comparison of API release profiles from different data sets is undertaken. The most common model-independent approach used to compare release profiles is the technique in which a difference (f_1) and similarity factor (f_2) proposed by Moore and Flanner [248] is calculated.

The comparison of dissolution profiles using the f_1 and f_2 fit factors is well established [245, 246, 248, 249]. The difference factor f_1 measures the percent error between the dissolution profile of a test and a reference product at all times and a percent error of zero (0) implies that the *in vitro* release profiles of the test and reference product are identical. The value for f_1 increases as the dissolution profiles become less similar [245, 246, 248, 249]. The difference factorcan be calculated using Equation 5.1.

$$f_1 = \left\{\frac{\sum_{t=1}^{n}|R_t - T_t|}{\sum_{t=1}^{n} R_t}\right\} \times 100 \qquad \textbf{Equation 5.1}$$

Where,

n = sampling number,
R_t = percent API from the reference product dissolved at time t, and
T_t = percent API from the test product dissolved at time t.

The similarity factor, f_2, is the logarithmic transformation of the sum-squared error of the difference in dissolution of an API from a test and reference product over all time points [248]. The value of f_2 lies between 0 and 100, and a value of 100 is indicative that the dissolution profiles of a test and reference product are identical. The FDA guidance on development, evaluation and application of *in vitro-in vivo* correlations on extended release oral dosage forms [249] recommends that at least three or four dissolution time points are to be used to calculate the similarity factor, f_2, effectively. The similarity factor is calculated using Equation 5.2.

$$f_2 = 50 \times \log\left\{\left[1 + \left(\frac{1}{n}\right)\sum_{t=1}^{n} w_t |R_t - T_t|^2\right] \times 100\right\} \qquad \textbf{Equation 5.2}$$

Where,

n = number of dissolution time points,
R_t = percent API from a reference product dissolved at time t,
T_t= percent API from a test product dissolved at time t, and
w_t= an optional weight factor, usually set at 1.

A value for f_1< 15 and for f_2 between 50 and 100 indicates that the dissolution profiles being compared are considered similar [248]. The Centre for Drug Evaluation and Research at FDA [249] has adopted the use of the similarity factor f_2 as a valid criterion for the comparison of *in vitro* dissolution profiles between test and reference products. Recommendations for the use of the f_2 similarity factor include that the number of sample points included in the calculation should not be limited to three or four time points and that at least one or more time point after 85 % of the label claim for the API has been released from the product [227, 228, 245, 250].The sensitivity of the test after this point may fail to permit discrimination between the two curves.

A major advantage of the $f1$ and f_2 factors is that they are easy to compute and result in a single value that is used to indicate the degree of closeness between the two *in vitro* dissolution profiles being compared. There are, however, limitations in the use of the similarity factor, including the fact that itfails to account for the shape of the dissolution profile, unequal spacing between time pointsof the profile and number of test units for each release profile data set [244, 245]. Furthermore, it is difficult to evaluate false positive and negative values using the similarity factor. Correlation of the similarity factor to a specific time point is difficult due to variability and therefore it is a challenge to evaluate the similarity of dissolution profiles.

A newer model-independent approach for the comparison of dissolution profiles of test to reference products has been developed by Gohel and Panchal [247] and themodel is used to calculate a similarity factor, (S_d) for thiscomparison. The Gohel similarity factor can be calculated using Equation 5.3.

$$S_d = \frac{\sum_{t=1}^{n-1}\left|\log\left(\frac{AUC_{R_t}}{AUC_{T_t}}\right)\right|}{n-1} \qquad \textbf{Equation 5.3}$$

Where,

n= number of data points collected during *in vitro* release testing,
AUC_{Rt} = area under the curve of API release from a reference product at time t, and
AUC_{Tt} = area under the curve of API release from a test product at time t.

An S_d value close to or zero is indicative that the dissolution profiles under investigation are similar. The advantage of using the Gohel similarity factor for the comparison of dissolution profiles is that this is a simple and flexible approach, since the dissolution data may be expressed as either an amount or percent release/dissolved [247] and the value for S_d can be used to infer a difference between the formulations tested as a percentage.

Other model-independent approaches that can be used to compare drug release profiles include the calculation of dissolution efficiency (DE) [251] and mean dissolution time (MDT) [252]. The DE of adosage form is defined as the area under the dissolution curve up to a specific time, t, expressed as a percentage of the area of a rectangle representing 100 % release after dissolution at that time, t[251]. DE can be calculated using Equation 5.4.

$$DE = \frac{\int_0^t y \times dt}{y_{100} \times t} \times 100\% \qquad \textbf{Equation 5.4}$$

Where,

y= the percent API dissolved at a time, t.

The MDT is a ratio test procedure that is an evaluation of the ratio of percent released/dissolved at a certain time point based on the calculation of AUC [252]. The MDT ratio is the sum of a specific fraction of the total dose in a dosage form that is released at specific times of the dissolution test [252].

The f_1 and f_2 factors were calculated and used to analyse dissolution data in this study as described by the FDA [249]to assess the similarity of dissolution profiles. In addition, S_d values were calculated due to the simplicity and ease of interpretation of this approach, and the value of the S_d was compared to f_1 and f_2 factors to establish whether a relationship existed between these factors.

5.3.2 Statistical methods

Statistical methods usinganalysis of variance canbe distinguished as one-way analysis of variance (ANOVA) ormultivariate analysis of variance (MANOVA) [253]. The statistical approach can be used to assess the difference between the mean of two sets of dissolution data at a single time point (ANOVA or t-student test) or at multiple time points (MANOVA). The advantage of using statistical methods for analysis of dissolution data is that variability and correlation factors are taken into account when comparing release profiles [243].

Repeated measurements may be necessary for the comparison of *in vitro* release profiles, of which time may be one. ANOVA is used to establish whether differences, if any, exist at specific time points of the dissolution profiles under comparison [243, 250]. A number of *post hoc* tests can be performed to determine the exact points of difference between dissolution profiles.These include the Least Significant Difference, Tukey's Multiple Range, Scheffé Method, Newman-Keuls and Dunnett's tests [243].

ANOVA-based methods of analysis do not rely on curve fitting procedures and do not reveal information about differences in the shape and levels of the dissolution data under comparison [229]. ANOVA analysis is criticised for being too discriminatory for the purposes of testing for difference ofdissolution profiles that may not necessarily reflect pharmaceutical differences during product use or assessment [253].

5.3.3 Model-dependent methods

Model-dependent methods have been extensively used as tools to provide information on the mechanisms that govern the release of API from a dosage form [254]. In addition, a model can be used to quantitatively predict the kinetics of API release from specific technologies[238]. Commonly used model-dependent methods that have been used to characterise dissolution profiles

include zero order [255], first order [256], Higuchi [257], Hixson-Crowell [258], Weibull [259, 260] and Korsmeyer-Peppas models [261].

5.3.3.1 *Zero order*

The dissolution of dosage forms that do not disintegrate or deaggregate prior to releasing at a constant rate per unit time can be fitted to a zero order model [245, 246]. Zero order release is the ideal target for sustained release technologies to facilitate prolonged pharmacological activity [255, 262]. The mathematical depiction of a zero order model is depicted by Equation 5.5.

$$Q_t = Q_0 + K_0 t \qquad \textbf{Equation 5.5}$$

Where,

Q_t = the amount of API released at time t,
Q_0 = the initial amount of API in solution at t = 0,
K_0= Zero order release rate constant, and
t = time.

5.3.3.2 *First order*

A first order kinetic model described by Gibaldi and Feldman [256] was used to characterise the absorption and/or elimination of certain molecules from biological systems. The first order kinetic model presented in Equation 5.6 may be applied to the modelling of dissolution test data in which sink conditions had been met [256, 263].

$$\ln Q_t = \ln Q_0 + K_1 t \qquad \textbf{Equation 5.6}$$

Where,

Q_t= the amount of API released at time = t,
Q_0= the initial amount of API in solution at t = 0,
K_1= the first order release rate constant, and
t = time.

Water-soluble API formulated into porous matrices are released according to a first order kinetic process and the rate of API release is usually proportional to the amount of API remaining to be released from the matrix [263]. The rate of release therefore declines over time as the amount of API remaining in the dosage form diminishes. This model can therefore be used to describe release from systems in which the release rate is concentration dependent [256].

5.3.3.3 *Higuchi*

The Higuchi model can be used to describe release of poorly soluble API from non-eroding matrices such as ointments and polymeric based systems [234, 257]. Higuchi described drug release as a diffusion process, fundamentally based on Fick's law. However, it is dependent on square root of time. This approach to describing API release can be used to characterise the dissolution process from several types of modified release technologies [152, 200, 234, 238, 257] and a simple form of the Higuchi equation is shown mathematically in Equation 5.7.

$$Q_t = K_H t^{1/2} \qquad \textbf{Equation 5.7}$$

Where,

Q_t = amount of API released at time t,
K_H = Higuchi dissolution constant, and
t = time.

The Higuchi model can be modified to describe diffusion through polymeric membranes that may occur in technologies where an insoluble film coatis used and solvent filled pores or cracks exist in the membrane [236]. To completely describe API transport through a polymeric membrane, the solute diffusion coefficient(s) of the molecule in the polymer phase in water , partitioning and pore size distribution must be considered to fully apply theHiguchi model [263]. The diffusion-based model of API release from coated systems identifies transport through the polymeric film as the rate-limiting step in the release process [227].

The Higuchi model has been made modified to facilitate the prediction of release kinetics from coated dosage forms [227, 236] through the use of Fick's 2nd law, provided the diffusion coefficient of the API in the film coating is known. Assuming that the beads exhibit a spherical geometry with a uniform coating and dissolution is tested under sink conditions, the relationship described in Equation 5.8 can be applied to the data.

$$\frac{m_t}{m_\infty} = 1 - e\left(-\frac{3D \times k_{part} \times r_{ex} \times t}{(r_{ex} - r_{in}) r_{in}^2}\right) \qquad \textbf{Equation 5.8}$$

Where,

m_t = absolute cumulative amount of API released at time t
m_∞ = absolute cumulative amount of API released at time infinity,
D = diffusion coefficient of the API within the membrane,
k_{part} =partition coefficient of the API between the membrane andreservoir,
r_{in} and r_{ex} are the inner and external radii of the coated bead.

5.3.3.4 *Hixson-Crowell*

The Hixon and Crowell model [258] describes the release of API from systems in which the area of the particle is directly proportional to the cube root of its volume. They developed a mathematical relationship to describe this relationship and this is defined in Equation 5.9. The cube root law can be applied to pharmaceutical dosage forms in which dissolution occurs in planes that are parallel to the surface ofthe dosage form for which the dimensions diminish proportionally while the geometrical shape of the dosage form is retained [244, 245]. The model assumes that the rate of release of API from a dosage form is limited by the dissolution rate of that compound and not by diffusion through a polymeric matrix.

$$Q_0^{1/3} - Q_t^{1/3} = K_s t \qquad \textbf{Equation 5.9}$$

Where,

Q_0 = the initial amount of API in the dosage form,
Q_t = the amount of API remaining in the dosage form,
K_s = a constant incorporating the surface volume relationship of the technology, and
t = time.

5.3.3.5 *Weibull*

The linearisation of the dissolution rates model [260] states that the empirical relationship proposed by Weibull [259] for the quantitation of dissolution rate data can be used to describe common types of dissolution curves as it combines the advantages of first order and log-normal data distributions . The Weibull model can be used to approximate the best linearisation of API release data from experimental and commercially available formulations.The general empirical equation for this model is depicted in Equation 5.10.

$$\log\left[-\ln\left(1-\left(\frac{Q_t}{Q_\infty}\right)\right)\right] = \beta \log t - \log \alpha \qquad \textbf{Equation 5.10}$$

Where,

Q_t = the amount of API remaining in a dosage form at time = t,
Q_∞= the maximum amount of API that can be released at infinite time from a dosage form,
β = shape parameter, obtained from the slope of the line,
α = scale parameter, and
t = time.

The Weibull model can be used to characterise the shape of a dissolution curve with the use of the Weibull shape parameter, β, and when assigned case 1 (β = 1) represents a sigmoidal or S-shaped with an upward curvature followed by a turning point, (case 2) in which case β > 1 or is parabolic. A higher initial value for slope that becomes consistent (case 3) will be reflected by β < 1 [259, 260].

5.3.3.6 *Korsmeyer-Peppas*

The Kosmeyer-Peppas model is a simple, semi-empirical model that is used to analyse API release data from dosage forms [261]. The model relates release to elapsed time by means of an exponential function [235, 264]. The relationship is referred to as the power law and is represented mathematically as Equation 5.11.

$$\frac{M_t}{M_\infty} = Kt^n \qquad \textbf{Equation 5.11}$$

Where,

$\frac{M_t}{M_\infty}$ = the fraction of API released at time = t,
K= Kinetic constant, and
n = Diffusion exponent for API release.

The model has been applied to different systems for the analysis of the API of a different solubility. The value of the exponent n is used to describe different release mechanisms [200, 234, 238, 239, 261, 264]. Specific values of n represent different mechanisms and/or types of release that may occur from specific geometries of dosage form and Table 5.1 provides a summary.

Table 5.1 *Relationship between the release exponent n and mechanism of API transport.*

Release Exponent	Shape	Transport Mechanism	Reference
0.43	Sphere	Fickian	[13, 17, 41]
0.43<n<0.85	Sphere	Anomalous	[5, 17, 24, 41]
0.85	Sphere	Case II transport	[5, 17, 24, 41, 45]
>1	Sphere	Super Case II transport	[11, 24, 41, 45]
0.45	Cylinder	Fickian	[5, 45]
0.5<n<0.89	Cylinder	Anomalous	[5, 45]
0.89	Cylinder	Case II transport	[5]

The relationships described in Table 5.1 reveal that API release from polymeric matrices described using Equation 5.11 may occur by one of four mechanisms of release, *viz*. Fickian diffusion, anomalous diffusion, Case II and super Case II transport. In order to understand Fickian or non-Fickian diffusion mechanisms, the release characteristics of the polymeric matrix used must be clarified [265]. Fickian diffusion occurs when n values are close to 0.5 and API release follows a diffusion process through a thin film. This is best described by Ficks 2nd law of diffusion. Anomalous transport occurs when API release deviates from Ficks law and where the mass transfer of API is both diffusion and swelling controlled [233, 265]. Case II transport represents API release that is zero-order and is generally observed when macromolecular relaxation of the rate controlling polymer controls release [246]. Super Case II transport occurs when delivery rates increase over time. The initial phase of the dissolution process can be characterised using Equation 5.11.

5.3.3.7 *Determination of goodness of fit*

Commonly used approaches to establishing a best fit model for API release use the correlation coefficient (R) [238], coefficient of determination (R^2) [266] and adjusted coefficient of determination (adjusted R^2) [266]. When comparing models with different numbers of parameters, it is recommended that the adjusted R^2 approach be used as it is a more meaningful criterion for the selection the best fit, compared to the R^2 [239, 266]. The R^2 value may increase or remain constant following the addition of new model parameters, whereas the adjusted R^2 may decrease to indicate whether or not the additional parameter improves the model or leads to over-fitting of experimental data [266].

The criterion of choice for establishing the best-fit model for CPT release from coated beads was the adjusted R^2 parameter. Models with the highest adjusted R^2 value were considered as those that the data were best fitted to were close to ideal release kinetics charactorised with R^2 value of 1. A value for the adjusted $R^2 > 0.950$ was considered acceptable for the purposes of comparison of the dissolution profiles for experimental dosage forms. The adjusted R^2 value was calculated using Equation 5.12 after fitting dissolution rate data for CPT to different models.

$$adjusted\ R^2 = 1 - \frac{(n-1)}{(n-p)}(1 - R^2) \qquad \textbf{Equation 5.12}$$

Where,

n = number of dissolution data points,
p = number of parameters in the model, and
R^2 = coefficient of determination.

5.3.4 Selection of appropriate statistical and mathematical models

A number of studies [228, 244, 246, 247] have evaluated dissolution profile data using model independent methods. There is a lack of standardisation as to which models should be used for the evaluation of dissolution from SR dosage forms. Model independent methods such as the use of f_1, f_2 and S_d have been described as useful for the comparison and assessment of dosage forms [228, 249], yet they provide little or no information on the kinetics and mechanisms of API release from a variety of modified release dosage forms. The approaches used for the analysis of the dissolution data in this study include f_1 and f_2 as they are advocated by regulatory authorities such as the FDA [249] and Human Medicine Evaluation Unit of The European Agency for the Evaluation of Medicinal Products (EMEA) [267]. Models based on statistical methods such as ANOVA and MANOVA, while having a place in academic research studies and being proposed for comparison of dissolution data [252, 253], are not advocated by the FDA and EMEA agencies and hence analyses using this approach were not performed. The FDA [249] and EMEA [267] recommend the use of only the f_2 factor for the comparison of dissolution profiles. For the purposes of these studies, f_1 and f_2 factors were calculated and both parameters had to meet the specifications for dissolution profiles to be declared similar or different.

Model-dependent mathematical approaches include empirical and semi-empirical models that can be applied to the evaluation of dissolution rate data. The use of model-dependent mathematical models permits elucidation of the mechanism and type of release that can be expected from modified release dosage forms that are based on a polymeric matrix scaffold [150, 156, 226, 229]. The adjusted R^2 value was used as the criterion to ascertain to which mathematical model the dissolution data for CPT were best fitted and Table 5.2 lists the studies.

Table 5.2 *Mathematical models used for the analysis of dissolution data.*

Mathematical models used to describe drug dissolution profile	
Zero order	$Q_t = Q_0 + K_0 t$
First order	$\ln Q_t = \ln Q_0 + K_1 t$
Higuchi model	$Q_t = K_H t^{1/2}$
Hixon-Crowell model	$Q_0^{1/3} - Q_t^{1/3} = K_s t$
Weibull model	$\log\left[-\ln\left(1 - \left(\frac{Q_t}{Q_\infty}\right)\right)\right] = \beta \log t - \log \alpha$
Korsmeyer-Peppas model	$\frac{M_t}{M_\infty} = K t^n$

As previously mentioned, *in vitro* dissolution testing is an essential quality control tool used to inform the development of safe and effective medicines [249]. Mathematical modelling is an important approach for assessing the mechanism of API release from a dosage form during the early stages of formulation development. The use of models facilitates the optimisation of API release characteristics from a delivery system, dosage form performance evaluation and evaluation of the impact of excipients on the mechanism of release. For the purposes of this study, a model-dependent mathematical approach was used to enhance the understanding of the impact of different levels of granulation fluid coating and curing conditions on the liberation of CPT from the coated beads delivered in a hard gelatin capsule.

5.4 RESULTS AND DISCUSSION

5.4.1 Similarity and difference factors

The dissolution data was assessed and the similarity and difference factors calculated for test batches CPT-002 – CPT-027 to a reference formulation that was batch CPT-001. The lack of a commercially available SR CPT formulation in South Africa led to development of CPT-001 that was used as reference since it was the initial formulation that satisfied the recommendations for modified/SR dissolution profiles in the USP [48] prior to screening and optimisation process. Test formulations included batches manufactured using different amounts of granulating fluid (CPT-003 – CPT-006), coated to different coating levels (CPT-007 – CPT-009) and batches manufactured using different curing conditions (CPT-010 – CPT-012), experimental design batches runs 1 to 12 (CPT-013 – CPT-024) and CPT release from optimised batches (CPT-025 – CPT-027). The results of model-independent analysis of dissolution profiles, *viz*. calculation of f_1, f_2 and S_d, are summarised in Table 5.3.

Table 5.3 *f_1, f_2 and S_d for CPT batches compared to CPT-001.*

Formulation	f_1	f_2	S_d
CPT-002	0.80	32.1	0.416
CPT-003	22.7	45.1	0.171
CPT-004	11.2	57.3	0.083
CPT-005	8.20	67.6	0.103
CPT-006	1.70	81.3	0.001
CPT-007	16.7	51.1	0.219
CPT-008	10.5	59.8	0.085
CPT-009	51.4	24.7	0.255
CPT-010	39.9	33.5	0.378
CPT-011	13.7	53.1	0.212
CPT-012	14.7	53.3	0.015
CPT-013	20.2	44.9	0.259
CPT-014	17.9	45.6	0.271
CPT-015	27.9	41.4	0.287
CPT-016	11.2	56.2	0.188
CPT-017	11.9	55.9	0.034
CPT-018	7.50	66.8	0.121
CPT-019	15.1	52.9	0.212
CPT-020	17.4	50.2	0.222
CPT-021	14.7	49.3	0.243
CPT-022	39.7	33.2	0.396
CPT-023	12.2	55.1	0.093
CPT-024	19.3	48.8	0.171
CPT-025	7.50	66.8	0.121
CPT-026	12.7	57.9	0.172
CPT-027	8.70	64.3	0.138

The dissolution of CPT from beads that had been manufactured with different amounts of diluted Surelease® dispersion 10 %, 15 % and 20 % w/w and then coated was investigated. Batches CPT-004 to CPT-006 were found to be comparable with f_2 values > 50, f_1 < 15, whereas the f_2 value for batch CPT-003 with 5 % w/w granulating fluid was 45.1 and f_1 value of 22.7, suggesting that there was a difference in the CPT release between the two formulations.

The f_2 values calculated for the comparison of CPT batches manufactured with different levels of coating revealed that batches CPT-007 and CPT-008 were similar to batch CPT-001. The corresponding $f_1$values determined for the same batches suggest similarity with the $f_1$values falling below 15. However, the CPT-009 batch prepapred to 25 % coating level was found to be

different when compared to the reference batch, CPT-001. In general, increasing the coating level led to a decrease in CPT releaseas depicted in Figure 4.24 in §4.4.2.6.1.

The dissolution profiles of batches of beads manufactured using different curing conditions, *viz.* batches CPT-011 and CPT-012, reveal that CPT release is similar to that observed for batch CPT-001.The $f_1$and f_2 values were 13.7, 14.7, 53.1 and 53.3 respectively. A relationship between f_2 and the similarity factor, S_d can be postulated since for batches in which the f_2 values were > 50 the S_d values were ≤ 0.212 and the larger the value for f_2, the lower the value of S_d. As the value for S_d tended towards a value of 0.25 increasing dissimilarity between dissolution profiles was observed. When the value for S_d was approximately 0.008 and lower there was an increase in the incidence of similarity of the dissolution profiles. It is therefore fairly difficult to set a limit for establishing similarity based on S_d alone.

Comparison of the release from CPT beads formulations was based on dissolution data for which at least 85 % CPT release was observed due to the sensitivity of f_1 and f_2. The calculation of f_1 and f_2 is based on differences in data and includes all time points, resulting in one value. The f_1 values for the optimised batches CPT-025 to CPT-027 ranged between 7.5 and 12.7 and f_2 values ranged from 57.9 to 66.8, which indicate similarity between the optimised products and the reference product. The results obtained supplement the results observed using exploratory methods of data analysis when comparing dissolution profiles.

The mean *in vitro* dissolution profiles of CPT release from Batch CPT-001and Batch CPT-025 – CPT-027, considered the test formulation,is depicted in Figure 5.2.

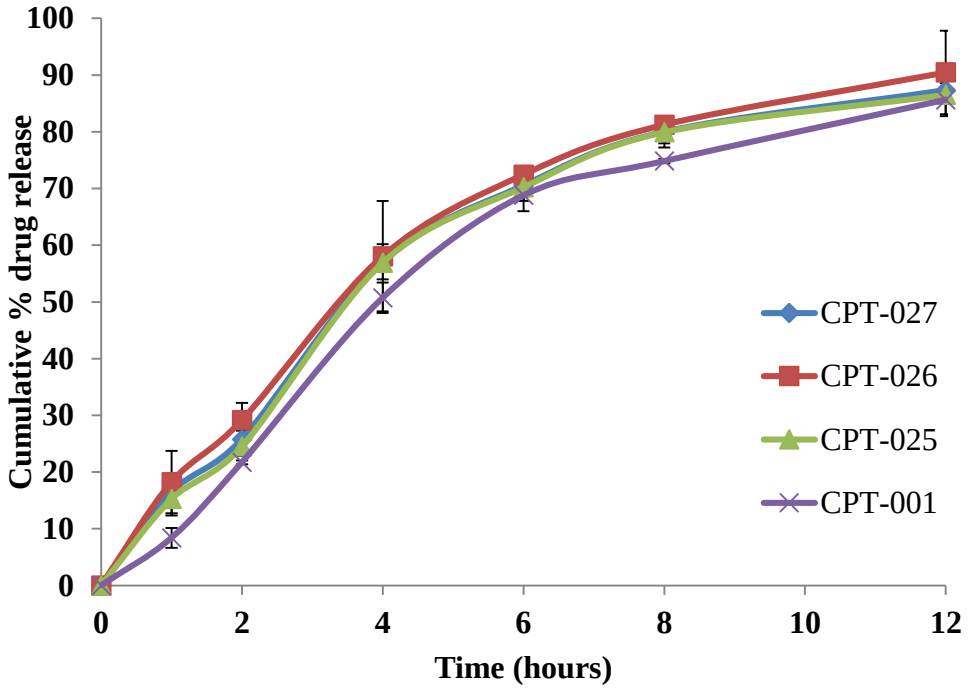

Figure 5.2 *In vitro dissolution profiles of CPT release from Batches CPT-001and CPT-025-CPT-027.*

The error bars observed at 1 hr, 6 hrs and 12 hrs overlap, suggesting that the two curves are similar and that the dissolution data for both batches may be considered similar at these times. Despite the simplicity and ease of using this approach, the method is not comprehensive. It does not categorically conclude that the two dissolution profiles being compared are significantly similar, as the error bars overlap only at some data points and not for all times under investigation. The application of this method is limited to a comparison of data at specific time points only and serves as an initial step in developing an understanding of data generated during dissolution testing. The f_1 values for all optimised batches were < 15 and the f_2 values were > 50, indicating that all optimised batches were similar to the reference product.

5.4.2 Mathematical modelling

5.4.2.1 Application of Korsmeyer-Peppas model

The mechanism by which CPT is released from the coated beads was determined by fitting dissolution data to selected mathematical models that were described in §5.3.3. The Korsmeyer-Peppas model was used to characterise the transport mechanism of CPT from each batch

manufactured in these studies. CPT release data were fitted to the Korsmeyer-Peppas model, which was modified to produce a linear plot of log of (M_t/M_∞) vs. log (t) to calculate the kinetic constants. These data were used to predict the mechanism of CPT release and are summarised in Table 5.4.

Table 5.4 *Korsmeyer-Peppas coefficients and best-fit parameters for batches CPT-001, and CPT-002 - CPT-027.*

	Korsmeyer-Peppas Parameters		
Formulation	**n**	**R^2**	**K_m**
CPT-001	0.959	0.947	0.104
CPT-002	0.328	0.996	0.436
CPT-003	0.804	0.923	0.169
CPT-004	0.905	0.914	0.127
CPT-005	0.786	0.943	0.152
CPT-006	0.943	0.936	0.105
CPT-007	0.606	0.982	0.231
CPT-008	0.719	0.969	0.159
CPT-009	0.652	0.934	0.088
CPT-010	0.449	0.956	0.359
CPT-011	0.531	0.956	0.242
CPT-012	0.808	0.947	0.119
CPT-013	0.542	0.933	0.263
CPT-014	0.472	0.982	0.289
CPT-015	0.552	0.974	0.276
CPT-016	0.608	0.974	0.216
CPT-017	0.868	0.979	0.109
CPT-018	0.756	0.955	0.161
CPT-019	0.611	0.976	0.224
CPT-020	0.609	0.639	0.229
CPT-021	0.519	0.978	0.262
CPT-022	0.395	0.992	0.394
CPT-023	0.867	0.975	0.138
CPT-024	0.757	0.976	0.177
CPT-025	0.756	0.955	0.161
CPT-026	0.685	0.969	0.193
CPT-027	0.724	0.959	0.171

5.4.2.2 *Effect of amount of granulation fluid*

The release exponent n for batches CPT-003 and CPT-005 was found to be 0.804 and 0.786, respectively suggesting that the mechanism of CPT release from these dosage forms is controlled by an anomalous process. These results suggest that for these batches, the mechanism of CPT release is controlled by more than one phenomenon, and therefore CPT is liberated by anomalous transport kinetics. An n value of between 0.43 and 0.85 for spherical shaped dosage forms is

usually indicative of anomalous transport (Table 5.1) and drug release that deviates from Ficks 2nd law. Several reports of complex dissolution profiles [147, 234, 238, 245, 246] have been characterised by anomalous transport mechanisms and the complexity of the CPT release process may involve diffusion, swelling and erosion of HPMC matrices. The values of n for batches CPT-004 and CPT-006 were 0.905 and 0.943, indicating that a Case II transport process was driving release. In this process a zero-order kinetic model occurs, in which macromolecular relaxation of polymers control CPT release [235].

5.4.2.3 *Effect of coating levels*

There was a slight increase in the n value from 0.606 to 0.719 for formulations manufactured using different coating levels *viz*. batches CPT-007 and CPT-008. The release mechanism of CPT from the beads was unaltered for all batches manufactured with different levels of coating. Despite the increase in thickness of the coating, CPT release occurred primarily via a non-Fickian diffusion controlled mechanism. The relationship between K_m and R^2 for the batches coated to different level is depicted in Figure 5.3.

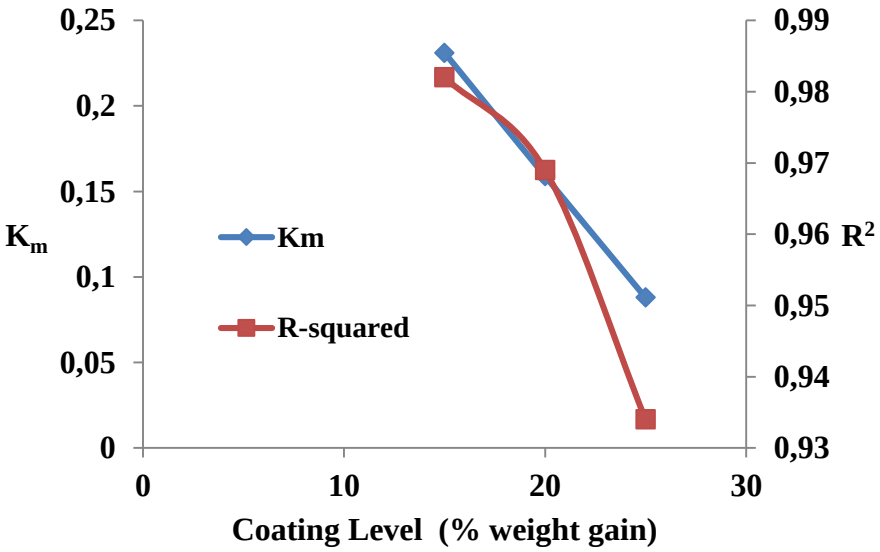

Figure 5.3 *Relationship between K_m, R^2 and coating level.*

The increased level of coating results in a decrease in water permeability as there is a barrier against the transport of water from the dissolution medium into the matrix within the bead. This is manifested by a decrease in the value for K_m to < 1, which falls into the realm of non-Fickian release in which CPT release is controlled by diffusion and swelling.

5.4.2.4 *Effect of curing*

The coefficient K_m incorporates aspects of the structure and geometric characteristics of dosage forms. An increase in the time for curing *viz*. batches CPT-010 to batch CPT-012 relative to a batch of coated beads that were not subject to curing, resulted in values of n value ranging between 0.449 and 0.808. The value for K_m decreased from 0.359 to 0.119. The results reveal that there is no direct relationship between the cumulative percent CPT released and the value of K_m, since batches CPT-010, CPT-011 and CPT-012 had different values for K_m. The different values for K_m can be partially attributed to a change in the geometric characteristics of the dosage form, primarily the coalescence of ethylcellulose particles over the bead surface through capillary effects during prolonged curing. The glass transition of the polymeric ethylcellulose affects the diffusivity of the poorly permeable CPT molecules in the membrane layer due to curing. Polymers with low glass transition temperatures possess higher diffusivity for API and do not hinder diffusion across film coats [268].

5.4.2.5 *Effect of formulation composition*

The value for the release exponent for batches CPT-013 - CPT-024 varied in the range of 0.472 to 0.868, indicating that the release mechanism from these dosage forms was controlled by an anomalous diffusion process. The value of n for batch CPT-022 was 0.395, and this is < 0.43, which implies that CPT release cannot be readily explained by the Korsmeyer-Peppas model. The inability to ascribe a mechanism of release to batch CPT-022 may in part be explained by changes in geometry of the dosage forms during dissolution testing and the excipients used to manufacture the batch. The value for n is affected by the change in the shape of matrices. In systems in which diffusion and transport within a matrix is important, the value will depend on the nature and type of excipients, degree of adhesion of binders and compatibility of excipients used in the technology [226]. Eudragit® RS PO, which contains a methacrylic acid copolymer, occupies free volume within the polymeric matrix. This creates a tortuous path for diffusion and results in a decreased diffusivity of dissolved CPT. The degree of tortuosity is dependent on the volume fraction of Eudragit® RS PO and the orientation and shape of these particles in the polymeric matrix [236]. As dissolution occurs, the matrix becomes more porous due to an increase in the void volume, as depicted in Figure 5.4 B. Incompatibility between excipients within the polymeric matrix may result in the formation of additional voids, leading to an increase in the free transport of CPT facilitated by concentration gradient or difference across the matrix.

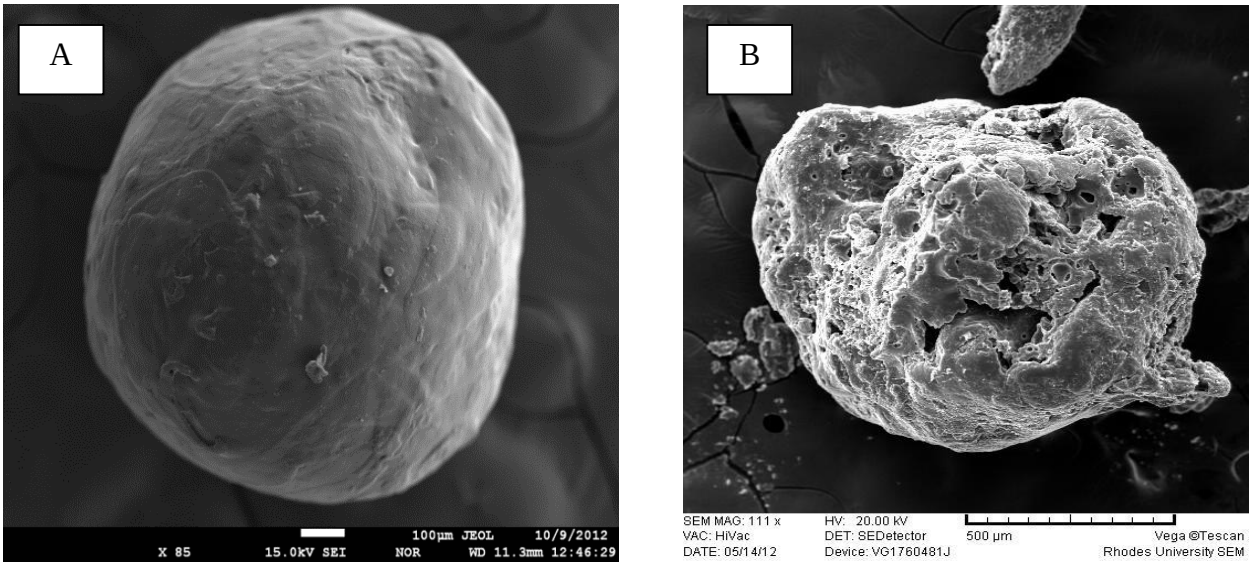

Figure 5.4 *SEM image of a coated bead prior to* ***(A)*** *and after 12 hours of dissolution* ***(B).***

5.4.2.6 Application of other mathematical models

The dissolution data generated from testing batches manufactured during formulation and process development of an extrusion-spheronisation process were used to establish the kinetics of CPT release. The dissolution data were fitted to different models, including zero order, first order, Higuchi, Hixon-Crowell and the Weibull model to determine dissolution kinetics. The results of model fitting are summarised in Table 5.5.

Table 5.5 *Results of modelling CPT dissolution data for batches CPT-001 - CPT-027.*

	Zero order		First order		Hixon-Crowell		Higuchi		Weibull		
Formulation	**K_0**	***R^2**	**K_1**	***R^2**	**K_{HC}**	***R^2**	**K_H**	***R^2**	***R^2**	**β**	**α**
CPT-001	7.603	0.898	0.171	0.986	0.289	0.617	28.353	0.953	0.983	1.275	0.101
CPT-002	6.775	0.777	0.314	0.937	0.249	0.443	27.422	0.962	0.915	0.736	0.489
CPT-003	8.241	0.825	0.252	0.943	0.302	0.608	31.821	0.931	0.975	1.241	0.166
CPT-004	7.784	0.827	0.188	0.937	0.304	0.632	29.834	0.919	0.957	1.255	0.126
CPT-005	7.307	0.852	0.164	0.942	0.289	0.618	27.968	0.944	0.974	1.091	0.153
CPT-006	7.253	0.867	0.149	0.946	0.299	0.661	27.346	0.933	0.968	1.231	0.104
CPT-007	7.518	0.895	0.227	0.989	0.279	0.578	28.737	0.989	0.996	0.971	0.231
CPT-008	6.965	0.935	0.159	0.992	0.281	0.627	26.004	0.985	0.992	0.995	0.159
CPT-009	3.142	0.889	0.041	0.931	0.211	0.589	12.011	0.982	0.947	0.713	0.091
CPT-010	7.461	0.779	0.318	0.997	0.267	0.487	30.056	0.957	0.991	0.914	0.387
CPT-011	6.359	0.834	0.137	0.949	0.259	0.533	24.964	0.972	0.983	0.772	0.263
CPT-012	6.466	0.916	0.121	0.975	0.281	0.658	24.078	0.968	0.988	1.038	0.119
CPT-013	6.939	0.882	0.183	0.978	0.267	0.525	27.392	0.973	0.983	0.849	0.286
CPT-014	6.674	0.852	0.173	0.989	0.259	0.515	26.147	0.988	0.993	0.753	0.316
CPT-015	7.824	0.851	0.276	0.981	0.279	0.551	30.388	0.971	0.981	0.988	0.279
CPT-016	7.102	0.867	0.169	0.953	0.276	0.576	27.307	0.968	0.981	0.908	0.224
CPT-017	7.022	0.927	0.139	0.969	0.294	0.689	25.779	0.941	0.987	1.131	0.106
CPT-018	7.489	0.876	0.178	0.975	0.291	0.625	28.411	0.953	0.981	1.077	0.161
CPT-019	7.557	0.898	0.218	0.996	0.281	0.587	28.748	0.982	0.985	0.968	0.224
CPT-020	7.551	0.887	0.224	0.995	0.283	0.578	28.912	0.984	0.995	0.975	0.231
CPT-021	6.763	0.855	0.166	0.984	0.263	0.533	26.412	0.986	0.998	0.801	0.282
CPT-022	7.314	0.806	0.464	0.901	0.261	0.476	29.282	0.976	0.922	0.946	0.395
CPT-023	8.637	0.931	0.351	0.937	0.314	0.679	31.869	0.958	0.989	1.383	0.118
CPT-024	8.592	0.915	0.369	0.948	0.305	0.641	32.151	0.969	0.799	0.898	0.212
CPT-025	7.489	0.876	0.178	0.976	0.291	0.625	28.411	0.953	0.981	1.077	0.161
CPT-026	7.593	0.885	0.201	0.995	0.287	0.605	28.908	0.971	0.993	1.031	0.193
CPT-027	7.474	0.879	0.181	0.982	0.288	0.617	28.394	0.959	0.984	1.048	0.173

***R^2 =adjusted R^2 calculated using Equation 5.12**

The release kinetics of batches CPT-003 – CPT-006 manufactured with different amounts of Surelease® E7-19010 as the granulating fluid were best fitted to the Weibull, first order and Higuchi models, using adjusted R^2 values as the best fit model determinant. The adjusted R^2 value for the Weibull model ranged between 0.957 and 0.975 and exhibited a better goodness of fit than that the first order and Higuchi models. Use of the Korsmeyer-Peppas model produced n values of 0.786 and 0.943, indicating that CPT transport was facilitated by an anomalous mechanism where the diffusion process of CPT and swelling of polymers modulate the release of CPT from the core. Dissolution data from CPT-007 – CPT-009 were well fitted to first order, Higuchi and the Weibull models. The adjusted R^2 for the Higuchi model was between 0.982 and 0.989, suggesting that the mechanism of CPT release is a diffusion-controlled process. An increase in coating levels from 15 % to 25 % weight gain (CPT-007 – CPT-009) appeared to have different effects on the adjusted R^2 value, but CPT release is primarily diffusion-controlled.

The results of fitting CPT release data and using the adjusted R^2 selection criteria identify the first order, Higuchi and Weibull models as the best models to describe CPT release from the optimised batches CPT-025, CPT-026 and CPT-027. The adjusted R^2 values for the optimised batches were in the range 0.953 -0.995.The magnitude of the adjusted R^2 for the first order and Weibull models were considerably closer to 1 compared to the adjusted R^2 value for the Higuchi model, which ranged between 0.953 -0.976. This suggests that diffusion is not the only mechanism that controls CPT release from the coated dosage forms. The results support the phenomenon that anomalous transport processes with some osmotic potential and hydrostatic pressure build-up play a role in CPT release.

The results indicate that mathematical modelling and identification of key parameters are important when evaluating CPT release mechanisms from bead dosage forms. Furthermore, the model parameters must be comprehensively defined before fitting experimental data to the models, as the shape of the dissolution profiles may be affected by experimental variables and consequently the results obtained from modelling studies may be skewed. When fitting dissolution data from coated formulations [237, 240, 241], it is necessary to correct the experimental lag time parameter to describe drug release from coated systems. However, this is tedious and involves the calculation of internal diameter, external diameter, diffusion coefficient of API in the core and coating. This was beyond the scope of this study and should be explored in future studies.

5.5 CONCLUSION

Mathematical modelling was used to elucidate mechanistic aspects of the transport processes specific to CPT release from coated bead formulations. Developing and understanding a comprehensive model for coated bead formulation is important for the development of *in vitro* release test methods for quality control in cases where the mechanism of release may be known or where a specific mechanism of release *in vivo*, is desirable. In such cases the *in vitro* release test may be optimised based on specific mechanistic requirements for CPT release. The optimisation of an *in vitro* release test method is essential for the exploration of an *in vitro-in vivo* correlation for a specific technology.This is pivotal in establishing a logical next step in the development and optimisation of novel formulations [147, 225, 234].

The evaluation of CPT release data formulations with different levels of granulating fluid using the Korsmeyer-Peppas model revealed that this approach was a discriminatory method and therefore most suitable as a tool for further product optimisation. The release exponent n was found to range between 0.786 and 0.943, suggesting that the release mechanism from the dosage form is controlled by anomalous diffusion and Case II transport mechanisms. The results suggest that there is a complex release process of CPT from coated spherical beads. This may involve osmotic potential and cracking of coating due to hydrostatic pressure build-up in the core of the beads. Increasing the amount of Surelease® E7-19010 from 5 % w/w to 20 % w/w resulted in variable effects on model fitting outcomes.

The effect of different coating levels resulted in a slight increase from 0.606 to 0.719 for the n value. The release mechanism of CPT from the coated beads was unaltered for all batches manufactured using different coating levels and the mechanism appeared to be primarily non-Fickian diffusion controlled. The increase in % weight gain resulted in a decrease in the permeability of the film coat that acts as a barrier to transport of water into the core of the bead matrix, with a resultant decrease in K_m to < 1 within the realm of non-Fickian mechanisms in which release deviates from Ficks law and is controlled by diffusion and swelling.

An increase in the time of curing up to 2 hours (CPT-010 - CPT-012) revealed that the value for the release exponent increased from 0.449 to 0.808 and the value for K_m varied between 0.359 and 0.119. The variability of the K_m values can be explained in part by the change in geometric characteristics of the dosage form primarily due to the coalescence of ethylcellulose particles on the surface of the beads through capillary effects as curing time was lengthened.

The glass transition of ethylcellulose may affect the diffusivity of poorly permeable CPT molecules due to the formation of a coherent film on the beads. The results of model fitting for the optimised batches CPT-025 – CPT-027 evaluated using adjusted R^2 values were in the range between 0.953 and 0.995. The magnitude of adjusted $R^2$was close to 1 compared to the adjusted R^2 value of theHiguchi model, which was in the range 0.953 to 0.976. This indicates that diffusion is not the only mechanism that controls CPT release from the coated beads.

In general, these results support the hypothesis that the hydration and swelling of polymers play a significant role in CPT release. The release mechanism includes transport of dissolution medium from the vessel reservoir into the core of the bead due to osmotic potential, dissolution of CPT, mass transfer of the dissolved CPT within the core, partitioning between the solution and polymeric film, and mass transfer of dissolved CPT through the film, ultimately to reach the bulk of the dissolution fluid.

Mathematical modelling has been successfully used to characterise and understand the mechanisms by which CPT is released from a bead technology manufactured using extrusion, spheronisation and coating processes.

CHAPTER SIX
CONCLUSIONS

CPT is an orally active ACE inhibitor that exhibits a diverse *in vivo* pharmacological profile. The primary activity of CPT is to block the conversion of AT-I to AT-II. CPT is used therapeutically for the treatment of hypertension, cardiac failure and diabetic nephropathy as it has an ability to alter binding on the ACE enzyme to reduce the conversion of AT II and increases plasma renin activity to lower the diastolic and systolic arterial blood pressure. CPT is prescribed to chronically ill patients and long-term use requires appropriate management due to limited toxicity. The antihypertensive effects of CPT last for up to 6 hours, which is related to the short plasma elimination half-life of the molecule. The presence of the sulphydryl moiety in the CPT molecule results in a sulphurous odour and facilitates oxidation of the parent compound to captopril disulphide conjugates that are eliminated via the kidneys. CPT exhibits undesirable adverse effects in patients who exhibit hypersensitivity to sulphur. These patients produce macula-papular skin rash. In addition, CPT may disturb taste, manifested by the loss of taste or the presence of a metallic taste. The development of a once or twice daily oral formulation of CPT would be of significant advantage and enhance patient adherence. In addition, the challenges exhibited by CPT use that include taste disturbance, instability and the characteristic sulphur odour may be minimised using sustained release delivery technologies.

CPT lacks the presence of a strong chromophore and therefore does not absorb in the UV-Vis region of electromagnetic spectrum. The quantitation of CPT was achieved using a validated HPLC method and a PDA detector with a fast scan spectrophotometer that has a low S/N ratio and wide wavelength range for scanning. This enhances the sensitivity of the method and can assess peak purity. CPT is a weakly acidic molecule and the pH of the mobile phase can affect the distribution of charged entities, thereby affecting the separation of CPT. In particular, the resolution and retention time of CPT can be altered through silanol interactions between the molecule and the stationary phase. A DOE approach using CCD was successfully used to optimise the chromatographic conditions for the analysis of CPT. The method was advantageous in respect of saving costs through minimal reagents and effective time use. The CCD approach permitted the investigation of interactive factors such as pH, MeOH content and column temperature on the chromatographic responses of the retention time of CPT and resulted in identification of method parameters that yielded an optimised separation with well-resolved and symmetrical peaks for CPT and the IS, SCY.

ANOVA was used to identify the significant factors that affected retention time and the resolution factor. The MeOH content in the mobile phase had the greatest impact on the retention time of CPT. An increase in MeOH content increased the overall polarity of the mobile phase, resulting in overall decrease in the retention time of CPT due to a decrease in solute particle interactions with silanol functional groups of the stationary phase. ANOVA revealed that the interaction of pH-MeOH content and pH-column temperature had significant and antagonistic effects on the symmetry of the CPT peak. The pH of the mobile phase is the most significant factor in the interactive model. It affects peak shape significantly, particularly if the compound of interest has ionisable functional groups that will elute at a different rate to unionised compounds, resulting in peak tailing. A quadratic polynomial equation was used to describe the relationship between the input variables and responses (output variables). The relationship was then used to establish the retention time of CPT and the optimum conditions for the separation. It permitted an evaluation of the combined effects of independent variables such as pH, MeOH content and column temperature due to linear antagonistic contributions.

The optimum chromatographic conditions were selected based on experimental data for which the CV was used as an indicator of the degree of precision with which the experiments were performed. The CV was 10.16 and 1.75 for retention time and A_s. The peaks for CPT and SCY were adequately separated with retention times of 3.5 and 6.8 minutes for the analytes. The analytical method was validated using ICH guidelines and was found to be simple, precise, accurate, selective, rapid and accurate and was appropriate to use for the analysis of CPT in its pure form over the concentration range 2 - 60 µg/mL and for the analysis of CPT in commercially available and prototype formulations.

The stability indicating RP-HPLC method revealed that CPT degrades in 0.1 M NaCl (100%), 30 % v/v H_2O_2 (98.02%), 0.1 M HCl (43.20%) and after exposure to 500W/m^2 (43.60%) light following exposure to these media for up to 8 hours. The stress studies yielded degradation products following exposure to neutral hydrolytic conditions at an elevated temperature of 80 °C and 0.1 M NaCl (46.3%) for 8 hours.

A number of preliminary studies were undertaken to establish the properties of CPT and potential excipients to ensure a suitable risk assessment for the development of a coated bead dosage form. SEM images of raw materials revealed the particle size and shape of the excipients.Materials had to be sieved prior to blending to facilitate the production of homogenous blends of powder of uniform content that would be suitable for further processing.

The results of powder flow analysis revealed that CPT, MCC and Eudragit® RS PO exhibited satisfactory flow properties, whereas HPMC K100M and HPMC E4M exhibited poor flow properties. These data were based on an assessment of the AOR, CI and HR. A glidant such as talc had to be included for successful blending and granulation prior to manufacturing beads. Following the addition of talc, most blends had measured values for the AOR and calculated values for CI and HR that fell within the range to suggest that the flow properties of the materials would be satisfactory to good.

DSC studies were used to assess the compatibility of CPT and CPT-excipient mixtures and revealed no significant shift in the melting point of CPT. The thermogram for CPT exhibited a T_{peak} at 110.93 °C. Similarly, FT-IR studies did not reveal any significant shifts in the absorption bands for CPT in the presence of excipients for all combinations except talc. Despite the limitations of FT-IR when it comes to providing insight into molecular changes that are necessary to fully understand prospective CPT-excipient interactions, the studies provide valuable information relating to the behaviour of blends of binary mixtures of CPT and excipients. No interactions were noted, and based on the combination of studies of flow properties, SEM, TGA, DSC and FT-IR, it was established that Methocel® K100M, Methocel® E4M, Avicel® PH102, Eudragit® RS PO and talc were suitable for use in formulation development studies designed to produce CPT beads. The dissolution of CPT in the presence and absence of ammonium oleate was studied and it was concluded that the anionic oleate did not interact with CPT, as shown by the similar release profile in the presence and absence of ammonium oleate. These results indicate that no potential interactions are likely to occur during processing and coating of CPT beads using Surelease® E-7-19010 as a granulation and coating material.

An increase in the amount of solid content in the granulation fluid from 5 % w/w to 20 % w/w resulted in a decrease in the extent of CPT release. SR was achieved using Surelease® as the granulating fluid in an attempt to suppress the initial burst effect usually observed with water soluble compounds. In addition, the concurrent use of hydrophilic HPMC K100M and E4M polymers that form a gel matrix on hydration in dissolution media further retarded CPT release. When the CPT dissolution data were fitted to the Korsmeyer-Peppas model for batches with increased granulation fluids, values of n between 0.786 and 0.943 emerged, suggesting that CPT release occurs via anomalous and Case II transport mechanisms. The results suggest that CPT release from the spherical coated beads may involve anomalous transport mechanisms

and the complexity of the CPT release process may encompass diffusion, swelling and erosion of HPMC based matrices.

CPT release diminished when the level of coating was increased from 15 – 25 % since the increase in coating levels increased the physical barrier around the core bead, which retards the release of CPT. A slight increase in the value for n from 0.606 to 0.719 suggested that the release of CPT from the coated beads was via a non-Fickian diffusion controlled mechanism. The increase in coating levels hinders the permeability of the coating and acts as a barrier to the transport of water.

CPT is classified as a BCS class III compound for which permeability is the rate-limiting step for absorption across epithelial cells of the GIT. Since CPT solvates rapidly, the rate of release is rapid and consequently absorption may be controlled by altering the availability of CPT with a coated multi-particulate bead technology. Preliminary prototype formulations were developed using different amounts of polymer, different levels of granulating fluid and coating, and curing time to identify a suitable composition and process that would produce SR beads with a dissolution profile that met the specifications for SR products in the USP. All batches of coated beads were manufactured by extrusion and spheronisation. Excipients such as Methocel® K100M, Methocel® E4M, Avicel® PH102, Eudragit® RS PO and talc were successfully used to produce SR beads that were then coated and have the potential to be used as a twice-daily drug delivery system. The coated beads formulations were selected for further optimisation as they offer several benefits in respect of flexibility in titrating doses for paediatric patients and reduce the risk of dose dumping, which is a characteristic observed when delivering water soluble API drugs.

A Plackett-Burman experimental design was used to screen the formulation composition of MCC, HPMC K100M, HPMC E4M, Eudragit® RS PO and process parameters such as extrusion and spheronisation speed, residence time, coating temperature, atomising airflow, spray rate and curing time on the manufacture of beads. The aforementioned factors were critical input variables for the manufacture of coated CPT beads. The Plackett-Burman design was used since it is an efficient approach that permits screening of a large number of significant factors in a short time and requires minimal resources. The responses monitored for the design included percent yield, AOR, friability, AR, sphericity, coating efficiency, cumulative percent CPT released at 2, 6 and 12 hrs. The limits for some of the responses were set to meet USP recommendations for the dissolution of API from the SR/modified release dissolution profile.

The quality attributes of the beads after production using extrusion-spheronisation and coating were also measured against appropriate specifications. The model that was developed demonstrates significant responses for the yield, AR, sphericity, coating efficiency and the amount of CPT, released at 2 and 12 hours. The p value were < 0.05, indicating that the beads exhibited satisfactory to good flow properties, were smooth and spherical, indicating that a capsule filling would be efficient. CPT release from this technology was sustained over the 12-hour test period.

The response variables for all formulations and process factors were analysed using Design-Expert® 8.0.4 software. ANOVA revealed that CPT release at 2 hours (p=0.0336) was significantly affected by the linear terms of MCC, Methocel® K100M and Eudragit® RS PO, spray rate and curing temperature in the model that were necessary to control the initial burst effect. The application of Surelease® E-7-19010 onto the surface of the beads produced a barrier that complements the rate of release retardant properties of the hydrophilic polymeric core, thereby reducing the rapid dissolution of CPT in the core and its release into the dissolution medium. An increase in the spray rate during coating was reflected by a decrease in the amount of CPT released at two hours. An increase in the spray rate resulted in smaller droplets that are deposited onto the surface of the bead rapidly.This associated with a thicker coating layer that retards release more effectively when compared to coats manufactured at lower spray rates. An increase in curing time facilitates complete coalescence of the polymer coat, resulting in production of a less permeable membrane that reduces the rate of CPT release and overcomes the burst effect.

CPT release at 12 hours was significantly affected by the MCC, HPMC K100M, HPMC E4M and Eudragit® RS PO content, AFR, spray rate and curing time. The use of contour plots verified the acceptance criterion of ensuring that at least 80 % CPT was released at 12 hours. HPMC is a hydrophilic non-ionic polymeric material that hydrates rapidly and swells to form a gel layer that can control the release of CPT. An increase in the amount of the more viscous HPMC K100M from 15 – 25 % resulted in a slower rate of CPT release due to the slower diffusion of the molecule through the viscous matrix. An increase in Eudragit® RS PO content from 7.5 to 15 % w/w increased the number of insoluble quaternary ammonium functional groups in the matrix, resulting in fewer pores and channels through which CPT can diffuse.This subsequently resulted in slower release.

ANOVA data for coating efficiency revealed that all individual parameters investigated were significant in ensuring the efficiency of the process. The coating efficiency ranged between 76.4 % and 98.6 % and the AFR and spray rate had the greatest impact on efficiency. A high AFR is associated with continuous mass transport of air in the coating chamber and consequently increases the evaporative capacity of the coating unit, which minimises over-wetting and agglomeration of beads.

The prediction error when comparing the responses for three batches of the optimised formulation (CPT-025 – CPT-027) with that from a reference product (CPT-001) was between -1.44 % and +0.78 %. This is a reasonable error of low magnitude that is reproducible (R^2 = 0.9996). The use of the Plackett-Burman approach was suitable for formulation composition and process parameter screening during the development of SR CPT beads. The beads were manufactured at an acceptable yield level with target quality attributes of good flow properties.

The use of an HPMC-based matrix coated with ethylcellulose to modulate the delivery of the highly water soluble and poorly permeable CPT molecule may result in release of the API by one of a number of mechanisms. As the API is water soluble, an osmotic gradient may in part provide a driving force for the influx of dissolution medium across the coating to dissolve CPT. The hydration and swelling of the polymers in the bead result in an increase in the diffusional path length for CPT and may increase the pressure in the interior of the bead.

The experimental design was successfully applied to the development of SR CPT beads that can be used for twice-daily dosing. The technology can be used to reduce the dosing frequency and this may enhance patient adherence to prescribed dosing regimens. The coated beads also provide a potential solution to the challenges of treating paediatric patients as dose adjustment when manufacturing extemporaneous products is easily achieved. It is likely that the coated beads will deliver CPT in a manner that will maintain drug levels in the therapeutically desirable range while reducing potential side effects such as the dry hacking cough, taste disturbances and maculo-papular rash associated with CPT. Further development and optimisation of the formulation and manufacturing process using RSM approaches such as CCD or Box-Behnken design studies are required to establish a scaled-up process for an optimised formulation. Furthermore, additional studies would be necessary to establish the long-term stability and shelf life of the optimised and scaled-up formulations.

REFERENCES

1. M.Ortegon, S.Lim, D.Chisholm, S.Mendis. Cost-effectiveness strategies to combat cardiovascular disease, diabetes and tobacco use in Sub-Saharan Africa and South East Asia: Mathematical modelling study. *British Medical Journal* 2012; **344**(607):1-15.

2. T.A.Gaziano, K.Steyn, D.J.Cohen, C.Milton, M.C.Weinstein, L.H.Opie. Cost-Effective Analysis of Hypertension Guidelines in South Africa: An absolute risk versus Blood Pressure Level. *Circulation* 2005; **112**(23):3569-3576.

3. H.Kadin. Captopril. In: K.Florey (editor): *Analytical Profiles of Drug Substances*. London: Academic Press; 1982, pp. 79-137.

4. D.Chen, H.Chen, H.Ku. Degradation rates of captopril in aqueous meduim through buffer catalyst oxidation. *Drug Development and Industrial Pharmacy* 1995; **21**(7):781-792

5. K.Tselios, C.Koumaras, M.B.Urowitz, D.D.Gladman. Do current arterial hypertension treatment guidelines apply to systematic lupus erythematosus patients? A critical appraisal. *Seminars in Arthritis and Rheumatism* 2014; **43**(4):521-525.

6. D.Mather, A.D.Harries, R.Zachariah, D.Enarson. A global framework for action to improve the primary care response to chronic non-communicable diseases: A solution to a neglected problem. *BioMed Central Public Health* 2009; **9**(355):1-7.

7. S.R.Hill, A.J.Smith. First Line medicines in the treatment of hypertension. *Australian Publisher* 2005; **28**(2):34-37.

8. Q.Bui. First Line Treatment for hypertension. *American Family Physicians* 2010; **81**(11):1333-1335.

9. C.S.Sweetman. *Martindale "The Complete Drug Reference"*. London: The Pharmaceutical Press; 2011; **39**(1), pp 156-159.

10. T.K.Lee, R.E.Notari. Kinetics and mechanism of captopril oxidation in aqueous solution under controlled oxygen partial pressure. *Pharmaceutical Research* 1987; **4**(2):98-103.

11. B.Gokul, J.Lee, K.Song, T.Panda, S.K.Rhee, C.H.Kim. Screening of Microorganisms Producing Esterase for the Production of (R)-β−Acetylmecraptoisobutyric acid from Methyl (R,S)-β−Acetylmercaptoisobutyrate. *Biotechnology and Bioprocess Engineering* 2000; **5**(1):57-60.

12. D.Burger, T.L.Reudelhuber, A.Mahajan, K.Chibule, E.D.Sturrock, R.M.Touyz. Effects of a domain-selective ACE inhibitor in a mouse model of chronic angiotensin II dependend hypertension. *Clinical Sciences* 2014; **127**:57-63.

13. D.Cushman, H.S.Cheung, M.Odentti. Design of Potent Competitive Inhibitors of Angiotensin-Converting Enzyme. Carboxyalkanoyl Amino Acids. *Biochemistry (Mosc)* 2001; **16**(25):5484-5491.

14. D.Cushman, M.Odentti, B.Rubin. Design of specific inhibitors of Angiotensin-Converting Enzyme: A new class of orally active Antihypertensive agents. *Science* 1977; **196**(4288):441-444.

15. W.Soudijin. Angiotensin Converting enzyme inhibitors. *Pharmaceutissch Weekblad Scientific Edition* 1982; **4**(5):154-158.

16. CAPOTEN®. Pharmacy Retailing (NZ) Ltd t/a Healthcare Logistics. 2010. New Zealand.

17. B.G.Katzung, S.B.Masters, A.J.Trevor. *Basic and Clinical Pharmacology*. Stamford: Appleton & Lang; 2011.**12** pp876-889.

18. A.H.El-Kamel, D.H.Al-Shora, Y.M.El-Sayed. Formulation and pharmacodynamic evaluation of captopril sustained release microparticles. *Journal of Microencapsualtion* 2006; **23**(4):389-404.

19. I.Jimenez-Martinez, T.Quirino-Barreda, L.Villafuerte-Robles. Sustained delivery of captopril from floating matrix tablets. *International Journal of Pharmaceutics* 2008; **362**(1-2):37-43.

20. J.Singh, D.H.Robinson. Controlled release captopril microcapsules:effect of ethyl cellulose viscosity grade on the *in vitro* dissolution from microcapsulesand tableted microcapsules. *Journal of Microencapsualtion* 1990; **7**(1):67-76.

21. A.Golik, R.Zaidenstein, V.Dishi, A.Blatt, N.Cohen, G.Cotter. Effects of Captopril and Enalapril on Zinc Metabolism in Hypertensive Patients. *The Journal of the American college of Nutrition* 2014; **17**(1):75-78.

22. R.R.Chirumamilla, R.Marchant, P.Nigam. Captopril and its synthesis from chiral intermediates. *Journal of Chemical Technology and Biotechnology* 2001; **76**(2):123-127.

23. R.Stefan, F.J.Van Staden, H.Y.Aboul-Enein. On-line assay of S-Captopril using an amperometric biosensor/sequential injection system. *Analytica Chimica Acta* 2012; **411**(1-2):51-158.

24. R.Stefan, F.J.Van Staden, H.Y.Aboul-Enein. A new construction for a potentiometric enantioselective membrane electrode - its utelization to the S-Captopril assay. *Talanta* 1999; **48**(5):1139-1143.

25. R.Stefan, F.J.Van Staden, H.Y.Aboul-Enein. Amperometric biosensors: sequential injection analysis system for simulteneous determination of S- and R-captopril. *Biosensors & Bioelectronics* 2000; **15**(1-2):1-5.

26. A.Isab, M.Wazeer. Solid and solution NMR studies of the complexation of Ag+ with the trans isomer of captopril: Biological activities of this high blood pressure drug along with its Ag+ complex. *Spectrochimica Acta Part A: Moleculer and Biomolecular Spectroscopy* 2006; **65**(1):191-195.

27. C.Richer, B.Giroux, P.F.Plouin, B.Maarek, J.F.Giudicelli. Captopril: Pharmacokinetics, antihypertensive and biological effects in hypertensive patints. *British Journal of Clinical Pharmacology* 1984; **17**(3):243-250.

28. E.Haber, T.Koerner, L.Page, B.KLiman, A.Purnode. Application of Radioimmunoassay for Angiotensin I to the Physiologic Measurements of Plasma Renin Activity in Normal Human Subjects. *The Journal of Clinical Endocrinology and Metabolism* 1969; **29**(10):1349-1355.

29. P.J.Wysocki, E.P.Kwiatkowaski, U.Kazimierczak. Captopril: An Angiotensin-Converting Enzyme Inhibitor, Promotes Growth of Immunogenic Tumors in Mice. *Clinacal Cancer Research* 2006; **12**(13):4095-4102.

30. M.Harrold. Angiotensin-Converting Enzyme Inhibitors; Angiotensin Antagonist and Calcium Channel Blockers. In: T.Lumke (editor): *Foye's Principles of Medicinal Chemistry*. Philadelphia: Williams & Wilkins; 2007, pp. 739-769.

31. P.R.Ribeiro, A.O.Santini, H.R.Pezza, L.Pezza. Potentiometric determination of captopril in pharmaceutical formulations. *Eclética Química* 2003; **28**(1):33-44.

32. Y.Huang, Y.Cheng, K.Alexander, D.Dollimore. The thermal analysis study of the drug captopril. *Thermochemica Acta* 2001; **367-368**:43-58.

33. R.M.Silverstein, F.X.Webster, D.Kiemle. Infrared Spectrometry. *Spectrometric Identification of Organic Compounds*. New York: Wiley and Sons,Inc; 2005, pp. 58-67.

34. *United States Pharmacopoea - National Formulary [USP-29/NF-24]*. The United States Pharmacopoeial Convention.Inc.; 2006.**29** (1) pp109-110

35. A.Ortiz, O.Arellano, E.Sansinenea, E.Bernes. Steroselective Crystallization as a Key Step for the Synthesis of New Epimers of Captopril Derivatives. *Journal of Mexican Chemical Society* 2007; **51**(4):245-258.

36. M.M.Hefnawy, M.A.Sultan, M.M.Al-Shehri. Direct Enantiomeric Resolution of Betaxolol with Application to Analysis of Pharamaceutical Products. In: H.Y.Aboul-Enein, I.W.Wainer (editors): *The Impact of Stereochemistrybon Drug Development and Use*. New York: John Wiley & Sons Inc.; 1997, pp. 1-19.

37. D.Nam, C.S.Lee, D.D.Ryu. An improved synthesis of captopril. *Journal of Pharmaceutical Sciences* 1984; **73**(12):1834-1844.

38. M.P.Feltrin, W.P.Almeida. A Synthesis of Captopril Through a Baylis-Hillman Reaction. *Synthetic communications: An International Journal for Rapid Communications of Synthetic Organic Chemistry* 2003; **33**(7):1141-1146.

39. C.H.Kim, W.K.Hong, I.Y.Lee, E.S.Choi, S.K.Rhee. Enhanced production of D-β− hydroxyisobutyric acid through strain improvement. *Journal of Biotechnology* 1999; **69**(1):75-79.

40. D.Seong, W.Paik, S.Baek. Strain development for the production of D-(-)-β− hydroxyisobutyric acid. *Biotechnology and Bioprocess Engineering* 1997; **2**(1):23-26.

41. P.Timmins, I.Jackson, Y.Wang. Factors affecting captopril stabilty in aqueous solution. *International Journal of Pharmaceutics* 1982; **11**(4):329-336.

42. S.A.Atlas. The Renin-Aldosterone Aldosterone System:Pathophysiologica; Role and Pharmacologic Inhibition. *Supplement to Journal of Managed Care Pharmacy* 2007; **13**(8):s9-s20.

43. C.J.Gibbon. Agents acting on the Renin-Angiotensin Sysytem. In: C.J.Gibbon (editor): *South African Medicine Formulary*. Cape Town: FA Print; 2010, pp. 159-161.

44. U.Brewster, M.Perrazella. Cardiorenal effects of the Renin-Aldosterone Angiotensin System. *Hospital Physicians* 2004; **40**:11-20.

45. F.N.Withrow, P.Dawson. Marked bradykinin-induced tissue plasminogen activator release in patients with heart failure maintained on long term angiotensin- converting enzyme inhibitor therapy. *Journal of the American College of Cardiologist* 2002; **40**(5):961-966.

46. J.J.Brugts, R.Ferrari, M.L.Simoons. Angiotensin-converting enzyme inhibition by Perindopril in the treatment of cardiovascular disease. *Expert Review of Cardiovascular Therapy* 2009; **7**(4):345-360.

47. E.J.Lewis, L.G.Hunsicker. The Effect of Angiotensin- Converting Enzyme Inhibition on Diabetic Nephropathy. *The New Engaland Journal of Medicine* 1993; **329**(20):1456-1462.

48. R.D.Minshall, S.J.Nedumgottil, R.Igic, S.F.Rabito. Potentiation of the effects of bradykinin on its receptor in the isolated guinea pig ileum. *Peptides* 2000; **21**(8):1257-1264.

49. A.B.Artkinson. Captopril and Hypertension. *Journal of the Royal Society of Medicine* 1981; **74**(8):636-637.

50. P.M.Mehta, K.Przyklenk, R.Kloner. Cardioprotective effects of captopril in myocardial ischaemia, ischaemia/reperfusion and infarction. *European Heart Journal (Suppliment B)* 1990; **11**:94-99.

51. M.A.Pfeffer, J.McMurray, E.J.Velazquez, J.L.Rulea, L.Kober, A.P.Maggioni. Valsatan, Captopril or both in Myocardial Infaction Complicated by Heart failure, Left Ventricular Dysfunction or Both. *The New Engaland Journal of Medicine* 2003; **349**(20):1893-1906.

52. L.D.Elving, J.F.Wetzels, E.De Nobel, A.J.Hoitsma, J.H.Berden. Captopril acutely lowers albuminuria in normotensive patients with diabetic nephropathy. *American Journal of Kidney Diseases* 1992; **20**(6):559-563.

53. W.L.Augenstein, K.Kulig, B.Rumack. Captopril Overdose Resulting in Hypotension. *Journal of the American Medical Association* 1988; **259**(22):3302-3305.

54. Application for inclusion of Captopril (Paediatrics). 17th Expert Committee on the Selection and Use of Essential Medicines. 17th Expert Committee on the Selection and Use of Essential Medicines , 1-7. 3-31-2009. Geneva, World Health Organisation.

55. A.Haywood, B.D.Glass. Liquid dosage forms extemporeneous prepared from commercially available products - considering new evidence on stability. *Journal of Pharmacy and Pharmaceutical Sciences* 2013; **16**(3):441-455.

56. S.L.Baker. A study of the use of Captopril in elderly hypertensive patients. *Age Ageing* 1988; **17**(1):17-20.

57. K.L.Duchin, S.M.Singhvi, D.A.Willard, B.H.Migdalof, D.N.McKinsty. Captopril Kinetics. *Clinical Pharmacology and Therapeutics* 1982; **31**(4):452-458.

58. O.H.Drummer, P.J.Worland, B.Jarrott. Tissue distribution of captopril, reducible captopril congugates and S-methylcaptopril in the rat. *Biochemical Pharmacology* 1983; **32**(10):1563-1568.

59. F.Zuninga, D.Loi, K.Ling, D.Tang-Liu. Idiosyncratic reactions and metabolism of sulphur- containing drugs. *Expert Opinion on Drug Metabolism & Toxicology* 2012; **8**(4):467-468.

60. S.Tiwari, N.Batra. Oral drug delivery system: A review. *American Journal of Life Sciences Research* 2014; **2**(1):27-35.

61. M.Amini, A.Zargi, H.Vatanpour. Sensetive high performance liquid chromatographic method for the determination of catopril in plasma. *Pharmaceutica Acta Helveticae* 1999; **73**(6):303-306.

62. T.Mirza, H.Tan. Determination of captopril in pharmaceutical tablets by anion-exchange HPLC using indirect photometric detection: A study in the systematic method development. *Journal of Pharmaceutics and Biomedical Analysis* 2001; **25**(1):39-52.

63. T.Ito, Y.Matsuki, H.Kurihara, T.Nambara. Sensetive method in the determination of captopril in biological fluids by gas chromatography-mass spectrometry. *Journal of Chromatography* 1987; **417**(1):79-87.

64. Y.Matsuki, K.Fukuhara, T.Ito, H.Ono, T.Yui. Determination of captopril in biological fluids by gas-liquid chromatography. *Journal of Chromatography* 2012; **188**(1):177-183.

65. O.H.Drummer, B.Jarrott, W.J.Louis. Combined gas chromatography-mass spectrometric procedure for the measurement of captopril and sulfur-congugated metabolites of captopril in plasma and urine. *Journal of Chromatography* 2012; **305**(1):83-93.

66. Z.Chik, A.M.Mustafa, Z.Mohamed, T.C.Lee. Analysis of captopril in human plasma using gas chromatography-mass spectrometry (GCMS) with solid-phase extraction (SPE). *Current Analytical Chemistry* 2012; **6**(4):329-333.

67. S.Vancea, S.Imre, G.Donath-Nagy, T.Bela, M.Nyulas, T.Muntean. Determination of free captopril in human plasma by liquid chromatography with mass spectrometry detection. *Talanta* 2012; **79**(2):436-441.

68. G.Lawson, H.Mulla, S.Tanna. Captopril determination in dried blood spot samples with LC-MS and LC-HRMS: A potential method for neonate pharmacokinetic studies. *Journal of Bioanalysis and Biomedicine* 2012; **4**(2):16-25.

69. F.R.Mansour, N.D.Danielson. Separation methods for captopril in pharmaceuticals and biological fluids. *Journal of Separation Science* 2012; **35**(10-11):1213-1226.

70. S.Hillaert, W.Van Den Bossche. Determination of captopril and its degradation products by capillary electrophoresis. *Journal of Pharmaceutics and Biomedical Analysis* 1999; **21**(1):65-73.

71. N.Rahman, M.Sigh, M.N.Hoda. Validation of simulteneous volumetric and spectrometric methods for the determination of captopril in pharmaceutical formulations. *Farmaco* 2012; **60**(6-7):569-574.

72. P.R.Ribeiro, L.Pezza, H.R.Pezza. A simple spectrophotometric method for the determination of captopril in pharmaceutical preparations using Ammonium Molybdate. *Eclética Química* 2010; **35**(3):179-188.

73. N.Sultana, M.S.Arayneb, S.Naveed. Simultaneous determination of captopril and statins in API, pharmaceutical formulations and in human serum by RP-HPLC. *Journal of the Chinese Chemical Society* 2010; **57**(3):378-383.

74. K.Czerwin'ska, E.Wyszomirska, T.Kaniewska. Identification and determination of selected medicines reducing hypertension by densitometric and gas chromatographic methods. *Acta Poloniae Pharmaceutica* 2001; **58**(5):331-318.

75. K.Kus'mierek, E.Bald. A simple liquid chromatography method for the determination of captopril in urine. *Chromatographia* 2012; **66**(1-2):71-74.

76. The ultimate guide to HPLC/UHPLC reversed phase selectivity. 2011. 5-6-2011.http://www.phenomenex.com/Info/WebDocumentServe/reversedguide.pdf accessed on 05/06/2011.

77. G.Lunn, N.R.Schumuff. *HPLC methods for pharmaceutical analysis.* New York: Wiley Interscience; 1999.

78. *Giudance for Industry: Bioanalytical Method Validation.* Food and Drug Administration. 2001. Center for Drug Evaluation and Research (CDRER). Rockville, US Department of Health and Human Services: 1-12. 2001.

s 79. *Guidance: Validation of Chromatographic Methods.* Center for Drug Evaluation and Research (CDER). Food and Drug Administration. 1994. Rockville: 1- 12. 1994.

80. S.M.Khamanga, R.B.Walker. The use of experimental design in the development of an HPLC-ECD method for the analysis of captopril. *Talanta* 2011; **83**(3):1037-1049.

81. L.Synder, J.Kirkland. *Introduction to modern liquid chromatography*. New York: John Wiley & Sons Inc., 2009.

82. R.J.Hamilton, P.A.Sewell. *Introduction to high performance liquid chromatography*. London: Chapman and Hill; 1982.

83. A.De Villers, F.Lestremau, R.Szucs, S.Gelabart. Evaluation of ultra-performance liquid chromatography: Part I. Possibilitiesand limitations. *Journal of Chromatography A* 2006; **1127**(1-2):60-69.

84. J.Mendham, R.C.Denney, J.Bessett, G.H.Jeffery. *Vogels Textbook of Quantitative Chemical Analysis*. Boston: Addison Wesley Publications; 2000.

85. L.C.Tan, P.W.Carr. Study of retention in reversed-phase liquid chromatography using linear solvation energy relationships: II. The mobile phase. *Journal of Chromatography A* 1998; **799**(1-2):1-19.

86. K.A.Dill. The mechanism of solute retention in reversed-phase liquid chromatography. *The Journal of Physical Chemistry* 1987; **91**(7):1980-1988.

87. Y.Kazakevick. High-performance liquid chromatography retension mechanism and their mathematical descriptions. *Journal of Chromatography A* 2006; **1126**(1-2):232-243.

88. F.Gritti, G.Guiochon. Critical contribution of nonlinear chromatography to the understanding of retention mechanism in reversed-phase liquid chromatography. *Journal of Chromatography A* 2005; **1099**(1-2):1-42.

89. T.H.Dzido, T.E.Kossowski, D.Matosiuk. Comparison of retension of aromatic hydrocarbons with polar groups in binary reversed-phase high performance liquid chromatography systems. *Journal of Chromatography A* 2002; **974**(2):167-183.

90. M.Jaroniec. Partition and displacement models in reversed-phase liquid chromatography with mixed eluents. *Journal of Chromatography A* 1993; **656**(1-2):37-50.

91. B.Nikolin, B.Imamovi, S.Medanhodzic-Vuk, M.Sober. High performance liquid chromatography in pharmaceutical analysis. *Bosnian Journal of Basic Medical Sciences* 2004; **4**(2):5-9.

92. A.Mendez, E.Bosch, M.Roses, U.Neune. Comparison of the acidity of residual silanol groups in several liquid chromatography columns. *Journal of Chromatography A* 2012; **986**(1):33-44.

93. P.R.Ribeiro, A.O.Santini, H.R.Pezza, L.Pezza. Potentiometric determination of captopril in pharmaceutical formulations. *Eclética Química* 2003; **28**(1):33-44.

94. Phenomenex® columns. 2012. 3-8-2012.http://www.phenomenex.com/Products/Part/00G-4252-E0 accessed on 03/08/2012.

95. H.A.Classens. Characterization of stationary phase for reversed-phase liquid chromatography: column testing, classification and chemical stability. 7-27. 1999. Eindhoven, Technische Universiteit Eindhoven.

96. H.Stulzer, M.Tagliari, G.Kuminek, P.Oliveira, C.Betrol, M.Silva. Development and validation of stability indicating LC method to quantify captopril in tablets of controlled release. *Chromatographia* 2010; **69**(Suppliment 2):123-128.

97. R.Bonfilio, M.B.De Araujo, H.R.N.Salgado. Recent applications of analytical techniques for quantitaive pharmaceutical analysis: A review. *WSEAS Transactions on Biology and Biomedicine* 2012; **7**(4):316-318.

98. J.McDay. Ecological method development for the detecting of Nitrosodimeethylaminein water using HPLC PDAD. 7-35. 2010. Michigan. USA, Eastern Michigan University.

99. I.Panderi, M.Parissi-Poulou. Determination of captopril and captopril-hydrochlorothiazide combination in tablets by derivative UV spectrophotometry. *International Journal of Pharmaceutics* 1992; **86**(2-3):99-106.

100. S.Perlman, J.Kirschbaum. High-Performance liquid chromatographic analyses of the antihypertensive drug captopril. *Journal of Chromatography A* 1981; **206**(2):311-317.

101. S.Denton, T.De Angelis, A.Yaccynch, W.Heineman, T.Gilbert. Oscillating mirror rapid scanning ultraviolet-visible cpectrometer as a detector for liquid chromatography. *Analytical Chemistry* 1976; **48**(1):20-24.

102. M.A.Milford. Waters® 2996 PDA Detector: Operator's guide. 1-124. 1996. Waters®. 5-6-2012.www.waters.com/webassets/cms/support/docs/71500023202rc.pdf accessed on 05/06/2012.

103. G.Shabir. Validation of high-performance liquid chromatography methods for pharmaceutical analysis: Understanding the differences and similarities between validation requirements of the US FDA, the US Pharmacopoeia and the International Conference on Harmonization. *Journal of Chromatography A* 2003; **987**(1-2):57-66.

104. D.Ivanovic, M.Medenica, A.Melanovic, B.Jancic. Validation of the RP-HPLC method for the ananlysis of hydrochlorothiazide and captopril in tablets. *Accreditation and Quality Assurance* 2004; **9**(1-2):76-81.

105. T.Jovanovic', B.Stanovic, Z.Koric'anac. Spectrophotometric investigation on complex fornmation of captopril with palladium (II) and its analytical application. *Journal of Pharmaceutical and Biomedical Analysis* 1995; **13**(3):213-217.

106. M.C.Ortiz, L.A.Sarabia. Response surface methodology. In: S.D.Brown, R.Tauler, B.Walczak (editors): *Comprehensive Chemometrics: Chemical and Biochemical Data Analysis*. Oxford: Elsevier; 2009, pp. 345-390.

107. M.Bezerra, R.Santelli, E.Oliveira, L.Villar, L.Escaleira. Response surface methodology (RSM) as atool for optimization in analytical chemistry. *Talanta* 2008; **76**(5):965-977.

108. P.Luliani, G.Carlucci, A.Marrone. Investigation of the HPLC response of NSAIDs by functional experimental design and multivariate regression analysis. Response optimization and new retention parameters. *Journal of Pharmaceutical and Biomedical Analysis* 2010; **51**(1):46-55.

109. S.P.Jones. Stability and response surface methodology. In: M.Hendricks, J.de Boer, A.K.Smilde (editors): *Robustness of analytica chemical methods and pharmaceutical technological products.*; 1996, pp. 11-77.

110. P.Hashemi, F.Raeisi, A.Ghiasvand, A.Rahimi. Reversed-phase dispersive liquid-liquid microextraction with central composite design oprimization for preconcentration and HPLC determination of oleuropein. *Talanta* 2012; **80**(5):1926-1931.

111. P.Barmpalexis, F.Kanase, E.Georgarakis. Developing and optimizing a validated isocratic reversed-phase high performance liquid chromatography separation of nimodipine and impurities in tablets using experimental design methodology. *Journal of Pharmaceutics and Biomedical Analysis* 2009; **49**(5):1192-1202.

112. W.Lough, I.Wainer. *High performance liquid chromatography: Fundamental principles and practice.* United Kingdom: Chapman and Hill; 1996.

113. *Guidance for Industry: Validation of Analytical Procedures and Methodology. Topic Q2B.* Center for Drug Evaluation and Research (CDER). Food and Drug Administration.1996. Rockville: 1-8. 1996.

114. *The European Medicines Agency, ICH Topic Q2 (R1). Validation of Analytical Procedures: Text and Methodology [CPMP/ICH/381/95]*.1995. London: 1-12. 1995.

115. *International Conference on Harmonizaton (ICH) of Technical Requirements for the registration of Pharmaceuticals for human use. Guidelines for Industry Q2A - Text on Validation of Analytical Procedures.* 1995. London: 1-10. 1995.

116. C.Chan, H.Lam, Y.Lee, X.Zhang. *Analytical Method and Validation of Instrument Performance Verification.* New York: John Wiley & Sons Inc., 2004.

117. D.Jenke. Chromatographic method validation: A review of current practices and procedures. 1. General concepts and guidelines. *Instrumentation Science and Technology* 1997; **25**(4):345-359.

118. J.Green. A practical guide to analytical method validation. *Analytical Chemistry* 1996; **68**(9):305A-309A.

119. T.Piano, A.Moore. Determination of LOD and LOQ of an HPLC method using four different techniques. *Pharmaceutical Technology* 1999; **23**(10):86-90.

120. A.I.Khalif. Photochemistry and free radical stabilization of the captodative centre. *Trends in Photochemistry and Photobiology* 2010; **12**:7-15.

121. S.Yoshioka, V.Stella. Chemical stability of drug substances. In: S.Yoshioka, V.Stella (editors): *Stability of Drugs and Dosage Forms.* New York: Kluwer Academic Publishers; 2002, pp. 3-138.

122. S.Ahmed, M.Rizk, F.Belal, F.Ibrahim, A.Sheribah. Stability-Indicating HPLC method for captopril through pre-column derivatization with Pd (II). *Journal of Liquid Chromatography and Related Technologies* 2006; **29**(4):521-532.

123. T.Hu, T.Chou. The Kinetics of Thiol-mediated decomposition of S-Nitrosothiols. *Journal of the American Association of Pharmaceutical Scientists* 2006; **8**(3):E485-E492.

124. M.Bhakshi, S.Singh. Development of validated stability-indicating assay methods: A Critical review. *Journal of Pharmaceutical and Biomedical Analysis* 2002; **28**(6):1011-1040.

125. S.S.Bharate, S.B.Bharate, A.N.Bajaj. Interactions and incompatibilities of pharmaceutical excipients with active pharmaceutical ingredients: A comprehensive review. *Journal of Excipients and Food Chemistry* 2010; **1**(3):3-26.

126. G.Steele, T.Austin. Preformulation investigations using small amounts of compound as an aid to candidate drug selection and early development. In: M.Gibson (editor): *Pharmaceutical Preformulation and Formulations: A practical guide from candidate drug selection to commercial dosage form.* New York: Informa Healthcare; 2009, pp. 17-129.

127. B.Lee. Pharmaceutical preformulation: Physicochemical properties of excipients and powders and tablet characterisation. In: S.C.Gad (editor): *Pharmaceutical Manufacturing Handbook: Production and Process.* New Jersey: John Wiley & Sons Inc., 2008, pp. 881-932.

128. G.Steele. Preformulation as an aid to product design in early drug development. In: M.Gibson (editor): *Pharmaceutical Preformulation and Formulations: A practical guide from candidate drug selection to commercial dosage forms.* New York: Informa Healthcare; 2009, pp. 188-246.

129. B.Bataille, A.Amourdedieu, D.Sonanglio, A.Terol, G.Cassanas, M.Jacob. Preformulation in extrusion-spheronisation: Behavioural study of two Microcel(R) cellulose grades. *Pharmazie* 2014; **52**(2):138-144.

130. S.K.Singh, S.Singh, N.R.Seth, Y.V.Ushir, R.Patel, A.Singh. Design, development and evaluationof domperidone pellets. *International Journal of Pharmaceutical Technology Reseach* 2009; **1**(3):885-891.

131. A. Kumar, P. Prathap, P.Venketeswararao, A. Babu, R. Babu, M. Shanthi. Development of itraconazole immediate release pellets by using HPMC loaded gelatin capsules. *International Journal of Biological & Pharmaceutical Research* 2012; **3**(7):904-910.

132. D. Huck. Particle shape - an important parameter in pharmaceutical manufacturing. Malvern Instruments Ltd. 2012. Worcestershire, UK, Malvern Instruments Ltd, Egnima Business Park. 12-4-2012.

133. Guidance for Industry: *PAT - A framework for innovative pharmaceutical development, manufacturing and quality assuarance.* Food and Drug Administration.2004: p 1-19. 2004.

134. J.Staniforth. Powder flow. In: M.E.Aulton (editor): *Pharmaceutics the science of dosage form design.* London: Churchill Livingstone; 2002, pp. 197-210.

135. H.G.Kristensen, T.Schaefer. Granulation: A review on pharmaceutical wet granulation. *Drug Development and Industrial Pharmacy* 1987; **13**(4-5):803-873.

136. A.Bodhmage. Correlation between physical properties and flowability indicators for fine powders. 8-49. 2006. Canada, University of Saskatchewan.

137. R.C.Rowe. Spheronisation: A novel pill making process. *Pharmaceutical International* 1985; **6**:119-123.

138. J.M.Newton. Extrusion and extruders. In: J.Shabrick, J.C.Boylans (editors): *Encyclopedia of pharmaceutical technology.* New York: Marcel Dekker Inc., 2002, pp. 1220-1236.

139. R.D.Shah, M.Kabadi, D.G.Pope, L.Augsburger. Physicomechanical characterisation of the extrusion-spheronisation process. 2. Rheological determinants for the successful extrusion and spheronisation. *Pharmaceutical Research* 1995; **12**(4):496-504.

140. K.E.Fielden, J.M.Newton. Movement of liquid through powder beds. *International Journal of Pharmaceutics* 1992; **79**(1-3):47-60.

141. K.E.Fielden, J.M.Newton, P.O'Brien, R.C.Rowe. Thermal studies on the interaction of water and microcrystalline cellulose. *Journal of Pharmacy and Pharmacology* 1988; **40**(10):674-678.

142. P.Kleinebudde. The crystallite-gel-model for microcrystalline cellulose in wet-granulation, extrusion and spheronisation. *Pharmaceutical Research* 1997; **14**(6):804-809.

143. K.Jess, H.Steckel. The extrusion and spheronisation of chitosan. *Pharmaceutical Technology* 2007; **19**(7):21-30.

144. J.J.Sousa, A.Sousa, F.Podczeck, J.M.Newton. Factors influencing the physical characteristics of pellets obtained by extrusion-spheronisation. *International Journal of Pharmaceutics* 2002; **232**(1-2):91-106.

145. J.J.Sousa, A.Sousa, M.J.Moura, F.Podczeck, J.M.Newton. The influence of core materials and film coating on the drug release from coated pellets. *International Journal of Pharmaceutics* 2002; **233**(1-2):111-122.

146. *Handbook of Pharmaceutical excipients*. London: Pharmaceutical Press; 2009.

147. J.Siepmann, H.Kranz, R.Bodmeier, N.A.Peppas. HPMC-matrices for the controlled drug delivery: A new model for combining diffusion, swelling and dissolution mechanisms and predicting the release kinetics. *Pharmaceutical Research* 1999; **16**(11):1748-1755.

148. P.Kleinebudde. Shrinking and swelling properties of pellets containing microcrystalline cellulose and low substituted hydroxypropylcellulose: I. Shrinking properties. *International Journal of Pharmaceutics* 1994; **109**(3):209-219.

149. P.Kleinebudde. Shrinking and swelling properties of pellets containing microcrystalline cellulose and low substituted hydroxypropylcellulose: II. Swelling properties. *International Journal of Pharmaceutics* 1994; **109**(3):221-227.

150. J.Siepmann. Mathematical modeling of controlled drug delivery based on hydroxypropyl methyl cellulose (HPMC). *Advanced Drug Delivery Reviews* 2001; **48**:139-157.

151. J.Siepmann, N.A.Peppas. Modeling of drug release from delivery systems based on hydroxypropyl methylcellulose (HPMC). *Advanced Drug Delivery Reviews* 2001; **48**(2-3):139-157.

152. M.R.Abbaspour, F.Sadeghi, H.Garekani. Preparation and characterisation of ibuprofen pellets based on Eudragit® RS PO and RL PO or their combination. *International Journal of Pharmaceutics* 2005; **303**(1-2):88-94.

153. S.C.Porter. Controlled release film coatings based on ethylcellulose. *Drug Development and Industrial Pharmacy* 1989; **15**(10):1495-1521.

154. A.G.Ozturk, S.S.Ozturk, B.O.Palsson, T.A.Wheatley, J.B.Dressman. Mechanism of release from pellets coated with an ethylcellulose-based film.*Journal of Controlled Release* 1990; **14**(3):203-213.

155. R.Bodmeier, O.Paeratakul. Process and formulation variables affecting the drug release from chlorpheniramine maleate-loaded beads coated with commercialand self aqueous ethyl cellulose pseudolatexes. *International Journal of Pharmaceutics* 1991; **70**(1-2):59-68.

156. F.Siepmann, A.Hoffman, B.Leclercq, B.Carlin, J.Siepmann. How to adjust desired drug release patterns from ethylcellulose-coated dosage forms. *Journal of Controlled Release* 2007; **119**(2):182-189.

157. R.K.Chang, C.H.Hisiao, J.R.Robinson. Review of aqueous coating techniques and preliminary data on release from a theophylline product. *Pharmaceutical Technology* 1987; **11**(3):56-68.

158. R.Bodmeier, O.Paeratakul. Mechanical properties of drug and wet cellulosic and acrylic polymer films prepared from aqueous colloidal polymer dispersions. *Pharmaceutical Research* 1994; **11**(6):882-888.

159. R.Bodmeier. Tableting of coated pellets. *European Journal of Pharmaceutics and Biopharmaceutics* 1997; **43**(1):1-8.

160. J.Wang, J.Hemenway, W.Chen, D.Desai, W.Early, S.Paruchuri. An evaluation of process parameters to improve coating efficiency of an active tablet film-coating process. *International Journal of Pharmaceutics* 2012; **427**(2):163-169.

161. F.Sadeghi, J.L.Ford, A.Rajabi-Siahboomi. The influence of drug type on the release profiles from Surelease-coated pellets. *International Journal of Pharmaceutics* 2003; **254**(2):123-135.

162. G.Pifferi, P.Santoro, M.Pedrano. Quality and functionality of excipients. *II Farmaco* 1999; **54**(1-2):1-14.

163. J.Burgees, E.Duffy, F.Etzler, A.J.Hickey. Particle size analysis: AAPS workshop report, cosponsored by the Food and Drug Administration and the United States Pharmacopeia. *The American Association of Pharmaceutical Scientist Journal* 2004; **6**(3):23-43.

164. J.J.Fitzpartick, L.Ahme. Food powder handling and processing: Industry problems, knowledge barriers and research opportunities. *Chemical Engineering and Processing: Process Intensification* 2005; **44**(2):209-214.

165. *United States Pharmacopoea-National Formulary [USP-29/NF-24]*. Uniformity of dosage units. Rockville Maryland 31[363].2008: pp375-376. 2008.

166. J.Cain. An alternative technique for determing ANSI/CEMA standard 550 flowability ratings for granular materials. *Powder Handling and Processing* 2002; **14**(3):218-220.

167. R.L.Carr. Evaluating flow properties of solids. *Chemical Engineering* 1965; **72**(2):163-169.

168. T.P.Garcia. Blending and blend uniformity: Rational design and formulation. In: L.Augsburger, S.W.Hoang (editors): *Pharmaceutical dosage forms: Tablets.* New York: Informa Healthcare; 2008, pp. 111-173.

169. *Guidance for Industry ANDAs: Blend uniformiy analysis.*Center for Drug Evaluation and Research (CDER). Food and Drug Administration. Rockville. 1999. pp 1-10. 1999.

170. A.S.El-Hagrasy, H.R.Morris, F.D'amico, R.A.Lodder, J.K.Drennen. Near-Infrared Spectroscopy and Imaging for the Monitoring of Powder Blend Homogeneity. *Journal of Pharmaceutical Sciences* 2001; **90**(9):1298-1307.

171. J.Guentensburger, P.Lamerio, A.Nyhuis, B.O'Connel, S.Tigher. A statistical approach to blend uniformity acceptance criteria. *Drug Development and Industrial Pharmacy* 1996; **22**(11):1055-1061.

172. R.J.Morgan. Thermal characterisation on composites. In: E.A.Turi (editor): *Thermal Characterisation on Polymeric Materials*. New York: Academic Press; 1997, pp. 56-97.

173. D.Giron. Contribution of thermal methods related techniques to the rational development of pharmaceuticals - Part 2. *Pharmaceutical Science & Technology Today* 1998; **1**(6):262-268.

174. R.Cavatur, N.Vemuri, Z.Chezan. Use of Isothermal microcalorimetry in pharmaceutical preformulation studies: Part III. Evaluation of excipient compartibility of new chemical entity. *Journal of Thermal analysis and Calorimetry* 2004; **78**(1):63-73.

175. D.Giron. Applications of themal analysis and coupled techniques in pharmaceutical industry. *Journal of Thermal analysis and Calorimetry* 2002; **68**(2):335-357.

176. *Thermogravimetric Analysis (TGA): A beginner's guide.* PerkinElmer®. Waltham. 2010: pp 1-19. 2010.

177. C.Betrol, A.Cruz, H.Stulzer, F.Murakami, M.Silva. Thermal decomposition kinetics and compatibility studies of primaquine under isothermal and non-isothermal conditions. *Journal of Thermal analysis and Calorimetry* 2010; **102**(1):187-192.

178. S.D.Clas, C.R.Dalton, B.C.Hancock. Differential scanning calorimetry: Applications in drug development. *Pharmaceutical Science & Technology Today* 1999; **2**(8):311-320.

179. P.Mura, M.Faucci, A.Manderioli, G.Bramanti, L.Ceccarelli. Compatibility study between ibuproxam and pharmaceutical excipicients using differential scanning calorimetry, hot-stage microscopy and scanning electron microscopy. *Journal of Pharmaceutical and Biomedical Analysis* 1998; **18**(1-2):151-163.

180. D.Wargo, J.K.Drennen. Near-Infrared spectroscopic characterisation of pharmaceutical powder blends. *Journal of Pharmaceutical and Biomedical Analysis* 1996; **14**(11):1415-1423.

181. R.M.Silverstein, G.C.Bassler. *Infrared spectrometry, in spectrometric identification of organic compounds.* New York: John Wiley & Sons, Inc., 1991.

182. A.F.Rawle. Particle morphology and characterisation in preformulation. In: M.C.Adeyeye, H.G.Brittain (editors): *Preformulation in solid dosage form development.* New York: Informa Healthcare; 2011, pp. 145-184.

183. M.Efentakis, M.Vlachou. Evaluation of high molecular weight poly(oxyethelene) (POLYOX) Polymer : Studies of flow properties release rate of furosemide and captopril from controlled release hard gelatin capsules. *Pharmacetical Development Technology* 2000; **5**(3):339-346.

184. J.Berman, D.E.Elinsiki, C.R.Gonzales, J.D.Hofer. Blend uniformity analysis: Validation and in-process testing. Technical report No 25.PDA. *PDA Journal of Pharmaceutical Sciences and Technology* 1997; **51**(Supplementary 3: i-iii):S1-S99.

185. H.Stulzer, P.Rodriques, T.Cardiso, J.Matos, M.Silva. Compatibility studies between Captopril and pharmaceutical excipients used in tablets formulations. *Journal of Thermal Analysis and Calorimetry* 2008; **91**(1):323-328.

186. S.M.Khamanga, R.B.Walker. Evaluation of rate of swelling and erosion of verapamil (VRP) sustained release matrix tablets. *Drug Development and Industrial Pharmacy* 2006; **32**(10):1139-1148.

187. S.A.Elkheshem. Interaction of verapamil hydrochloride with Carbopol® 934P and its effect on the release rate of the drug and water uptake of the polymer matrix. *Drug Development and Industrial Pharmacy* 2001; **27**(9):925-934.

188. D.E.Bugay. Characterisation of the solid-state: 2. Spectroscopic techniques. *Advanced Drug Delivery Reviews* 2001; **48**(1):43-65.

189. Y.Qui, G.Zhang. Research and development aspects of oral controlled release systems. In: D.L.Wise (editor): *Handbook of pharmaceutical controlled release technology*. New York: Marcel Dekker Inc., 2000, pp. 465-503.

190. Y.Qui. Rational design of oral modified-release drug delivery systems. In: Y.Qui, G.Zhang, L.Lui, W.R.Porler (editors): *Developing solid oral dosage forms: Pharmaceutical theory and practice*. San Diego: Academic Press; 2009, pp. 469-499.

191. J.Chatchawalsaisin, F.Podczeck, J.M.Newton. The preparation by extrusion/spheronisation and the properties of pellets containing drugs, microcrystalline cellulose and glyceryl monostearate. *European Journal of Pharmaceutical Sciences* 2005; **24**(1):35-48.

192. D.Blanque, H.Sternagel, F.Podczeck, J.M.Newton. Some factors influencing the formation and in vitro drug release from matrix pellets prepared by extrusion/spheronisation. *International Journal of Pharmaceutics* 1995; **119**(2):203-211.

193. B.Abramsson, A.Ungell. Biopharmaceutical support in formulation development. In: M.Gibson (editor): *Pharmaceutical Preformulation and Formulation: A Practical Guide from Candidate Drug Selection to Commercial Dosage Form*. New York: Informa Healthcare; 2009, pp. 247-288.

194. I.Ghebre-Sellassie. Pellets: A general overview. In: I.Ghebre-Sellassie (editor): *Pharmaceutical pelletization Technology.* New York: Marcel Dekker Inc., 1989, pp. 1-14.

195. J.Kramer, H.Blume. Biopharmaceutical aspects of multiparticulates. In: I.Ghebre-Sellassie (editor): *Multiparticualte oral drug delivery.* New York: Marcel Dekker Inc., 1994, pp. 307-332.

196. M.K.Vuppala, D.M.Parikh, H.R.Bhagat. Application of powder-layering technology and film coating for manufacture of sustained-release pellets using a rotary fluid bed processor. *Drug Development and Industrial Pharmacy* 1997; **23**(7):687-694.

197. J.Vertommen, R.Kinget. The influence of five selected processing and formulation variables on the particle size , particle size distribution and friability of pellets produced by a rotary processor. *Drug Development and Industrial Pharmacy* 1997; **23**(1):39-46.

198. S.Watano, E.Shimoda, Y.Osako. Measurement of physical strength of pharmaceutical extruded pellets. *Chemical and Pharmaceutical Bulletin (Tokyo)* 2002; **50**(1):26-30.

199. D.F.Erkoboni. Extrusion-Spheronisation as a granulation technique. In: D.M.Parikh (editor): *Handbook of pharmaceutical granulation technology.* New York: Marcel Dekker Inc., 1997, pp. 333-365.

200. J.Siepmann, A.Streubel, N.A.Peppas. Understanding and predicting drug release from the hydrophilic matrix tablets using "Sequential Layer" model. *Pharmaceutical Research* 2002; **19**(3):306-314.

201. H.Rashid, J.Heinamaki, O.Antikainen, J.Yliruusi. Influence of the centrifugal granulating process on the properties of layered pellets. *European Journal of Pharmaceutics and Biopharmaceutics* 2001; **51**(3):227-234.

202. H.Kanbe, T.Hayashi, Y.Onuki, T.Sonobe. Manufacture of fine spherical granules by an extrusion/spheronisation method. *International Journal of Pharmaceutics* 2007; **337**(1-2):56-62.

203. M.Thommes, P.Kleinebudde. Properties of pellets manufactured by wet extrusion/spheronisation process using ê-Carrageenan: Effect of process parameters. *American Association of Pharmaceutical Sciences* 2007; **8**(4):E1-E8.

204. R.D.Shah, M.Kabadi, D.G.Pope, L.Augsburger. Physicomechanical characterization of the extrusion-spheronisation process. 2. Rheological determinants for the successful extrusion and spheronisation. *Pharmaceutical Research* 1995; **12**(4):496-504.

205. R.E.O'Conner, J.B.Schwartz. Extrusion and spheronisation technology. In: I.Ghebre-Sellassie (editor): *Pharmaceutical Pelletization Technology*. New York: Marcel Dekker Inc., 1989, pp. 187-215.

206. A.D.Reynolds. A new technique for the production of spherical particles. *Manufacturing Chemist and Aerosol News* 1970; **41**(1):40-43.

207. F.Baert, J.Remon, D.Massart. Correlation of extrusion forces, raw materials and sphere characteristics. *Journal of Pharmacy and Pharmacology* 1992; **44**(8):676-684.

208. P.Linkson, J.Glostonbury. The mechanism of granule growth in wet pelletizing. *Transactions of the Instituition of Chemical Engineers* 1973; **51**:251-259.

209. K.Sastry, D.Fuerstenau. Mechanism of agglomerates growth in green pelletization. *Powder Technology* 1973; **7**(2):97-105.

210. V.P.Mehrotra, K.Sastry. Moisture requirements and role of ash and microporosity in pelletization of coal fines. *Powder Technology* 1986; **47**(1):51-59.

211. H.Leuenburger, G.Imanidis. Monitoring of mass transfer processes to control moist agglomeration. *Pharmaceutical Technology* 1986; **3**:56-73.

212. S.Srivastaval, G.Mirshra. Fluid bed technology: Overview and parameters for process selection. *International Journal of Pharmaceutical Sciences and Drug Research* 2010; **2**(4):236-246.

213. D.E.Würster. Air-suspension technique of coating drug particles. *Journal of the American Pharmacist Association* 1959; **XLVIII**(8):451-454.

214. F.N.Christensen, P.Bertelsen. Qualitative description of the Würster-based fluid bed coating process. *Drug Development and Industrial Pharmacy* 1997; **23**(5):451-463.

215. J.Swarbrick, J.C.Boylans. Fluid bed dryer, granulator and coaters. In: J.Shabrick (editor): *Encyclopedia of pharmaceutical technology.* New York: Marcel Dekker Inc., 1992, pp. 171-173.

216. M.Wesseling, R.Bodmeier. Drug release from beads coated with an aqueous colloidal ethylcellulose dispersion, Aquacoat®, or an organic ethylcellulose solution. *European Journal of Pharmaceutics and Biopharmaceutics* 1999; **47**(1):33-38.

217. R.O.Williams, J.Lui. Influence of processing and curing conditions on beads coated with an aqueous dispersion of cellulose acetate pthalate. *European Journal of Pharmaceutics and Biopharmaceutics* 2000; **49**(2):243-252.

218. R.O.Williams, J.N.Brown. Dissolution of Modified-release oral dosage forms. In: A.Palmieri (editor): *Dissolution Theory, Methodology and Testing.* Hockessin: Dissolution Technologies Inc., 2007, pp. 196-231.

219. E.Jorgensen, D.Bhagwat. Development of dissolution tests for oral extended- release products. *Pharmaceutical Science & Technology Today* 1998; **1**(3):128-135.

220. D.C.Montgomery. *Design and analysis of experiments.* New York: John Wiley & Sons Inc., 2001: 45 -97.

221. M.A.Howard. The application of polyethyleneoxide (PolyOx) and methoxypropylethylene glycol (Carbowax Sentry) in the production of extruded spheronized beads with a high drug load.38-129. 2004. Missouri, Univercity of Missouri-Kansas City.

222. S.V.Sasty, M.A.Khan. Aqueous based polymeric dispersion: Plackett-Burman design for the screenin of formulation variables of Atenolol Gastrointestinal therapeutic system. *Pharmaceutica Acta Helveticae* 1998; **73**(2):105-112.

223. S.R.Shah, R.H.Parikh, J.R.Chavda, N.R.Sheth. Application of Plackett-Berman screening design for preparing glibenclamide nanoparticles for dissolution enhancement. *Powder Technology* 2012; **235**:405-411.

224. R.Gandhi, Y.Ashokraj, C.L.Kaul, R.Panchagnula. Using extrusion-spheronisation to develop: Controlled-release formulations of Azithromycin. *Pharmaceutical Technology* 2005; **29**(1):68-86.

225. G.Khan, J.Zhu. Ibuprofen release kinetics from controlled-release tablets granulated with aqueous polymeric dispersion of ethylcellulose. II. Influence of several parameters and coexcipients. *Journal of Controlled Release* 1998; **56**(1-3):127-134.

226. K.E.Uhrich, S.M.Canizzaro, R.S.Langer, K.M.Shakesheff. Polymeric systems for controlled drug release.*Chemical Review* 1999; **99**:3181-3198.

227. E.Kaunisto, S.Abrahmsen-Alami, P.Borgquist, A.Larsson, B.Nilsson, A.Axelsson. A mechanistic modelling approach to polymer dissolution using magnetic resonace microimaging. *Journal of Controlled Release* 2010; **147**(2):232-241.

228. N.H.Anderson, M.Bauer, N.Boussac, R.Khan-Malek, P.Munden, M.Sardaro. An evaluation of the fit factors and dissolution efficiency for the comparison of *in-vitro* disssolution profiles. *Journal of Pharmaceutical and Biomedical Analysis* 1998; **17**(4):811-822.

229. T.O`Hara, A.Dunne, J.Butlet, J.Devane. A review of methods used to compare dissolution profile data. *Plasma Sources, Science and Technology* 1998; **1**(5):214-223.

230. T.Bussemer, N.A.Peppas, R.Bodmeier. Time-Dependent mechanical properties of polymeric coatings used in rapturable pulsatile release dosage forms. *Drug Development and Industrial Pharmacy* 2003; **29**(6):623-630.

231. Y.Cuppok, S.Muschert, M.Marucci, J.Hjaertstam, F.Siepman. Drug release mechanisms from Kollicoat SR:Eudragit NE coated pellets.*International Journal of Pharmaceutics* 2011; **409**(1-2):30-37.

232. S.Conti, L.Maggi, L.Segale, E.Ochhoa Machiste, U.Conte, P.Granier, et al. Matrices containing NaCMC and HPMC: 2. Swelling and release mechanism study. *International Journal of Pharmaceutics* 2007; **333**(1):143-151.

233. M.Grassi, L.Zema, M.Sangalli, A.Maroni, F.Giordano, A.Gazzaniga. Modeling of drug release from partially coated matrices made of a high viscosity HPMC.*International Journal of Pharmaceutics* 2004; **276**(1-2):107-114.

234. J.Siepmann, N.A.Peppas. Hydrophilic matrices for controlled drug delivery: An improved mathematical model to predict the resulting drug release kinetics. *Pharmaceutical Research* 2000; **17**(10):1290-1298.

235. A.Andover, M.Giona, M.Grassi. Analysis of controlled release in disordered structures: A percolation model. *Journal of Membrane Science* 1996; **113**(1):21-30.

236. B.Narasimhan. Mathematical models describing polymer dissolution: consequences for drug delivery.*Advanced Drug Delivery Reviews* 2001; **48**(2):195-210.

237. M.Marucci, J.Hjaertstam, G.Ragnarsson, F.Iselau, A.Axelsson. Coated formulation: new insight into the release mechanism and changes in the film properties with a novel release cell.*Journal of Controlled Release* 2009; **136**(3):206-212.

238. P.Colombo, R.Bettini, P.Santo, A.D.Ascentiis, N.A.Peppas. Analysis of the swelling and release mechanisms from drug delivery systems with emphasis on drug solubility and water transport. *Journal of Controlled Release* 1996; **39**(2):231-237.

239. A.R.Khare, N.A.Peppas. Swelling/deswelling of anionic copolymer gels. *Biomaterials* 1995; **16**(7):559-567.

240. M.Marucci, A.Holmgren, H.Carisson, A.Jarke, A.Johansson, C.von Corswant. Non-Uniformity of pellets coating: Effect on the dose release profile and how to improve

the coating process by reducing the electrostatic charging of pellets. *Chemical and Biochemical Engineering* 2012; **26**(4):379-384.

241. M.Marucci, G.Ragnarsson, B.Nilsson, A.Axelsson. Osmotic pumping release from ethyl-hydroxypropyl-cellulose-coated pellets: a new mechanistic model.*Journal of Controlled Release* 2010; **142**(1):53-60.

242. J.Siepmann, N.A.Peppas. Modelling of drug release from delivery systems based on hydroxypropyl methylcellulose (HPMC). *Advanced Drug Delivery Reviews* 2001; **48**(2-3):139-157.

243. J.C.Chow, F.Y.Ki. Statistical comparison between dissolution profiles of drug products.*Journal of Biopharmaceutical Statistics* 1997; **7**(2):241-258.

244. W.W.Hauk, T.Foster, E.Sheinin, T.Cecil, W.Brown, M.Marques, et al. Oral dosage form performance tests: New dissolution approaches. *Pharmaceutical Research* 2005; **22**(2):182-187.

245. P.Costa. An alternate method to the evaluation of similarity factor in dissolution testing. *International Journal of Pharmaceutics* 2001; **220**(1-2):77-83.

246. P.Costa, J.Lobo. Modelling and comparison of dissolution profiles. *European Journal of Pharmaceutical Sciences* 2001; **13**(2):123-133.

247. M.C.Gohel, M.K.Panchal. Comparison of *in vitro* dissolution profiles using a novel, model independent approach. *Pharmaceutical Technology* 2000; **24**(1):92-101.

248. J.W.Moore, H.H.Flanner. Mathematical comparison of dissolution profiles. *Pharmaceutical Technology* 1996; **20**(6):64-74.

249. *Guidance for industry. Extended release oral dosage forms: Development, evaluation and application of in vitro/in vivo correlations*. U.S Department of Health and Human Services, Food and Drug Administration, Centre for Drug Evaluation and Research (CDER). September. (1997). BP2. 1-27.1997.

250. K.Tahara, Y.Yamamoto, T.Nishihata. Application of model-independent and model analysis for the investigation of the effect of drug solubility on its release rate from hydroxylpropyl methylcelluose sustained release tablets. *International Journal of Pharmaceutics* 1996; **133**(1):17-27.

251. K.A.Khan. The concept of dissolution efficiency. *Journal of Pharmacy and Pharmacology* 1975; **27**(1):48-49.

252. K.C.Khoo, M.Gibaldi, R.K.Brazzell. Comparsion of statistical moment parameters to C_{max} and t_{max} for detecting differences *in- vivo* dissolution rates.*Journal of Pharmaceutical Sciences* 1985; **74**(12):1340-1342.

253. N.Yuksel, A.E.Kanik, T.Baykara. Comparison of *in vitro* dissolution profiles by ANOVA-based model-dependent and independent methods. *International Journal of Pharmaceutics* 2000; **209**(1-2):57-67.

254. J.W.Mauger, D.Chilko, S.Howard. On the analysis of dissolution data. *Drug Development and Industrial Pharmacy* 1986; **12**(7):969-992.

255. K.Baveja, K.V.Ranga Rao, K.Padmalatha Devi. Zero-order release hydrophilic matrix tablets of β-adrenergic blockers. *International Journal of Pharmaceutics* 1987; **39**(1):39-45.

256. M.Gibaldi, S.Feldman. Establishment of sink conditions in dissolution rate determinations-theoretical considerations and applications in to non-disintegrating dosage forms. *Journal of Pharmaceutical Sciences* 1967; **56**(10):1238-1242.

257. T.Higuchi. Mechanism of sustained-action medication. Theoretical analysis of rate of release of solid drugs dispersed in solid matrices. *Journal of Pharmaceutical Sciences* 1963; **52**:1145-1149.

258. A.W.Hixon, J.H.Crowell. Dependence of reaction velocity upon surface and agitation. *Industrial and Engineering Chemical Reasearch* 1931; **23**(8923):931.

259. W.Weibull. A statistical distribution function of wide applicability. *Journal of Applied Mechanics* 1951; **18**:293-297.

260. F.Langerbuncher. Linearization of the dissolution rate curves by the Weibull distribution. *Journal of Pharmacy and Pharmacology* 1972; **24**(12):979-981.

261. R.W.Korsmeyer, R.Gumy, E.Doelker, P.Buri, N.A.Peppas. Mechanisms of solute release from porous hydrophilic polymers. *International Journal of Pharmaceutics* 1983; **15**(1):25-35.

262. R.K.Chang. Time dependent diffusivity as a mechanism for regulating drug release from slab matrix systems: Theoretical models. *Journal of Pharmaceutical Sciences* 1986; **75**(7):717-718.

263. J.G.Wagner. Interpretation of percent dissolved-time plots derived from *in-vitro* testing of conventional tablets and capsules. *Journal of Pharmaceutical Sciences* 1969; **58**(10):1253-1257.

264. C.S.Brazel, N.A.Peppas. Modelling of drug release from swellable polymers. *European Journal of Pharmaceutics and Biopharmaceutics* 2000; **49**(1):47-58.

265. M.Grassi, G.Grassi. Mathematical modelling and controlled drug delivery: Matrix systems. *Current Drug Delivery* 2005; **2**:97-116.

266. A.Saltelli, I.M.Sobol. About the use of rank transformation in sensitivity analysis of model output. *Reliability Engineering and System Safety* 1995; **50**(3):225-239.

267. European Agency for the Evaluation of Medicial Products. Human Medicines Evaluation Unit,Jully 1999. Note for guidance on quality of modified release products. A. Oral dosage forms; B.Transdermal dosage forms; Section I (Quality), CPMP/QWP/604/96.1999. 4-5-2012.

268. S.C.George, S.Thomas. Transport phenomena through polymeric systems. *Progress in Polymer Science* 2001; **26**(6):985-1017.

APPENDIX I
BATCH PRODUCTION RECORDS

Note that only the production records for batch CPT-001 is included here. The batch production records for batches CPT-002 to CPT-027 are available on request.

RHODES UNIVERSITY, FACULTY OF PHARMACY
GRAHAMSTOWN, SOUTH AFRICA, 6140

BATCH PRODUCTION RECORD

Product name:	Captopril beads	**Page:**	1 of 4
Batch ID:`	CPT-001	**Batch size:**	200 g

MANUFACTURING APPROVALS

Batch record issued by_____ Date_____
Master record issued by_____ Date_____

RHODES UNIVERSITY, FACULTY OF PHARMACY
GRAHAMSTOWN, SOUTH AFRICA, 6140

BATCH PRODUCTION RECORD

Product name: Captopril beads **Page:** 2 of 4
Batch ID: CPT-001 **Batch size:** 200 g

MATERIALS AND QUANTITIES

Material	Rhodes No.	Quantity (% w/w)	Amount dispensed (g)	Dispensed by	Checked by
CPT	5103-02-348-C	20	40		
Avicel® PH 102	RM000038	42.5	75		
Methocel® K100M	RM000024	15	30		
Methocel® E4M	RM000032	10	20		
Eudragit® RS PO	RM000023	7.5	15		
Talc	RM000050	5	10		

EQUIPMENT VERIFICATION

Description	Type	Verified by	Confirmed by
Mixing	Silversonmagnetic stirrer		
Sieve	1400 μm mesh size 0.315, 0.80 and 1.25 mm Mesh DIN 4188		
Weighing balance	Mettler AG 135 top loading balance		
Blender	Kenwood Multi-Pro FP580planetary mixer		
Extrusion	Model 20 Caleva® extruder		
Spheroniser	Caleva® MBS 250 spheroniser		
Fluid bed drier	STREA-1™ Classic Fluid Bed Processor		

RHODES UNIVERSITY, FACULTY OF PHARMACY
GRAHAMSTOWN, SOUTH AFRICA, 6140

BATCH PRODUCTION RECORD

Product name: Captopril beads **Page:** 3 of 4
Batch ID: CPT-001 **Batch size:** 200 g

MANUFACTURING PROCEDURE

Step	Procedure	Time	Done by	Checked by
1	Dilute 25 % m/v Surelease® E-7-19010 to 15 % m/v solids (SSC) stirring at 400 rpm for 2 hoursusing a magnetic stirrer.			
2	Separately screen weighed amounts of the following materials through a 1400 μm mesh size screen: CPT, Avicel® PH 102, Eudragit® RS PO, talc, Methocel® K100M and E4M.			
3	Blend the powders using a Kenwood Multi-Pro FP580planetary mixer at low speed for 20 minutes.			
4	Manually spray diluted SSC dispersion (1) onto the powder mixture while blending at low speed for an additional 3 minutes.			
5	Load the granules into the gravimetric feeder of Model 20 Caleva® extruder with the impeller speed set at 35 rpm.			
6	Spheronise the extrudate for1 6 minutes in a 300 mmdiameter crosshatched friction plate Caleva® MBS 250 spheroniser immediately on harvesting.			
7	Dry the wet beads in a fluid bed processorfor 25 minutes withthe inlet air temperature was set at 50 °Cand an atomising air flow rate of 115 m^3/hr.			
8	Coat the dried beads using fluid bed processor fitted with 121 mm Würster insert, diluted SSC dispersion (1) sprayed at a rate of 2.0g/min, through a 1.2 mm nozzle with an atomising air flow pressure set at 115 m^3/hr. The inlet air temperature was set at 60±2°C.			
9	Cure beads at 40 °C for 1hour. Sieve dried beads using a set of standard sieves with a nominal screen sizes of 1.25 mm, 0.80 mm and 0.3125 mm.			
10	Calculate the % yield and load the coated beads into opaque yellow size 1 hard gelatin capsules. Pack the capsules in a sealed plastic bag until analysis.			

RHODES UNIVERSITY, FACULTY OF PHARMACY
GRAHAMSTOWN, SOUTH AFRICA, 6140

BATCH PRODUCTION RECORD

Product name: Captopril beads **Page:** 4 of 4
Batch ID: CPT-001 **Batch size**: 200 g

SIGNATURE AND INITIAL REFRENCE

Full Name (Print)	Signature	Initials	Date

APPENDIX II
BATCH SUMMARIES

RHODES UNIVERSITY, FACULTY OF PHARMACY
GRAHAMSTOWN, SOUTH AFRICA, 6140

BATCH SUMMARY CPT-001

Formulator:	Farai Mhaka	**Extrusion-spheronisation time (start):**	09:00
Product:	Captopril beads	**(end):**	10:10
Manufactured date:	14/06/2012	**Coating time (start):**	10:10
Batch number:	CPT-001	**(end):**	11:30
Batch size:	200 g		

Formula

Material	Rhodes No.	Quantity (% w/w)	Amount dispensed (g)
CPT	5103-02-348-C	20	40.34
Avicel® PH 102	RM000038	40	80.15
Methocel® K100M	RM000024	15	30.09
Methocel® E4M	RM000032	7.5	15.12
Eudragit® RS PO	RM000023	15	30.05
Talc	RM000050	2.5	5.14

Release profile of CPT-001

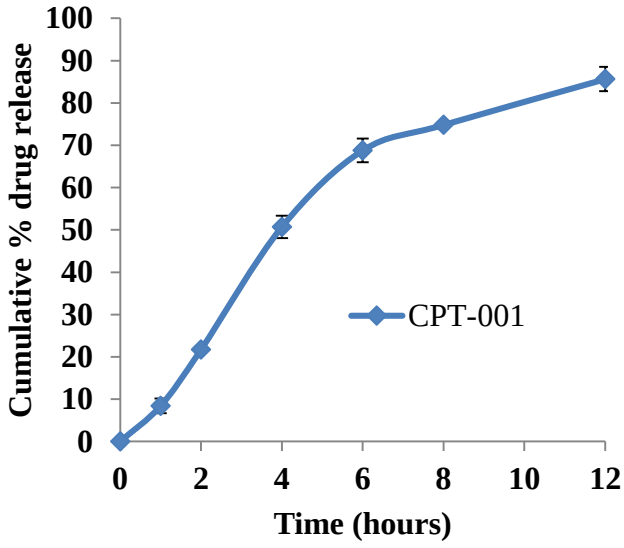

SEM

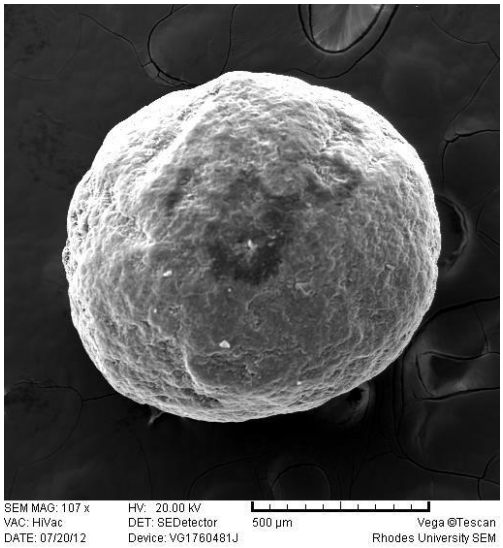

Temperature:	23.8 ˚C	**Friability:**	0.43±0.05 %
Humidity:	60.0%	**Aspect ratio:**	1.04±0.74
Weight obtained:	171.2 g	**Drug content:**	96.4±0.9 %
Yield:	85.6 %	**Coating efficiency:**	84.6 %

Comments

Smooth spherical beads obtained

RHODES UNIVERSITY, FACULTY OF PHARMACY
GRAHAMSTOWN, SOUTH AFRICA, 6140

BATCH SUMMARY CPT-002

Formulator:	Farai Mhaka	**Extrusion-spheronisation time (start):**	13:00
Product:	Captopril beads	**(end):**	14:10
Manufactured date:	14/06/2012	**Coating time (start):**	14:10
Batch number:	CPT-002	**(end):**	15:30
Batch size:	200 g		

Formula

Material	Rhodes No.	Quantity (% w/w)	Amount dispensed (g)
CPT	5103-02-348-C	20	40.08
Avicel® PH 102	RM000038	40	80.11
Methocel® K100M	RM000024	15	30.07
Methocel® E4M	RM000032	7.5	15.32
Eudragit® RS PO	RM000023	15	30.24
Talc	RM000050	2.5	5.13

Release profile of CPT-002

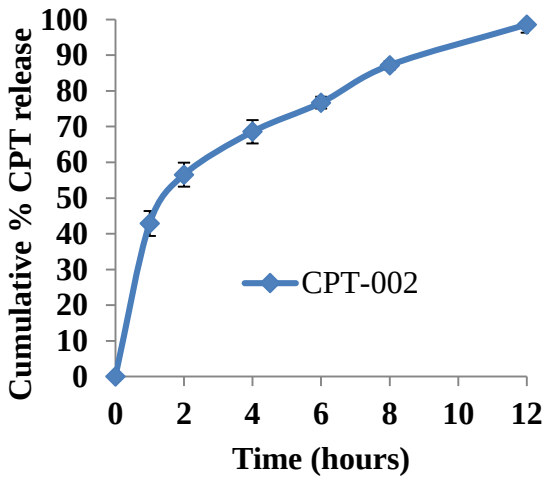

SEM

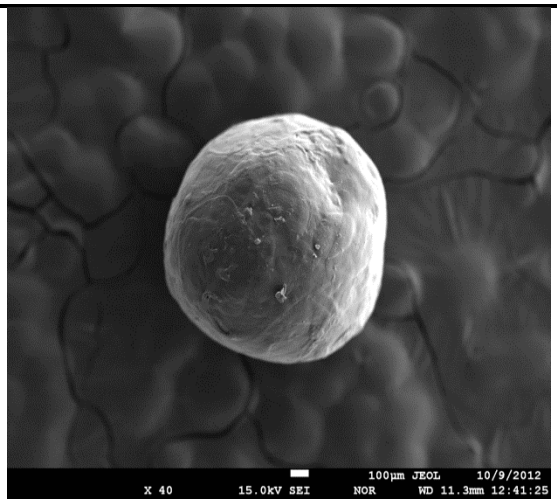

Temperature:	23.7 ˚C	**Friability:**	0.96±0.18 %
Humidity:	59.5%	**Aspect ratio:**	1.01±0.62
Weight obtained:	166.4 g	**Drug content:**	98.4±1.9 %
Yield:	83.2 %	**Coating efficiency:**	86.9 %

Comments

Smooth spherical beads obtained

RHODES UNIVERSITY, FACULTY OF PHARMACY
GRAHAMSTOWN, SOUTH AFRICA, 6140

BATCH SUMMARY CPT-003

Formulator:	Farai Mhaka	**Extrusion-spheronisation time (start):**	16:00
Product:	Captopril beads	**(end):**	17:10
Manufactured date:	14/06/2012	**Coating time (start):**	17:10
Batch number:	CPT-003	**(end):**	18:30
Batch size:	200 g		

Formula

Material	Rhodes No.	Quantity (% w/w)	Amount dispensed (g)
CPT	5103-02-348-C	20	39.87
Avicel® PH 102	RM000038	40	80.13
Methocel® K100M	RM000024	15	29.89
Methocel® E4M	RM000032	7.5	15.17
Eudragit® RS PO	RM000023	15	29.93
Talc	RM000050	2.5	4.98

Release profile of CPT-003

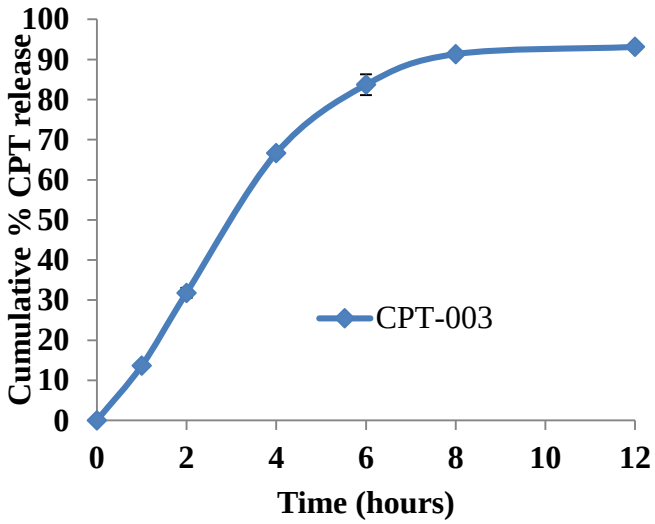

SEM

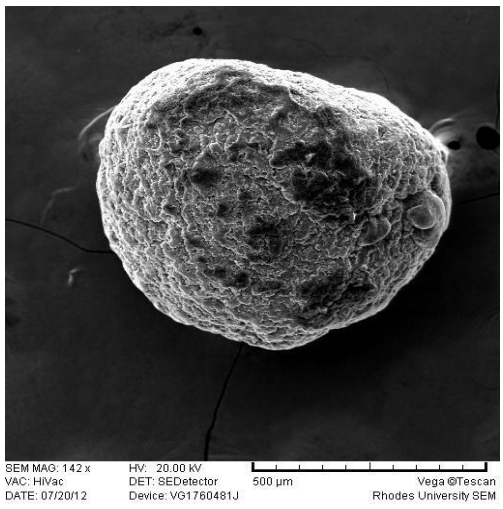

Temperature:	23.5 ˚C	**Friability:**	0.74±0.13 %
Humidity:	59.8%	**Aspect ratio:**	1.08±0.28
Weight obtained:	185.23 g	**Drug content:**	87.1±2.2 %
Yield:	92.6 %	**Coating efficiency:**	77.2 %

Comments

Smooth spherical beads obtained

RHODES UNIVERSITY, FACULTY OF PHARMACY
GRAHAMSTOWN, SOUTH AFRICA, 6140

BATCH SUMMARY CPT-004

Formulator:	Farai Mhaka	**Extrusion-spheronisation time (start):**	09:00
Product:	Captopril beads	**(end):**	10:10
Manufactured date:	16/06/2012	**Coating time (start):**	10:10
Batch number:	CPT-004	**(end):**	11:30
Batch size:	200 g		

Formula

Material	Rhodes No.	Quantity (% w/w)	Amount dispensed (g)
CPT	5103-02-348-C	20	40.07
Avicel® PH 102	RM000038	40	79.79
Methocel® K100M	RM000024	15	30.06
Methocel® E4M	RM000032	7.5	15.10
Eudragit® RS PO	RM000023	15	29.87
Talc	RM000050	2.5	5.18

Release profile of CPT-004

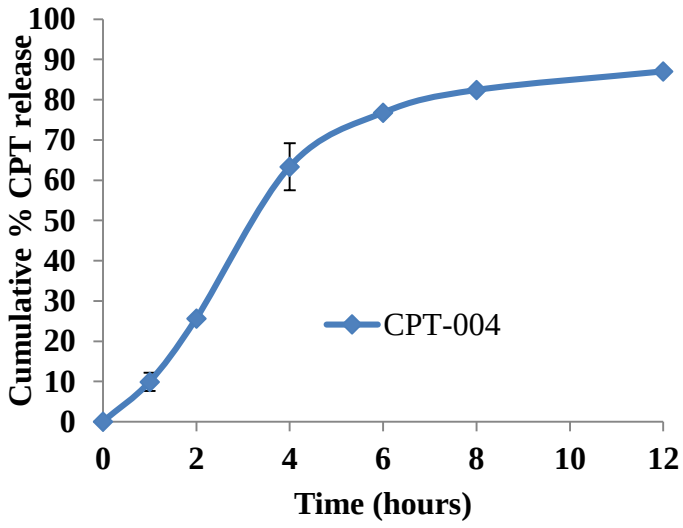

SEM

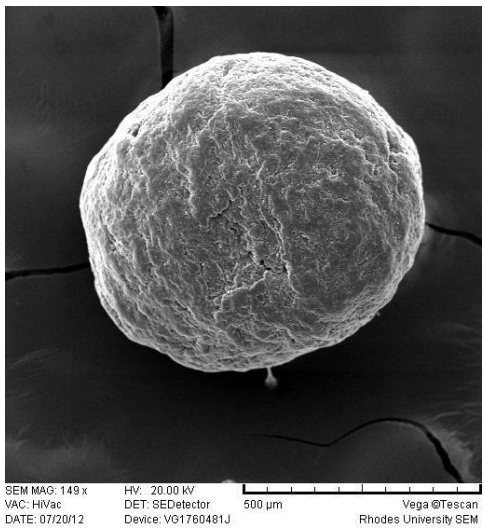

Temperature:	23.1 ˚C	**Friability:**	0.67±0.17 %
Humidity:	60.2%	**Aspect ratio:**	1.03±0.12
Weight obtained:	187.06 g	**Drug content:**	91.4±0.8 %
Yield:	93.6 %	**Coating efficiency:**	92.6 %

Comments

Smooth spherical beads obtained

RHODES UNIVERSITY, FACULTY OF PHARMACY
GRAHAMSTOWN, SOUTH AFRICA, 6140

BATCH SUMMARY CPT-005

Formulator:	Farai Mhaka	**Extrusion-spheronisation time (start):**	13:00
Product:	Captopril beads	**(end):**	14:10
Manufactured date:	16/06/2012	**Coating time (start):**	14:10
Batch number:	CPT-005	**(end):**	15:30
Batch size:	200 g		

Formula

Material	Rhodes No.	Quantity (% w/w)	Amount dispensed (g)
CPT	5103-02-348-C	20	40.58
Avicel® PH 102	RM000038	40	80.12
Methocel® K100M	RM000024	15	30.07
Methocel® E4M	RM000032	7.5	14.85
Eudragit® RS PO	RM000023	15	30.06
Talc	RM000050	2.5	5.25

Release profile of CPT-005

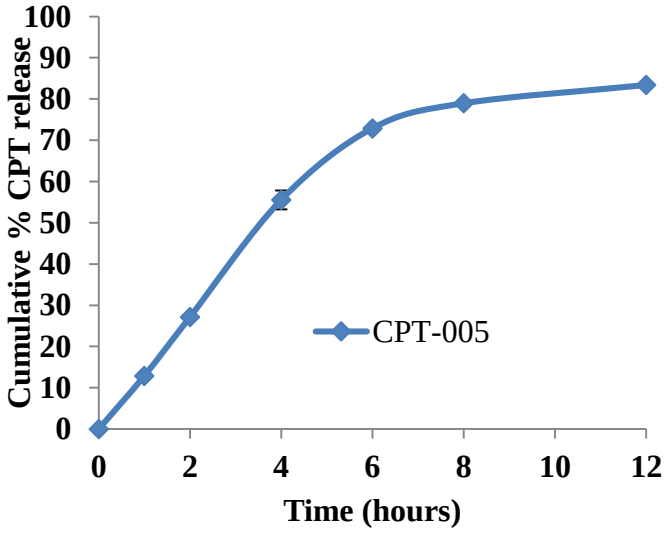

SEM

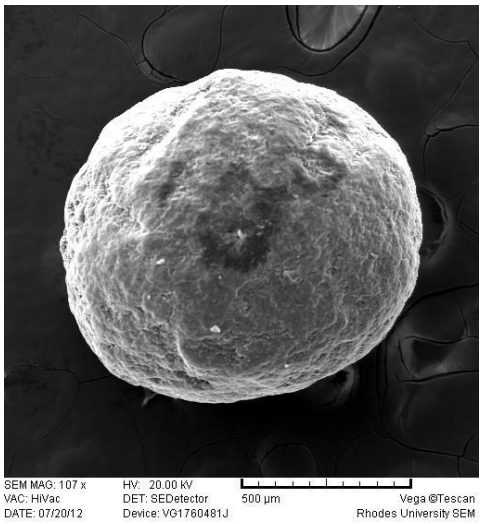

Temperature:	22.9 ˚C	**Friability:**	0.83±0.34 %
Humidity:	60.0%	**Aspect ratio:**	1.09±0.14
Weight obtained:	171.76 g	**Drug content:**	86.7±3.4 %
Yield:	85.9 %	**Coating efficiency:**	84.7 %

Comments

Smooth spherical beads obtained

RHODES UNIVERSITY, FACULTY OF PHARMACY
GRAHAMSTOWN, SOUTH AFRICA, 6140

BATCH SUMMARY CPT-006

Formulator:	Farai Mhaka	**Extrusion-spheronisation time (start):**	17:00
Product:	Captopril beads	**(end):**	18:10
Manufactured date:	16/06/2012	**Coating time (start):**	18:10
Batch number:	CPT-006	**(end):**	19:35
Batch size:	200 g		

Formula

Material	Rhodes No.	Quantity (% w/w)	Amount dispensed (g)
CPT	5103-02-348-C	20	39.95
Avicel® PH 102	RM000038	40	80.05
Methocel® K100M	RM000024	15	30.17
Methocel® E4M	RM000032	7.5	15.21
Eudragit® RS PO	RM000023	15	29.96
Talc	RM000050	2.5	5.07

Release profile of CPT-006

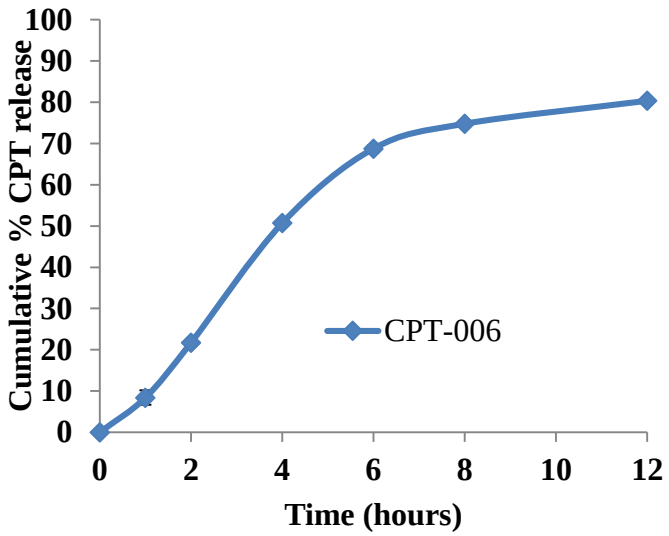

SEM

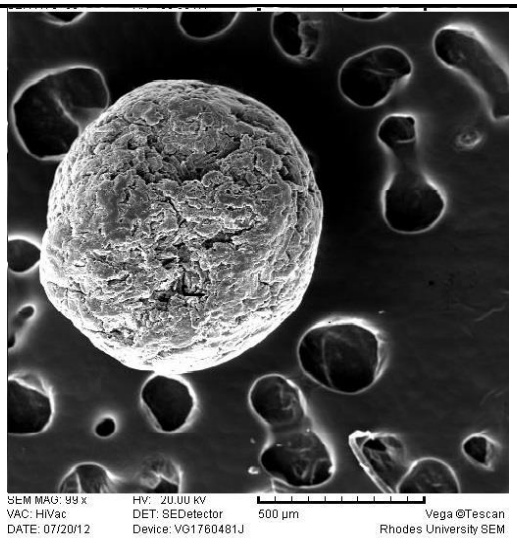

Temperature:	22.7 ˚C	**Friability:**	0.52±0.07 %
Humidity:	59.5%	**Aspect ratio:**	1.14±0.09
Weight obtained:	176.27 g	**Drug content:**	83.4±5.1 %
Yield:	88.1 %	**Coating efficiency:**	86.8 %

Comments

Smooth spherical beads obtained

RHODES UNIVERSITY, FACULTY OF PHARMACY
GRAHAMSTOWN, SOUTH AFRICA, 6140

BATCH SUMMARY CPT-007

Formulator:	Farai Mhaka	**Extrusion-spheronisation time (start):**	08:00
Product:	Captopril beads	**(end):**	09:10
Manufactured date:	18/06/2012	**Coating time (start):**	09:10
Batch number:	CPT-007	**(end):**	10:25
Batch size:	200 g		

Formula

Material	Rhodes No.	Quantity (% w/w)	Amount dispensed (g)
CPT	5103-02-348-C	20	40.14
Avicel® PH 102	RM000038	40	80.23
Methocel® K100M	RM000024	15	30.31
Methocel® E4M	RM000032	7.5	14.86
Eudragit® RS PO	RM000023	15	30.04
Talc	RM000050	2.5	5.11

Release profile of CPT-007

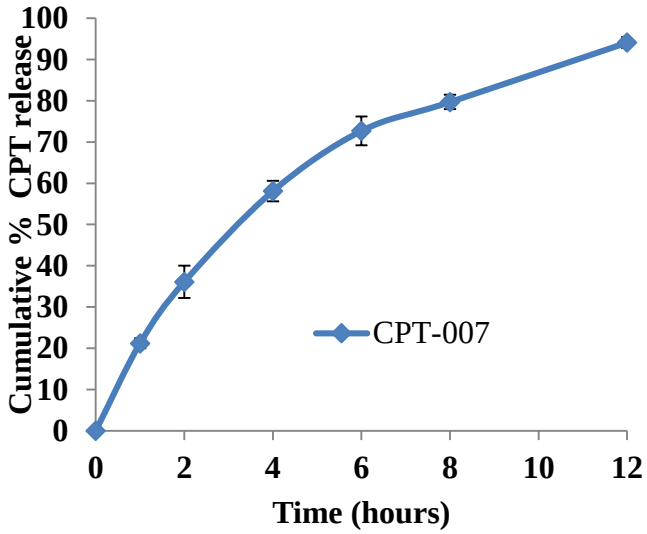

SEM

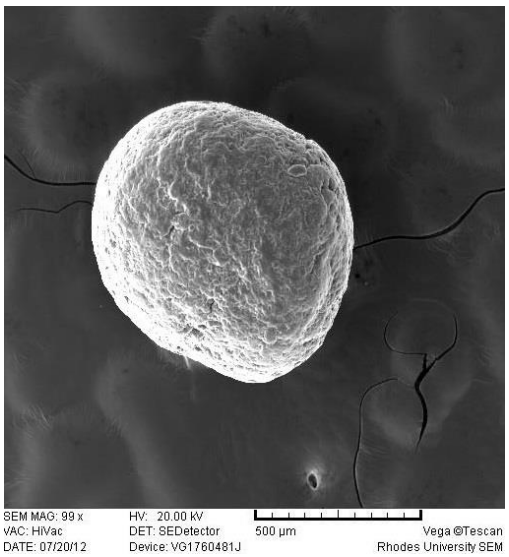

Temperature:	23.0 ˚C	**Friability:**	0.75±0.27 %
Humidity:	60.0 %	**Aspect ratio:**	1.18±0.15
Weight obtained:	163.95 g	**Drug content:**	90.6±2.3 %
Yield:	81.9 %	**Coating efficiency:**	83.7 %

Comments

Spherical beads obtained

RHODES UNIVERSITY, FACULTY OF PHARMACY
GRAHAMSTOWN, SOUTH AFRICA, 6140

BATCH SUMMARY CPT-008

Formulator:	Farai Mhaka	**Extrusion-spheronisation time (start):**	12:00
Product:	Captopril beads	**(end):**	13:10
Manufactured date:	18/06/2012	**Coating time (start):**	13:10
Batch number:	CPT-008	**(end):**	14:25
Batch size:	200 g		

Formula

Material	Rhodes No.	Quantity (% w/w)	Amount dispensed (g)
CPT	5103-02-348-C	20	40.11
Avicel® PH 102	RM000038	40	80.05
Methocel® K100M	RM000024	15	30.25
Methocel® E4M	RM000032	7.5	15.09
Eudragit® RS PO	RM000023	15	30.04
Talc	RM000050	2.5	5.16

Release profile of CPT-008

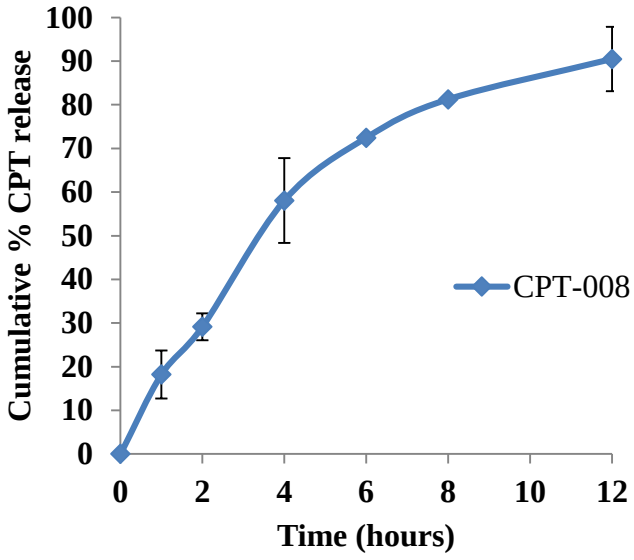

SEM

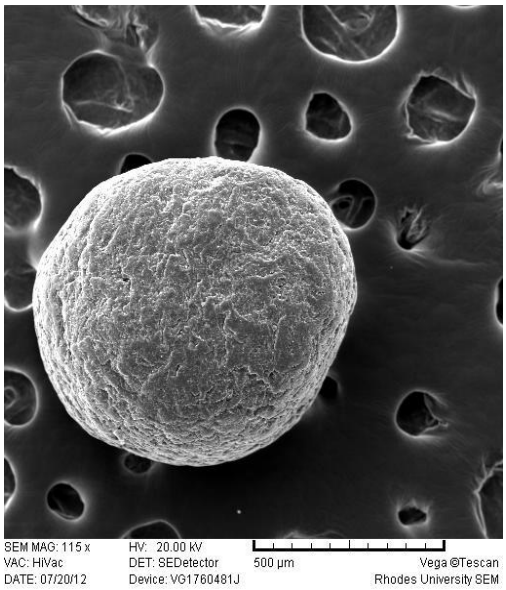

Temperature:	23.0 ˚C	**Friability:**	0.47±0.11 %
Humidity:	60.0 %	**Aspect ratio:**	1.01±0.13
Weight obtained:	168.85 g	**Drug content:**	94.7±3.5 %
Yield:	84.4 %	**Coating efficiency:**	92.5 %

Comments

Smooth spherical beads obtained

RHODES UNIVERSITY, FACULTY OF PHARMACY
GRAHAMSTOWN, SOUTH AFRICA, 6140

BATCH SUMMARY CPT-009

Formulator:	Farai Mhaka	**Extrusion-spheronisation time (start):**	18:00
Product:	Captopril beads	**(end):**	19:10
Manufactured date:	18/06/2012	**Coating time (start):**	19:10
Batch number:	CPT-009	**(end):**	20:25
Batch size:	200 g		

Formula

Material	Rhodes No.	Quantity (% w/w)	Amount dispensed (g)
CPT	5103-02-348-C	20	39.86
Avicel® PH 102	RM000038	40	80.15
Methocel® K100M	RM000024	15	30.07
Methocel® E4M	RM000032	7.5	14.88
Eudragit® RS PO	RM000023	15	30.19
Talc	RM000050	2.5	5.16

Release profile of CPT-009

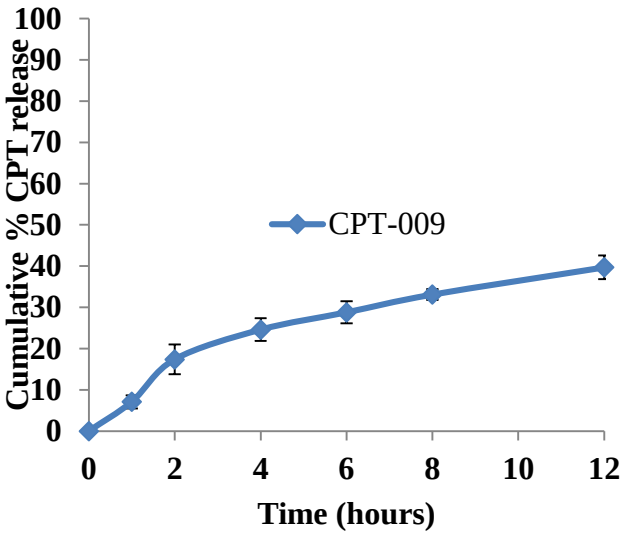

SEM

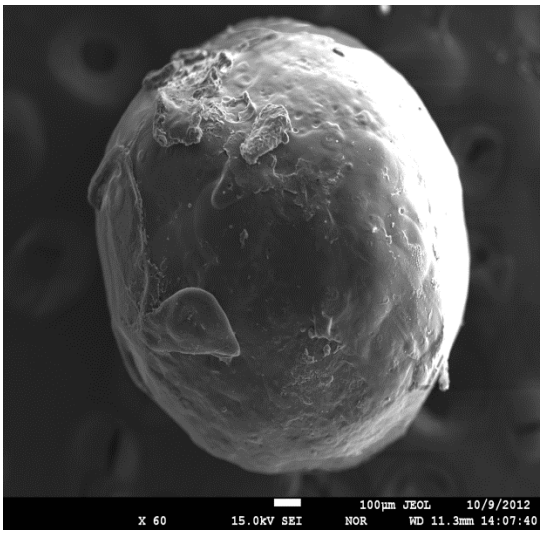

Temperature:	22.7 ˚C	**Friability:**	0.24±0.04 %
Humidity:	60.0 %	**Aspect ratio:**	1.27±0.15
Weight obtained:	131.37 g	**Drug content:**	77.4±1.5 %
Yield:	65.7 %	**Coating efficiency:**	95.8 %

Comments

Spherical beads obtained

RHODES UNIVERSITY, FACULTY OF PHARMACY
GRAHAMSTOWN, SOUTH AFRICA, 6140

BATCH SUMMARY CPT-010

Formulator:	Farai Mhaka	**Extrusion-spheronisation time (start):**	09:00
Product:	Captopril beads	**(end):**	10:10
Manufactured date:	20/06/2012	**Coating time (start):**	10:10
Batch number:	CPT-010	**(end):**	10:40
Batch size:	200 g		

Formula

Material	Rhodes No.	Quantity (% w/w)	Amount dispensed (g)
CPT	5103-02-348-C	20	39.93
Avicel® PH 102	RM000038	40	80.07
Methocel® K100M	RM000024	15	30.14
Methocel® E4M	RM000032	7.5	15.31
Eudragit® RS PO	RM000023	15	30.07
Talc	RM000050	2.5	5.13

Release profile of CPT-010

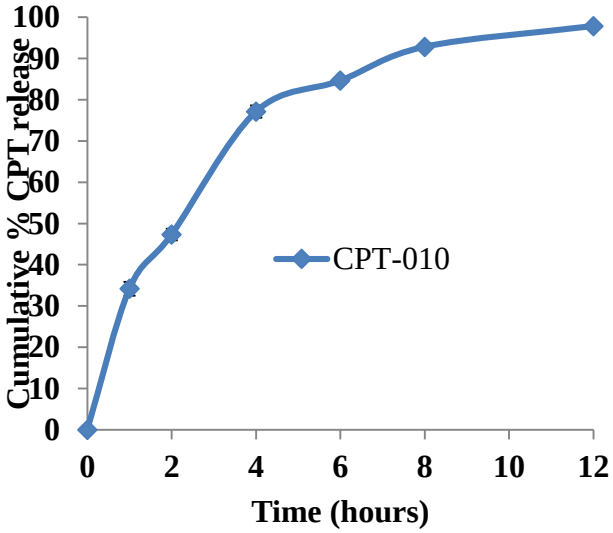

SEM

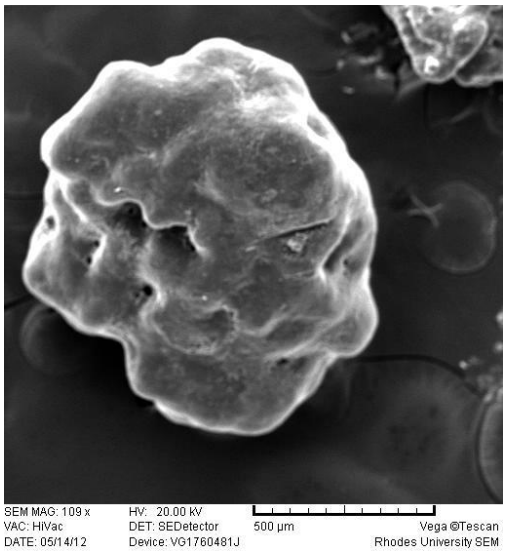

Temperature:	22.8 ˚C	**Friability:**	0.16±0.06 %
Humidity:	60.0 %	**Aspect ratio:**	1.37±0.28
Weight obtained:	124.51 g	**Drug content:**	72.9±2.1 %
Yield:	62.2 %	**Coating efficiency:**	76.5 %

Comments

Beads obtained tend to agglomerate due to incomplete coalescence and resulted in low yield.

RHODES UNIVERSITY, FACULTY OF PHARMACY
GRAHAMSTOWN, SOUTH AFRICA, 6140

BATCH SUMMARY CPT-011

Formulator:	Farai Mhaka	**Extrusion-spheronisation time (start):**	13:00
Product:	Captopril beads	**(end):**	14:10
Manufactured date:	20/06/2012	**Coating time (start):**	14:10
Batch number:	CPT-011	**(end):**	15:25
Batch size:	200 g		

Formula

Material	Rhodes No.	Quantity (% w/w)	Amount dispensed (g)
CPT	5103-02-348-C	20	40.11
Avicel® PH 102	RM000038	40	80.48
Methocel® K100M	RM000024	15	29.76
Methocel® E4M	RM000032	7.5	15.15
Eudragit® RS PO	RM000023	15	30.44
Talc	RM000050	2.5	5.32

Release profile of CPT-011

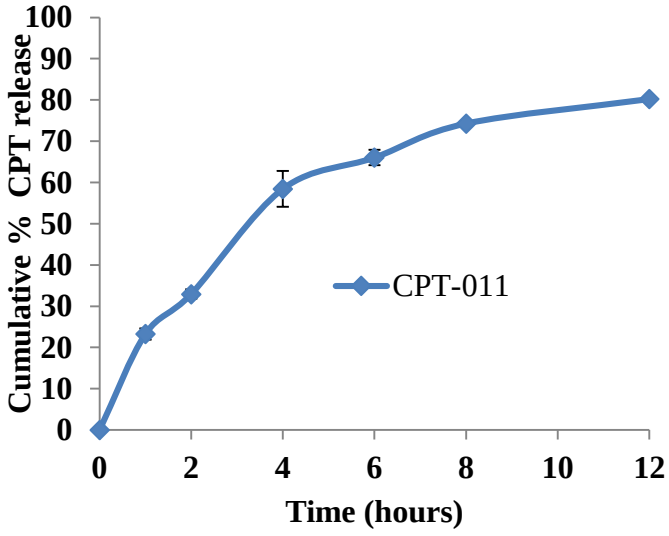

SEM

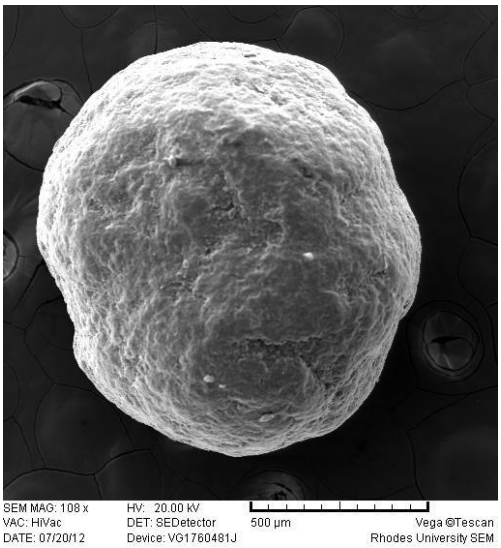

Temperature:	22.9 ˚C	**Friability:**	0.73±0.23 %
Humidity:	59.0 %	**Aspect ratio:**	1.08±0.25
Weight obtained:	158.32 g	**Drug content:**	83.4±3.7 %
Yield:	79.16 %	**Coating efficiency:**	89.8 %

Comments

Spherical beads obtained

RHODES UNIVERSITY, FACULTY OF PHARMACY
GRAHAMSTOWN, SOUTH AFRICA, 6140

BATCH SUMMARY CPT-012

Formulator:	Farai Mhaka	**Extrusion-spheronisation time (start):**	18:00
Product:	Captopril beads	**(end):**	19:10
Manufactured date:	20/06/2012	**Coating time (start):**	19:10
Batch number:	CPT-012	**(end):**	21:30
Batch size:	200 g		

Formula

Material	Rhodes No.	Quantity (% w/w)	Amount dispensed (g)
CPT	5103-02-348-C	20	40.25
Avicel® PH 102	RM000038	40	80.18
Methocel® K100M	RM000024	15	30.25
Methocel® E4M	RM000032	7.5	15.15
Eudragit® RS PO	RM000023	15	30.23
Talc	RM000050	2.5	5.16

Release profile of CPT-012

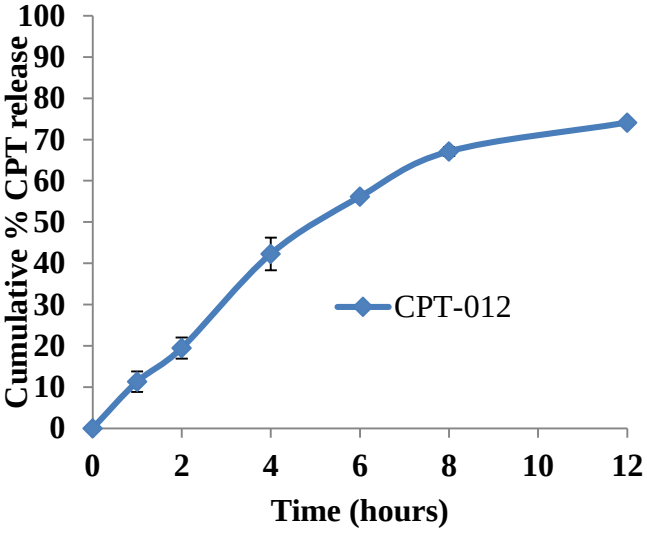

SEM

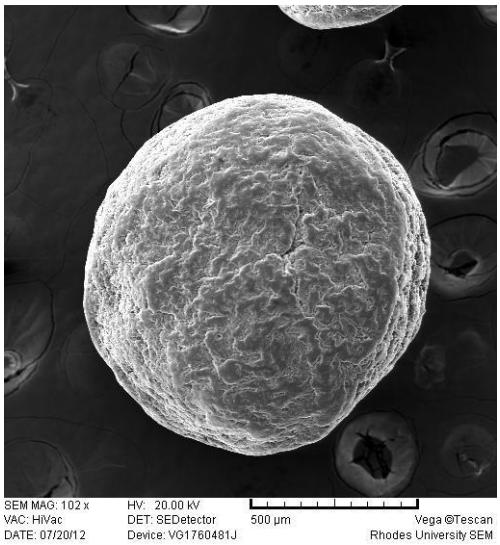

Temperature:	22.9 ˚C	**Friability:**	0.41±0.35 %
Humidity:	59.0 %	**Aspect ratio:**	1.09±0.12
Weight obtained:	186.43 g	**Drug content:**	84.1±4.3 %
Yield:	93.2 %	**Coating efficiency:**	79.7 %

Comments

Spherical beads obtained

RHODES UNIVERSITY, FACULTY OF PHARMACY
GRAHAMSTOWN, SOUTH AFRICA, 6140

BATCH SUMMARY CPT-013

Formulator:	Farai Mhaka	**Extrusion-spheronisation time (start):**	09:00
Product:	Captopril beads	**(end):**	10:10
Manufactured date:	04/07/2012	**Coating time (start):**	10:10
Batch number:	CPT-013	**(end):**	11:30
Batch size:	200 g		

Formula

Material	Rhodes No.	Quantity (% w/w)	Amount dispensed (g)
CPT	5103-02-348-C	20	40.46
Avicel® PH 102	RM000038	40	80.09
Methocel® K100M	RM000024	15	30.93
Methocel® E4M	RM000032	15	30.05
Eudragit® RS PO	RM000023	7.5	16.95
Talc	RM000050	2.5	5.09

Release profile of CPT-013

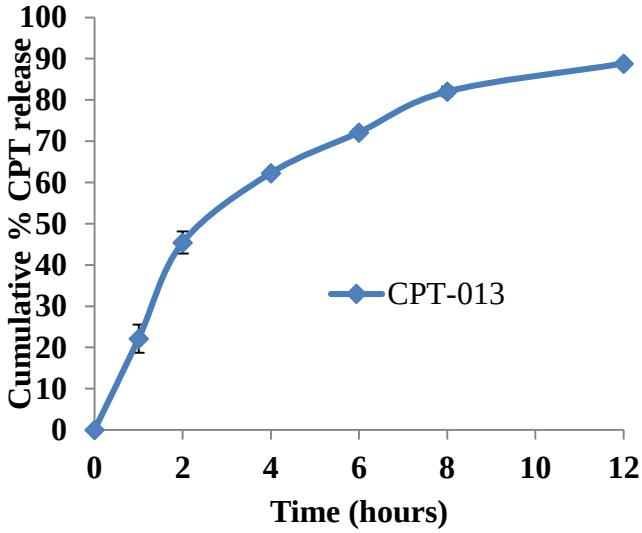

SEM

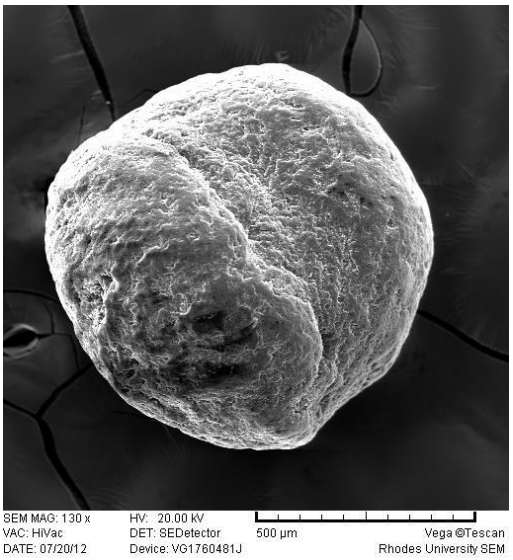

Temperature:	22.9 ˚C	**Friability:**	0.79±0.23 %
Humidity:	59.0 %	**Aspect ratio:**	1.27±0.12
Weight obtained:	140.82 g	**Drug content:**	86.1±3.3 %
Yield:	70.4 %	**Coating efficiency:**	82.4 %

Comments

Slightly dumb-bell shaped beads obtained

RHODES UNIVERSITY, FACULTY OF PHARMACY
GRAHAMSTOWN, SOUTH AFRICA, 6140

BATCH SUMMARY CPT-014

Formulator:	Farai Mhaka	**Extrusion-spheronisation time (start):**	13:00
Product:	Captopril beads	**(end):**	14:10
Manufactured date:	04/07/2012	**Coating time (start):**	14:10
Batch number:	CPT-014	**(end):**	15:30
Batch size:	255 g		

Formula

Material	Rhodes No.	Quantity (% w/w)	Amount dispensed (g)
CPT	5103-02-348-C	20	40.31
Avicel® PH 102	RM000038	50	100.35
Methocel® K100M	RM000024	15	30.53
Methocel® E4M	RM000032	25	50.22
Eudragit® RS PO	RM000023	15	30.61
Talc	RM000050	2.5	5.02

Release profile of CPT-014

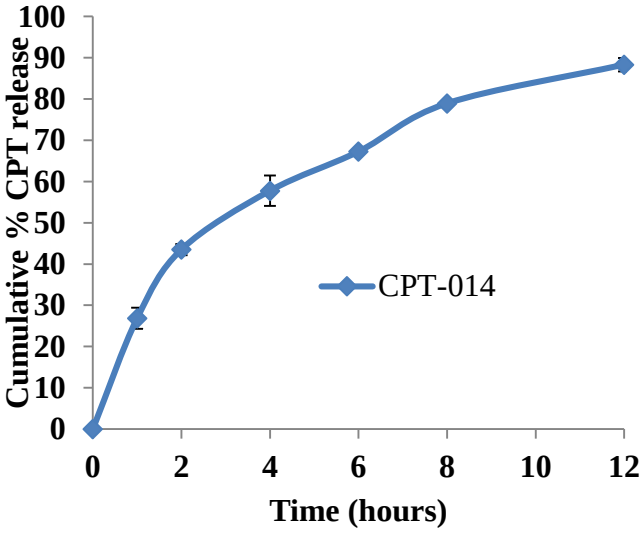

SEM

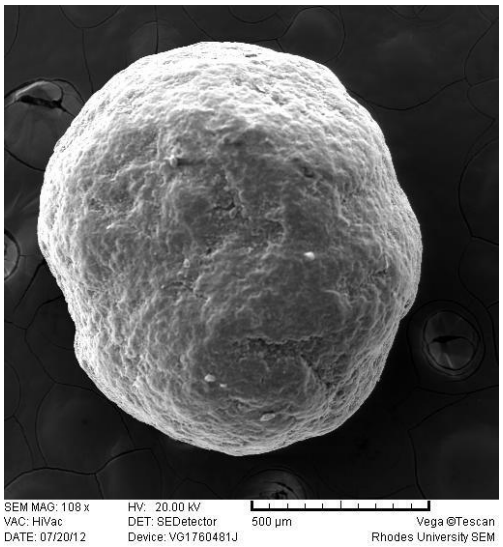

Temperature:	23.0 ˚C	**Friability:**	0.79±0.23 %
Humidity:	60.0 %	**Aspect ratio:**	1.31±0.07
Weight obtained:	233.07 g	**Drug content:**	88.8±4.1 %
Yield:	91.4 %	**Coating efficiency:**	97.9 %

Comments

Slightly dumb-bell shaped beads obtained

RHODES UNIVERSITY, FACULTY OF PHARMACY
GRAHAMSTOWN, SOUTH AFRICA, 6140

BATCH SUMMARY CPT-015

Formulator:	Farai Mhaka	**Extrusion-spheronisation time (start):**	17:00
Product:	Captopril beads	**(end):**	18:10
Manufactured date:	04/07/2012	**Coating time (start):**	18:10
Batch number:	CPT-015	**(end):**	19:30
Batch size:	255 g		

Formula

Material	Rhodes No.	Quantity (% w/w)	Amount dispensed (g)
CPT	5103-02-348-C	20	40.31
Avicel® PH 102	RM000038	50	100.36
Methocel® K100M	RM000024	25	49.89
Methocel® E4M	RM000032	15	29.70
Eudragit® RS PO	RM000023	15	29.78
Talc	RM000050	2.5	5.06

Release profile of CPT-015

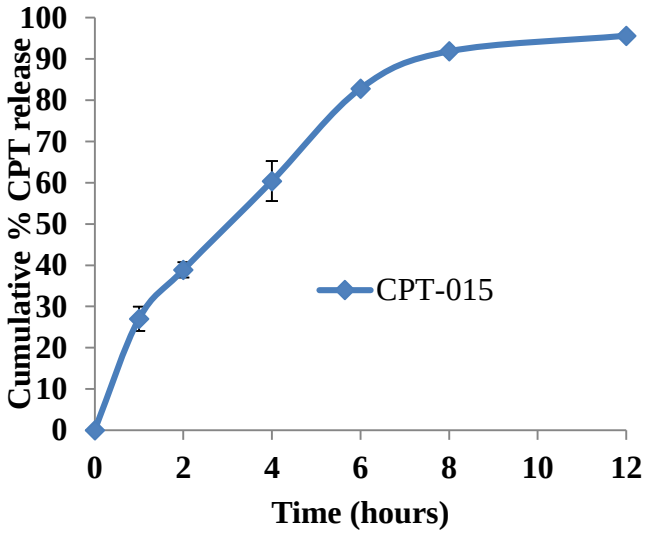

SEM

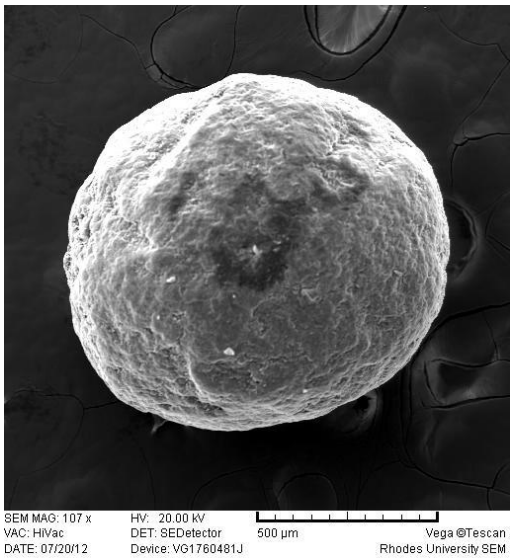

Temperature:	22.5 ˚C	**Friability:**	0.92±0.17 %
Humidity:	60.0 %	**Aspect ratio:**	1.02±0.02
Weight obtained:	191.51 g	**Drug content:**	94.1±0.9 %
Yield:	75.1 %	**Coating efficiency:**	86.1 %

Comments

Smooth spherical beads obtained

RHODES UNIVERSITY, FACULTY OF PHARMACY
GRAHAMSTOWN, SOUTH AFRICA, 6140

BATCH SUMMARY CPT-016

Formulator:	Farai Mhaka	**Extrusion-spheronisation time (start):**	09:30
Product:	Captopril beads	**(end):**	10:40
Manufactured date:	05/07/2012	**Coating time (start):**	10:40
Batch number:	CPT-016	**(end):**	12:00
Batch size:	260 g		

Formula

Material	Rhodes No.	Quantity (% w/w)	Amount dispensed (g)
CPT	5103-02-348-C	20	41.58
Avicel® PH 102	RM000038	50	100.51
Methocel® K100M	RM000024	25	49.82
Methocel® E4M	RM000032	25	49.46
Eudragit® RS PO	RM000023	7.5	15.89
Talc	RM000050	2.5	5.81

Release profile of CPT-016

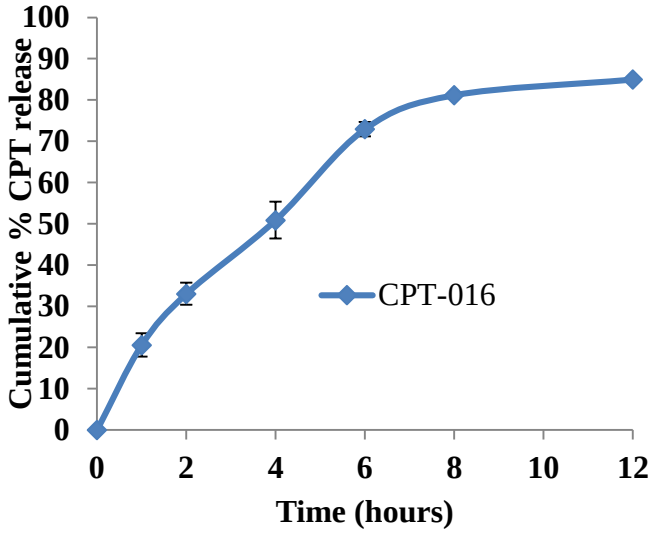

SEM

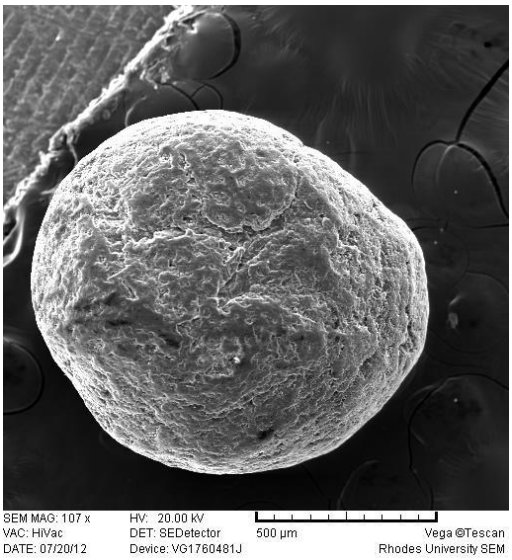

Temperature:	22.5 ˚C	**Friability:**	0.86±0.08 %
Humidity:	60.0 %	**Aspect ratio:**	1.22±0.14
Weight obtained:	193.41 g	**Drug content:**	91.8±1.5 %
Yield:	74.4 %	**Coating efficiency:**	89.1 %

Comments

Smooth spherical beads obtained

RHODES UNIVERSITY, FACULTY OF PHARMACY
GRAHAMSTOWN, SOUTH AFRICA, 6140

BATCH SUMMARY CPT-017

Formulator:	Farai Mhaka	**Extrusion-spheronisation time (start):**	14:30
Product:	Captopril beads	**(end):**	15:40
Manufactured date:	05/07/2012	**Coating time (start):**	15:40
Batch number:	CPT-017	**(end):**	17:00
Batch size:	255 g		

Formula

Material	Rhodes No.	Quantity (% w/w)	Amount dispensed (g)
CPT	5103-02-348-C	20	40.39
Avicel® PH 102	RM000038	40	80.14
Methocel® K100M	RM000024	25	49.25
Methocel® E4M	RM000032	25	50.35
Eudragit® RS PO	RM000023	15	30.03
Talc	RM000050	2.5	5.24

Release profile of CPT-017

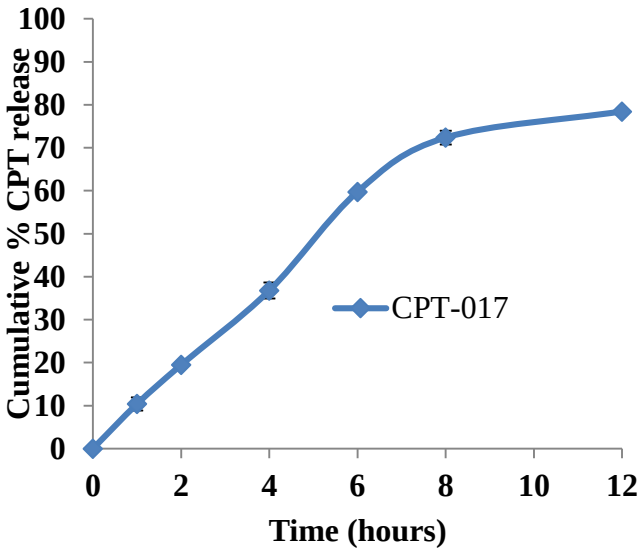

SEM

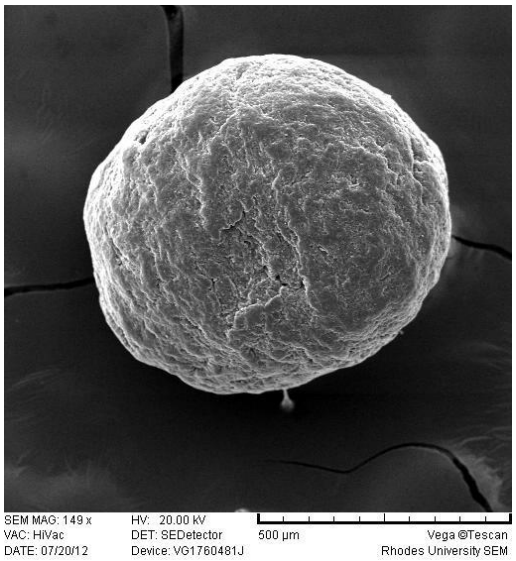

Temperature:	23.0 ˚C	**Friability:**	0.99±0.17 %
Humidity:	60.0 %	**Aspect ratio:**	1.04±0.10
Weight obtained:	189.75 g	**Drug content:**	84.9±0.7 %
Yield:	74.4 %	**Coating efficiency:**	78.7 %

Comments

Smooth spherical beads obtained

RHODES UNIVERSITY, FACULTY OF PHARMACY
GRAHAMSTOWN, SOUTH AFRICA, 6140

BATCH SUMMARY CPT-018

Formulator:	Farai Mhaka	**Extrusion-spheronisation time (start):**	17:30
Product:	Captopril beads	**(end):**	18:40
Manufactured date:	05/07/2012	**Coating time (start):**	18:40
Batch number:	CPT-018	**(end):**	20:00
Batch size:	215 g		

Formula

Material	Rhodes No.	Quantity (% w/w)	Amount dispensed (g)
CPT	5103-02-348-C	20	41.08
Avicel® PH 102	RM000038	40	80.16
Methocel® K100M	RM000024	15	30.69
Methocel® E4M	RM000032	15	29.71
Eudragit® RS PO	RM000023	15	31.18
Talc	RM000050	2.5	5.24

Release profile of CPT-018

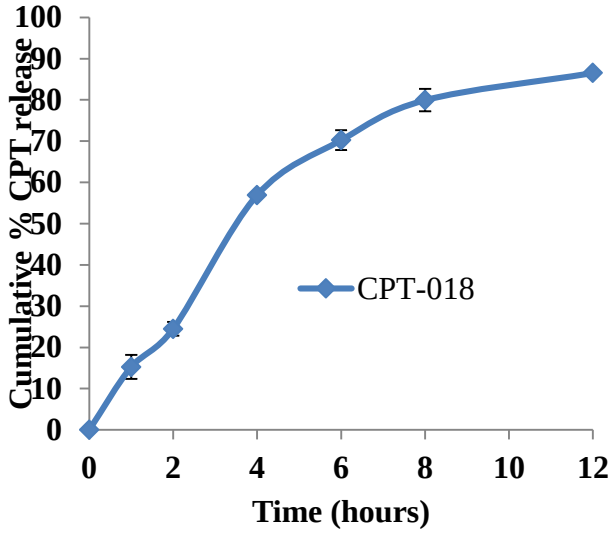

SEM

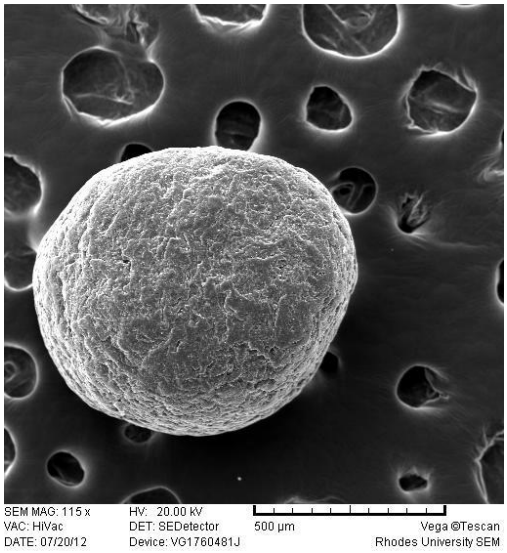

Temperature:	22.8 ˚C	**Friability:**	0.53±0.11 %
Humidity:	60.0 %	**Aspect ratio:**	0.91±0.22
Weight obtained:	188.55 g	**Drug content:**	87.4±2.1 %
Yield:	87.7 %	**Coating efficiency:**	90.7 %

Comments

Smooth spherical beads obtained

RHODES UNIVERSITY, FACULTY OF PHARMACY
GRAHAMSTOWN, SOUTH AFRICA, 6140

BATCH SUMMARY CPT-019

Formulator:	Farai Mhaka	**Extrusion-spheronisation time (start):**	08:00
Product:	Captopril beads	**(end):**	09:10
Manufactured date:	06/07/2012	**Coating time (start):**	09:10
Batch number:	CPT-019	**(end):**	10:30
Batch size:	220 g		

Formula

Material	Rhodes No.	Quantity (% w/w)	Amount dispensed (g)
CPT	5103-02-348-C	20	40.75
Avicel® PH 102	RM000038	50	99.44
Methocel® K100M	RM000024	15	29.82
Methocel® E4M	RM000032	15	30.05
Eudragit® RS PO	RM000023	7.5	15.24
Talc	RM000050	2.5	4.42

Release profile of CPT-019

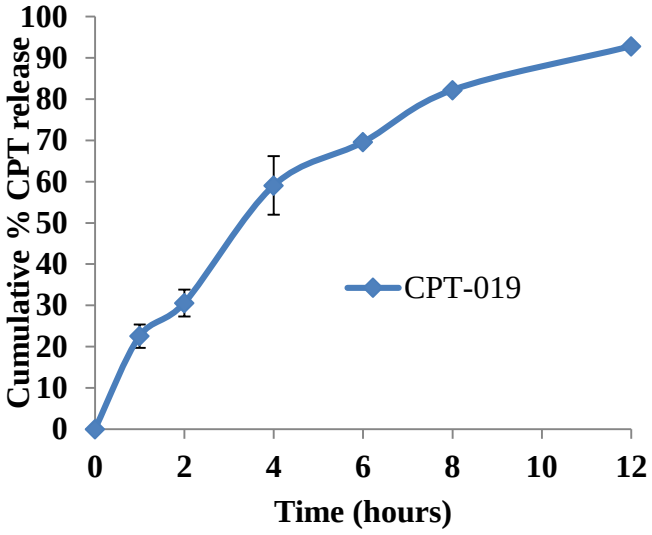

SEM

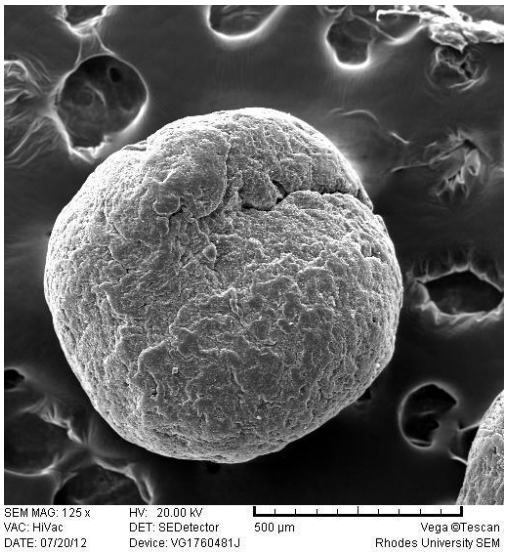

Temperature:	23.0 ˚C	**Friability:**	0.89±0.24 %
Humidity:	60.0 %	**Aspect ratio:**	0.81±0.12
Weight obtained:	180.09 g	**Drug content:**	79.7±1.9 %
Yield:	81.9 %	**Coating efficiency:**	76.4 %

Comments

Smooth spherical beads obtained

RHODES UNIVERSITY, FACULTY OF PHARMACY
GRAHAMSTOWN, SOUTH AFRICA, 6140

BATCH SUMMARY CPT-020

Formulator:	Farai Mhaka	**Extrusion-spheronisation time (start):**	12:00
Product:	Captopril beads	**(end):**	13:10
Manufactured date:	06/07/2012	**Coating time (start):**	13:10
Batch number:	CPT-020	**(end):**	14:30
Batch size:	220 g		

Formula

Material	Rhodes No.	Quantity (% w/w)	Amount dispensed (g)
CPT	5103-02-348-C	20	40.12
Avicel® PH 102	RM000038	40	80.77
Methocel® K100M	RM000024	15	30.30
Methocel® E4M	RM000032	25	49.39
Eudragit® RS PO	RM000023	7.5	15.73
Talc	RM000050	2.5	5.37

Release profile of CPT-020

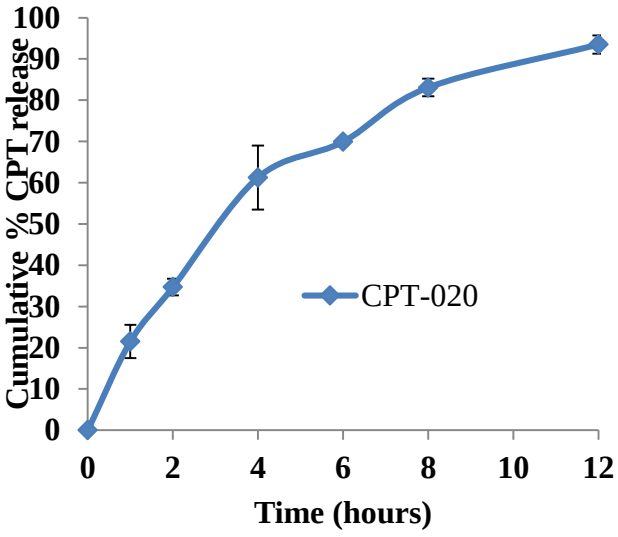

SEM

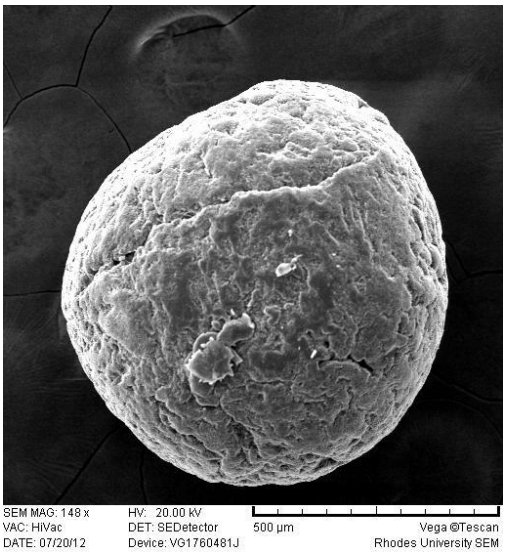

Temperature:	23.0 ˚C	**Friability:**	0.92±0.30 %
Humidity:	60.0 %	**Aspect ratio:**	1.08±0.05
Weight obtained:	152.26 g	**Drug content:**	86.5±3.9 %
Yield:	69.2 %	**Coating efficiency:**	92.1 %

Comments

Smooth spherical beads obtained

RHODES UNIVERSITY, FACULTY OF PHARMACY
GRAHAMSTOWN, SOUTH AFRICA, 6140

BATCH SUMMARY CPT-021

Formulator:	Farai Mhaka	**Extrusion-spheronisation time (start):**	17:00
Product:	Captopril beads	**(end):**	18:10
Manufactured date:	06/07/2012	**Coating time (start):**	18:10
Batch number:	CPT-021	**(end):**	19:30
Batch size:	235 g		

Formula

Material	Rhodes No.	Quantity (% w/w)	Amount dispensed (g)
CPT	5103-02-348-C	20	40.74
Avicel® PH 102	RM000038	40	80.88
Methocel® K100M	RM000024	25	50.50
Methocel® E4M	RM000032	15	30.40
Eudragit® RS PO	RM000023	15	30.18
Talc	RM000050	2.5	6.08

Release profile of CPT-021

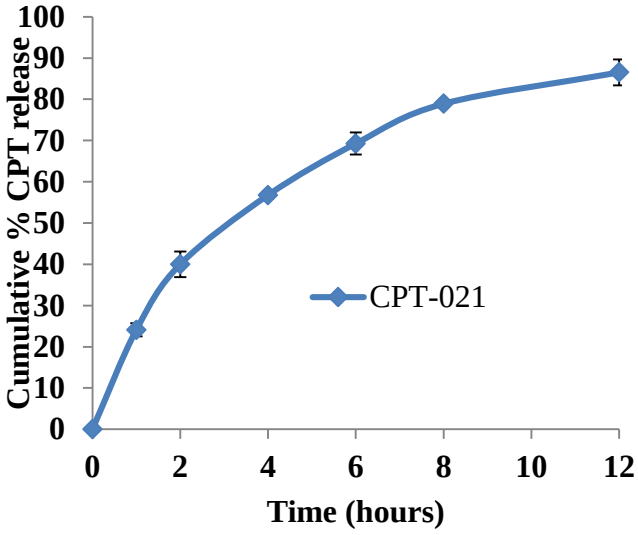

SEM

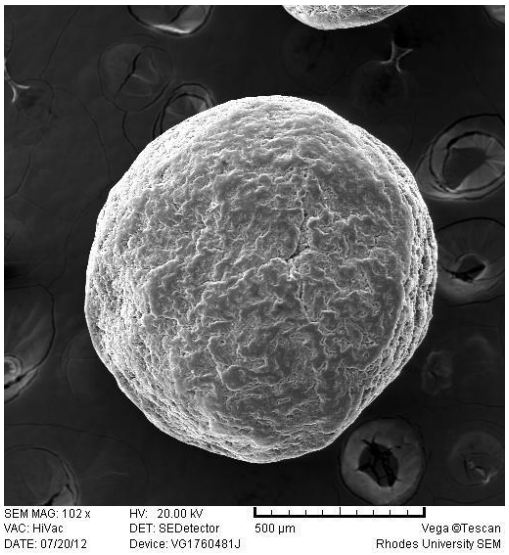

Temperature:	23.0 ˚C	**Friability:**	0.43±0.04 %
Humidity:	60.0 %	**Aspect ratio:**	0.91±0.22
Weight obtained:	211.15 g	**Drug content:**	89.4±1.1 %
Yield:	85.9 %	**Coating efficiency:**	98.6 %

Comments

Smooth spherical beads obtained

RHODES UNIVERSITY, FACULTY OF PHARMACY
GRAHAMSTOWN, SOUTH AFRICA, 6140

BATCH SUMMARY CPT-022

Formulator:	Farai Mhaka	**Extrusion-spheronisation time (start):**	09:00
Product:	Captopril beads	**(end):**	10:10
Manufactured date:	07/07/2012	**Coating time (start):**	10:10
Batch number:	CPT-022	**(end):**	11:30
Batch size:	255 g		

Formula

Material	Rhodes No.	Quantity (% w/w)	Amount dispensed (g)
CPT	5103-02-348-C	20	40.65
Avicel® PH 102	RM000038	50	100.95
Methocel® K100M	RM000024	15	30.05
Methocel® E4M	RM000032	25	49.81
Eudragit® RS PO	RM000023	15	30.52
Talc	RM000050	2.5	5.82

Release profile of CPT-022

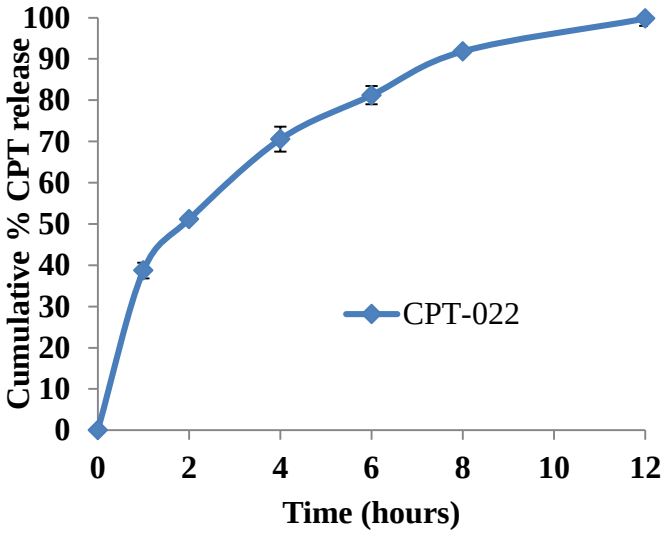

SEM

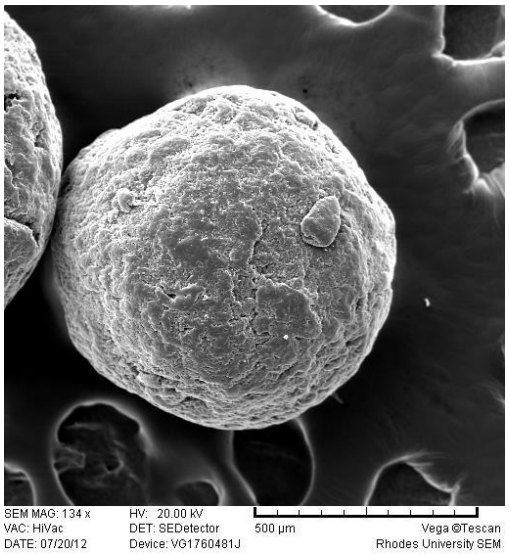

Temperature:	23.0 ˚C	**Friability:**	0.52±0.16 %
Humidity:	60.0 %	**Aspect ratio:**	0.98±0.07
Weight obtained:	216.19 g	**Drug content:**	93.5±2.5 %
Yield:	84.8 %	**Coating efficiency:**	84.6 %

Comments

Smooth spherical beads obtained

RHODES UNIVERSITY, FACULTY OF PHARMACY
GRAHAMSTOWN, SOUTH AFRICA, 6140

BATCH SUMMARY CPT-023

Formulator:	Farai Mhaka	**Extrusion-spheronisation time (start):**	13:00
Product:	Captopril beads	**(end):**	14:10
Manufactured date:	07/07/2012	**Coating time (start):**	14:10
Batch number:	CPT-023	**(end):**	15:30
Batch size:	240 g		

Formula

Material	Rhodes No.	Quantity (% w/w)	Amount dispensed (g)
CPT	5103-02-348-C	20	40.07
Avicel® PH 102	RM000038	40	80.46
Methocel® K100M	RM000024	25	49.72
Methocel® E4M	RM000032	25	49.73
Eudragit® RS PO	RM000023	7.5	16.35
Talc	RM000050	2.5	5.27

Release profile of CPT-023

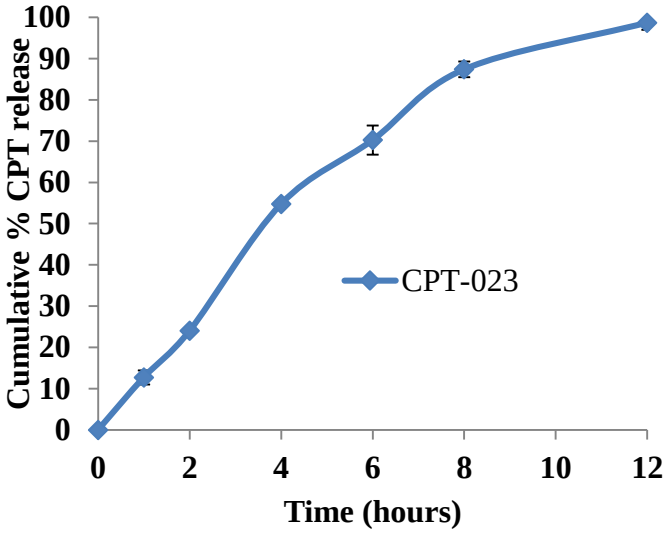

SEM

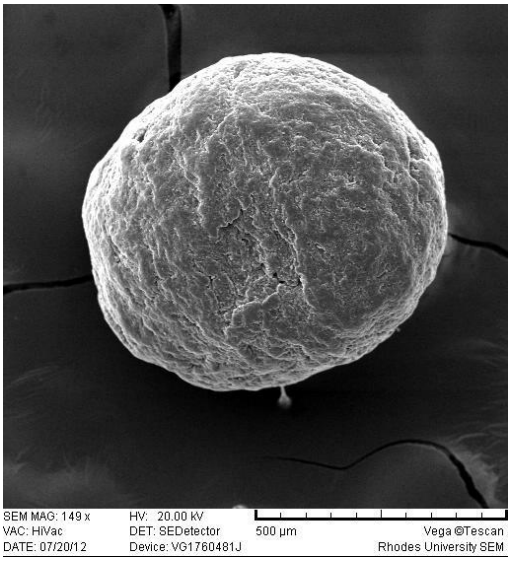

Temperature:	23.0 ˚C	**Friability:**	0.56±0.20 %
Humidity:	60.0 %	**Aspect ratio:**	1.01±0.03
Weight obtained:	196.44 g	**Drug content:**	95.8±3.0 %
Yield:	81.9 %	**Coating efficiency:**	83.1 %

Comments

Smooth spherical beads obtained

RHODES UNIVERSITY, FACULTY OF PHARMACY
GRAHAMSTOWN, SOUTH AFRICA, 6140

BATCH SUMMARY CPT-024

Formulator:	Farai Mhaka	**Extrusion-spheronisation time (start):**	17:00
Product:	Captopril beads	**(end):**	18:10
Manufactured date:	07/07/2012	**Coating time (start):**	18:10
Batch number:	CPT-024	**(end):**	19:30
Batch size:	240 g		

Formula

Material	Rhodes No.	Quantity (% w/w)	Amount dispensed (g)
CPT	5103-02-348-C	20	40.69
Avicel® PH 102	RM000038	50	100.29
Methocel® K100M	RM000024	25	50.12
Methocel® E4M	RM000032	15	30.15
Eudragit® RS PO	RM000023	7.5	15.15
Talc	RM000050	2.5	5.29

Release profile of CPT-024

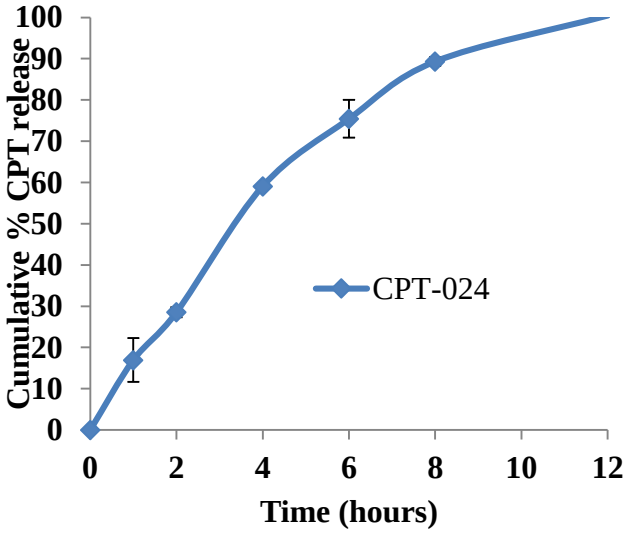

SEM

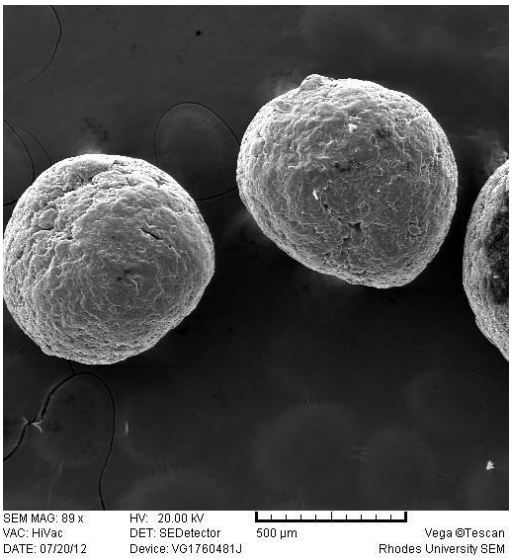

Temperature:	23.0 ˚C	**Friability:**	0.43±0.14 %
Humidity:	60.0 %	**Aspect ratio:**	1.06±0.07
Weight obtained:	201.14 g	**Drug content:**	95.3±2.6 %
Yield:	83.8 %	**Coating efficiency:**	98.4 %

Comments

Smooth spherical beads obtained

RHODES UNIVERSITY, FACULTY OF PHARMACY
GRAHAMSTOWN, SOUTH AFRICA, 6140

BATCH SUMMARY CPT-025

Formulator:	Farai Mhaka	**Extrusion-spheronisation time (start):**	09:00
Product:	Captopril beads	**(end):**	10:10
Manufactured date:	25/08/2012	**Coating time (start):**	10:10
Batch number:	CPT-025	**(end):**	11:30
Batch size:	240 g		

Formula

Material	Rhodes No.	Quantity (% w/w)	Amount dispensed (g)
CPT	5103-02-348-C	20	40.76
Avicel® PH 102	RM000038	41.2	82.45
Methocel® K100M	RM000024	23.1	46.20
Methocel® E4M	RM000032	24.95	50.12
Eudragit® RS PO	RM000023	8.4	16.87
Talc	RM000050	2.5	5.15

Release profile of CPT-025

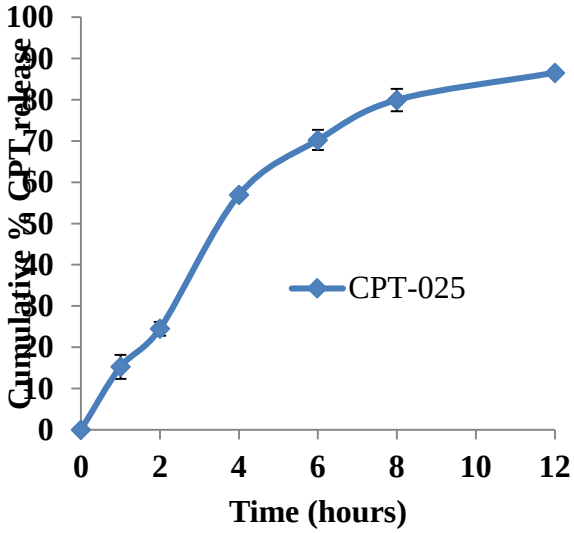

SEM

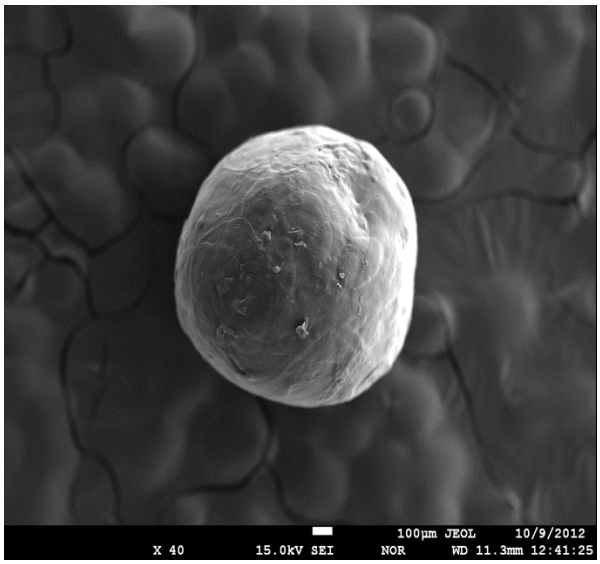

Temperature:	23.0 ˚C	**Friability:**	0.78±0.33 %
Humidity:	60.0 %	**Aspect ratio:**	1.04±0.09
Weight obtained:	202.81 g	**Drug content:**	98.7±2.1 %
Yield:	84.5 %	**Coating efficiency:**	91.2%

Comments

Smooth spherical beads obtained

RHODES UNIVERSITY, FACULTY OF PHARMACY
GRAHAMSTOWN, SOUTH AFRICA, 6140

BATCH SUMMARY CPT-026

Formulator:	Farai Mhaka	**Extrusion-spheronisation time (start):**	13:00
Product:	Captopril beads	**(end):**	14:10
Manufactured date:	25/08/2012	**Coating time (start):**	14:10
Batch number:	CPT-026	**(end):**	15:30
Batch size:	240 g		

Formula

Material	Rhodes No.	Quantity (% w/w)	Amount dispensed (g)
CPT	5103-02-348-C	20	40.64
Avicel® PH 102	RM000038	41.2	82.38
Methocel® K100M	RM000024	23.1	46.17
Methocel® E4M	RM000032	24.95	49.87
Eudragit® RS PO	RM000023	8.4	16.74
Talc	RM000050	2.5	5.05

Release profile of CPT-026

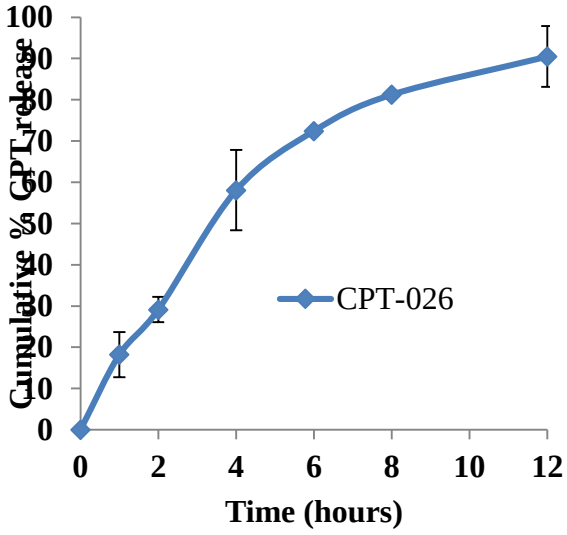

SEM

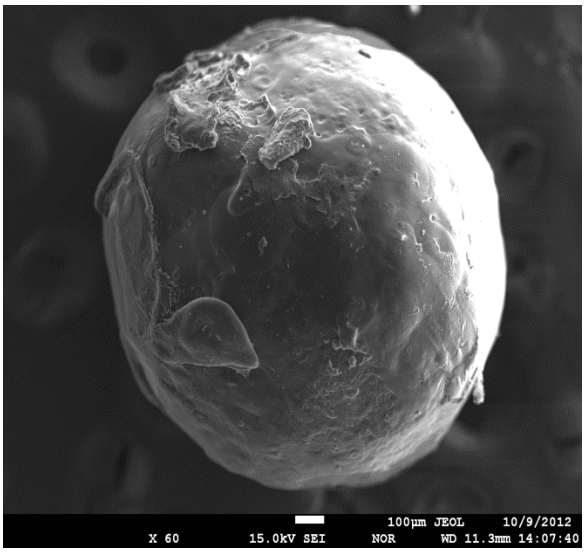

Temperature:	23.0 ˚C	**Friability:**	0.84±0.47 %
Humidity:	60.0 %	**Aspect ratio:**	1.05±0.12
Weight obtained:	204.48 g	**Drug content:**	97.4±1.3 %
Yield:	85.2 %	**Coating efficiency:**	90.8%

Comments

Smooth spherical beads obtained

RHODES UNIVERSITY, FACULTY OF PHARMACY
GRAHAMSTOWN, SOUTH AFRICA, 6140

BATCH SUMMARY CPT-027

Formulator:	Farai Mhaka	**Extrusion-spheronisation time (start):**	17:00
Product:	Captopril beads	**(end):**	18:10
Manufactured date:	25/08/2012	**Coating time (start):**	18:10
Batch number:	CPT-027	**(end):**	19:30
Batch size:	240 g		

Formula

Material	Rhodes No.	Quantity (% w/w)	Amount dispensed (g)
CPT	5103-02-348-C	20	39.94
Avicel® PH 102	RM000038	41.2	82.48
Methocel® K100M	RM000024	23.1	46.27
Methocel® E4M	RM000032	24.95	50.03
Eudragit® RS PO	RM000023	8.4	16.91
Talc	RM000050	2.5	5.13

Release profile of CPT-027

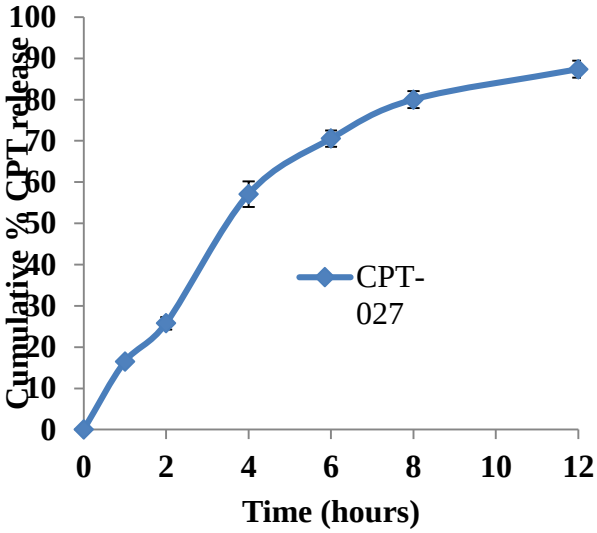

SEM

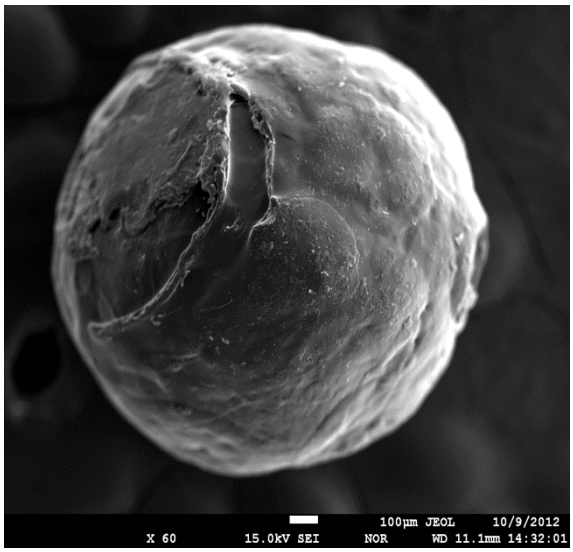

Temperature:	23.0 ˚C	**Friability:**	0.82±0.26 %
Humidity:	60.0 %	**Aspect ratio:**	1.04±0.04
Weight obtained:	204.96 g	**Drug content:**	96.8±1.3 %
Yield:	85.4%	**Coating efficiency:**	91.5%

Comments

Spherical beads obtained